UCSF
UC San Francisco Electronic Theses and Dissertations

Title
Rational design of selective, irreversible kinase inhibitors: A structural bioinformatics approach

Permalink
https://escholarship.org/uc/item/7hh975dz

Author
Cohen, Michael Steven

Publication Date
2006

Peer reviewed|Thesis/dissertation

eScholarship.org Powered by the California Digital Library
University of California

Copyright 2006

by

Michael Steven Cohen

Dedicated to my family, especially my wife, Misha

For their encouragement, prayers, and love

ars ago Meriwether Lewis, William Clark and a select group of
iscovery) set out on an expedition across the uncharted territory
ase. The primary purpose of their journey was to discover the
Pacific (Northwest Passage) to use for commerce. Though they
onexistent transcontinental water route, their pioneering efforts
te with unanticipated adventures and exciting discoveries. My
F followed a similar trajectory-what initially seemed doomed to
much greater than I could have ever imagined. And like the
ose courage, skill, and teamwork was integral to a triumphant
been many people who have contributed, both directly and
ful completion of my doctoral degree. I relish in the opportunity
atitude to them.

hanking my thesis advisor, the inimitable Jack Taunton, whose
passion for science is unparalleled. Being one of Jack's first
e opportunity to work very closely with him in the lab. I entered
molecular biology experience and Jack spent a great deal of
echniques necessary to get my project off the ground. He
critically and independently about my thesis work, and taught
ortant biological problems. Jack, I will forever be indebted for
. Along with Jack, Kevan Shokat and Kip Guy, my two other
s, deserve special mention. They have been a major source
piration, and have contributed immensely to my development
y want to thank Kevan for his sage guidance and ceaseless
fruitful collaboration.

I am very grateful for the diverse, collaborative, and dynamic atmosphere of which is arguably, unmatched by any other institution. Many people have d my graduate experience, and I owe a special debt of gratitude to the following uals: Chao Zhang, a gifted and brilliant scientist that contributed much tually to my thesis work; Hans Luecke and Matt Simon for showing me how to ore effectively; and PJ Alaimo, now a Professor at Seattle University, for his wise l and encouraging words, especially during the more difficult times.

My fellow labmates, the Tauntonians, have profoundly fostered my intellectual sonal development. I want to specifically thank: Carl Co, who was there with me lab's inception, for teaching me how to pour a gel and the stimulating ations into the wee hours of the morning; Nathan Gushwa for simultaneously g sound advice and comic relief, being my gym buddy, and beautifying our lab impressive collection of orchids; Jennifer Garrision for pouring through countless f my writing and providing me with food and drink on more than one occasion; Vong for patiently listening to my ramblings about the meaning of life and related effrey Henise for endowing me with his impressive knowledge of chemistry and cle engines; Haralambos "Bellos" Hadjivassiliou for his unrelenting work ethic ned projects forward and his infectious fervor for life; and lastly, Sarah Arriola for the lab in order and always providing a helping hand. I will never forget our ether, both in and out of the lab. The bonds we share shall never be broken-dship and mentorship have truly left an indelible mark on my life!

am especially thankful for the many friendships that have developed during my CSF. The former "boy band" and fellow colleagues: Peter Madrid, Nathan ian Yeh, and Carl Co. You have always been genuine, consistent, and caring d I'm blessed to have you in my life. I will forever remember all the great trips ogether-especially our epic snowboarding adventures in Tahoe. Thanks for

ɔol that much more bearable! I also want to acknowledge Richard
seph Ho, and John Lee for their fellowship in brotherly love; your
ınsel have allowed me to see God's handiwork in the daily grind of

to acknowledge Valerie Ohman and Christine Olson for their
ɜss occasions and a willingness to always go the extra mile.
morning conversations, especially the ones about family. Chris,
surrogate mother in San Francisco-your nurturing spirit has
ɔly to my success.
fortunate to have an amazing family who has lovingly provided
ɔver the years. They deserve a huge piece of this degree. My
git Cohen, taught me that I must tenaciously pursue my dreams.
ɜd my passions in science and did everything possible to make
ı my goals. My brother, Ben, and my sister, Stephanie, have
the importance of family and made sure that I kept a balanced
my wife's family: Lawrence, Penny, Candice, Emily, and Molly.
ers, especially while writing this thesis, have impacted my life
ever describe. Thank you for love and genuinely caring about

st event that happened during graduate school, or my entire life,
ıy beautiful bride, Misha. She is truly a "wife of noble character"
s wisdom beyond her years. Misha, your unconditional love and
ıe to heights I never knew I could obtain. Your innumerable
g words and encouraging scriptures always provided me much
you for all your sacrifices and for patiently standing by my side
ıd prayer warrior. You are truly an undeserved blessing!

ke to express my deepest thanks to Jesus, without whom all of
le. Even in the most challenging times, He has been there,
'ing me strength to persevere beyond my perceived limitations.
'er!

ıg through Him who gives me strength." Philippians 4:13

is a reproduction of material previously published. Chapter 2
permission from: Cohen, M.S., Zhang, C., Shokat, K.M., and
informatics-Based Design of Selective, Irreversible Kinase
318 (2005), Copyright 2006 American Association for the
Chapter 3 is reproduced in part with permission from: Cohen,
and Taunton, J. A Clickable Inhibitor Reveals Context-
p90 RSK. *Nature Chemical Biology*, submitted.

ational design of selective, irreversible kinase inhibitors: a structural bioinformatics approach

Michael Steven Cohen

Jack Taunton, Ph.D.

Abstract

human genome encodes approximately 500 protein kinases, which are myriad cellular processes essential for homeostasis. Small molecule t potently and selectively block the activity of kinases are not only useful as cisely dissect the cellular role of their molecular targets, but also have alue.

kinase inhibitors target the ATP-binding pocket because it makes favorable vith small, hydrophobic molecules. Although some potent and selective tive inhibitors have been identified, the vast majority do not distinguish highly conserved ATP binding sites shared among all kinases. The few selective ATP-competitive inhibitors were primarily identified using high-creening, followed by demanding medicinal chemistry performed in al companies. We therefore sought an alternative strategy that would laborious process. This dissertation describes a structural bioinformatics e rational design of selective, irreversible kinase inhibitors. These efforts gn and synthesis of fmk (a fluoromethylketone-substituted pyrrolo[2,3-e first potent and selective irreversible inhibitor of the C-terminal kinase f the p90 ribosomal protein kinases 1 and 2 (RSK1 and RSK2).

nd the utility of fmk as a cellular probe of RSK CTD-dependent signaling, d fmk-pa, a propargylamine analog that is more potent thank fmk in lls, and can be coupled to a reporter tag via the bioorthogonal click sess covalent modification of RSK1 and RSK2 in cells. These improved mk-pa were exploited to demonstrate that activation of RSK1 and RSK2 pendently of the CTD. Fmk-pa was also used in two-step competitive s to screen Michael acceptor-substituted pyrrolo[2,3-*d*]pyrimidines against K CTD in mammalian cells. We found that compounds capable of forming ond with the targeted cysteine in the CTD were RSK1-selective. *vitro* experiments suggested that this isoform selectivity is achieved by ences in the rate of covalent bond formation.

s

uction

mary 2

:ture and function of protein kinases 4

-competitive kinase inhibitors 15

:lusion 32

'ences 34

ural bioinformatics-based design of selective, irreversible inhibitors

act 45

uction 46

ts and Discussion 48

usion 60

imental 62

ences 81

able inhibitor reveals context-dependent autoactivation of p90

ct 86

ction 87

and Discussion 88

sion 98

ental 99

ces 105

orm-selective p90 RSK inhibitors identified by a two-step

petition labeling approach

stract 110

oduction 111

ults and Discussion 113

clusion 119

erimental 120

erences 131

generation p90 RSK inhibitors

ract 134

duction 135

lts and Discussion 137

rimental 144

ences 155

sions and future directions

ences 162

d ^{13}C NMR spectra 164

List of Figures and Sc

Figure 1-1
Crystal structure of the cat

Scheme 1-1
Biochemical reaction catal

Figure 1-2
Chemical structure of FS

Figure 1-3
DDC selectively reacts w

Figure 1-4
PKA as a paradigm for c

Figure 1-5
ATP-competitive kinase

Figure 1-6
Connolly surface represe
atom type) bound to the

Figure 1-7
Development of a poten
hypothesis

Figure 1-8
ATP-competitive kinase
only in the autoinhibited

Figure 1-9
Connolly surface repre
atom type) bound to th

Figure 1-10
The rational design of
HER-1 and HER-2

Figure 1-11
Electrophilic EGFR/HE

Figure 1-12
Competition-based as

Figure 1-13
Affinity chromatograp
family cellular target

Figures and Schemes

-1
tructure of the catalytic domain of the tyrosine kinase, Src 3

1-1
cal reaction catalyzed by protein kinases 4

2
structure of FSBA 8

3
ctively reacts with acidic amino acids in proteins 10

4
paradigm for catalytic domain architecture 12

5
etitive kinase inhibitors that exploit the threonine gatekeeper pocket 17

6
urface representation of the crystal structure of PP1 (colored by
bound to the Src-family kinase, Hck 18

nt of a potent and selective Lck inhibitor based on the extension 21

titive kinase inhibitors that exploit an allosteric pocket present
utoinhibited state 22

rface representation of the crystal structure of Gleevec (colored by
ound to the catalytic domain of Abl 23

design of a selective, ATP-competitive, electrophilic inhibitor of
HER-2 26

EGFR/HER-2 inhibitors inspired by PD 18393 28

based assay developed by Ambit biosciences 30

atography of immobilized kinase inhibitors as an approach to
ar targets 32

tion mechanism 48

ioinformatics guides the design of electrophilic inhibitors of protein kinases 49

1
f pyrrolo[2,3-*d*]pyrimidine **2.3** 50

2
f cmk and bmk 51

fmk 51

dent inhibition of WT RSK2 CTD 53

fmk-biotin 53

eling of WT, but not mutant RSK2 by fmk-biotin 54

versible targeting of RSK1 and RSK2 by fmk-biotin 55

on EGF-activated RSK2 56

on WT and M498T MSK1 57

and fmk on WT and cysteine-engineered Src-family kinases 58

expressing V281C but not WT v-Src, revert to a flat morphology t with cmk 59

nk-biotin 59

eling of Val281Cys v-Src, but not WT v-Src by cmk-biotin 59

k-BODIPY 60

Figure 2-11
Cmk-BODIPY preferentially labels V281C v-Src 60

Scheme 3-1
Synthesis of fmk-BODIPY 88

Figure 3-1
Fmk-BODIPY irreversibly targets RSK, but displays only modest selectivity and potency in cells 89

Figure 3-2
Covalent modification of RSK by fmk-pa is unaffected by serum in the incubation medium, whereas covalent modification by fmk-BODIPY is significantly decreased 90

Scheme 3-2
Synthesis of fmk-pa 91

Figure 3-3
Irreversible, selective, and potent inhibition of RSK by fmk-pa 91

Figure 3-4
Fmk-pa reveals a RSK CTD-dependent pathway for rpS6 phosphorylation 93

Figure 3-5
Parallel pathways leading to rpS6 phosphorylation 94

Figure 3-6
Fmk-pa and click chemistry reveal the existence of a CTD-independent pathway for RSK Ser386 phosphorylation 96

Figure 3-7
Alternative RSK Ser386 phosphorylation by a putative hydrophobic motif (HM) kinase, which bypasses the CTD 97

Figure 3-8
Neither rapamycin (mTOR/raptor inhibitor) nor SB 203580 (p38 MAPK inhibitor) block LPS-stimulated Ser386 phosphorylation 98

Figure 4-1
Chemical structures of pyrrolo[2,3-*d*]pyrimidines substituted with an electrophile at the C-6 position 112

Figure 4-2
Two distinct RSK bands are targeted by fmk-pa in intact cells 112

Scheme 4-1
Synthesis of Michael acceptor-substituted pyrrolo[2,3-*d*]pyrimidines I 113

Scheme 4-2
Synthesis of Michael acce

Figure 4-3
Two-step competition labe
inhibitors in cells

Figure 4-4
Time-dependent, covalen

Figure 4-5
Sequence alignment of t
human RSK1 and RSK2

Scheme 5-1
Synthesis of enone-BOD

Figure 5-1
Fmk-BODIPY is more k

Scheme 5-2
Synthesis of secondary

Scheme 5-3
Synthesis of fmk-cp

Scheme 5-4
Synthesis of fmk-pip

Figure 5-2
Effects of N-7 fmk deri
phosphorylation

Figure 5-3
Secondary amine fmk

Figure 5-4
Fmk-mpe is not an eff

Figure 5-5
Exploring the size thr
a competition labeling

Figure 6-1
Designer oxindole-b

acceptor-substituted pyrrolo[2,3-*d*]pyrimidines II 114

labeling as a method to screen RSK1 and RSK2 CTD 115

lent modification of the CTD of RSK1 and RSK2 118

f the Gly-rich loop located in the CTD active site of
K2 119

DIPY 136

kinetically selectivity than enone-BODIPY in intact cells 136

amine derivatives of fmk 137

138

138

atives on PMA-stimulated RSK Ser386 139

ariants exhibit remarkable cellular potency 140

tive clickable probe of the CTD of RSK1 and RSK2 141

ine gatekeeper pocket of RSK2 CTD using
say 143

l electrophilic inhibitor 161

List of Tables

Table 2-1 52
IC_{50} values (in μM) for fmk and the pyrrolo[2,3-*d*]pyrimidine scaffold against the kinase activities of wild-type (WT) and mutant RSK2 CTDs

Table 3-1 95
Variable inhibition of Ser386 RSK phosphorylation by fmk and fmk-pa

Table 4-1 116
IC_{50} values of pyrrolo[2,3-*d*]pyrimidines derivatives against RSK1 and RSK2 in cells

Chapter 1

Introduction

ranslational, covalent modification of amino acids provides exquisite ein function. Reversible protein phosphorylation is a major regulatory mechanism in eukaryotic cells and contributes to complex avior, such as learning and memory, in metazoans[1]. Its discovery igo from studies of glycogen metabolism has fueled an explosion of ating the role of protein phosphorylation in cellular physiology[2]. The lyze phosphorylation and dephosphorylation events in cells are known s and phosphatases, respectively. It is well established that these the circuitry of cellular signal transduction pathways that integrate and llular cues. In this way, reversible phosphorylation plays an essential ular processes, such as proliferation, differentiation, and migration. tral importance in these molecular pathways, the aberrant regulation rylation plays a casual role in many human diseases. For example, n of protein kinases by mutations or other genetic legions has been ral cancers, inflammatory diseases, and neuronal disorders. Not kinases have become a significant class of therapeutic targets in the stry[3].

91 protein kinase domains encoded by the human genome and they onserved catalytic domain of approximately 250 amino acids[1]. The composed of two lobes; the abundant cellular substrate, ATP, binds ft formed between these lobes (**Figure 1-1**). The majority of kinase highly homologous ATP-binding site, and must compete with high rations of ATP[4]. Consequently, identifying small molecules that ntly target only one, or even a fraction, of cellular kinases is a

Figure 1-1. Crystal structu
atom type) is bound in a hy

Nevertheless, several
been identified that i
that these inhibitors
throughput screenin
companies. Structura
orientation of some
binding site that are
used to generate ph
inhibitors to improv
inhibitors for kinases

In the ensui
function of kinases
small molecules. p

-1. Crystal structure of the catalytic domain of the tyrosine kinase, Src (1FMK)[5]. ATP (colored by e) is bound in a hydrophobic cleft between the small N-terminal and large C-terminal lobes.

ıeless, several structurally distinct classes of active site-directed inhibitors have entified that indeed exhibit remarkable selectivity[6-11]. It is noteworthy, however, ese inhibitors were not rationally designed, but rather discovered by high-put screening and intense medicinal chemistry efforts within pharmaceutical ies. Structural and mutagenesis studies have demonstrated the precise binding on of some of these inhibitors, revealing subtle differences in or near the ATP-site that are exploited by these inhibitors. Such efforts can be (and have been) generate pharmacophore models that guide not only the modification of known s to improve their potency and selectivity, but also the rational design of for kinases which do not have structural information available[8,12].

the ensuing paragraphs of this introduction, I will expand on the structure and of kinases, and describe strategies used to inhibit the activity of kinases with ecules. Particular attention will be given to ATP-competitive inhibitors and how

et of them achieve their selectivity, as this provides a foundation for my thesis

ıre and function of protein kinases

The specific chemical reaction catalyzed by kinases is the transfer of the γ-ate group of ATP to tyrosine, serine, and threonine amino acids of their protein es (**Scheme 1-1**).

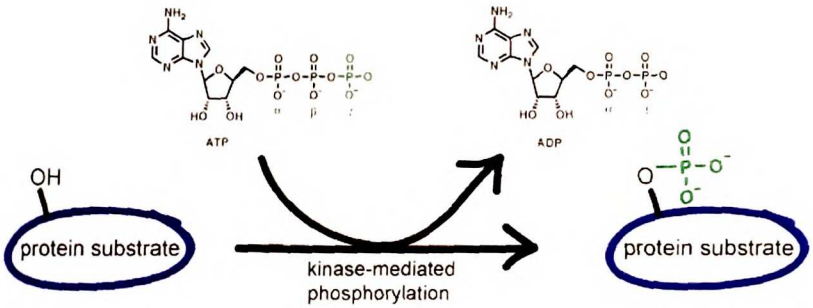

1. Biochemical reaction catalyzed by protein kinases.

ılent conjugation of the γ-phosphate group to these amino acids can have effects on protein function, including changes in protein activity, stability, ar localization, and interactions with other proteins via phosphorylation-t binding motifs[13]. The human kinase superfamily can be segregated into two ses: the serine/threonine kinases (~65%) and the tyrosine kinases (~25%)[1]. A l class, known as dual-specific kinases that phosphorylate both tyrosine and no acids of proteins, are less well understood.

e of the first kinases to be purified was cyclic AMP-dependent protein kinase 'n as PKA). PKA was isolated from rabbit skeletal muscle by Edwin G. Krebs kers in 1968[14]. This serine/threonine kinase exists as a tetramer consisting of ytic domains and two regulatory domains; the binding of the second r, cyclic AMP, to the regulatory domain acts as an allosteric switch that

releases, and thereby a

cyclic-AMP can regulate

kinases in cellular sign

activated by extracellul

particular case, the reg

decades, detailed che

general paradigm for u

attempt to summarize

on the chemical-based

describing these studi

techniques were integ

crystallography, and

myself included).

Chemical-based lab

Chemical-bas

reactive group (elec

acid side chains. C

activity, particularly

directed covalent in

This equat

complex, [EI], foll

inhibitor complex,

and thereby activates the catalytic domains[15]. The significant discovery that ? can regulate the kinase activity of PKA supported, for the first time, a role for cellular signaling cascades (i.e. multiple kinases in intracellular pathways y extracellular inputs) that mediate important physiological processes (in this ase, the regulation of glycogenolysis by adrenaline)[2]. During the next several letailed chemical, mutagenesis, and structural studies on PKA provided a adigm for understanding the structure and function of protein kinases[16]. I will summarize some of the salient results of these studies, focusing particularly nical-based labeling strategies used to identify active site amino acids. Briefly hese studies serves an important pedagogical purpose since these powerful were integral for correlating structure with function in the absence of protein phy, and have long been forgotten by this new generation of scientists ded).

ased labeling strategies: some basics to consider

nical-based labeling strategies often exploit small molecules that contain an p (electrophile) capable of forming a covalent bond with nucleophilic amino ins. Covalent modification of an enzyme can lead to an irreversible loss of cularly if the electrophilic small molecule targets the active site. Active site- lent inhibitors can be described by the following equation (**1.1**)[17]:

$$[E] + [I] \underset{}{\overset{K_i}{\rightleftharpoons}} [EI] \xrightarrow{k_2} [E\text{-}I] \qquad (\mathbf{1.1})$$

quation describes the rapid, reversible formation of an enzyme-inhibitor followed by a slower, irreversible reaction to yield the covalent enzyme- lex, [E-I]. K_i (M) is the reversible dissociation constant and k_2 (s^{-1}) is the

ovalent bond formation. k_2 can be influenced by several factors, including the ation of [EI], the nucleophilicity of the residue being covalently modified, and the of the electrophile. The total enzyme concentration, $[E_T]$, is equal to the sum of e enzyme states described in equation (**1.1**) ($[E_T] = [E] + [EI] + [E\text{-}I]$), according nciples of mass balance. A first-order differential equation (**1.2**) that describes **1.1**) is as follows:

$$\frac{d[E\text{-}I]}{dt} = k_{obs}([E_T]-[E\text{-}I]) \qquad (\mathbf{1.2})$$

$$k_{obs} = \frac{k_2[I]}{K_i + [I]} \qquad (\mathbf{1.3})$$

ved rate, k_{obs}, can be obtained by determining the enzyme activity as a time in the presence of increasing inhibitor concentrations. Plotting the of the enzyme activity versus time (Kitz-Wilson plot) yields a straight line in slope is equal to k_{obs}. If the reciprocal of k_{obs} versus the reciprocal of [I] is th k_2 and K_i can be obtained according to equation (**1.3**). These kinetic nd equilibrium and rate constants are important to consider as I elaborate on directed, electrophilic reagents since these variables describe their mode of

rporation of a chemical tag into an electrophilic reagent can be used to e proteins, or peptides derived from proteolysis, that contain the modified s) and thereby aid in their isolation and identification. Classically, this was introducing a radioactive tag (such as ^{14}C) into the reagent. An advantage egy is that introduction the radioactive element does not change the nd therefore inhibitory, properties of the molecule. Several disadvantages

the radioactive handle can be synthetically challenging, costly, and ne case of ^{125}I, which is volatile). Another common strategy is to tag, such as biotin or a fluorescent molecule, which is useful not ion of the covalently targeted proteins, but also in their isolation. of these types of affinity tags can significantly disrupt interactions hilic reagent and its protein target. To circumvent this problem, ave recently developed bioorthogonal coupling strategies in which affinity tag is introduced after covalent modification of the target two strategies will be relevant to my thesis work on irreversible ribed in Chapters 2 and 3. For now, we focus on electrophilic radioactive tags used to define the conserved, catalytically within the ATP-binding pocket of PKA.

no acids within the ATP-binding site of PKA, especially those s, Susan S. Taylor and coworkers used a chemical-based advantage of an ATP analogue, *p*-fluorosulphonylbenzoyl 5'- hich was developed as an affinity reagent for ATP-binding . FSBA contains an electrophilic fluorosulphonyl (shown in blue) modifying nucleophilic amino acids (e.g. lysine, cysteine and

ubunit of PKA (cPKA)

FSBA (0.9 mM), the

inhibited in a time-

, consistent with an

of inactivation. This

nted by preincubation

ggesting that FSBA

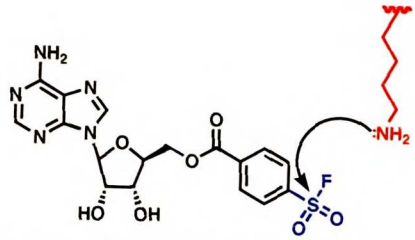

Figure 1-2. Chemical structure of FSBA. The conserved catalytic lysine in kinases (red) reacts covalently with the fluorosulphonyl electrophile (blue).

site as ATP. FSBA exhibited pseudo first-order inhibition and of cPKA, suggesting that it forms a reversible enzyme-inhibitor ovalent inactivation, in accordance with equation (**1.1**). The (K_i) and the rate of covalent inhibition (k_2) were also determined (K_i = 57 μM and k_2 = 3.64 x 10^{-2} min^{-1}). Using a radioactive which ^{14}C was incorporated into the carbonyl carbon of the benzoyl hey showed that a single lysine in cPKA was covalently modified. lucidation of the amino acid sequence of bovine cPKA (the first sequence to be determined[25]), researchers were able to strate that Lys72 (bovine numbering) was the site of covalent SBA[26]. Using a similar method, the Krebs laboratory showed that catalytic subunit cyclic GMP-dependent protein kinase (PKG) was hich corresponded to Lys72 of PKA[27]. These results suggested l lysines are in the same position in the ATP binding pocket of the teracting with the phosphate backbone of ATP.

ears of the aforementioned studies, a landmark paper was 1984, in which FSBA was used to demonstrate that protein ingle family, despite having different amino acid substrate ly, the researchers found that the tyrosine kinase $p60^{src}$ (v-Src),

the transforming protei

reacted with FSBA in a

site of modification by

PKG. Sequence align

PKG, and p60^{src} reveal

as two glycines, now

The sequence simil

suggested to the a

structurally and funct

FSBA contin

active site amino a

demonstrate t

isoquinolinesulfona

Preincubation with

dependent manner

experiment using

the kinase active

FSBA-modified pr

kinases (and othe

competition lab

simultaneously[30,3

Diego, CA, has

later application

structurally relat

reacted with a

reactions[32].

nsforming protein of Rous sarcoma virus (discovered just four years prior), also d with FSBA in an ATP competitive manner. They subsequently showed that the modification by FSBA was Lys295, homologous to Lys72 of PKA and the lysine in Sequence alignments of the amino acids within the ATP binding region of PKA, nd p60^{src} revealed the absolute conservation of the FSBA-reactive lysine as well glycines, now know to be part of the glycine-rich loop important for ATP binding. equence similarities and shared sensitivity to FSBA among these kinases ted to the authors that protein kinases share a common ancestor and are ally and functionally homologous.

FSBA continued to be a useful chemical tool with applications beyond identifying ite amino acids in ATP utilizing enzymes. For example, FSBA was used to strate that the kinase inhibitor, *N* -[2-(methylamino)ethyl]-5-linesulfonamide (H-8), specifically targeted the ATP binding site of PKA[29]. ation with H-8 prevented the labeling of PKA by FSBA in a concentration-nt manner. This is the first example, to my knowledge, of a competition labeling ent using an electrophilic reagent to demonstrate the binding of an inhibitor to se active site. The development of an antibody that specifically recognizes odified proteins not only provided an alternative to using [^{14}C]-FSBA to identify and other ATP utilizing enzymes) from cell lysates, but also a strategy to use ion labeling to profile inhibitor specificity against several kinases ously[30,31]. More recently, ActivX, a biotechnology company based in San A, has designed FSBA derivatives containing fluorescent affinity tags for the lication (http://www.activx.com). FSBA has also inspired the design of a y related electrophilic reagent, in which the *p*-fluorosulphonylbenzoyl was with an *o*-phthaldialdehyde, to facilitate the identification of substrate-kinase s[32].

Another electrophilic reagent that identified invariant amino acids in the ATP-ng site was dicylcohexylcarbodiimide (DCC), which reacts chemoselectively with amino acids (Asp and Glu) in proteins to form an *O*-acylurea adduct (**Figure 1-**

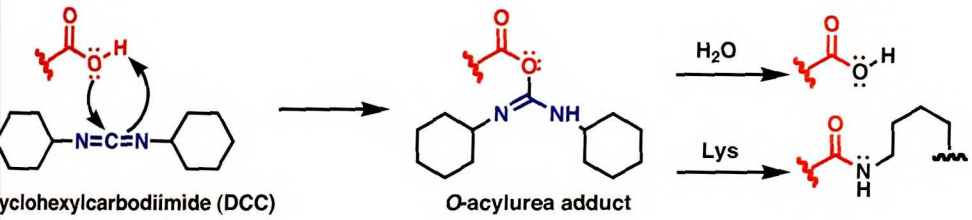

1-3. DCC selectively reacts with acidic amino acids in proteins. Acidic amino acids (red) in the ATP pocket react with the carbodiimide electrophile to form an *O*-acylurea adduct, which can react further her water to regenerate the acidic amino acid or a proximal lysine amino acid to generate a peptide n both cases, dicyclohexyurea (DCU) is liberated from the protein.

l on the proposed mechanism of phosphoryl transfer, the Taylor laboratory ned that acidic amino acids may be important for chelating the divalent metal, required for catalysis. It was hypothesized that DCC, because of the hydrophobic exyl groups, would selectively partition into the hydrophobic ATP-binding pocket of nd react with proximal acidic amino acids[34]. Indeed, DCC inhibited the kinase in an ATP competitive manner and exhibited pseudo first-order inhibition and on kinetics, similar to FSBA (K_i = 60 μM and k_2 = 1.8 x 10^{-2} min^{-1}). Initial attempts ify the modified amino acids using [^{14}C]DCC were unsuccessful due to the loss of olabel from the protein, most likely due to reaction of the *O*-acylurea adduct with lysines (**Figure 1-3**). Cleverly, the researchers pretreated PKA with acetic de to mask the reactive lysines and block intramolecular cross-linking. nt with DCC followed by [^{14}C]glycine ethyl ester to trap the *O*-acylurea adduct duce a radioactive tag via peptide bond formation, allowed for the unequivocal

ıation as Asp184 as the major site of DCC modification[35]. Glu91 was also l as a minor product. Interestingly, in later work they demonstrated that DCC s an intramolecular cross-link between Asp184 and Lys72, providing strong that these residues are close proximity in the ATP binding pocket[36].

everal other electrophilic reagents were used to "chemically" map the ATP- and -binding site of PKA and thereby provide insight into structure and function e crystal structure was solved[37,38]. For the sake of brevity, I will exclude these and move on to structural and mutagenesis studies of PKA that beautifully ted the chemical-based strategies, and provided a more complete picture of tic mechanism of kinases.

l and mutagenesis studies

1991, the Taylor and Sowadski laboratories solved the first protein kinase y X-ray crystallography[39]. The structure is a ternary complex of the catalytic PKA bound to ATP and a high affinity inhibitor peptide derived from the heat- ein kinase inhibitor (PKI). Since many of the features of the catalytic domain among kinases, a brief description of this structure, as well as more recent will serve as a paradigm for the entire kinase family.

catalytic domain of PKA consists of two lobes: an N-terminal lobe composed parallel β-sheets and a conserved α-helix (called helix C) and a larger, C- e dominated by α-helices (**Figure 1-4a**). ATP binds in a deep cleft at the f the two lobes where catalysis occurs. The adenine ring of ATP forms van der Waals interactions with hydrophobic amino acids in a pocket within nal lobe. The N6 and N7 position of the adenine ring form hydrogen bonds to backbone in the hinge region, which is important for anchoring ATP in the ormation for catalysis (**Figure 1-4b**). It is interesting to note that all ATP

ompetitive kinase inhibitors exploit at least one of these hydrogen bonds and disruption f these interactions leads to a significant decrease in binding affinity[40].

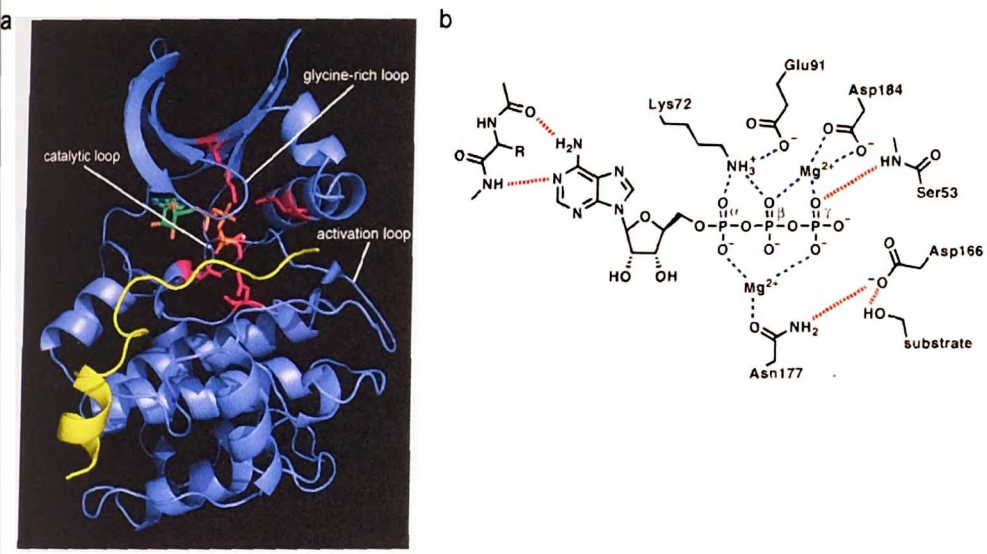

ure 1-4. PKA as a paradigm for catalytic domain architecture (a) Ribbon diagram of the X-ray structure[39] he catalytic domain of PKA bound to ATP (colored by atom type) and the peptide inhibitor, PKI(aa5-24) lored yellow). The absolutely conserved amino acids are colored magenta. The metal ions are shown as te circles. (b) The kinase active site[13,16]. Interactions between ATP and the invariant active site amino ls are shown (hydrogen bonding in red, and ionic interactions in blue).

The triphosphate moiety of ATP is stabilized and oriented for phosphoryl transfer amino acids emanating from the N-terminal lobe and several conserved loops, uding the glycine-rich, catalytic, and activation loops (**Figure 1-4a,b**). In the N- ninal lobe, Lys72 in the middle of β-strand three forms an ion pair with Glu91 of the x C and directly contacts the α and β phosphates, which is thought to stabilize ATP ng catalysis. Consistent with this notion, mutation of Lys72 to alanine in *charomyces cervisiae* PKA resulted in 5700-fold decrease in the second order rate stant, k_{cat}/K_M (ATP)[41]. Further, mutation of the lysine (corresponding to Lys72 of) to alternate amino acids (e.g. methionine, arginine, alanine) in several tyrosine ses resulted in complete loss of catalytic activity and biological function in cells[42,43].

For exa

transfor

G-K-q-

strand

The p

PKA

confo

nydro

nydro

cata

ndu

hy

ch

pe

w

p

s

e, unlike wild type v-Src, the K295M mutant failed to induce cellular
on in infected cells[42].

glycine-rich loop[44], which contains a highly conserved sequence motif (G-X-
here ϕ is usually either a tyrosine or phenylalanine), is located between β-
and two in the N-terminal lobe and forms the roof of the active site cleft.
of this loop is very dynamic as determined by multiple crystal structures of
apo-, adenosine bound-, and ATP bound-states[45]. In the active
, the glycine-rich loop clamps down on ATP and provides a critical
d via the backbone amide of Ser53 to the γ-phosphate[46]. Removal of this
nd by mutation of Ser53 to proline resulted in a significant decrease in
ity. As the glycine-rich loop is highly mobile, it thought to facilitate the
ding of inhibitors that target the active site[45].

talytic loop forms the floor of the active site and is anchored in position by
contacts to the C-terminal lobe. This loop contains Asp166, which is in
y to the peptide substrate hydroxyl group and presumably acts as a
and Asn171, which not only orients Asp166 toward the incoming substrate
bond, but also binds a Mg^{2+} ion that directly interacts with the α and γ
nd is required for catalysis. Replacement of Asp166 to alanine in
s cervisiae PKA lead to a mutant enzyme that exhibited a 350-fold
without affecting the K_M for ATP or a peptide substrate, consistent with
alytic base[41].

vation loop begins (moving from the N to C terminus) at the base of the
the highly conserved DFG motif, and wraps down into the C-terminal lobe
es a docking site for the peptide substrate. Asp184, which is part of the
ds a Mg^{2+} ion (different from Asn171) that interacts with the β and γ

phosphor
complex
catalys
phosph
is invo
for cat
some
contro
termi
conti

also
how
phy
an
in
th
c
s

on of Asp184 to alanine in *Saccharomyces cervisiae* PKA resulted in ıctivity, providing strong evidence that this Mg^{2+} is essential for orientation of Asp184 is predominately controlled by the te of Thr197 in the middle of activation loop; when phosphorylated, it work of hydrogen bonds and ionic interactions that position Asp184 ıtion loop phosphorylation is a requirement for full catalytic activity of kinases[47]. Phe185 of the DFG motif also contributes to the 184 by making important hydrophobic contacts with helix C in the N- s interaction is thought to lock helix C into a catalytically active ıat Glu91 is properly oriented to form a critical ion pair with Lys72.

ce making up the peptide-binding site is diverse among kinases, osphorylation of specific substrates through distinct interactions; n of this region is in general structurally consistent. The consensus tif for PKA is R-R-X-S/T-ϕ (where ϕ is a hydrophobic amino acid), ids in the C-terminus of the activation loop contribute to the specific ein substrates that contain this motif. Consensus phosphorylation etermined for many other kinases using peptide libraries and these uggest their cellular substrates[13]; however, they are not always the specificity required in cells since many kinases share similar ylation motifs. Therefore, many kinase substrates have evolved guide the specific interaction with kinases in cells[48].

ons of kinases in the autoinhibited state

imately 50 kinase structures have been solved, both in the active tes[47]. These structures have provided insight into the complex ctivity. In the active state, the overall architecture of the catalytic

ighly similar across the entire kinase family. By contrast, the autoinhibited kinases display much more structural heterogeneity, revealing the nal plasticity of kinases[49]. In particular, the conformation of the activation is diverse in sequence, varies widely among kinases in their autoinhibited as their active states. The ability of kinases to interconvert between the active bited states is mediated by various mechanisms, including phosphorylation sites (e.g. within the activation loop) as well as interactions with modular g SH2 and SH3 domains in Src-family of tyrosine kinases[50]) that extend catalytic core. The activation loop and helix C undergo the largest structural en toggling between the two states and these movements can be coupled. g is mediated by direct interactions of the DFG motif at the N-terminus of the op with ionic and hydrophobic interactions in helix C[47]. In some cases, the of the activation loop is not coupled to changes in the orientation of helix C. t all kinases are equivalent in their ability to adopt discrete conformations of n loop and helix C in the autoinhibited state, and this contributes to the eir regulation as well as their ability to be selectively targeted by inhibitors.

titive kinase inhibitors

s of protein kinases are useful as tools for elucidating kinase function in works and as drugs for human diseases. Most kinase inhibitors bind the ATP-binding site (i.e. ATP-competitive), which provides a deep pocket that can accommodate small molecules of various shapes and entioned previously, this region of the catalytic domain is highly conserved s in their active states, making the identification inhibitors that discriminate closely related conformers a challenge. Moreover, the potency of these n reported as an IC_{50} (50% inhibitory concentration), critically depends not

only on the their intrin

$K_{M,ATP}$. The relationsh

In the absence of AT

the concentration of

30 μM and [ATP] (

needed to inhibit 50

Despite these imp

that target the act

inhibitors that targe

in their autoinhibite

inhibitors of both

revealed the mo

addressed below

Finally, methods

be described. T

correlate kinase i

Selective ATP-C

A point t

state of kinase

primarily contai

kinases. Rece

trinsic binding affinity, K_i, but also on the concentration of ATP and the nship between these variables is given by equation (**1.4**)[51]:

$$IC_{50} = K_i\left(1 + \frac{[ATP]}{K_{M,\,ATP}}\right) \qquad (\mathbf{1.4})$$

ATP, the $IC_{50} = K_i$; however, this situation does not exist in cells where f ATP is in the low-millimolar range. Assuming an average $K_{M,\,ATP}$ of of 5 mM in cells, the concentration of an ATP-competitive inhibitor)% of the kinase activity in cells must be 100-fold greater than the K_i! ediments, there are several examples of ATP-competitive inhibitors ve state with remarkable selectivity and potency. Another class of : an allosteric binding pocket found in a subset of kinases specifically l state has been described[12]. Structural and mutagenesis studies on asses bound to the active and autoinhibited states of kinases have cular basis for their potency and selectivity, which will be briefly Inhibitors that target kinases irreversibly will also be discussed. ed to assess kinase inhibitor selectivity both *in vitro* and in cells will e latter strategies provide valuable information that can be used to itor target selectivity with cellular function.

petitive kinase inhibitors that target the active state

annot be emphasized enough is that inhibitors that target the active often non-selective. This is because many of these inhibitors same amino acids in the ATP-binding pocket that are found in all sing a pharmacophore model based on the analysis of multiple

ystal structures of

ighly conserved 'fea

ypes of inhibitors[52].

he natural product

inase inhibitors kn

ability of kinase inh

ocket[12]. Subtle d

rofound effects on

One region

hydrophobic pocke

inhibitors exhibit a

hey all contain arc

crystal structures of kinases bound to promiscuous inhibitors, researchers identified five highly conserved features of the active site that invariably form interactions with these types of inhibitors[52]. An example of a small molecule that conforms to this analysis is the natural product, staurosporine, which is one of the most potent and broadly active kinase inhibitors known. Selectivity among different kinases is often achieved by the ability of kinase inhibitors to exploit regions of the active site outside of the ATP-binding pocket[12]. Subtle differences in these regions, or the ability to access them, can have profound effects on selectivity.

One region that is widely exploited by several different classes of inhibitors is a hydrophobic pocket adjacent to the ATP binding site[53-56] (**Figure 1-5**). Although these inhibitors exhibit a broad range of potencies and selectivies against different kinases, they all contain aromatic substituents that occupy this lipophilic cavity.

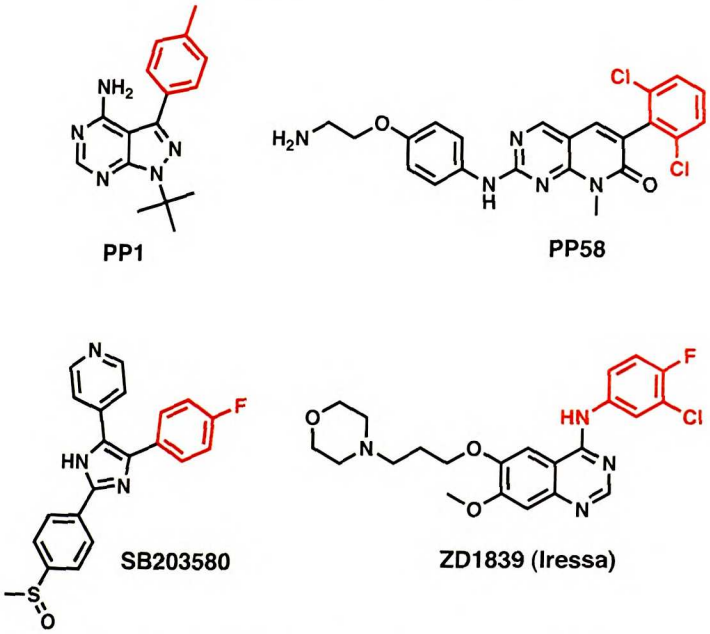

Figure 1-5. ATP-competitive kinase inhibitors that exploit the threonine gatekeeper pocket. The aromatic portion of the molecule that occupies the hydrophobic cavity pocket is colored red. PP1[12] and PP58[57] were originally described as Src-family selective inhibitors, but are now known to target several other threonine gatekeeper-containing kinases. ZD1839 (Iressa) is a clinically approved drug for the treatment of lung adenocarcinoma and non-small-cell lung carcinoma (NSCLC)[58]. It targets EGFR and is one of the most potent and selective kinase inhibitors known. SB203580 is a very potent and selective inhibitor of the tyrosine/threonine kinases, p38α and p38β mitogen-activated protein kinases (MAPK)[59,60].

ss to this pocket is predominately controlled by a single amino acid that is referred the "gatekeeper."[54] A threonine gatekeeper or smaller amino acid allows access to ocket whereas larger substituents, such as methionine, sterically occlude the cavity ice. This is clearly illustrated in the crystal structure of the Src-family selective or, PP1[61] (which is based on a pyrazolo[3,4-*d*]pyrimidine scaffold), bound to the mily kinase, hematopoietic cell kinase (Hck) in the autoinhibited form (full length ning that SH2 and SH3 domains, and not phosphorylated in the activation loop) **e 1-6**)[62]. It should be noted that PP1 does not discriminate between the active toinhibited states. PP1 makes two hydrogen bonds to the backbone hinge region s orients it in a similar position to the adenine ring of ATP. The *p*-tolyl substituent ing from the C-5 position of PP1 occupies the lipophilic cavity defined by Thr338 n Hck numbering), which is positioned at the top-entrance of the pocket. Placed ottom-entrance of the pocket is Ala403, which immediately precedes Asp404 of served DFG motif, and it is also important, although to a much lesser extent, for ng access to the cavity.

proximately 50% of tyrosine kinases and 10% of serine/threonine kinases reonine gatekeeper, suggesting that they would be sensitive to inhibition by ecules that can present aromatic groups to the hydrophobic cavity[3]. Indeed, PP1 was originally identified as a Src-family selective inhibitor, it also targets r threonine gatekeeper-containing tyrosine kinases, and even distantly related eonine kinases that have less than 20% sequence identity with tyrosine the catalytic domain[54]. However, PP1 seems to be the most selective toward at also contain an alanine in the DFG –1 position (all Src-family kinases have at this position). For example, PP1 has a 50-fold greater selectivity for the kinase, lymphocyte-specific kinase (Lck), than for the receptor tyrosine idermal growth factor receptor (EGFR), which has threonine in the DFG –1 $_{50}$ of 5 nM versus 250 nM, respectively)[61]. Nonetheless, mutagenesis studies uivocally demonstrated that the threonine gatekeeper is the main selectivity ng access to the hydrophobic pocket for PP1 as well as the other inhibitors **igure 1-5**; mutation of the threonine gatekeeper to methionine or isoleucine in targets of these inhibitors renders them resistant to inhibition[53,54]. By nases normally resistant to PP1 could be made sensitive by introduction of a or smaller, gatekeeper. The identification of the threonine gatekeeper as a vity determinant for PP1 guided the development of a chemical genetic hat could be used to generate novel orthogonal kinase/inhibitor pairs[63,64]. d involves mutating the gatekeeper position to either an alanine or a glycine enlarged lipophilic pocket that uniquely accepts a PP1 derivative containing or similarly large) group, which is too large to fit in the hydrophobic pocket of e kinases normally targeted by PP1. This chemical genetic strategy has led ancements in our understanding of the role kinases play in cellular signaling

ATP-co

the hy

Compa

non-hy

adive

Furth

amo

FP1

sele

cata

pre

hy

ho

si

TP-competitive kinase inhibitors that selectivity target the autoinhibited state

The crystal structure of PP1 bound to Hck in the autoinhibited state revealed that e hydrophobic cavity occupied by the *p*-tolyl group of PP1 is largely unoccupied. omparing this structure to the crystal structure of active Lck[66] bound to AMP-PNP (a on-hydrolyzable ATP analog) shows that the hydrophobic pocket is much smaller in the tive conformation, which seems to be generally true for the Src-family kinases[62]. urther, the size and shape of the hydrophobic pocket in the autoinhibited form varies mong the Src-family kinases[49]. Based on these observations, it was hypothesized that P1 analogs that have extended aromatic groups at C-5 would be able to bind lectively to the autoinhibited state, thus preventing the kinase from attaining a talytically relevant conformation[62]. Furthermore, inhibitors of this type might exhibit eater isoform selectivity among Src-family kinases because of differences in the ophilic pocket. Isoform selective inhibitors would not only be useful to unravel their lividual roles in cellular signaling, but also as potential therapeutics that exhibit lower e-effects due to broad-spectrum activity against all Src-family kinases.

The first class of Src-family-directed kinase inhibitors that appeared to selectively get the autoinhibited versus active conformation were targeted against Lck, which is a rapeutic target for autoimmune and inflammatory diseases due to its crucial role in T- signaling. Guided by PP1, an inhibitor based on a pyrrolo[2,3-*d*]pyrimidine scaffold t has a *p*-phenoxyphenyl group at C-5 (PP-OPh) was designed to occupy the arged hydrophobic pocket found in the autoinhibited conformation (**Figure 1-7**)[67]. OPh was first tested against two Lck constructs: down-regulated Lck (Lck64-509, inhibited) and the catalytic domain of Lck (Lckcd, active). The down-regulated form ck contains the SH2 and SH3 domains that maintain it in the autoinhibited state; ever, it does have a low level catalytic activity that can be measured via an *in vitro* se assay. PP-OPh was remarkably potent against Lck64-509 (IC_{50} = 16 nM), with

-50-fold selectivity

values for PP1 deta

were 0.15 nM and

than Lok64-509, a

these studies show

lead not only to in

and autoinhibited

modeling, and cry

which exhibits rem

vitro and in anim

survival in rats i

structural basis

crystallographic a

Figure 1-7. Dev
aromatic substit
selectively target
is larger in the
short elongation

over Lckcd in the presence of 1 mM ATP (IC_{50} = 1000 nM). The IC_{50} ermined in the presence of 5 μM ATP against Lckcd and Lck64-509 0.25 nM, respectively. PP-OPh inhibited Src 70-fold more weakly though the activation state of Src was not known. Nevertheless, ed that increasing the occupancy of the hydrophobic pocket could eased potency, but also to increased selectivity between the active ates. Several years of intense structure-activity relationship (SAR), allographic studies eventually led to the identification of A-770041, rkable isoform selectivity for Lck versus other Src-family kinases *in* s[68]. Further, A-770041 at 10 mg/kg/day significantly increased a model of organ transplant rejection. An understanding of the r its selectivity over other Src-family kinases awaits further ysis.

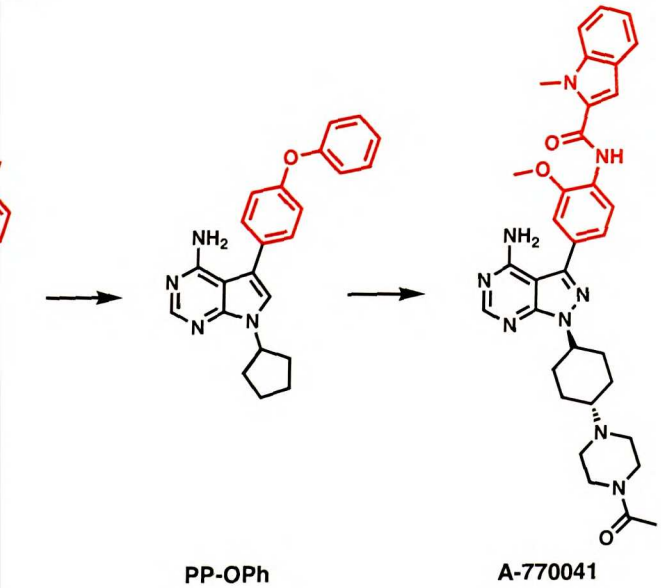

of a potent and selective Lck inhibitor based on the extension hypothesis. The t occupy the hydrophobic pocket are colored red. PP-OPh was designed to nhibited versus active form of Lck based on the idea that the hydrophobic pocket ed conformation[67]. A-770041 is a highly advanced Lck inhibitor developed by rally active and efficacious in animals[68].

ural basis for the selectivity of another class of ATP-competitive kinase
1-8) that target the autoinhibited state was initially realized by the
of STI571 (Gleevec) bound to the catalytic domain of the Abelson
Abl) in the autoinhibited (not phosphorylated in the activation loop)
Gleevec selectively targets three kinases: Abl, the platelet-derived
ptor-α (PDGFR-α), and stem-cell factor receptor kinase (KIT).

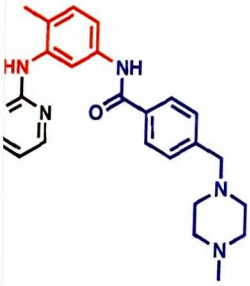

TI571 (Gleevec)

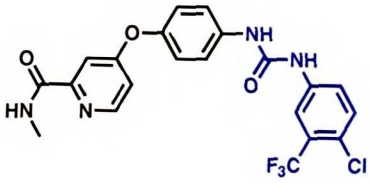

Bay43-9006 (Nexavar)

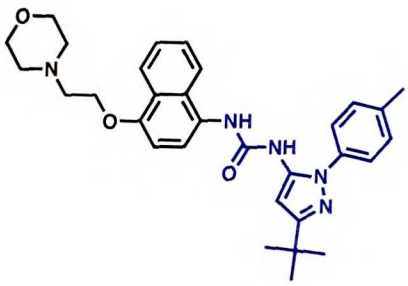

BIRB796

petitive kinase inhibitors that exploit an allosteric pocket present only in the
substituents that target the allosteric site are colored blue. The aromatic substituents
nobic pocket are colored red. STI571 (Gleevec) is the first small molecule kinase
pproval for the treatment of several cancers, including chronic myeloid leukemia
ly, gastrointestinal stromal tumors (GIST)[71]. The causative agent of CML targeted
a disregulated Abl kinase fusion protein. PDGFR-α and KIT are implicated in the
Gleevec occupies the lipophilic cavity defined by the threonine gatekeeper as well as
ated by the "DFG out" configuration[70]. Bay43-9006 (Nexavar) is also a clinically
and is one of the most promiscuous inhibitors of this type[72]. BIRB796 is a very
MAPK that binds with picomolar affinity[73]. Interestingly, both BIRB796 and Nexavar
yl ureas precursors identified as hits in initial high-throughout screening libraries.

Figure 1-9. Connolly surface representation of the crystal structure of Gleevec (colored by atom type) bound to the catalytic domain of Abl[69]. The "DFG out" conformation in the inactive form creates an allosteric pocket that is occupied by the piperazinyl-substituted benzamide portion of Gleevec.

In this configuration, the side chain of Phe382 (human Abl numbering) would sterically clash with the phosphate backbone of ATP. Within the allosteric pocket, the amide group of Gleevec makes two key hydrogen bonds with the side chain of Glu286 (absolutely conserved glutamic acid that emanates from helix C) and the NH amide from Asp381 (absolutely conserved aspartic acid of the DFG). The "DFG out" conformation is unique not only to the autoinhibited versus active form of Abl, but also among other kinases in their autoinhibited state. For example, the DFG motif in the autoinhibited form of Hck is in a position that would sterically clash with Gleevec. Therefore the selectivity of Gleevec for Abl versus other closely related Src family kinases seems to reside in the unique conformation of the DFG motif. The fact that Gleevec also targets KIT and

PDGF

these

of Gle

confo

occur

rece

(Ne

nig

BR

kn

Ge

an

e

s

s

t

:h threonine gatekeeper kinases) with similar potencies suggests that can adopt the "DFG out" conformation. Indeed, a recent crystal structure ınd to autoinhibited KIT demonstrates that it binds to a similar "DFG out" ıs found in Abl[74]. Whether the "DFG out" conformation is a naturally ırmation or induced by inhibitor binding is unclear.

:nown how many kinases can attain the "DFG out" conformation, but the ries of several new inhibitors, including BIRB796[73] and Bay43-9006[72] **ıure 1-8**), that exploit this conformation in their targets suggests that it widespread than previously assumed. Analysis of the crystal structure of d to p38 MAPK[73] and Nexavar bound to B-Raf[75] (a serine/threonine that both inhibitors exploit the allosteric pocket in a similar way to ıake the same hydrogen bond contacts (via the urea group instead of the ec). The selectivity profiles of BIRB796 and Nexavar are vastly different ey are based on similar diaryl urea precursors: BIRB796 is extremely d p38 MAPK whereas Nexavar targets B-Raf as well as several other e and tyrosine kinases with similar potencies. Although the origin of selectivity differences is not known, one conclusion that can be drawn is ences in the size and shape of the allosteric site determined by the local ıence and overall architecture of the kinase active site can be selectively right combination of aromatic substituents on the urea scaffold.

competitive, electrophilic kinase inhibitors

ously discussed, ATP-competitive kinase inhibitors must effectively h intracellular ATP concentrations (low millimolar) to block the activity of ells. For this reason, ATP-competitive, electrophilic inhibitors capable of ersible covalent bond (i.e. dissociation rate of zero) with their target(s)

are advantageous over their reversible ATP-competitive counterparts. Despite the fact that these types of inhibitors are often associated with metabolic instability and off-target effects due to non-specific akylation of irrelevant targets, there are several examples of selective ATP-competitive, electrophilic inhibitors. There are at least three reasons for the success of these inhibitors: (1) they contain an electrophile that is sufficiently unreactive so as to target an amino acid nucleophile only by a proximity-accelerated mechanism governed by reversible binding (i.e. binding is thermodynamically versus kinetically controlled), (2) they are based on a scaffold that binds with high affinity ($IC_{50} \leq$ μM in the presence of 100 μM ATP) to its target, and (3) they target amino acid nucleophiles (e.g. cysteine) not conserved among the kinase family, unlike the broad-spectrum inhibitor, FSBA (**Figure 1-2**), which targets the absolutely conserved catalytic lysine.

The first example of a selective ATP-competitive, electrophilic kinase inhibitor was designed against EGFR (HER-1) and the related human epidermal growth factor receptors, HER-2 and HER-4. Both classes of receptor tyrosine kinases are overexressed in many types of cancer and are therefore therapeutic targets. Previous work by scientists at Parke-Davis had established that EGFR and HER-1, HER-2 (as well as seven other kinases, including HER-4, not known at the time of their publication, determined by a structure-based sequence alignment performed in our laboratory) have a non-conserved cysteine (Cys773, human EGFR numbering) in the ATP binding pocket[76]. They demonstrated that a thiol-containing derivative of adenosine (2'-thioadenosine) could inhibit EGFR in a time-dependent manner ($k_2 = 2 \times 10^{-3}\ s^{-1}$) *in vitro*, consistent with an irreversible mode of inactivation (**Figure 1-10**). The site of covalent modification by 2'-thioadenosine was not identified; however, 1 mM DTT reversed inhibition by 2'-thioadenosine suggesting that it forms a disulfide bond with a cysteine in

the AT

weak

design

Parke

(phe

deve

know

app

ng pocket. Even though 2'-thioadenosine is not a useful inhibitor due to its and promiscuity, it does indeed provide a conceptual framework for the ctive, irreversible kinase inhibitors that target non-conserved cysteines.

g on their studies with 2'-thioadenosine, David W. Fry and coworkers at rationally designed an electrophilic inhibitor[77] based on a 4-quinazoline scaffold[6] (**Figure 1-10**). EGFR and HER-2 inhibitors m this scaffold are among the most potent and selective kinase inhibitors e such compound, described previously, Iressa (**Figure 1-5**), is a clinically er drug.

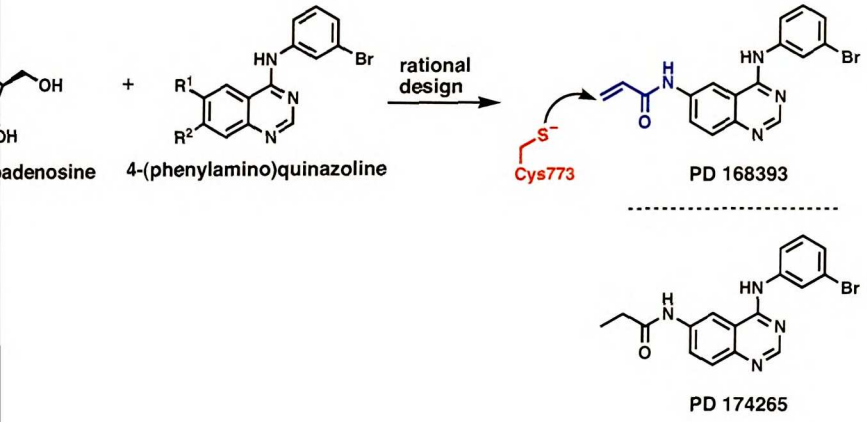

rational design of a selective, ATP-competitive, electrophilic inhibitor of EGFR and HER-ine was shown to covalently inactivate HER-1 by forming a disulfide bond between the 2'-ue) and Cys773 (colored red). PD 153035 was the first of a series of 4-azolines reported in the literature to very selectively and potently inhibit EGFR and HER-2 which is based on a similar 4-(phenylamino)quinazoline scaffold, was designed to alkylate ylamide electrophile is colored blue. PD 174265 is a reversible congener of PD 168393.

roposed binding mode of 4-(phenylamino)quinazoline-based inhibitors to del of the kinase domain of EGFR, the researchers designed PD 168393, rylamide electrophile, a Michael acceptor, was appended to C6 of the g (**Figure 1-10**). Acrylamides can react chemoselectively with cysteine e Michael addition reaction at physiological pH. PD 168393 potently

inhibited the kinase activity of EGFR *in vitro,* however was equipotent to a reversible analog that contained an ethylamide in place of the acrylamide (PD 174265). In cells, PD 168393 inhibited EGFR autophosphorylation in an irreversible manner and a ^{14}C labeled derivative irreversibly associated with EGFR and HER-2. Tandem mass spectrometry was used to shown that Cys773 is the predominate sight of covalent modification by PD 168393. Mutation of Cys773 to serine abolished alkylation by PD 168393; however, PD 168393 and PD 174265 inhibited the S773C EGFR mutant with similar potencies. These results together demonstrate that while PD 168393 irreversibly inactivates EGFR both *in vitro* and in cells, it does not appear that the electrophile provides increased potency, possibly because the starting scaffold alone targets EGFR with such high affinity. Nevertheless, PD 168393 exhibited superior anti-tumor activity compared to PD 174265 in a mouse cancer model[77].

The discovery of PD 168393 established that electrophilic kinase inhibitors could exhibit increased anti-tumor activity compared to their reversible congeners. Consequently, several large pharmaceutical companies devoted much effort to developing electrophilic EGFR inhibitors as potential cancer drugs. During these efforts, other Michael acceptors were found to be effective, including butynamides, as exemplified by CI-387,785 (**Figure 1-11**)[79]. Two electrophilic EGFR/HER-2 inhibitors, CI-1033[80] and EKB-569[81] (**Figure 1-11**), have now entered Phase II clinical trials for the treatment of non-small-cell lung carcinoma (NSCLC). Moreover, recent studies have demonstrated that electrophilic EGFR/HER-2 inhibitors, including CI-387,785 and EKB-569, can overcome resistance caused by a gatekeeper mutation in the EGFR kinase domain (T790M, human EGFR numbering) that renders Iressa and related compounds ineffective[82].

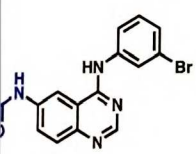

CI-387,785

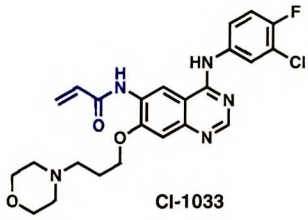

CI-1033

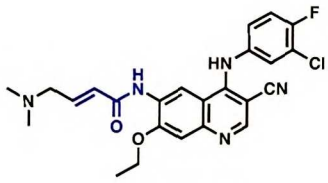

EKB-569

1-11. Electrophilic EGFR/HER-2 inhibitors inspired by PD 18393. CI-387,785[79] is similar to PD except that it contains a butynamide instead of an acrylamide. CI-1033[83] has an acrylamide similar to 393, but is more structurally related to Iressa. EKB-569[84] is based on a 4-(phenylamino)-3-nitrile-e scaffold and has a substituted acrylamide that contains a tertiary amine thought to act as a general talyst to accelerate the Michael addition reaction. Electrophiles are colored blue.

ds used to evaluate kinase inhibitor selectivity

Save a few exceptions (some mentioned in the previous sections), the majority of only used kinase inhibitors are non-selective (i.e. have more than one target), makes the interpretation of their cellular phenotypes as well as mechanism of in diseases potentially complicated. Therefore, the development of experimental ds to comprehensively evaluate the selectivity of kinase inhibitors across the kinase family as well as other non-kinase targets is needed. In recent years, l approaches have been developed to address this challenge, and in the aphs below I will briefly highlight some of them. The information garnered from ypes of analyses is essential if kinase inhibitors are to be used effectively as al tools to delineate the individual roles of kinases in signal transduction ys.

Kinases that share high sequence homology are usually sensitive to structurally compounds; however, subtle differences in the amino acid sequence that affect nformational plasticity of the kinase can be exploited to achieve remarkable ity even among closely related isoforms (e.g. Lck-selective inhibitors described in vious section). On the other hand, kinases that possess low sequence homology targeted by the same set of inhibitors and often share similar structure activity

elationsh

they sha

sequenc

from pe

experim

ATP i

kinase

384-w

Until

more

12

(Up

kin

G

p (SAR) profiles. Kinases of this type are referred to as SAR homologs as e structural similarities within the inhibitor binding pocket(s) despite limited homology[85]. In both cases, these selectivity trends are not easily discerned rming sequences alignments or comparing structures and must be determined ally.

vitro kinase activity assays that monitor the incorporation of the γ-phosphate of a peptide or protein substrate are the most common approach for profiling bitor selectivity[86,87]. These types of assays have been adapted to 96- and rmat to facilitate the profiling of many inhibitors and kinases simultaneously. tly, however, only a small panel of kinases was commercially available. Now, 200 kinases from representative members of all subfamilies (approximately human kinase genome) are available from at least two different companies nd Invitrogen). A major limitation of these assays is that they require active s inhibitors that selectively target the inactive kinases may be missed (e.g.

alternative approach to *in vitro* kinase activity assays that does not rely on activity was developed by Ambit biosciences[88]. This method is based on a assay that measures direct binding (determination of K_d values) to the ATP-. Kinases are expressed in *E. coli* as fusions to T7 bacteriophage, and a t potent kinase inhibitor (e.g staurosporine) is derivitized with biotin to bind to port containing streptavidin (**Figure 1-12**). The phage-tagged kinases are vith the immobilized inhibitor and the test inhibitor is added at increasing ons. If the test inhibitor binds directly to the ATP-binding site or an allosteric srupts binding of the immobilized inhibitor, the phage-tagged kinase will be rom the immobilized inhibitor, which can be measured quantitatively with nsitivity (single molecule) by a traditional plaque assay or quantitative

polymerase chain reaction (qPCR). This approach was used to screen 20 known kinase inhibitors (research compounds, inhibitors in phase trials, and FDA-approved drugs) against 113 kinases from all major subfamilies. Binding constants (K_d values) were determined for inhibitors that were effective below 10 μM.

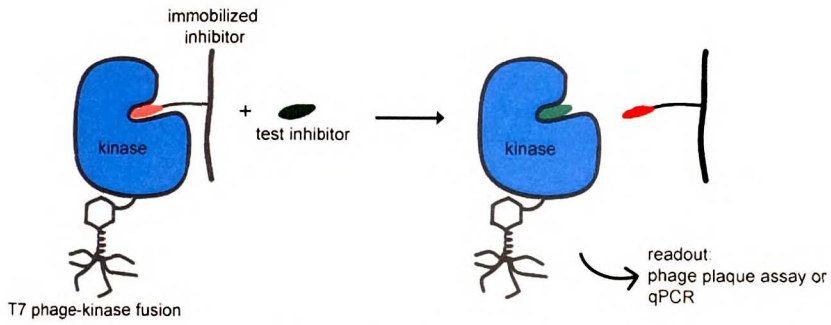

Figure 1-12. Competition-based assay developed by Ambit biosciences. Used to rapidly and efficiently screen kinase inhibitors against several hundred kinases.

The profiling of these inhibitors against this broad panel of kinases identified several unknown off-targets in addition to their primary targets. For example, EKB-569 (**Figure 1-11**), which was previously thought to be a very selective EGFR/HER-2 inhibitor, targeted 56 out of 113 kinases, and three with K_d values similar to EGFR. The cyclin G-associated kinase (GAK), a serine/threonine kinase with low sequence identity to EGFR (~20%), is an example of the latter. Interestingly, Iressa (**Figure 1-5**) also inhibited GAK and EGFR with similar potencies. These results suggest that GAK and EGFR are SAR homologs; however, a broader panel of inhibitors with different chemotypes needs to be tested to validate this claim.

The competition-based assay has at least three important advantages over *in vitro* kinase activity assays that are worth mentioning. First, this approach allows for the rapid generation of a diverse panel of kinases (already applied to 235 kinases) using phage display technology that avoids time-consuming and labor intensive protein purifications. Second, by measuring direct binding, it circumvents the need for ATP,

which can
values an
assay fo
micromol
method
develop

immob
suppo
protei
(MS/
unkn
seri
mhi
Inte
fu
a

which can complicate the interpretation of selectivity results due to the disparity of $K_{M,\ ATP}$ values among kinases (which can range from 1-600 μM for protein kinases). Third, the assay has a wide dynamic range (measure affinities from low-picomolar to mid-micromolar), due to the low concentrations kinases used. The disadvantages of this method include the inability to know the activation state of the kinase and the need to develop immobilized probes for kinases that do not bind to the ones currently used.

A complementary approach to the latter methods is affinity chromatography of immobilized inhibitors. In this strategy, kinase inhibitors are conjugated to a solid support (e.g. sepharose) and added to cell or tissue lysates to enrich for binding proteins. The captured proteins are then identified using tandem mass spectrometry (MS/MS) methods. A recently published example using this method identified 20 unknown cellular targets of Iressa (**Figure 1-13**)[89]. Two of these are the serine/threonine kinases, GAK and Rip-like interacting CLARP kinase (RICK), potently inhibited by Iressa as determined by follow-up *in vitro* kinase activity assays. Interestingly, GAK was also identified as a target of Iressa using the Ambit screen, giving further evidence that GAK is a *bone fide* off-target kinase. This approach has been applied to more than 15 structurally distinct kinase inhibitors and has revealed both kinase and non-kinase off-targets[90]. A caveat to this strategy is that often the most abundant cellular proteins are identified even though they are only weakly inhibited by the "free" compound. Therefore affinity chromatography can suggest novel off-targets, however, subsequent *in vitro* kinase assays need to be performed to truly determine inhibitor selectivity profiles.

All three described *in vitro* methods suffer from the drawback that they are not always predictive of cellular selectivity profiles. For example, an inhibitor may exhibit similar binding affinities for kinase a and b *in vitro*, however the same inhibitor may be 10-fold more potent for kinase a in cells due to differences in $K_{M,\ ATP}$ and/or

ɔrmational states relevant only in cells. Therefore, methods are needed to 'mine the selectivity of inhibitors in a cellular context.

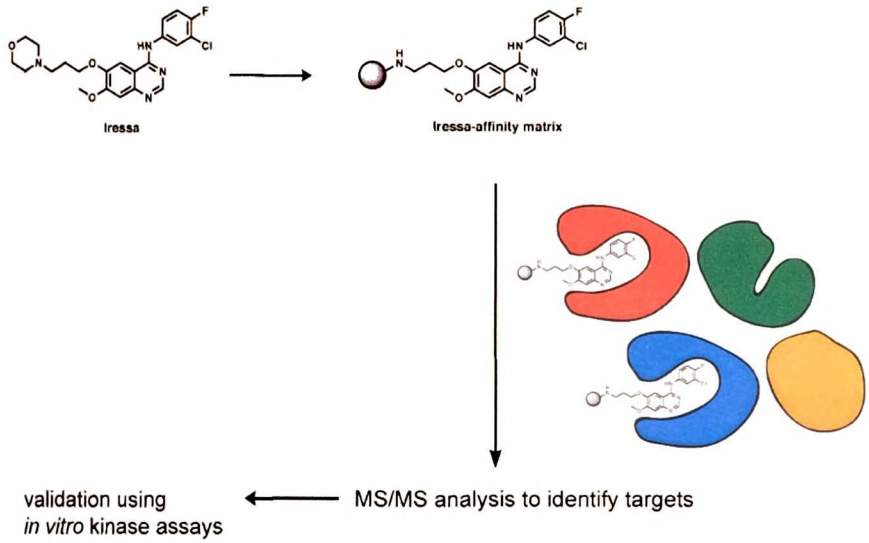

e 1-13. Affinity chromatography of immobilized kinase inhibitors as an approach to identify cellular s. An Iressa variant was conjugated to sepharose and added to a Hela cell lysates to identify Iressa-g proteins. Enriched proteins are subjected to trypsin digestion followed by LC-MS/MS to identify s. Iressa is then tested against the putative targets *in vitro* to determine binding constants (IC_{50} or K_d, ding on the assay).

clusion

Protein kinases are key regulatory enzymes in eukaryotes. Although they are :urally and functionally homologous within the catalytic core, peripheral domains of es give rise to their diverse modes of regulation and conformational plasticity. tive, small molecule inhibitors of kinases can be used to precisely dissect the role ases in signaling networks. Most kinase inhibitors target the essentially invariant ɔinding pocket and are therefore non-selective across the family. Increasingly, ver, examples of inhibitors that exploit regions outside the ATP-binding pocket (e.g. ıine gatekeeper and allosteric pocket) are being discovered, and these types of ors can exhibit remarkable selectivity, even among closely related isoforms. theless, it is important to stress that many, if not all, of these inhibitors were not

y designed, but rather serendipitously discovered and later optimized by s SAR studies requiring intense medicinal chemistry efforts. It is no surprise at most potent and selective kinase inhibitors have been provided by eutical companies.

My thesis work has been directed toward the rational design of irreversible nhibitors that target nonconserved cysteines within the ATP binding pocket, as inspired, in part, by discovery of electrophilic EGFR family inhibitors. In the pter I will elaborate on the approach we used to guide the design of a potent ctive p90 ribosomal protein S6 kinase inhibitor (RSK) inhibitor, named fmk[91]. he success of our strategy was the availability of chemical (SAR), genetic nesis), and structural (crystallography) studies that defined the protein kinase ophore. Chapter 3 describes the design and synthesis of an analog of fmk, mk-pa that can monitor covalent RSK modification in cells, and was used to that RSK autoactivation is dependent on the cell type and stimulation condition. was further exploited, as elaborated in Chapter 4, to screen a panel of nilic inhibitors using a competition-based assay, which revealed several nds that exhibit isoform selectivity. Finally, Chapter 5 describes the nent of third-generation RSK inhibitors that exhibit increased cellular potency fmk.

Referenc

1. Ma
pr
2. C
(
3. H
4.
5.
6.
7.
8.
9

References

1. Manning, G., Whyte, D. B., Martinez, R., Hunter, T. & Sudarsanam, S. The protein kinase complement of the human genome. *Science* **298**, 1912-34 (2002).
2. Cohen, P. The origins of protein phosphorylation. *Nat Cell Biol* **4**, E127-30 (2002).
3. Knight, Z. A. & Shokat, K. M. Features of selective kinase inhibitors. *Chem Biol* **12**, 621-37 (2005).
4. Lawrence, D. S. & Niu, J. Protein kinase inhibitors: the tyrosine-specific protein kinases. *Pharmacol Ther* **77**, 81-114 (1998).
5. Xu, W., Harrison, S. C. & Eck, M. J. Three-dimensional structure of the tyrosine kinase c-Src. *Nature* **385**, 595-602 (1997).
6. Fry, D. W. et al. A specific inhibitor of the epidermal growth factor receptor tyrosine kinase. *Science* **265**, 1093-5 (1994).
7. Lee, J. C., Kassis, S., Kumar, S., Badger, A. & Adams, J. L. p38 mitogen-activated protein kinase inhibitors--mechanisms and therapeutic potentials. *Pharmacol Ther* **82**, 389-97 (1999).
8. Traxler, P. & Furet, P. Strategies toward the design of novel and selective protein tyrosine kinase inhibitors. *Pharmacol Ther* **82**, 195-206 (1999).
9. Bold, G. et al. New anilinophthalazines as potent and orally well absorbed inhibitors of the VEGF receptor tyrosine kinases useful as antagonists of tumor-driven angiogenesis. *J Med Chem* **43**, 2310-23 (2000).
10. Kelly, L. M. et al. CT53518, a novel selective FLT3 antagonist for the treatment of acute myelogenous leukemia (AML). *Cancer Cell* **1**, 421-32 (2002).
11. Rusnak, D. W. et al. The effects of the novel, reversible epidermal growth factor receptor/ErbB-2 tyrosine kinase inhibitor, GW2016, on the growth of human

al and tumor-derived cell lines in vitro and in vivo. *Mol Cancer Ther* **1**, 85-94
).

Y. & Gray, N. S. Rational design of inhibitors that bind to inactive kinase
rmations. *Nat Chem Biol* **2**, 358-64 (2006).

s, J. A. Kinetic and catalytic mechanisms of protein kinases. *Chem Rev*
2271-90 (2001).

, D. A., Perkins, J. P. & Krebs, E. G. An adenosine 3',5'-monophosphate-
ndant protein kinase from rabbit skeletal muscle. *J Biol Chem* **243**, 3763-5
).

M., Salas, M. L. & Lipmann, F. Mechanism of activation by adenosine 3':5'-
monophosphate of a protein phosphokinase from rabbit reticulocytes. *Proc*
cad Sci U S A **67**, 408-14 (1970).

r, S. S. et al. cAMP-dependent protein kinase: a framework for a diverse
of enzymes. *Cold Spring Harb Symp Quant Biol* **53 Pt 1**, 121-30 (1988).

ngoni, A. G. *Enzyme kinetics: a modern approach* (John Wiley and Sons,
New Jersey, 2003).

s, A. E., Adam, G. C. & Cravatt, B. F. Activity-based protein profiling in vivo
a copper(i)-catalyzed azide-alkyne [3 + 2] cycloaddition. *J Am Chem Soc*
4686-7 (2003).

dlo, D. J. & Bertozzi, C. R. A strategy for functional proteomic analysis of
sidase activity from cell lysates. *Angew Chem Int Ed Engl* **43**, 5338-42
).

s, A. E. & Cravatt, B. F. Profiling enzyme activities in vivo using click
istry methods. *Chem Biol* **11**, 535-46 (2004).

, H. et al. Chemistry in living cells: detection of active proteasomes by a
ep labeling strategy. *Angew Chem Int Ed Engl* **42**, 3626-9 (2003).

22. Ale
imp
en
23. Zo
ca
[
(
24.
25.
26.
27
2

22. Alexander, J. P. & Cravatt, B. F. Mechanism of carbamate inactivation of FAAH: implications for the design of covalent inhibitors and in vivo functional probes for enzymes. *Chem Biol* **12**, 1179-87 (2005).

23. Zoller, M. J. & Taylor, S. S. Affinity labeling of the nucleotide binding site of the catalytic subunit of cAMP-dependent protein kinase using p-fluorosulfonyl-[14C]benzoyl 5'-adenosine. Identification of a modified lysine residue. *J Biol Chem* **254**, 8363-8 (1979).

24. Wyatt, J. L. & Colman, R. F. Affinity labeling of rabbit muscle pyruvate kinase by 5'-p-fluorosulfonylbenzoyladenosine. *Biochemistry* **16**, 1333-42 (1977).

25. Shoji, S. et al. Complete amino acid sequence of the catalytic subunit of bovine cardiac muscle cyclic AMP-dependent protein kinase. *Proc Natl Acad Sci U S A* **78**, 848-51 (1981).

26. Zoller, M. J., Nelson, N. C. & Taylor, S. S. Affinity labeling of cAMP-dependent protein kinase with p-fluorosulfonylbenzoyl adenosine. Covalent modification of lysine 71. *J Biol Chem* **256**, 10837-42 (1981).

27. Hashimoto, E., Takio, K. & Krebs, E. G. Amino acid sequence at the ATP-binding site of cGMP-dependent protein kinase. *J Biol Chem* **257**, 727-33 (1982).

28. Kamps, M. P., Taylor, S. S. & Sefton, B. M. Direct evidence that oncogenic tyrosine kinases and cyclic AMP-dependent protein kinase have homologous ATP-binding sites. *Nature* **310**, 589-92 (1984).

29. Hagiwara, M., Inagaki, M. & Hidaka, H. Specific binding of a novel compound, N-[2-(methylamino)ethyl]-5-isoquinolinesulfonamide (H-8) to the active site of cAMP-dependent protein kinase. *Mol Pharmacol* **31**, 523-8 (1987).

30. Wang, Q. M., Srinivas, P. R., Harrison, M. L. & Geahlen, R. L. Partial purification and characterization of the lck protein-tyrosine kinase from bovine thymus. *Biochem J* **279 (Pt 2)**, 567-74 (1991).

31. Pa

pr

32. N

i

33. I

34.

35.

36

31. Parker, P. J. Antibodies to fluorylsulfonylbenzoyladenosine permit identification of protein kinases. *FEBS Lett* **334**, 347-50 (1993).

32. Maly, D. J., Allen, J. A. & Shokat, K. M. A mechanism-based cross-linker for the identification of kinase-substrate pairs. *J Am Chem Soc* **126**, 9160-1 (2004).

33. Buechler, J. A., Toner-Webb, J. A. & Taylor, S. S. Carbodiimides as probes for protein kinase structure and function. *Methods Enzymol* **200**, 487-500 (1991).

34. Toner-Webb, J. & Taylor, S. S. Inhibition of the catalytic subunit of cAMP-dependent protein kinase by dicyclohexylcarbodiimide. *Biochemistry* **26**, 7371-8 (1987).

35. Buechler, J. A. & Taylor, S. S. Identification of aspartate-184 as an essential residue in the catalytic subunit of cAMP-dependent protein kinase. *Biochemistry* **27**, 7356-61 (1988).

36. Buechler, J. A. & Taylor, S. S. Dicyclohexylcarbodiimide cross-links two conserved residues, Asp-184 and Lys-72, at the active site of the catalytic subunit of cAMP-dependent protein kinase. *Biochemistry* **28**, 2065-70 (1989).

37. Bramson, H. N. et al. Modification of the catalytic subunit of bovine heart cAMP-dependent protein kinase with affinity labels related to peptide substrates. *J Biol Chem* **257**, 10575-81 (1982).

38. Buechler, J. A., Vedvick, T. A. & Taylor, S. S. Differential labeling of the catalytic subunit of cAMP-dependent protein kinase with acetic anhydride: substrate-induced conformational changes. *Biochemistry* **28**, 3018-24 (1989).

39. Zheng, J. H., Knighton, D. R., Parello, J., Taylor, S. S. & Sowadski, J. M. Crystallization of catalytic subunit of adenosine cyclic monophosphate-dependent protein kinase. *Methods Enzymol* **200**, 508-21 (1991).

40. Noble, M. E., Endicott, J. A. & Johnson, L. N. Protein kinase inhibitors: insights into drug design from structure. *Science* **303**, 1800-5 (2004).

41. Gibb
Syst
unr
of t
42. Sn
AT
tu
43. K
f
44.
45.
46.
4

Gibbs, C. S., Knighton, D. R., Sowadski, J. M., Taylor, S. S. & Zoller, M. J. Systematic mutational analysis of cAMP-dependent protein kinase identifies unregulated catalytic subunits and defines regions important for the recognition of the regulatory subunit. *J Biol Chem* **267**, 4806-14 (1992).

Snyder, M. A., Bishop, J. M., McGrath, J. P. & Levinson, A. D. A mutation at the ATP-binding site of pp60v-src abolishes kinase activity, transformation, and tumorigenicity. *Mol Cell Biol* **5**, 1772-9 (1985).

Kamps, M. P. & Sefton, B. M. Neither arginine nor histidine can carry out the function of lysine-295 in the ATP-binding site of p60src. *Mol Cell Biol* **6**, 751-7 (1986).

Wong, L., Jennings, P. A. & Adams, J. A. Communication pathways between the nucleotide pocket and distal regulatory sites in protein kinases. *Acc Chem Res* **37**, 304-11 (2004).

Taylor, S. S. et al. PKA: a portrait of protein kinase dynamics. *Biochim Biophys Acta* **1697**, 259-69 (2004).

Aimes, R. T., Hemmer, W. & Taylor, S. S. Serine-53 at the tip of the glycine-rich loop of cAMP-dependent protein kinase: role in catalysis, P-site specificity, and interaction with inhibitors. *Biochemistry* **39**, 8325-32 (2000).

Nolen, B., Taylor, S. & Ghosh, G. Regulation of protein kinases; controlling activity through activation segment conformation. *Mol Cell* **15**, 661-75 (2004).

Biondi, R. M. & Nebreda, A. R. Signalling specificity of Ser/Thr protein kinases through docking-site-mediated interactions. *Biochem J* **372**, 1-13 (2003).

Huse, M. & Kuriyan, J. The conformational plasticity of protein kinases. *Cell* **109**, 275-82 (2002).

Sicheri, F. & Kuriyan, J. Structures of Src-family tyrosine kinases. *Curr Opin Struct Biol* **7**, 777-85 (1997).

31. Che
the
end
32. An
hi
33. B
c
T
34.
35.
36.
37.
38

51. Cheng, Y. & Prusoff, W. H. Relationship between the inhibition constant (K1) and the concentration of inhibitor which causes 50 per cent inhibition (I50) of an enzymatic reaction. *Biochem Pharmacol* **22**, 3099-108 (1973).

52. Aronov, A. M. & Murcko, M. A. Toward a pharmacophore for kinase frequent hitters. *J Med Chem* **47**, 5616-9 (2004).

53. Blencke, S. et al. Characterization of a conserved structural determinant controlling protein kinase sensitivity to selective inhibitors. *Chem Biol* **11**, 691-701 (2004).

54. Liu, Y. et al. Structural basis for selective inhibition of Src family kinases by PP1. *Chem Biol* **6**, 671-8 (1999).

55. Wang, Z. et al. Structural basis of inhibitor selectivity in MAP kinases. *Structure* **6**, 1117-28 (1998).

56. Wilson, K. P. et al. The structural basis for the specificity of pyridinylimidazole inhibitors of p38 MAP kinase. *Chem Biol* **4**, 423-31 (1997).

57. Klutchko, S. R. et al. 2-Substituted aminopyrido[2,3-d]pyrimidin-7(8H)-ones. structure-activity relationships against selected tyrosine kinases and in vitro and in vivo anticancer activity. *J Med Chem* **41**, 3276-92 (1998).

58. Barker, A. J. et al. Studies leading to the identification of ZD1839 (IRESSA): an orally active, selective epidermal growth factor receptor tyrosine kinase inhibitor targeted to the treatment of cancer. *Bioorg Med Chem Lett* **11**, 1911-4 (2001).

59. Cuenda, A. et al. SB 203580 is a specific inhibitor of a MAP kinase homologue which is stimulated by cellular stresses and interleukin-1. *FEBS Lett* **364**, 229-33 (1995).

60. Lee, J. C. et al. A protein kinase involved in the regulation of inflammatory cytokine biosynthesis. *Nature* **372**, 739-46 (1994).

61. Ha
kin
ZI
62. S
t
63.
64.
65.
66.
6

61. Hanke, J. H. et al. Discovery of a novel, potent, and Src family-selective tyrosine kinase inhibitor. Study of Lck- and FynT-dependent T cell activation. *J Biol Chem* **271**, 695-701 (1996).

62. Schindler, T. et al. Crystal structure of Hck in complex with a Src family-selective tyrosine kinase inhibitor. *Mol Cell* **3**, 639-48 (1999).

63. Alaimo, P. J., Shogren-Knaak, M. A. & Shokat, K. M. Chemical genetic approaches for the elucidation of signaling pathways. *Curr Opin Chem Biol* **5**, 360-7 (2001).

64. Bishop, A. C. et al. A chemical switch for inhibitor-sensitive alleles of any protein kinase. *Nature* **407**, 395-401 (2000).

65. Specht, K. M. & Shokat, K. M. The emerging power of chemical genetics. *Curr Opin Cell Biol* **14**, 155-9 (2002).

66. Yamaguchi, H. & Hendrickson, W. A. Structural basis for activation of human lymphocyte kinase Lck upon tyrosine phosphorylation. *Nature* **384**, 484-9 (1996).

67. Arnold, L. D. et al. Pyrrolo[2,3-d]pyrimidines containing an extended 5-substituent as potent and selective inhibitors of lck I. *Bioorg Med Chem Lett* **10**, 2167-70 (2000).

68. Burchat, A. et al. Discovery of A-770041, a src-family selective orally active lck inhibitor that prevents organ allograft rejection. *Bioorg Med Chem Lett* **16**, 118-22 (2006).

69. Nagar, B. et al. Crystal structures of the kinase domain of c-Abl in complex with the small molecule inhibitors PD173955 and imatinib (STI-571). *Cancer Res* **62**, 4236-43 (2002).

70. Schindler, T. et al. Structural mechanism for STI-571 inhibition of abelson tyrosine kinase. *Science* **289**, 1938-42 (2000).

71. Dr
On
72. Ly
in
73. P
t
74. (
75.
76.
77.
78

71. Druker, B. J. Molecularly targeted therapy: have the floodgates opened? *Oncologist* **9**, 357-60 (2004).

72. Lyons, J. F., Wilhelm, S., Hibner, B. & Bollag, G. Discovery of a novel Raf kinase inhibitor. *Endocr Relat Cancer* **8**, 219-25 (2001).

73. Pargellis, C. et al. Inhibition of p38 MAP kinase by utilizing a novel allosteric binding site. *Nat Struct Biol* **9**, 268-72 (2002).

74. Mol, C. D. et al. Structural basis for the autoinhibition and STI-571 inhibition of c-Kit tyrosine kinase. *J Biol Chem* **279**, 31655-63 (2004).

75. Wan, P. T. et al. Mechanism of activation of the RAF-ERK signaling pathway by oncogenic mutations of B-RAF. *Cell* **116**, 855-67 (2004).

76. Singh, J. et al. Structure-based design of a potent, selective, and irreversible inhibitor of the catalytic domain of the erbB receptor subfamily of protein tyrosine kinases. *J Med Chem* **40**, 1130-5 (1997).

77. Fry, D. W. et al. Specific, irreversible inactivation of the epidermal growth factor receptor and erbB2, by a new class of tyrosine kinase inhibitor. *Proc Natl Acad Sci U S A* **95**, 12022-7 (1998).

78. Fry, D. W. Inhibition of the epidermal growth factor receptor family of tyrosine kinases as an approach to cancer chemotherapy: progression from reversible to irreversible inhibitors. *Pharmacol Ther* **82**, 207-18 (1999).

79. Discafani, C. M. et al. Irreversible inhibition of epidermal growth factor receptor tyrosine kinase with in vivo activity by N-[4-[(3-bromophenyl)amino]-6-quinazolinyl]-2-butynamide (CL-387,785). *Biochem Pharmacol* **57**, 917-25 (1999).

80. Campos, S. et al. Multicenter, randomized phase II trial of oral CI-1033 for previously treated advanced ovarian cancer. *J Clin Oncol* **23**, 5597-604 (2005).

11. Yoshin
recep
cell l
(200
12. Kwa
acc
13. Sm
ep
(
s
14.
65.
66

Yoshimura, N. et al. EKB-569, a new irreversible epidermal growth factor receptor tyrosine kinase inhibitor, with clinical activity in patients with non-small cell lung cancer with acquired resistance to gefitinib. *Lung Cancer* **51**, 363-8 (2006).

Kwak, E. L. et al. Irreversible inhibitors of the EGF receptor may circumvent acquired resistance to gefitinib. *Proc Natl Acad Sci U S A* **102**, 7665-70 (2005).

Smaill, J. B. et al. Tyrosine kinase inhibitors. 17. Irreversible inhibitors of the epidermal growth factor receptor: 4-(phenylamino)quinazoline- and 4-(phenylamino)pyrido[3,2-d]pyrimidine-6-acrylamides bearing additional solubilizing functions. *J Med Chem* **43**, 1380-97 (2000).

Wissner, A. et al. Synthesis and structure-activity relationships of 6,7-disubstituted 4-anilinoquinoline-3-carbonitriles. The design of an orally active, irreversible inhibitor of the tyrosine kinase activity of the epidermal growth factor receptor (EGFR) and the human epidermal growth factor receptor-2 (HER-2). *J Med Chem* **46**, 49-63 (2003).

Frye, S. V. Structure-activity relationship homology (SARAH): a conceptual framework for drug discovery in the genomic era. *Chem Biol* **6**, R3-7 (1999).

Davies, S. P., Reddy, H., Caivano, M. & Cohen, P. Specificity and mechanism of action of some commonly used protein kinase inhibitors. *Biochem J* **351**, 95-105 (2000).

Bain, J., McLauchlan, H., Elliott, M. & Cohen, P. The specificities of protein kinase inhibitors: an update. *Biochem J* **371**, 199-204 (2003).

Fabian, M. A. et al. A small molecule-kinase interaction map for clinical kinase inhibitors. *Nat Biotechnol* **23**, 329-36 (2005).

Brehmer, D. et al. Cellular targets of gefitinib. *Cancer Res* **65**, 379-82 (2005).

90. Daub, H. Characterisation of kinase-selective inhibitors by chemical proteomics. *Biochim Biophys Acta* **1754**, 183-90 (2005).

91. Cohen, M. S., Zhang, C., Shokat, K. M. & Taunton, J. Structural bioinformatics-based design of selective, irreversible kinase inhibitors. *Science* **308**, 1318-21 (2005).

Chapter 2

Structural bioinformatics-based design of selective, irreversible kinase inhibitors

Abstract

The active sites of 491 human protein kinase domains are highly conserved, making the design of selective inhibitors a formidable challenge. We used a structural bioinformatics approach to identify two selectivity filters, a threonine and a cysteine, at defined positions in the active site of p90 ribosomal protein S6 kinase (RSK). A fluoromethylketone inhibitor, designed to exploit both selectivity filters, potently and selectively inactivated RSK1 and RSK2 in mammalian cells. Kinases with only one selectivity filter were resistant to the inhibitor, yet they became sensitized after genetic introduction of the second selectivity filter. Thus, two amino acids that distinguish RSK from other protein kinases are sufficient to confer inhibitor sensitivity.

Introduction

Phosphorylation of serine, threonine, and tyrosine residues is a primary mechanism for regulating protein function in eukaryotic cells. Protein kinases, the enzymes that catalyze these reactions, regulate essentially all cellular processes and have thus emerged as therapeutic targets for many human diseases [1]. Small-molecule inhibitors of the Abelson tyrosine kinase (Abl) and the epidermal growth factor receptor (EGFR) have been developed into clinically useful anti-cancer drugs [2,3]. Selective inhibitors can also increase our understanding of the cellular and organismal roles of protein kinases. However, nearly all kinase inhibitors target the adenosine triphosphate (ATP) binding site, which is well conserved even among distantly related kinase domains. For this reason, rational design of inhibitors that selectively target even a subset of the 491 related human kinase domains continues to be a daunting challenge.

Structural and mutagenesis studies have revealed key determinants of kinase inhibitor selectivity, including a widely exploited selectivity filter in the ATP binding site known as the "gatekeeper". A compact gatekeeper (such as threonine) allows bulky aromatic substituents, such as those found in the Src-family kinase inhibitors, PP1 and PP2, to enter a deep hydrophobic pocket [4-6]. In contrast, larger gatekeepers (methionine, leucine, isoleucine, or phenylalanine) restrict access to this pocket. A small gatekeeper provides only partial discrimination between kinase acitve sites, however, as ~20% of human kinases have a threonine at this position. Gleevec, a drug used to treat chronic myelogenous leukemia, exploits a threonine gatekeeper in the Abl kinase domain, yet it also potently inhibits the distantly related tyrosine kinases, c-KIT and the platelet-derived growth factor receptor (PDGFR) [7].

We therefore sought a second selectivity filter that could be discerned from a primary sequence alignment. Among the 20 amino acids, cysteine has unique chemical reactivity and is commonly targeted by electrophilic inhibitors. In the case of cysteine

protease

every cy

inhibitor

cysteine

reactive

report,

simult

unqu

(RSK

dom

are

eq

su

fu

c

protease inhibitors, the reactive cysteine is not a selectivity filter, because it is found in every cysteine protease and is essential for catalysis. Electrophilic, cysteine-directed inhibitors of the EGFR kinase domain have also been reported [8], but here again, the cysteine does not act as a selectivity filter, because neither the electrophile nor the reactive cysteine is required for potent, selective inhibition by these compounds. In this report, we describe the rational design of selective kinase inhibitors that require the simultaneous presence of a threonine gatekeeper and a reactive cysteine, which are uniquely found in the C-terminal kinase domain of p90 ribosomal protein S6 kinases (RSK).

In humans there are four RSK isoforms (RSK1-4) and they all contain two kinase domains, a C-terminal kinase domain (CTD) and N-terminal kinase domain (NTD) that are connecting by a regulatory linker region (**Figure 2-1**). RSK are ubiquitously expressed, however there is variable tissue distribution of the individual isoforms suggesting that they may have specific, non-compensatory roles. Indeed, loss of function mutations in the RSK2 gene cause Coffin-Lowry Syndrome, a human disorder characterized by severe mental retardation [9], suggesting that RSK2 is important for brain development.

RSK are downstream effectors of the Ras-mitogen activated protein kinase (MAPK) pathway and are activated by a complicated sequence of phosphorylation events (**Figure 2-1**). First, the MAPK extracellular regulated kinases (ERK) bind to a docking site in the C-terminus and phosphorylates Thr577 (human RSK2 numbering) in the activation loop and at least one other serine (Ser369) in the linker region[10,11]. The activated CTD then autophosphorylates Ser386 in a hydrophobic motif (shared among other AGC family kinases) located in the linker region, which creates a docking site for 3-phosphoinositide-depedent protein kinase1 (PDK1). Docking of PDK1 to the phosphorylated hydrophobic motif stimulates its kinase activity, which then

phosphor

phosphor

the activ

Fig

To

p

T

D

phosphorylates Ser227 in the activation loop of the NTD. Upon PDK1 dissociation, the phosphorylated hydrophobic motif is thought to bind to the NTD near helix C, stabilizing the active conformation, although no structural evidence exists for this mechanism.

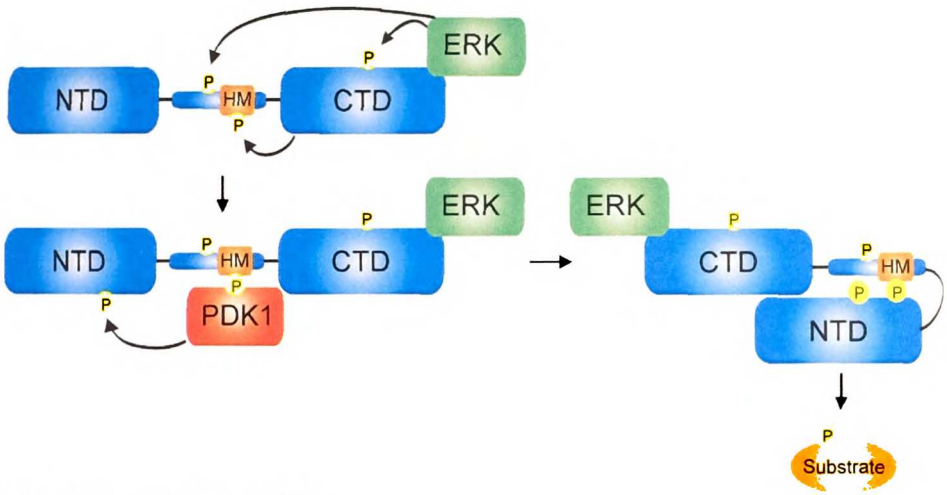

Figure 2-1. RSK activation mechanism.

To date, more than 20 proposed RSK substrates involved in diverse physiological processes have been reported, including translational regulation (eIF4B[12], eEF2K[13], Tuberin[14]), transcriptional regulation (ATF4[15], FOS[16], SRF[17]), cell survival (BAD[18,19], DAPK[20]), and cytoskeletal reorganization (FNLa[21]); however, whether these are actually physiological relevant substrates remains to be determined. A small molecule inhibitor of RSK would be a valuable tool toward this effort.

Results and Discussion

Structural bioinformatics guides the design of electrophilic inhibitors

We used a kinome-wide sequence alignment [1,22] to search for cysteines that, together with a threonine gatekeeper, could form a covalent bond with an inhibitor in the ATP pocket. We focused on the conserved glycine-rich loop, which interacts with the triphosphate of ATP and is one of the most flexible structural elements of the kinase domain [23]. A cysteine near this solvent-exposed loop is likely to have a lower pK_a and

therefore
related
C-termi
valine.
and R5
the R5

therefore be more reactive than a cysteine buried in the hydrophobic pocket. Out of 491 related kinase domains in the human genome [1], we found eleven with a cysteine at the C-terminal end of the glycine-rich loop (**Figure 2-2a**), a position usually occupied by valine. We next examined the gatekeeper in these kinases. The CTD of RSK1, RSK2, and RSK4, have a threonine gatekeeper, whereas the remaining nine kinases, including the RSK3 CTD, have larger gatekeepers (**Figure 2-2a**).

a

		nonconserved cysteine ↓		gatekeeper ↓
Src	[276]	LGQGCFGEVWMGTWNG	[333]	SEEP---IYIVTEYMSKGSL
RSK1	[424]	IGVGSYSVCKRCVHKA	[480]	DDGKH--VYLVTELMRGGEL
RSK2	[428]	IGVGSYSVCKRCIHKA	[484]	DDGKY--VYVVTELMKGGEL
RSK3	[421]	IGVGSYSVCKRCVHKA	[477]	DDGKF--VYLVMELMRGGEL
RSK4	[432]	IGVGSYSVCKRCIHAT	[488]	DDGRY--VYLVTDLMKGGEL
MSK1	[432]	LGEGSFSICRKCVHKK	[489]	HDQLH--TFLVMELLNGGEL
MSK2	[395]	LGQGSFSVCRRCRQRQ	[452]	HDQLH--TYLVLELLRGGEL
PLK1	[59]	LGKGGFAKCFEISDAD	[121]	EDNDF--VFVVLELCRRRSL
PLK2	[88]	LGKGGFAKCYEMTDLT	[150]	EDKEN--IYILLEYCSRR-S
PLK3	[29]	LGKGGFARCYEATDTE	[91]	EDADN--IYIFLELCSRK-S
NEK2	[14]	IGTGSYGRCQKIRRKS	[75]	IDRTNTTLYIVMEYCEGGDL
MEKK1	[1300]	IGLGAFSSCYQAQDVG	[1371]	CEKSN--YNLFIEWMAGGSV

b

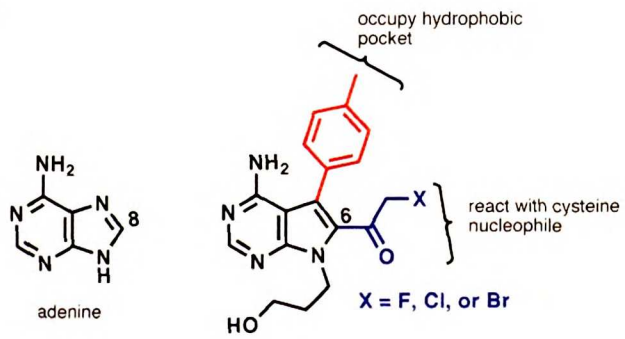

Figure 2-2. Structural bioinformatics guides the design of electrophilic inhibitors of RSK-family protein kinases. (**a**) Sequence alignment of the eleven human kinases with a cysteine selectivity filter at the C-terminal end of the glycine-rich loop. Of these eleven, RSK1, RSK2, and RSK4 are the only kinases with a threonine selectivity filter in the gatekeeper position. Src, which has a threonine gatekeeper but lacks the cysteine, is shown for comparison. (**b**) Chemical structures of adenine and the rationally designed halomethylketone pyrrolopyrimidines, cmk and fmk.

To exploit both selectivity filters in RSK-family kinases, we needed a scaffold that could present an electrophile to the cysteine while occupying the hydrophobic pocket defined by the gatekeeper. Crystal structures of kinases with bound ATP analogs all reveal van der Waals contacts between a conserved valine, analogous to the cysteine

we ide

design

scaffo

The

Struc

f. V

dista

of th

Sy

S

s

h

we identified in RSK (**Figure 2-2a**), and the adenine C-8 position. We therefore designed and synthesized electrophilic inhibitors based on a pyrrolo[2,3-*d*]pyrimidine scaffold that were substituted with halomethylketones at the C-6 position (**Figure 2-2b**). The *p*-tolyl substituent was designed to occupy the putative hydrophobic pocket. Structurally related pyrazolo[3,4-*d*]pyrimidines interact similarly with Src-family kinases [4-6]. We hypothesized that the electrophilic halomethylketones would be within striking distance of the key cysteine in RSK1, RSK2, and RSK4, and that kinases with only one of the two selectivity filters would be resistant to the inhibitors.

Synthesis of halomethylketone derivatives

Arnold and coworkers reported an efficient synthesis of pyrrolo[2,3-*d*]pyrimidine Src-family kinase inhibitors[24]. Using a similar route, pyrrolo[2,3-*d*]pyrimidine **2.3** was synthesized in five steps from commercially available materials (**Scheme 2-1**). The hydroxypropyl substituent at the N-7 position was installed to facilitate attachment of an affinity tag, such as biotin.

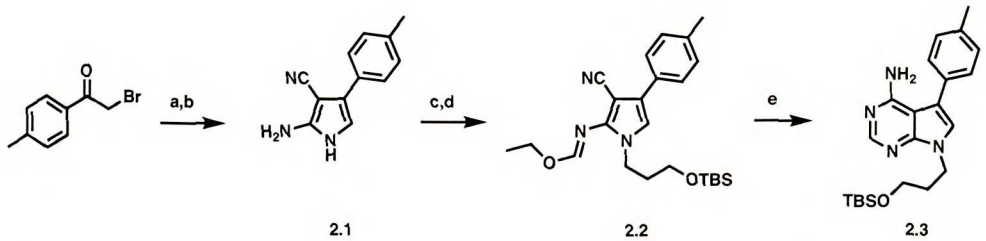

Scheme 2-1. Synthesis of pyrrolo[2,3-*d*]pyrimidine **2.3**. Reagents and conditions: a. potassium phthalimide, DMF; b. malononitrile, MeOH, H_2O, NaOH (91% yield over 2 steps); c. triethyl orthoformate, acetic anhydride; d. NaH, DMF, then 3-(*t*-butyldimethylsilyloxy)propyl iodide (70% yield over 2 steps); e. NH_3, MeOH (61% yield).

Halomethylketones **2.8** (bmk), **2.9** (cmk), and **2.13** (fmk) were synthesized as illustrated in **Scheme 2-2 and Scheme 2-3**. Briefly, selective bromination of **2.3** proceeded in quantitative yield with *N*-bromosuccinimide to give **2.4**. Conversion of this intermediate to enol ether **2.5** was accomplished by a palladium-catalyzed Stille reaction with α-

(ethoxyvinyl)tributyl tin. Enol ether **2.5** served as a key intermediate from which all halomethylketones were synthesized in two to six steps.

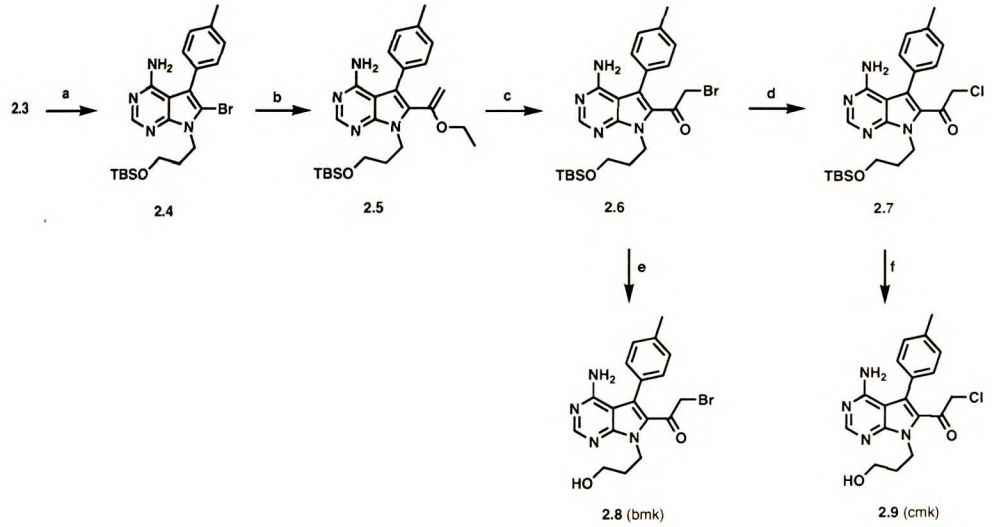

Scheme 2-2. Synthesis of cmk and bmk. Reagents and conditions: a. *N*-bromosuccinimide, DMF (99% yield); b. α-(ethoxyvinyl)tributyl tin, $Pd[P(Ph)_3]_4$, toluene (80% yield); c. *N*-bromosuccinimide, $NaHCO_3$, H_2O, DMF, -20°C (60% yield); d. LiCl, acetone (100% yield); e. 1 N HBr, THF (40% yield); f. 1 N HCl, THF (50% yield).

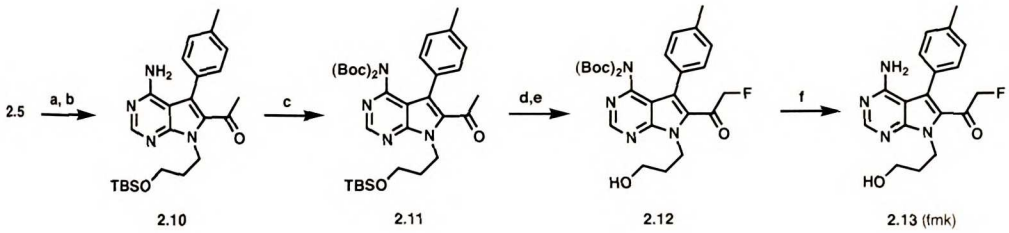

Scheme 2-3. Synthesis of cmk. Reagents and conditions: a. 1 N HCl, THF; b. imidazole, t-butyldimethylsilyl chloride, DMF (76% yield over 2 steps); c. $(Boc)_2O$, DMAP, THF (78% yield); d. LDA, THF, then N-fluorobenzenesulfonimide; e. 1 N HCl, THF (60% yield over 2 steps); f. 1 N HCl, dioxane (70% yield).

Bromomethylketone **2.8** (bmk) was synthesized via bromination of enol ether **2.5** with *N*-bromosuccinimide at –20°C, followed by removal of the *O*-silyl protecting group with 1 N HBr (Use of HCl instead led to a ~1:1 mixture of bmk and cmk). S_N2 displacement of the bromide of **2.6** with chloride, followed by deprotection with 1 N HCl afforded chloromethylketone **2.9** (cmk). Hydrolysis of enol ether **2.5** with 1 N HCl resulted in concomitant removal of the *O*-silyl protecting group; however, it could be easily

reinstalled using standard conditions to give ketone **2.8**. *N*-diboc protection of ketone **2.8** followed by treatment with LDA transiently generated the enolate of **2.11**, which could be reacted with the electrophilic fluorinating reagent, *N*-fluorobenzenesulfonimide, to yield the *N*-diboc-fluoromethylktone **2.12** (N-diboc-fmk). *N*-Boc deprotection of **2.12** with TFA gave the desired **2.13** (fmk) in good yield.

Potent inhibition of RSK CTD by fmk is dependent on two selectivity filters

We first tested the electrophilic pyrrolopyrimidines against the RSK2 CTD in vitro (*21*). Fmk (**Table 2-1**) cmk, and bmk inhibited RSK2 CTD activity with similar potencies, but we focused on fmk because of its greater chemical stability. In fact, bmk was completely unstable in aqueous solution, limiting its utility in cells. To test whether both selectivity filters were required for fmk sensitivity, we expressed two CTD mutants, C436V, in which Cys436 was replaced with Val, and T493M, in which Thr493 was replaced with Met.

	WT	C436V	T493M
fmk	0.015 ± 0.001	>10	3.4 ± 0.3
scaffold	1.2 ± 0.08	0.43 ± 0.14	>30

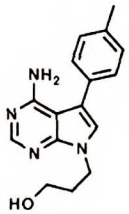

2.14 (scaffold)

Table 2-I. IC_{50} values (in μM) for fmk and the pyrrolo[2,3-*d*]pyrimidine scaffold against the kinase activities of wild-type (WT) and mutant RSK2 CTDs. RSK2 CTDs were expressed in *E. coli* as His_6-tagged proteins and activated by incubation with bacterially expressed His_6-ERK2 and ATP. Kinase assay conditions: 30 min inhibitor pretreatment, 1 nM RSK2 CTD, 0.1 mM ATP, 0.1 mM "CTD-tide" substrate [25]. WT and mutant CTDs had similar kinase activities.

Fmk was a potent and selective inhibitor of wild-type (WT) RSK2 (IC_{50} = 15 nM), with greater than 600- and 200-fold selectivity over the C436V and T493M mutants, respectively (**Table 2-1**). The electrophilic fluoromethylketone group is required for potent inhibition, as the parent scaffold (**2.14**) is 80-fold weaker than fmk toward WT

RSK2 CTD (**Table 2-1**). Fmk (1 μM) exhibited time-dependent inactivation of RSK2 CTD, with a half-time of less than 10 min in the presence of 1 mM ATP (**Figure 2-3**). Both selectivity filter mutants were not inhibited under these conditions. The time-dependent inhibition of fmk against WT RSK2 CTD is consistent with an irreversible mode of inactivation.

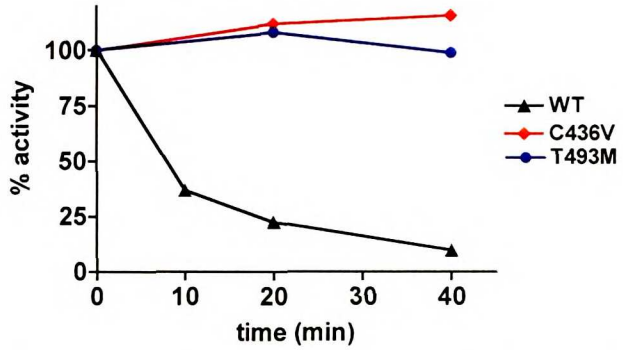

Figure 2-3. Time-dependent inhibition of WT RSK2 CTD. WT, C436V, and T493M RSK2 CTD (100 nM) were treated with fmk (1 μM) in the presence of 1 mM ATP for the indicated time intervals. After diluting the reactions 100-fold, kinase activity was measured as described in **Table 2-1**.

To test whether fmk forms an irreversible covalent bond with RSK2, we prepared a biotinylated derivative (fmk-biotin, see **Scheme 2-4**). Briefly, **2.15** was prepared in a two-step, one-pot sequence involving formation of an imidazole ester intermediate, followed by reaction with *N*-Boc-1,4-diaminobutane. Removal of the *N*-boc protecting groups followed by conjugation with biotin-NHS afforded **2.16** (fmk-biotin).

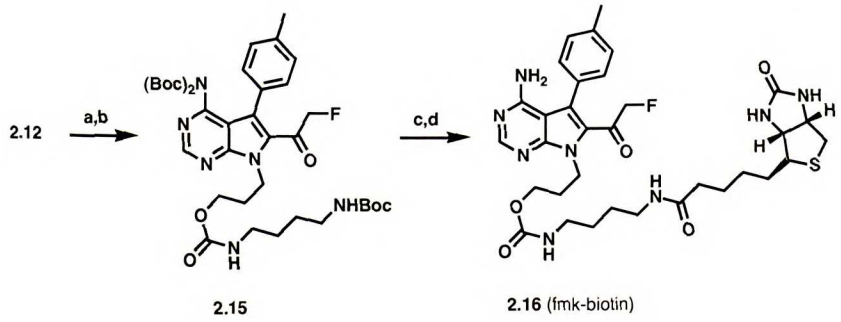

Scheme 2-4. Synthesis of fmk-biotin. Reagents and conditions: a. carbonyldiimidazole, DIPEA, CH_2Cl_2, then *N*-Boc-1,4-diaminobutane (69% yield); c. TFA, CH_2Cl_2; d. biotin-NHS, DIPEA, DMF (71% yield over 2 steps).

Fmk-biot

as show

horsera

labeled

pocket

Fig

wit

de

R

Fmk-biotin reacted irreversibly with WT RSK2, but not with the selectivity filter mutants, as shown by denaturing gel electrophoresis and Western blot analysis with streptavidin-horseradish peroxidase (**Figure 2-4**). ERK2, required to activate RSK2 in vitro, was not labeled by fmk-biotin, despite the presence of a solvent-exposed cysteine in its ATP pocket [26].

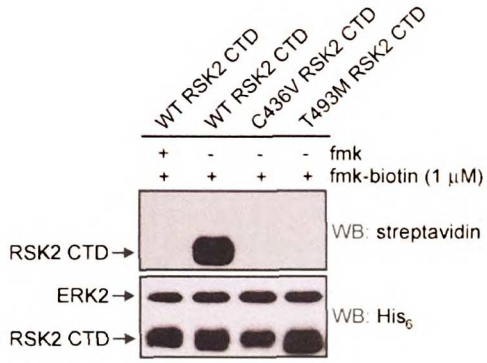

Figure 2-4. Covalent labeling of WT, but not mutant RSK2 by fmk-biotin. His_6-RSK2 CTDs were treated with 1 μM fmk-biotin in the presence of His_6-ERK2 for 1 hour. Proteins were resolved by SDS-PAGE and detected by Western blot with streptavidin-horseradish peroxidase (HRP) or antibodies to His_6.

Remarkable kinetic selectivity of fmk-biotin in cell lysates

We next tested the selectivity of fmk-biotin in a human epithelial cell lysate containing thousands of potentially reactive proteins. Fmk-biotin (1 μM) reacted with only two proteins, and labeling was abolished by pretreatment with 1 μM fmk (**Figure 2-5a**). These ~90 kD proteins were shown to be RSK1 and RSK2 by quantitative immunodepletion with specific antibodies (**Figure 2-5b**).

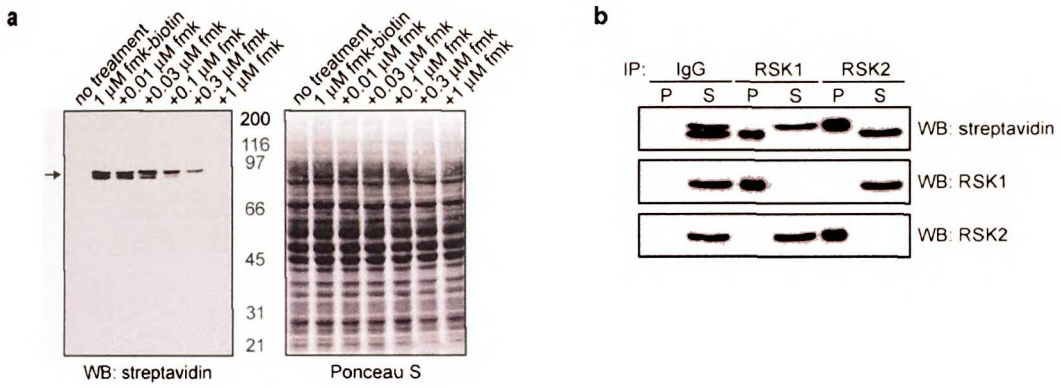

Figure 2-5. Selective, irreversible targeting of RSK1 and RSK2 by fmk-biotin. (**a**) Targeting of two ~90 kD proteins in human epithelial cell lysates by fmk-biotin. HEK-293 cell lysates were treated with the indicated concentrations of unlabeled fmk and then with 1 μM fmk-biotin. Proteins were resolved by SDS-PAGE, transferred to nitrocellulose, and stained with Ponceau S (right panel). Proteins labeled with biotin-fmk were detected with streptavidin-HRP (left panel). (**b**) Identification of RSK1 and RSK2 as biotin-fmk targets. HEK-293 lysates were treated with 1 μM biotin-fmk. Proteins were immunoprecipitated with control IgG, RSK1-specific polyclonal antibodies, or a RSK2-specific monoclonal antibody (Santa Cruz Biotechnology). Immunoprecipitates (P) and supernatants (S) were analyzed by Western blot with streptavidin-HRP and antibodies to RSK1 and RSK2.

Fmk potently inhibits RSK activity in cells

The only known substrate of the RSK2 CTD is Ser386 of RSK2 itself[27,28]. Phosphorylation of Ser386 creates a docking site for phosphoinositide-dependent kinase 1 (PDK1), which then phosphorylates and activates the N-terminal kinase domain (NTD)[29]. The activated NTD then phosphorylates downstream substrates. Treatment of serum-starved COS-7 cells with EGF induced Ser386 phosphorylation of endogenous RSK2, which was inhibited by fmk with an EC_{50} of ~200 nM (**Figure 2-6a**). Thus, the CTD appears to be the primary kinase responsible for EGF-stimulated Ser386 phosphorylation, consistent with results obtained with kinase-inactive mutants[27,28]. Fmk (10 μM) had no effect on EGF-stimulated phosphorylation of ERK1 or ERK2 (**Figure 2-6b**), the MAP kinases directly upstream of RSK2. This result further highlights the selectivity of fmk, as the signaling pathway leading to ERK activation involves at least three protein kinases (EGFR, Raf, and MEK), two of which (EGFR and Raf) have

threonine gatekeepers, as well as potentially reactive cysteines in their ATP binding pockets.

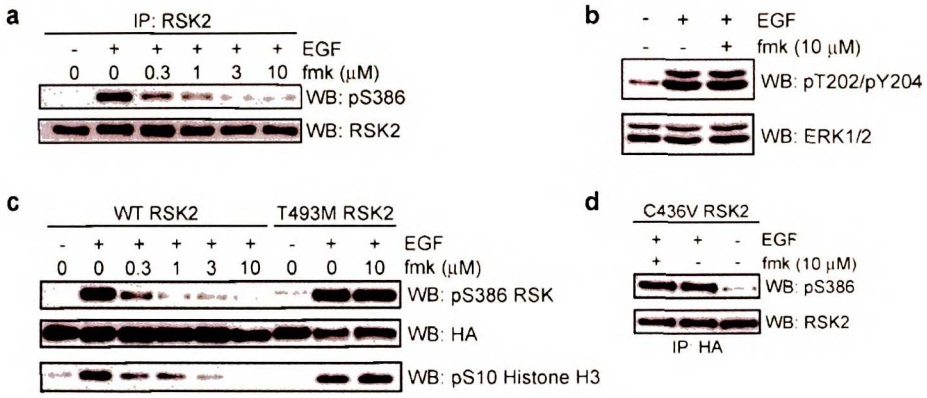

Figure 2-6. Effect of fmk on EGF-activated RSK2. (**a**) Inhibition of EGF-stimulated RSK2 autophosphorylation by fmk. COS-7 cells were deprived of serum for 20 hours, then treated with the indicated concentrations of fmk. Cells were stimulated for 10 min with EGF (1 ng/mL). RSK2 was immunoprecipitated and analyzed by Western blot with antibodies to phospho-Ser386 RSK (Cell Signaling Technology) and total RSK2. (**b**) Failure of fmk to inhibit EGF-stimulated activation of ERK1 and ERK2. Serum-starved COS-7 cells were treated with or without 10 μM fmk, then stimulated with EGF as in (**a**). Doubly phosphorylated and total ERK1 and ERK2 were detected by Western blot (both antibodies from Cell Signaling Technology). (**c**) Inhibition of EGF-stimulated histone H3 phosphorylation in cells expressing WT RSK2, but not T493M RSK2. COS-7 cells were transfected with HA-tagged WT or T493M RSK2. 24 hours post-transfection, cells were serum-starved for 3 hours, then treated with the indicated concentrations of fmk. Cells were stimulated with EGF (150 ng/mL) for 25 min and subsequently lysed in Laemmli sample buffer. Proteins were resolved by SDS-PAGE and detected by Western blot with antibodies specific for phospho-Ser386 RSK, the HA epitope (Roche), or phospho-Ser10 histone H3 (Upstate). (**d**) Mutation of Cys436 to Val in RSK2 confers resistance to fmk. COS-7 cells were transfected with HA-tagged C436V RSK2. 48 hours post-transfection, cells were deprived of serum for 23 hours and then treated with either fmk (10 μM) or DMSO for 90 min. After stimulation for 10 min with EGF (30 ng/mL), HA-tagged C436V RSK2 was immunoprecipitated from cell lysates. Proteins were resolved by SDS-PAGE and detected by Western blot with antibodies against phospho-Ser386 RSK or RSK2.

We next tested whether inhibition of the CTD by fmk could block signaling downstream of RSK2. In cells transfected with WT RSK2, treatment with EGF induced phosphorylation of histone H3 at Ser10, which was completely blocked by fmk (**Figure 2-6c**). By contrast, histone H3 phosphorylation was unaffected by up to 10 μM fmk in cells expressing the RSK2 gatekeeper mutant, T493M. Mutation of the cysteine selectivity filter to valine (C436V) also conferred complete resistance to fmk (**Figure 2-6d**).

Introduction of absent selectivity filter confers sensitivity to fmk and cmk

Similar to RSK-family kinases, the mitogen- and stress-activated kinases, MSK1 and MSK2, have two kinase domains. The CTD of MSK1 has a cysteine analogous to Cys436 of RSK2 (Fig. 1A), but unlike RSK2, MSK1 has a methionine gatekeeper. Fmk had no effect on histone H3 phosphorylation mediated by WT MSK1 (**Figure 2-7a**). By contrast, an MSK1 mutant with a threonine gatekeeper was potently inhibited. Thus, despite having only ~40% sequence identity to RSK2, MSK1 became equally sensitive to fmk once the second selectivity filter was introduced. Fmk had no effect on phorbol ester-stimulated histone H3 phosphorylation in nontransfected fibroblasts (**Figure 2-7b**), consistent with a dominant role for endogenous MSK1 and MSK2 in this pathway [30].

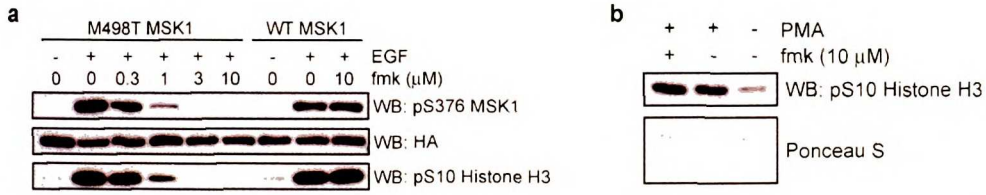

Figure 2-7. Effect of fmk on WT and M498T MSK1. (**a**) Inhibition of MSK1 by fmk after mutation of Met498 to Thr. COS-7 cells were transfected with HA-tagged WT or M498T MSK1. MSK1 autophosphorylation and histone H3 phosphorylation were assessed as in **Figure 2-6c**. (**b**) Fmk does not inhibit PMA-stimulated histone H3 phosphorylation in NIH-3T3 fibroblasts. Cells were deprived of serum for 24 hours, then treated with fmk (10 mM) or DMSO for 90 min. After stimulation for 20 min with PMA (100 ng/mL), histones were isolated, resolved by SDS-PAGE and analyzed by Ponceau S staining and Western blot with phospho-Ser10 histone H3 antibodies (Upstate).

Pyrrolo[2,3-*d*]pyrimidines inhibit Src-family kinases such as Fyn[31], raising the possibility that they might be susceptible to reversible inhibition by our designed halomethylketones. WT Fyn was weakly inhibited by cmk and fmk, with IC_{50} values of ~4 μM (compared to an IC_{50} value of 15 nM for fmk against RSK2). By contrast, cmk and fmk potently inhibited a Fyn mutant in which Val285 was replaced with Cys (IC_{50} values of 1 nM and 100 nM, respectively). Similarly, at concentrations that completely inhibited RSK2 in cells, neither cmk nor fmk reversed the cellular phenotypes induced by v-Src (with a Thr in the gatekeeper position) (**Figure 2-8a,b**). By contrast, cmk (and less

recently, fr

tyrosine ph

was replac

bond fro

synthesis

WT v-Sr

block le

(omit-E

showe

predo

of oth

muc

hyd

potently, fmk) promoted morphological reversion (**Figure 2-9**) and reduced global tyrosine phosphorylation in NIH-3T3 cells expressing a v-Src mutant in which Val281 was replaced with Cys (**Figure 2-8a,b**). Consistent with a mechanism involving covalent bond formation, a biotinylated derivative of cmk (cmk-biotin, see **Scheme 2-5**, synthesized using a similar route to fmk-biotin) irreversibly labeled V281C v-Src, but not WT v-Src (**Figure 2-10**). Treatment of cells with 1 μM cmk is sufficient to completely block labeling of V281C v-Src by cmk-biotin. Finally, a fluorescent derivative of cmk (cmk-BODIPY, see **Scheme 2-6**, synthesized using a similar route to cmk-biotin) showed remarkable selectivity when added to NIH-3T3 cells, with V281C v-Src being the predominantly labeled protein (**Figure 2-11**). By contrast to V281C v-Src, weak labeling of other proteins was not competed by 3 μM cmk pretreatment. Therefore, we attribute much of the non-specific labeling to the BODIPY fluorophore, which is bulkier and more hydrophobic than cmk itself.

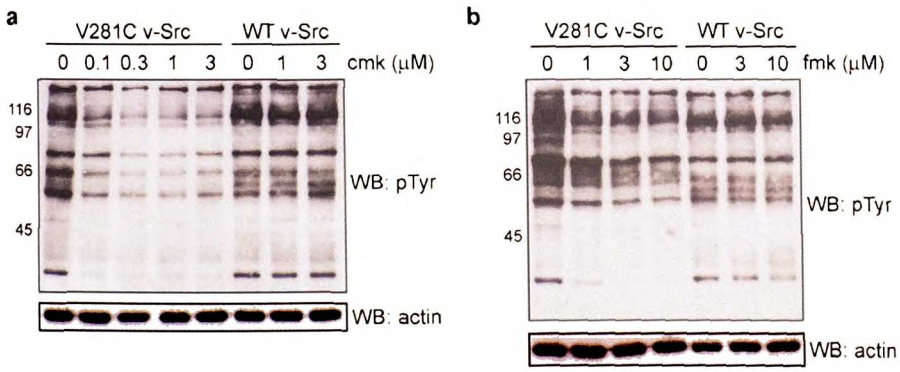

Figure 2-8. Effect of cmk and fmk on WT and cysteine-engineered Src-family kinases. (**a**) Cmk reduces steady-state phosphotyrosine levels in NIH-3T3 cells stably expressing V281C v-Src, but not WT v-Src. Both v-Src constructs also contained a threonine in the gatekeeper position. Cells were treated with the indicated concentrations of cmk for 1 hour. Whole-cell lysates were resolved by SDS-PAGE and phosphotyrosine-containing proteins were detected by Western blot with the 4G10 antibody (Upstate). To control for protein loading, the blot was reprobed with an actin antibody. (**b**) Inhibition of tyrosine phosphorylation in v-Src expressing cells by fmk was assessed as in (**a**).

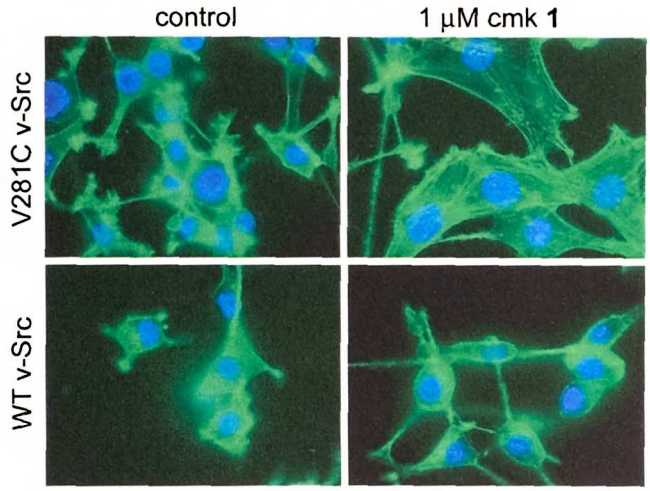

Figure 2-9. NIH-3T3 cells expressing V281C but not WT v-Src, revert to a flat morphology upon treatment with cmk. Cells were treated with or without cmk (1 μM) for 16 hours. Fixed cells were stained with phalloidin-FITC and DAPI to visualize actin filaments (green) and nuclei (blue). Cells expressing V281C v-Src acquired actin stress fibers upon treatment with cmk (75% of treated cells, n=220 vs. 6% of untreated cells, n=153), whereas fewer than 2% of the cells expressing WT v-Src and treated with cmk had actin stress fibers (n=83).

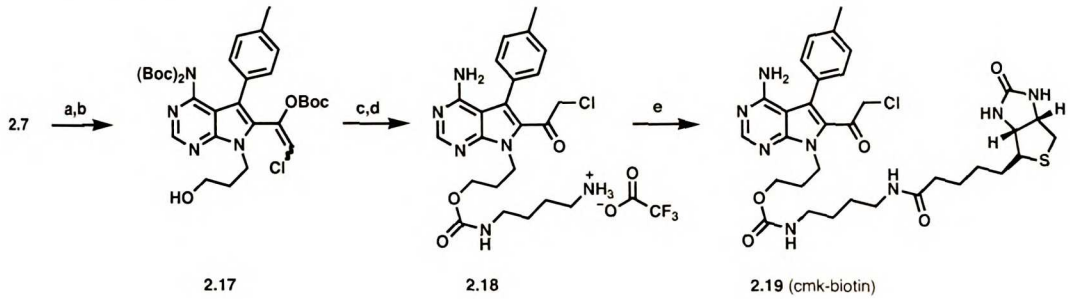

Scheme 2-5. Synthesis of cmk-biotin. Reagents and conditions: a. $(Boc)_2O$, DMAP, THF; b. 1 N HCl, THF (84% yield over 2 steps); c. carbonyldiimidazole, DIPEA, CH_2Cl_2, then *N*-Boc-1,4-diaminobutane (69% yield); d. TFA, CH_2Cl_2 (73% over 2 steps); e. biotin-NHS, DIPEA, DMF (70% yield).

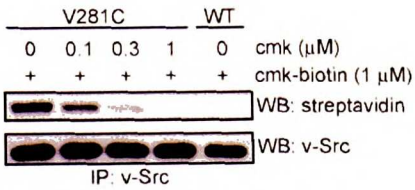

Figure 2-10. Irreversible labeling of Val281Cys v-Src, but not WT v-Src by cmk-biotin. NIH-3T3 cells expressing either V281C or WT v-Src were pretreated with varying concentrations of cmk for 1 h at 37°C. After washing the cells, lysates were prepared and treated with cmk-biotin (1 μM). v-Src was immunoprecipitated and detected by Western blot with streptavidin-HRP and a v-Src antibody. Pretreatment of cells with 1 μM cmk completely prevents subsequent labeling by cmk-biotin.

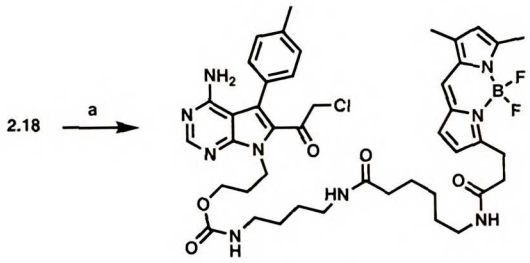

2.20 (cmk-BODIPY)

Scheme 2-6. Synthesis of cmk-BODIPY. Reagents and conditions: a. BODIPY FL-NHS, DIPEA, DMF (100% yield).

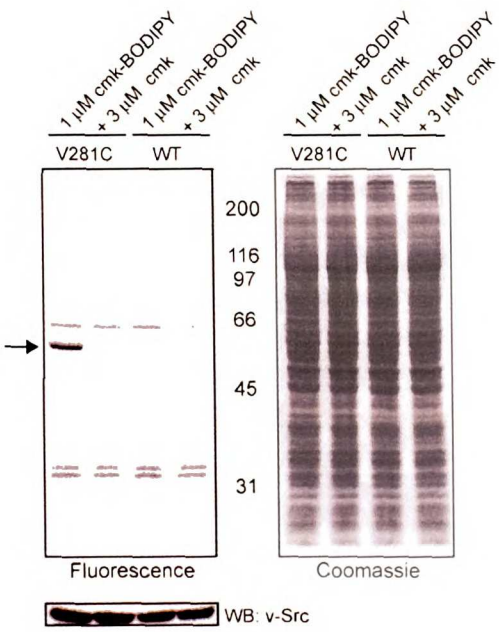

Figure 2-11. Cmk-BODIPY preferentially labels V281C v-Src. NIH-3T3 cells expressing either WT or V281C v-Src were treated with 3 μM cmk or DMSO control, followed by 1 μM cmk-BODIPY. After treatment, cells were washed with cold PBS and lysates were prepared. Proteins were resolved by 10% SDS-PAGE and detected by in-gel fluorescence scanning, followed by Western blotting with an antibody to v-Src.

Conclusion

In this study, we have rationally designed halomethylketone-substituted inhibitors whose molecular recognition by protein kinases requires the simultaneous presence of

two selectivity filters: a cysteine following the glycine-rich loop and a threonine in the gatekeeper position. We estimate that ~20% of human kinases have a solvent-exposed cysteine in the ATP pocket. Because of the structural conservation of the pocket, it should be possible to predict the orientation of these cysteines. In addition, there are many reversible kinase inhibitors whose binding modes have been characterized by x-ray crystallography. The integration of both types of information should allow the design of scaffolds that exploit selectivity filters other than the gatekeeper, as well as the appropriate sites for attaching electrophilic substituents.

Expe

Chem

Gene

and

dow

sol

rea

pe

2

in

V

S

Experimental

Chemical synthesis

General. ^{1}H and ^{13}C NMR spectra were recorded on a Varian 400 spectrometer at 400 and 100 MHz, respectively. Chemical shifts were reported as parts per million (ppm) downfield from an internal tetramethylsilane standard (δ = 0.0 for ^{1}H NMR) or from solvent references. Low-resolution electrospray ionization mass spectra (EI^{+}-MS) were recorded on a Waters Micromass ZQ 4000 spectrometer. LC/MS (MS: EI^{+}) was performed on a Waters AllianceHT LC/MS with a flow rate of 0.2 mL/min (monitored at 210 nm and 260 nm) using an Xterra MS C18 column (Waters). High-resolution electron impact mass spectra (HRMS) were recorded on a Micromass VG70E spectrometer by Yuequan Sun at the University of California-San Francisco Biomedical Mass Spectrometry Center. For air- and water-sensitive reactions, glassware was oven- or flame-dried prior to use and reactions were performed under argon. Dichloromethane, dimethylformamide, methanol, tetrahydrofuran, toluene, and diisopropylamine were dried using the solvent purification system manufactured by Glass Contour, Inc. (Laguna Beach, CA). All other solvents were of ACS chemical grade (Fisher) and used without further purification unless otherwise indicated. Commercially available starting reagents were used without further purification. Many of the pyrrolo[2,3-*d*]pyimidine compounds were sparingly soluble in acetonitrile and concentration from this solvent often yielded a nice solid. 6-((4,4-difluoro-5,7-dimethyl-4-bora-3a,4a-diaza-*s*-indacene-3-propionyl)amino)hexanoic acid, succinimidyl ester (BODIPY FL-NHS) was purchased from Invitrogen and used without further purification Analytical and preparative thin layer chromatography were performed with silica gel 60 F_{254} glass plates (EM Science). Flash chromatography was conducted with 230-400 mesh silica gel (Selecto Scientific). High performance liquid chromatography (HPLC) was performed on a Prostar 210 (Varian)

with a fl

prepara

Amino

MeO

meth

temp

colle

of p

δ 7

3-

with a flow rate of 10 mL/min (monitored at 210 nm and 260 nm) using a COMBI-A C18 preparatory column (Peeke Scientific).

Amino pyrrole **2.1**. To a solution of malononitrile (3.24 g, 48.9 mmol) in 6:1:1 MeOH/48% aq. (w/w) $NaOH/H_2O$ (56 mL) was added 2-phthalimido-4'-methylacetophenone (10.5 g, 37.6 mmol). The reaction mixture was stirred at room temperature for 1 h after which the product precipitated out of solution. The solid was collected by filtration, washed with H_2O, CH_2Cl_2, and hexanes to give 6.7 g (91% yield) of pyrrole **1** as a brown solid: R_f 0.70 (10% $MeOH/CH_2Cl_2$); ^{1}H NMR (400 MHz, CD_3OD) δ 7.409 (d, J = 7.6 Hz, 2H), 7.08 (d, J = 7.6 Hz, 2H), 6.36 (s, 1H), 4.83 (br s 2H), 2.27 (s, 3H); ^{13}C NMR (100 MHz, CD_3OD) (partial) δ 136.9, 130.1, 126.6, 120.1, 109.0, 21.1.

N-alkyl pyrrole iminoether **2.2**. A solution of pyrrole **2.1** (5 g, 25.3 mmol) in triethyl orthoformate (30 mL) was treated with acetic anhydride (0.5 mL) and refluxed for 1 h. After cooling to room temperature, the solvent was removed *in vacuo*. The crude pyrrole iminoether was azeotropically dried with toluene (2 x 10 mL) and carried on directly to the next step.

To a suspension of NaH (60% in oil, 0.9 g, 23.4 mmol) in 20 mL of DMF at room temperature was added a solution of the crude pyrrole iminoether in 10 mL of DMF. After stirring for 30 min, 3-(*t*-butyldimethylsilyloxy)propyl iodide[32] (7.0 g, 23.4 mmol) was added over 10 min. After stirring for an additional 3 h, the solvent was removed *in vacuo* and the residue was purified by flash chromatography (10-50% ethyl acetate/hexanes) to afford 5 g (70% yield) of *N*-alkyl pyrrole iminoether **2.2** as a brown oil: R_f 0.8 (4:1 hexanes/ethyl acetate); ^{1}H NMR (400 MHz, $CDCl_3$) δ 8.43 (s, 1H), 7.47 (d, J = 8.0 Hz, 2H), 7.16 (d, J = 8.0 Hz, 2H), 6.62 (s, 1H), 4.32 (q, J = 8.0 Hz, 2H), 3.96 (t, J = 7.2 Hz,

2H), 3.59 (t, J = 5.6 Hz, 2H), 2.33 (s, 3H), 1.91-1.82 (m, 2H), 1.37 (t, 3H), 0.88 (s, 9H), 0.03 (s, 6H); ^{13}C NMR (100 MHz, $CDCl_3$) δ 158.2, 144.1, 136.8, 130.5, 129.7, 126.2, 125.0, 118.5, 115.6, 63.4, 59.7, 43.1, 33.4, 26.1, 21.4, 18.5, 14.2.

Pyrrolo[2,3-*d*]pyrimidine-OTBS **2.3**. *N*-alkyl pyrrole iminoether **2.2** (18.0 g, 42.3 mmol) was dissolved in MeOH (100 mL) and transferred to 350 mL sealed-tube reaction vessel. Argon gas was then bubbled through the solution for 15 min. The reaction vessel was submerged in a dry ice/MeOH bath and NH_3 gas was bubbled through the solution for 15 min. The reaction vessel was quickly sealed with a Teflon screw cap (fitted with a rubber O-ring) and allowed to warm to room temperature. The reaction was stirred for 4 days at 50°C and then submerged in an ice bath. The NH_3 gas was slowly released. The solvent was removed *in vacuo* and the crude product purified by flash chromatography (3:2 ethyl acetate/hexanes with 1% Et_3N) to give 10.1 g (61% yield) of **2.3** as a light-brown solid: R_f 0.41 (1:1 hexanes/ethyl acetate); ^1H NMR (400 MHz, $CDCl_3$) δ 8.32 (s, 1H), 7.37 (d, J = 8.4 Hz, 2H), 7.26 (d, J = 8.0 Hz, 2H), 6.92 (s, 1H), 5.1 (br s, 2H), 4.34 (t, J = 6.8 Hz, 2H), 3.65 (t, J = 6.0 Hz, 2H), 2.41 (s, 3H), 2.10-2.05 (m, 2H), 0.91 (s, 9H), 0.05 (s, 6H); ^{13}C NMR (100 MHz, $CDCl_3$) δ 156.9, 151.9, 150.6, 136.8, 132.0, 129.7, 128.7, 123.2, 115.8, 101.3, 59.8, 41.5, 33.0, 25.9, 21.1, 18.2; EI^+-MS 419 $[M+Na]^+$, 397 $[M+H]^+$.

Bromide-OTBS **2.4**. To a solution of **2.3** (1.5 g, 3.78 mmol) in DMF (20 mL) was added *N*-bromosuccinimide (0.74 g, 4.16 mmol) and the mixture stirred for 24 h protected from light. The reaction was diluted with ether (100 mL) and washed with water (3 x 200 mL). The combined aqueous fractions were extracted with ether (3 x 50 mL). The combined organic fractions were dried over anhydrous Na_2SO_4, filtered, and concentrated *in vacuo* to give 1.77 g (99% yield) of bromide-OTBS **2.4** as a brown solid: R_f 0.59 (100% ethyl

acetate); ^{1}H NMR

8.0 Hz, 2H), 5.0 (t

2.1 (m, 2H), 0.9/1

475 [M]$^+$.

Enol ether-OTB

mL) was adde

through the sc

mmol) was qu

in vacuo and

hexanes/ethy

solid: R_f 0.25

7.31 (d, J =

1H), 4.33 (t,

= 6.0 Hz, 2

6H); ^{13}C N

130.2, 129

489 [M+Na

Bromom

DMF (2

bromosu

dark. A

saturat

over a

colum

acetate); ^{1}H NMR (400 MHz, $CDCl_3$) δ 8.21 (s, 1H), 7.35 (d, *J* = 8.0 Hz, 2H), 7.30 (d, *J* = 8.0 Hz, 2H), 5.0 (br s, 2H), 4.41 (t, *J* = 6.8 Hz, 2H), 3.73 (t, *J* = 6.0 Hz, 2H), 2.43 (s, 3H), 2.1 (m, 2H), 0.91 (s, 9H), 0.06 (s, 6H); EI$^+$-MS 500 $[M+2+Na]^+$, 497 $[M+Na]^+$, 477 $[M+2]^+$, 475 $[M]^+$.

Enol ether-OTBS **2.5**. To a solution of bromide **2.4** (389 mg, 0.82 mmol) in toluene (10 mL) was added a-(ethoxyvinyl)tin (0.390 mL, 1.15 mmol). Argon gas was bubbled through the solution for 10 min. Tetrakis(triphenylphosphine)palladium (95 mg, 0.082 mmol) was quickly added and mixture was refluxed for 16 h. The solvent was removed in vacuo and the crude product was purified by flash chromatography (50-100% hexanes/ethyl acetate) to give enol ether-OTBS **2.5** (304 mg, 80% yield) as a yellow solid: R_f 0.25 (1:1 hexanes/ethyl acetate); ^{1}H NMR (400 MHz, $CDCl_3$) δ 8.31 (s, 1H), 7.31 (d, *J* = 8.0 Hz, 2H), 7.22 (d, *J* = 8.0 Hz, 2H), 4.99 (br s, 2H), 4.39 (d, *J* = 2.0 Hz, 1H), 4.33 (t, *J* = 6.0 Hz, 1H), 4.17 (d, *J* = 2.0 Hz, 2H), 3.84 (q, *J* = 6.8 Hz, 2H), 3.73 (t, *J* = 6.0 Hz, 2H), 2.40 (s, 3H), 2.1 (m, 2H), 1.34 (t, *J* = 7.2 Hz, 3H), 0.89 (s, 9H), 0.05 (s, 6H); ^{13}C NMR (100 MHz, $CDCl_3$) δ 157.3, 152.4, 152.0, 150.2, 137.1, 131.9, 130.9, 130.2, 129.4, 114.9, 101.7, 91.6, 63.6, 61.2, 41.2, 33.5, 26.1, 21. 4, 18.5, 14.6; EI$^+$-MS 489 $[M+Na]^+$, 467 $[M+H]^+$.

Bromometylketone-OTBS **2.6** (bmk-OTBS). To a solution of **2.5** (81 mg, 0.17 mmol) in DMF (2 mL) and H_2O (0.006 mL) at –20°C was added $NaHCO_3$ (22 mg, 0.26 mmol). *N*-bromosuccinimide (31 mg, 0.17 mmol) was added and mixture was stirred at rt in the dark. After 15 min, the reaction was diluted with ethyl acetate (20 mL) and washed with saturated Na_2SO_3 (1 x 10 mL) and H_2O (1 x 10 mL). The organic fraction was dried over anhydrous Na_2SO_4, filtered, and concentrated *in vacuo*. Rapid purification by flash column chromatography (1:1 hexanes/ethyl acetate) gave 52 mg (60% yield) of **2.6** as a

yellow solid: R_f 0.6 (100% ethyl acetate); ^{1}H NMR (400 MHz, $CDCl_3$) δ 8.31 (s, 1H), 7.32 (s, 4H), 4.60 (t, J = 6.8 Hz, 2H), 3.69 (s, 2H), 3.67 (t, J = 6.0 Hz, 2H), 2.43 (2. 3H), 2.1 (m, 2H), 0.91 (s, 9H), 0.06 (s, 6H); EI$^+$-MS 519 $[M+2]^+$, 517 $[M]^+$.

Chloromethylketone-OTBS **2.7** (cmk-OTBS). To a solution of **2.6** (318 mg, 0.615 mmol) in acetone (1 mL) was added saturated LiCl. After 1 h, the reaction was diluted with ethyl acetate (20 mL) and washed with H_2O (1 x 5 mL) and brine (1 x 5 mL). The organic fraction was dried over anhydrous Na_2SO_4, filtered, and concentrated *in vacuo*. Rapid purification by flash column chromatography (1:1 hexanes/ethyl acetate) gave 291 mg (100% yield) of **2.7** as a yellow solid: R_f 0.6 (100% ethyl acetate); ^{1}H NMR (400 MHz, $CDCl_3$) δ 8.35 (s, 1H), 7.35 (s, 4H), 5.0 (br s, 2H), 4.68 (t, J = 6.8 Hz, 2H), 3.92 (s, 2H), 3.71 (t, J = 6.6 Hz, 2H), 2.48 (s, 3H), 2.01 (m, 2H); ^{13}C NMR (100 MHz, $CDCl_3$) δ 191.5, 185.1, 177.5, 158.8, 155.4, 139.7, 130.6, 130.3, 129.5, 127.8, 124.5, 61.0, 48.2, 41.6, 33.7, 29.6, 25.9, 21.4, 18.3; EI$^+$-MS 497 $[M+2+Na]^+$, 495 $[M+Na]^+$, 475 $[M+2]^+$, 473 $[M]^+$.

Bromomethylketone **2.8** (bmk). To a solution of **2.6** (18 mg, 0.035 mmol) in THF (1 mL) at 0°C was added 1 N HBr (0.33 mL). After stirring for 30 min at 0°C and 2 h at rt, the reaction was diluted with ethyl acetate (5 mL) and washed with saturated $NaHCO_3$ (1 x 5 mL) and H_2O (1 x 5 mL). The organic fraction was dried over anhydrous Na_2SO_4, filtered, and concentrated *in vacuo*. Purification by preparative HPLC (30-100% MeOH gradient over 15 min; 10 mL/min; retention time, 11.9 min), afforded **2.8** (bmk) (5 mg, 36% yield) as an off-white solid: ^{1}H NMR (400 MHz, $CDCl_3$) d 8.36 (s, 1H), 7.38 (br s, 4H), 5.0 (br s, 2H), 4.66 (t, J = 5.6 Hz, 2H), 3.74 (s, 2H), 3.46 (m, 2H), 2.49 (s, 3H), 2.10 (m, 2H); ^{13}C NMR (100 MHz, $CDCl_3$) d 185.4, 159.0, 155.6, 151.9, 139.9, 130.4, 130.3,

129.5, 128.1, 124.7, 1

HRMS (EI) Calcd for C

Chloromethylketone 2

(32 mg, 0.067 mmol)

for 30 min at 0°C an

washed with saturate

was dried over anhy

preparative HPLC (

11.2 min), afforded

$CDCl_3$) d 8.36 (s, 1

4.67 (t, J = 6.0 Hz,

(100 MHz, $CDCl_3$

124.8, 102.1, 57.7

Calcd for $C_{18}H_{19}Cl$

Methylketone-OT

in toluene (20 m

bubbled through

mg, 0.307 mmol

removed *in vac*

mL). After stir

ethyl acetate (5

was extracted

fraction was b

mL). The com

129.5, 128.1, 124.7, 102.1, 57.7, 40.5, 34.3, 32.9, 21.4; ES^+-MS 405 $[M + 2]^+$, 403 $[M]^+$; HRMS (EI) Calcd for $C_{18}H_{19}BrN_4O_2$ 402.0691, found 402.0699.

Chloromethylketone **2.9** (cmk). To a solution of the silyl-protected chloromethylketone (32 mg, 0.067 mmol) in THF (1 mL) at 0°C was added 1 N HCl (0.33 mL). After stirring for 30 min at 0°C and 2 h at rt, the reaction was diluted with ethyl acetate (5 mL) and washed with saturated $NaHCO_3$ (1 x 5 mL) and brine (1 x 5 mL). The organic fraction was dried over anhydrous Na_2SO_4, filtered, and concentrated *in vacuo*. Purification by preparative HPLC (30-100% MeOH gradient over 15 min; 10 mL/min; retention time, 11.2 min), afforded **2.9** (cmk) (11 mg, 46% yield) as a white solid: ^1H NMR (400 MHz, $CDCl_3$) d 8.36 (s, 1H), 7.37 (d, J = 8.0 Hz, 2H), 7.36 (d, J = 8.0 Hz, 2H), 5.0 (br s, 2H), 4.67 (t, J = 6.0 Hz, 2H), 3.93 (s, 2H), 3.40 (m, 2H), 2.49 (s, 3H), 2.10 (m, 2H); ^{13}C NMR (100 MHz, $CDCl_3$) d 185.1, 159.1, 155.8, 151.8, 140.0, 130.5, 130.3, 129.5, 128.1, 124.8, 102.1, 57.7, 48.2, 40.6, 32.9, 21.4; ES^+-MS 361 $[M + 2]^+$, 359 $[M]^+$; HRMS (EI) Calcd for $C_{18}H_{19}ClN_4O_2$ 358.1196, found 358.1196.

Methylketone-OTBS **2.10** (mk-OTBS). To a solution of bromide **2.4** (1.46 g, 3.07 mmol) in toluene (20 mL) was added α-(ethoxyvinyl)tin (1.24 mL, 3.68 mmol). Argon gas was bubbled through the solution for 10 min. Tetrakis(triphenylphosphine)palladium (355 mg, 0.307 mmol) was quickly added and mixture was refluxed for 16 h. The solvent was removed *in vacuo* and the crude product was dissolved in THF (10 mL) and 1N HCl (3 mL). After stirring for 12 h at room temperature, the reaction mixture was diluted with ethyl acetate (50 mL) and washed with saturated $NaHCO_3$ (200 mL). The crude product was extracted from the organic fraction with 1 N HCl (2 x 150 mL). The acidic aqueous fraction was brought to pH~8 with NaOH and then extracted with ethyl acetate (2 x 150 mL). The combined organic fractions were dried over Na_2SO_4, filtered, and concentrated

in vacuo to give 850 mg

^{1}H NMR (400 MHz, CDC

2H), 2.46 (s, 3H), 2.08

based on ^{1}H NMR, was

To a solution c

added imidazole (450

3.14 mmol). After stirr

into 150 mL of 10%

The organic fraction

and concentrated

acetate/hexanes) pro

acetate); ^{1}H NMR (4

J = 6.8 Hz, 2H), 3.6

6H); ^{13}C NMR (10

129.9, 129.7, 123.9

N-diboc methylke

2.10 (780 mg, 1.

DMAP (44 mg, 0

room temperatur

washed with 0.5

dried over Na_2S

chromatography

(4:1 hexanes/et

(t, J = 6.8 Hz, 2

in vacuo to give 850 mg (85% yield) of the TBS-deprotected ketone as an off-white solid: ^{1}H NMR (400 MHz, $CDCl_3$) δ 8.35 (s, 1H), 7.34 (s, 4H), 4.67 (t, *J* = 5.6 Hz, 2H), 3.40 (m, 2H), 2.46 (s, 3H), 2.08 (m, 2H), 2.0 (s, 3H). The crude product, which was >95% pure based on ^{1}H NMR, was used in the next reaction without further purification.

To a solution of the crude ketone (850 mg, 2.62 mmol) in DMF (15 mL) was added imidazole (450 mg, 6.60 mmol) followed by *t*-butyldimethylsilyl chloride (474 mg, 3.14 mmol). After stirring for 12 h at room temperature, the reaction mixture was poured into 150 mL of 10% citrate buffer [pH 4.0] and extracted with ethyl acetate (200 mL). The organic fraction was washed with brine (1 x 200 mL), dried over Na_2SO_4, filtered, and concentrated *in vacuo*. Purification by flash chromatography (1:1 ethyl acetate/hexanes) provided **2.10** (876 mg, 76% yield over 3 steps): R_f 0.70 (100% ethyl acetate); ^{1}H NMR (400 MHz, $CDCl_3$) δ 8.28 (s, 1H), 7.28 (s, 4H), 5.10 (br s, 2H), 4.60 (t, *J* = 6.8 Hz, 2H), 3.66 (t, *J* = 6.0 Hz, 2H), 2.41 (s, 3H), 1.94 (s, 3H), 0.85 (s, 9H), 0.05 (s, 6H); ^{13}C NMR (100 MHz, $CDCl_3$) δ 192.0, 158.8, 154.9, 151.0, 138.8, 131.7, 130.1, 129.9, 129.7, 123.9, 102.0, 61.1, 41.3, 33.8, 30.9; EI^+-MS 439.1 $[M+H]^+$.

<u>*N*-diboc methylketone-OTBS **2.11** (*N*-diboc mk-OTBS)</u>. To a solution of methylketone **2.10** (780 mg, 1.78 mmol) in THF (10 mL) was added $(Boc)_2O$ (1.16 g, 5.33 mmol). DMAP (44 mg, 0.36 mmol) was quickly added and the mixture was stirred for 2.5 h at room temperature. The reaction mixture was diluted with ethyl acetate (150 mL) and washed with 0.5 N HCl (200 mL) followed by brine (200 mL). The organic fraction was dried over Na_2SO_4, filtered, and concentrated *in vacuo*. Rapid purification by flash chromatography (1:5 ethyl acetate/hexanes) gave 884 mg (78% yield) of **2.11**: R_f 0.50 (4:1 hexanes/ethyl acetate); ^{1}H NMR (400 MHz, $CDCl_3$) δ 8.51 (s, 1H), 7.17 (s, 4H), 4.70 (t, *J* = 6.8 Hz, 2H), 3.64 (t, *J* = 6.0 Hz, 2H), 2.37 (s, 3H), 1.98 (s, 3H), 1.23 (s, 18H), 0.85

(s, 9H), 0.05 (s, 6H); ^{13}

129.3, 122, 114, 83.2, 6

N-diboc fluoromethyl

diisopropylamine (0.3

hexanes, 0.657 mL,

0°C. After 30 min, th

THF (2.5 mL) was a

min, then cooled to –

was added dropwise

25 min, saturated N

saturated NH_4Cl (1

fraction was dried c

was dissolved in 3:

mixture was dilute

(100 mL) followed

filtered, and conc

acetate/hexanes)

R_f 0.50 (100% eth

Hz, 2H), 7.20 (d,

(t, 1H), 3.41 (m,

$CDCl_3$) δ 189.4 (c

128.75, 123.5, 1

100% MeCN [0.

15.12 min; purity

(s, 9H), 0.05 (s, 6H); ^{13}C NMR (100 MHz, $CDCl_3$) δ 194, 153.8, 150.1, 138.1, 134, 129.9, 129.3, 122, 114, 83.2, 60.7, 41.5, 33.6, 31.2, 27.8, 25.9, 21.3, 18; EI^+-MS 639.2 $[M+H]^+$.

<u>*N*-diboc fluoromethylketone **2.12** (*N*-diboc fmk)</u>. A solution of THF (3 mL) and diisopropylamine (0.32 mL, 2.28 mmol) was cooled to -78°C. *n*-Butyllithium (2.48 M in hexanes, 0.657 mL, 1.63 mmol) was added and the reaction mixture was warmed to 0°C. After 30 min, the reaction was cooled to –78°C and **2.11** (800 mg, 1.25 mmol) in THF (2.5 mL) was added dropwise. The reaction mixture was warmed to 0°C over 20 min, then cooled to –78°C. *N*-fluorobenzenesulfonimide (631 mg, 2 mmol) in THF (2 mL) was added dropwise and the reaction mixture was warmed to room temperature. After 25 min, saturated NH_4Cl (1 mL) was added and the reaction mixture was poured into saturated NH_4Cl (150 mL) and extracted with ethyl acetate (100 mL). The organic fraction was dried over Na_2SO_4, filtered, and concentrated *in vacuo*. The crude product was dissolved in 3:1 THF/1 N HCl (12 mL). After 3 h at room temperature, the reaction mixture was diluted with ethyl acetate (100 mL) and washed with saturated $NaHCO_3$ (100 mL) followed by brine (100 mL). The organic fraction was dried over Na_2SO_4, filtered, and concentrated *in vacuo*. Purification by flash chromatography (1:4 ethyl acetate/hexanes) afforded **2.12** (408 mg, 60% yield over 2 steps) as an off-white solid: R_f 0.50 (100% ethyl acetate); ^1H NMR (400 MHz, $CDCl_3$) δ 8.91 (s, 1H), 7.24 (d, J = 8 Hz, 2H), 7.20 (d, J = 8 Hz, 2H), 4.70 (t, J = 6.0 Hz, 2H), 4.60 (d, J_{HF} = 47 Hz, 2H), 3.70 (t, 1H), 3.41 (m, 2H), 2.42 (s, 3H), 2.05 (m, 2H), 1.29 (s, 18H); ^{13}C NMR (100 MHz, $CDCl_3$) δ 189.4 (d, J_{CF} = 19 Hz), 155.25, 154.5, 154.0, 149.8, 139.2, 131.1, 129.7, 129.4, 128.75, 123.5, 114.2, 85.1, 83.5, 83.3, 58.2, 41.0, 32.9, 27.7, 21; LC/MS (LC: gradient 0-100% MeCN [0.1% HCO_2H] over 30 min, 0.2 mL/min flow rate, MS: EI^+): retention time, 15.12 min; purity, 95%; 543.1 $[M+H]^+$.

Fluo

dioxi

rem

sat

ove

(5

wi

8

2

1

3

Fluoromethylketone **2.13** (fmk). **2.12** (46 mg, 0.085 mmol) was dissolved in 1 N HCl in dioxane (1 mL) and stirred for 2 h at 0˚C, and 3 h at room temperature. The solvent was removed *in vacuo* and the crude product was partitioned between CH_2Cl_2 (10 mL) and saturated $NaHCO_3$ (10 mL). The organic fraction was washed with brine (200 mL), dried over Na_2SO_4, filtered, and concentrated *in vacuo*. Purification by flash chromatography (5% MeOH in CH_2Cl_2) afforded the desired **2.13** (fmk) (19 mg, 70% yield) as an off-white solid: ^{1}H NMR (400 MHz, $CDCl_3$) δ 8.37 (s, 1H), 7.38 (d, J = 8 Hz, 2H), 7.34 (d, J = 8 Hz, 2H), 4.95 (br s, 2H), 4.72 (t, J = 5.6 Hz, 2H), 4.62 (d, J_{HF} = 47 Hz, 2H), 3.46 (m, 2H), 2.49 (s, 3H), 2.10 (m, 2H); ^{13}C NMR (100 MHz, $CDCl_3$) (partial) δ 155.8, 140.0, 130.5, 129.3, 57.7, 40.7, 32.9, 21.4; HRMS (EI) Calcd for $C_{18}H_{19}FN_4O_2$ 342.1492, found 342.1502; HPLC (gradient 30-100% MeOH over 15 min, 10 mL/min flow rate): retention time, 10.3 min; purity, 100%.

Pyrrolo[2,3-d]pyrimidine **2.14** (scaffold). To a solution of **2.3** (49 mg, 0.123 mmol) in THF (3 mL) at 0 ^{0}C was added 1 N HCl (0.5 mL). After stirring for 1 h 30 min at 0 ^{0}C and 30 min at room temperature, the reaction mixture was diluted with ethyl acetate (10 mL) and washed with saturated $NaHCO_3$ (1 x 10 mL) and brine (1 x 10 mL). The organic fraction was dried over anhydrous Na_2SO_4, filtered, and concentrated in vacuo to provide 35 mg (100% yield) of **2.14** as a clear film; Compound **2.14** was found to be 99% pure by HPLC (30-100% MeOH gradient over 15 min; 0.75 mL/min flow rate; retention time for **2.14** was 9.3 min); ^{1}H NMR (400 MHz, $CDCl_3$) d 8.27 (s, 1H), 7.36 (d, J = 8.0 Hz, 2H), 7.27 (d, J = 8.3 Hz, 2H), 6.91 (s, 1H), 5.4 (br s, 2H), 4.35 (t, J = 5.6 Hz, 2H), 3.46 (t, J = 5.6 Hz, 2H), 2.41 (s, 2H), 1.96 (m, 2H); ^{13}C NMR (100 MHz, $CDCl_3$) d 157.2, 151.8, 150.6, 137.0, 131.6, 129.7, 128.6, 122.7, 116.6, 100.7, 57.5, 40.6, 33.3, 21.1; HRMS (EI) Calcd for $C_{16}H_{18}N_4O_2$ 282.1480, found 282.1477.

fluoromethylketone carbamate **2.15**. To a solution of **2.12** (59 mg, 0.11 mmol) in CH_2Cl_2 (1 mL) was added DIPEA (0.015 mL, 0.085 mmol), followed by carbonyldiimidazole (14 mg, 0.085 mmol). After stirring for 2 h at room temperature, *N*-Boc-1,4-diaminobutane (26 mg, 0.14 mmol) was added. After 3 h, additional *N*-Boc-1,4-diaminobutane (16 mg, 0.085 mmol) was added and the reaction was stirred for 2 h at room temperature. The reaction mixture was diluted with ethyl acetate (30 mL) and washed with 0.5 N HCl (10 mL) followed by brine (30 mL). The organic fraction was dried over Na_2SO_4, filtered, and concentrated *in vacuo*. Purification by flash chromatography (3:2 ethyl acetate/hexanes) gave 57 mg (69% yield) of **2.15**: R_f 0.50 (100% ethyl acetate); ^{1}H NMR (400 MHz, $CDCl_3$) δ 8.94 (s, 1H), 7.27 (d, J = 8 Hz, 2H), 7.23 (d, J = 8 Hz, 2H), 4.84 (m, 2H), 4.66-4.63 (d, J_{HF} = 47 Hz, 2H), 4.13 (m, 2H), 3.06 (m, 4H), 2.46 (s, 3H), 2.16 (m, 2H), 1.42 (s, 9H), 1.42 (m, 4H), 1.31 (s, 18H); LC/MS (LC: gradient 0-100% MeCN [0.1% HCO_2H] over 30 min, 0.2 mL/min flow rate, MS: EI^+): retention time, 17.69 min; purity, >95%; 757.2 $[M+H]^+$.

flouromethylketone-biotin **2.16** (fmk-biotin). To a solution of **2.15** (20 mg, 0.026 mmol) in CH_2Cl_2 (0.3 mL) was added TFA (0.3 mL) at 0°C. After slowly warming the reaction mixture to room temperature over a period of 2 h, solvent was removed *in vacuo*. A portion of the crude boc-deprotected product (5.6 mg, 0.0084 mmol) was dissolved in DMF (0.1 mL). Biotin-NHS (5 mg, 0.01 mmol) was added followed by DIPEA (3.9 mg, 0.03 mmol). After stirring for 12 h at room temperature, the reaction mixture was concentrated *in vacuo*. Purification by preparative HPLC (30-100% MeOH gradient over 15 min; 10 mL/min) afforded the desired **2.16** (fmk-biotin); ^{1}H NMR (400 MHz, $CDCl_3$) δ 8.27 (s, 1H), 7.37 (d, J = 8 Hz, 2H), 7.31 (d, J = 8 Hz, 2H), 6.59 (br s, 1H), 6.02 (br s, 1H), 5.22 (br s, 1H), 4.73 (t, 2H), 4.63 (d, J_{HF} = 47 Hz, 2H), 4.50 (t, 1H), 4.38 (m, 1H), 4.13 (2H), 3.21 (4H), 2.94 (dd, J = 14 Hz, J = 4 Hz, 1H), 2.72 (d, J = 12 Hz), 2.48 (s, 3H),

2.16

unde

Chl

TH

0.0

(5

o

P

2.16 (m, 2H), 0.90-0.70 (m, 6H) [Note: some protons not accounted for because they are underneath large solvent peak ~1.5 ppm].

Chloromethylketone enol carbonate **2.17**. To a solution of **2.7** (50 mg, 0.11 mmol) in THF (0.60 mL) was added $(Boc)_2O$ (210 mg, 0.420 mmol), followed by DMAP (6.5 mg, 0.053 mmol). After stirring for 2h 40 min at rt, the mixture was diluted with ethyl acetate (5 mL) and washed with 10 % citrate buffer pH 4.0 (1 x 5 mL) and brine (1 x 5 mL). The organic fraction was dried over anhydrous Na_2SO_4, filtered, and concentrated *in vacuo* to provide 62 mg of the crude enol carbonate silyl ether. This compound was dissolved in THF (1 mL) and treated at 0°C with 1 N HCl (0.33 mL). After 3 h, the reaction was diluted with ethyl acetate (5 mL) and washed with saturated $NaHCO_3$ (1 x 5 mL) and brine (1 x 5 mL). The organic fraction was dried over anhydrous Na_2SO_4, concentrated, and purified by flash column chromatography (50-100 % hexanes/ethyl acetate) to provide **2.17** (49 mg, 84% over two steps): R_f 0.40 (1:1 hexanes/ethyl acetate); ^{1}H NMR (400 MHz, $CDCl_3$) δ 8.83 (s, 1H), 7.35 (d, J = 8 Hz, 2H), 7.16 (d, J = 8 Hz, 2H), 5.88 (s, 1H), 4.50 (t, 2H), 3.52 (t, 3H), 2.40 (s, 3H), 2.0 (m, 2H), 1.49 (s, 9H), 1.28 (s, 18H).

Chloromethylketone carbamate **2.18**. **2.17** (51 mg, 0.077 mmol) was azeotropically dried with toluene under high vacuum and dissolved in CH_2Cl_2 (0.5 mL). DIPEA (0.015 mL, 0.085 mmol) was added, followed by 1,1'-carbonyldiimidazole (14 mg, 0.085 mmol). After stirring for 1 h at rt, *N*-Boc-1,4-diaminobutane (16 mg, 0.085 mmol) was added. After 5 h 40 min, and additional 1.1 equivalents of *N*-Boc-1,4-diaminobutane (16 mg, 0.085 mmol) was added. After 8 h, the reaction was diluted with ethyl acetate (5 mL) and washed with 10% sodium citrate buffer (1 x 5 mL) and brine (1 x 5 mL). The organic fraction was dried over anhydrous Na_2SO_4, filtered, and concentrated *in vacuo*. Rapid purification by flash chromatography (1:1-2:1 ethyl acetate/hexanes) gave 43 mg of the

N-boc-protected carbam

of the boc-protected c

added TFA (0.7 mL).

were removed *in vacu*

EI-MS 497 [M+2+Na]

Chloromethylketone-

DMF (0.1 mL) at rt

(0.007 mL, 0.04 mm

HPLC (30-100% M

afford 9 mg (70% y

[M+Na]$^+$. ^{1}H NMR (

Hz, 2H), 6.46 (br s

1H), 4.12 (t, *J* = 8

2.65 (m, 2H), 2.48

some protons no

ppm].

Chloromethylket

mmol) in DMF (

mmol), followed

were removed

CH_2Cl_2/MeOH)

(400 MHz, CD

7.30 (d, *J* = 8

6.10 (s, 1H), s

N-boc-protected carbamate, which was used immediately in the next step. To a solution of the boc-protected carbamate (43 mg, 0.056 mmol) in CH_2Cl_2 (0.8 mL) at 0°C was added TFA (0.7 mL). After warming to room temperature and stirring for 3 h, solvents were removed *in vacuo* to yield 26 mg (73% over three steps) of **2.17** as the TFA salt; EI^+-MS 497 $[M+2+Na]^+$, 495 $[M+Na]^+$, 475 $[M+2]^+$, 473 $[M]^+$.

Chloromethylketone-biotin **2.19** (cmk-biotin). To a solution of **2.18** (9 mg, 0.02 mmol) in DMF (0.1 mL) at rt was added Biotin-NHS (13 mg, 0.038 mmol), followed by DIPEA (0.007 mL, 0.04 mmol). After 24 h, the crude mixture was purified directly by preparative HPLC (30-100% MeOH gradient over 15 min; 10 mL/min; retention time, 12.2 min) to afford 9 mg (70% yield) of **2.19** (cmk-biotin) as a white solid; EI^+-MS 723 $[M+2+Na]^+$, 721 $[M+Na]^+$. ^1H NMR (400 MHz, $CDCl_3$) δ 8.27 (s, 1H), 7.38 (d, *J* = 8 Hz, 2H), 7.35 (d, *J* = 8 Hz, 2H), 6.46 (br s, 1H), 6.09 (br s, 1H), 4.70 (t, *J* = 8 Hz, 2H), 4.49 (m, 1H), 4.34 (m, 1H), 4.12 (t, *J* = 8 Hz, 2H), 3.93 (s, 2H), 3.70 (m, 2H), 3.24 (m, 2H), 2.88 (m, 1H), 2.73-2.65 (m, 2H), 2.48 (s, 3H), 2.31 (t, *J* = 8 Hz, 2H), 2.15 (m, 4H), 1.70-1.62 (m, 4H). [Note: some protons not accounted for because they are underneath large solvent peak ~1.5 ppm].

Chloromethylketone-BODIPY **2.20** (cmk-BODIPY). To a solution of **2.18** (4 mg, 0.008 mmol) in DMF (0.1 mL) at room temperature was added BODIPY FL-NHS (5 mg, 0.009 mmol), followed by DIPEA (0.003 mL, 0.016 mmol). After 24 h in the dark, the solvents were removed *in vacuo* and the mixture was purified by flash chromatography (10:1 CH_2Cl_2/MeOH) to give **2.20** (cmk-BODIPY) as a red solid in quantitative yield: ^1H NMR (400 MHz, $CDCl_3$) δ 11.2 (br s, 2H), 8.23 (s, 1H), 8.00 (s, 1H), 7.37 (d, *J* = 8 Hz, 2H), 7.30 (d, *J* = 8.4 Hz, 2H), 7.1 (s, 1H), 6.86 (d, *J* = 3.6 Hz, 1H), 6.23 (d, *J* = 3.6 Hz, 1H), 6.10 (s, 1H), 5.80 (m, 2H), 4.70 (t, 2H), 4.04 (t, 2H), 3.92 (s, 2H), 3.68 (m, 2H), 3.25-3.06

(m, 6H), 2.68 (s), 2.60 (t, J = 7.6 Hz, 2H), 2.53 (s, 3H), 2.46 (s, 3H), 2.23 (s, 3H), 2.1 (m, 2H), 1.46-1.37 (m, 10H); EI^+-MS 884 $[M+2+Na]^+$, 882 $[M+Na]^+$.

Cell culture and retroviral transfection. NIH-3T3, HEK-293, and COS-7 cells were cultured in Dulbecco's modified Eagle's medium (DMEM) supplemented with 10% fetal bovine serum. pBabe-puro retroviral vectors encoding WT and V281C v-Src were transfected into the Phoenix packaging cell line to obtain retroviruses, which were used to infect NIH-3T3 cells with puromycin selection (2.0 mg/mL) for 10 days [33]. Both v-Src constructs also contained an I338T gatekeeper mutation. All mutations were introduced by QuikChange mutagenesis (Stratagene) and confirmed by sequencing.

In vitro kinase assays: RSK2 CTD. The pET28b expression vector encoding His_6-RSK2 CTD (aa415-740) was provided by Yuguo Feng and Tom Alber (University of California, Berkeley). The His_6-ERK2 expression vector was provided by Melanie Cobb (University of Texas, Southwestern). Both kinases were expressed (separately) in E. coli and purified by immobilized nickel affinity chromatography. WT, C436V, and T493M RSK2 CTDs (500 nM) were activated by His_6-ERK2 (~500 nM) in 20 mM Hepes [pH 8.0], 10 mM $MgCl_2$, 2 mM *tris*(2-carboxyethyl)phosphine (TCEP), and 200 μM ATP for 1 hour at 30°C. Activated RSK2 CTDs (1 nM) in 20 mM Hepes [pH 8.0], 10 mM $MgCl_2$, 2 mM *tris*(2-carboxyethyl)phosphine (TCEP), 0.2 mg/mL BSA, and 100 μM ATP were preincubated with inhibitor (seven concentrations, in triplicate) for 30 min at rt. Kinase reactions were initiated by the addition of 5 μCi of $[\gamma\text{-}^{32}P]$ATP (6000 Ci/mmol, NEN) and 100 μM peptide substrate (RRQLFRGFSFVAK, CTD-tide) [25], and performed for 20 min at rt. Kinase activity was determined using the standard disk phosphocellulose assay,

based on counts per m

fit using PRISM 4.0 to

Labeling of RSK2 C

fmk (1 μM) for 1 hou

$MgCl_2$, 2mM TCEP,

RSK2 CTD was first

labeling reaction w

were separated by

probed with 1:5,00

detection, then rep

Labeling of en

Preparation and

mM Hepes [pH 7

by mechanical f

clarified by cent

Nap5 column (A

To remove end

incubated with

4°C. Preclear

concentrations

was terminat

separated by

based on counts per minute (cpm) of ^{32}P transferred to the peptide susbtrate. Data were fit using PRISM 4.0 to obtain IC_{50} values (expressed as the mean ± S.D.).

Labeling of RSK2 CTD with fmk-biotin. RSK2 CTDs (2 nM) were treated with biotin-fmk (1 μM) for 1 hour in the presence of 2 nM ERK2, 20 mM Hepes (pH 8.0), 10 mM $MgCl_2$, 2mM TCEP, 0.2 mg/mL BSA, and 100 μM ATP. In a separate experiment, WT RSK2 CTD was first treated with 0.5 μM unlabeled fmk before adding biotin-fmk. The labeling reaction was terminated by the addition of Laemmli sample buffer. Proteins were separated by 10% SDS-PAGE and transferred to nitrocellulose. The blot was probed with 1:5,000 streptavidin-HRP followed by enhanced chemiluminescence (ECL) detection, then reprobed with 1:1,000 His_6-HRP antibody (Pierce).

Labeling of endogenous RSK1/2 with fmk-biotin in HEK-293 cell lysates. *Preparation and labeling of HEK-293 cell lysates.* HEK-293 cells were lysed at 4˚C (20 mM Hepes [pH 7.4] and 200 mM NaCl, protease inhibitor cocktail). Lysis was achieved by mechanical force using a syringe equipped with a 28G needle. The lysates were clarified by centrifugation at 12,000 rpm for 20 min. Clarified lysates were applied to a Nap5 column (Amersham) equilibrated with 20 mM Hepes [pH 7.4] and 200 mM NaCl. To remove endogenous biotinylated proteins, 1 mL of lysate (4 mg/mL total protein) was incubated with 100 μL of streptavidin-conjugated agarose beads (Pierce) overnight at 4˚C. Precleared lysates (30 μL, 120 μg total protein) were pretreated with increasing concentrations of fmk for 1 hour followed by fmk-biotin (1 μM) for 1 hour at rt. Labeling was terminated by the addition of 30 μL of Laemmli sample buffer. Proteins were separated by 10% SDS-PAGE and transferred to nitrocellulose. Total protein was

visualized by staining

milk, the blot was prob

Immunodepletion of

and RSK2. HEK-293

proteins) was treate

1% NP40 and 0.01%

either rabbit IgG (S

affinity purified RS

4°C, followed by i

4°C. The immune

mM NaCl, 1% NP

µL SDS sample b

each condition wa

10% SDS-PAGE

streptavidin-HRP

1:1,000 RSK1 a

EGF-stimulate

(1 x 10 cm pla

subsequently t

stimulation for

at 4°C (RSK

10% glycerol,

Clarified lysa

kg) for 2 ho

visualized by staining the blot with Ponceau S. After destaining and blocking with 5% milk, the blot was probed with 1:5,000 streptavidin-HRP, followed by ECL detection.

Immunodepletion of biotinylated proteins with monospecific antibodies against RSK1 and RSK2. HEK-293 cell lysate (4 mg/mL, 200 μL, depleted of endogenous biotinylated proteins) was treated with fmk-biotin (1 μM) for 1 hour at rt, followed by the addition of 1% NP40 and 0.01% SDS (final concentrations). The lysate was incubated with 2 μg of either rabbit IgG (Sigma), a RSK2 monoclonal antibody (Santa Cruz Biotechnology), or affinity purified RSK1 polyclonal antibodies (Santa Cruz Biotechnology) for 2 hours at 4°C, followed by incubation with 25 μL Protein G/Sepharose (Amersham) overnight at 4°C. The immune complexes were washed three times with 20 mM Hepes [pH 7.4], 200 mM NaCl, 1% NP40, and 0.01% SDS and once without detergent, resuspended in 200 μL SDS sample buffer (2x), and boiled for 10 min. To 50 μL of the supernatants from each condition was added 50 μL of Laemmli sample buffer. Proteins were separated by 10% SDS-PAGE and transferred to nitrocellulose. The blot was probed with 1:5,000 streptavidin-HRP, followed by ECL detection. The blot was reprobed sequentially with 1:1,000 RSK1 and RSK2 antibodies.

EGF-stimulated autophosphorylation of endogenous RSK2. Confluent COS-7 cells (1 x 10 cm plate per experimental condition) were deprived of serum for 20 hours and subsequently treated with the indicated concentrations of fmk for 90 min at 37°C. After stimulation for 10 min with EGF (1 ng/mL), cells were washed with cold PBS, and lysed at 4°C (RSK lysis buffer: 50 mM Tris [pH 7.4], 1% NP40, 5 mM EDTA, 150 mM NaCl, 10% glycerol, protease inhibitor cocktail, and phosphatase inhibitor I/II cocktail (Sigma)). Clarified lysates (1 mg total protein) were incubated with a monoclonal RSK2 antibody (2 μg) for 2 hours at 4°C, followed by incubation with Protein G/Sepharose for 1 hour.

immunoprecipitates w

antibody (Cell Signal

Aliquots of the initial

Tnr202/Tyr204 ERK1

RSK2 or ERK1/2 (Ce

Expression of HA

expression vectors

Bjorbaek (Harvard

respectively. Co

(Invitrogen). 24 h

then treated with

(150 ng/mL) for 2

µL/well). Protein

with phospho-S

were reprobed w

In vitro kinase

(BL21-DE3) as

IC_{50} determina

ng/mL BSA)

the presence

peptide subs

performed fr

phosphocell

peptide sus

Immunoprecipitates were analyzed by Western blot with a phospho-Ser386 RSK antibody (Cell Signaling Technology; called "Ser380" based on RSK1 numbering). Aliquots of the initial cell lysates were also analyzed by Western blot with phospho-Thr202/Tyr204 ERK1/2 antibody (Cell Signaling Technology). Blots were reprobed with RSK2 or ERK1/2 (Cell Signaling Technology) antibodies.

Expression of HA-tagged RSK2 and MSK1 in COS-7 cells. Wild-type pMT2 expression vectors encoding HA-tagged RSK2 and MSK1 were provided by Christian Bjorbaek (Harvard Medical School) and Martin Frodin (Glostrup Hospital, Denmark), respectively. Confluent COS-7 cells were transfected with Lipofectamine 2000 (Invitrogen). 24 hours post-transfection, cells were deprived of serum for 3 hours and then treated with the indicated concentrations of fmk. Cells were stimulated with EGF (150 ng/mL) for 25 min, washed with cold PBS, and lysed in Laemmli sample buffer (200 μL/well). Proteins were separated by 10% SDS-PAGE and analyzed by Western blot with phospho-Ser386 RSK or phospho-Ser10 histone H3 antibodies (Upstate). Blots were reprobed with the 12CA5 monoclonal HA antibody (Roche).

In vitro kinase assays: Fyn. Wild-type (WT) and V285C Fyn were expressed in *E. coli* (BL21-DE3) as glutathione S-tranferase (GST) fusions as described previously [34]. For IC_{50} determinations, WT and V285C Fyn (in 50 mM Tris [pH 8.0], 10 mM $MgCl_2$, and 1 mg/mL BSA) were pretreated with varying concentrations of the inhibitors for 30 min in the presence of 100 μM ATP. Kinase reactions were initiated by the addition of 100 μM peptide substrate (LEEIYGEFKKK) and 1 μCi of [γ-^{32}P]ATP (6000 Ci/mmol, NEN) and performed for 15 min at rt. Kinase activity was determined using the standard disk phosphocellulose assay, based on counts per minute (cpm) of ^{32}P transferred to the peptide susbtrate [35].

PNA-stimulated his

Confluent NIH-3T3 ce

(10 μM) or DMSO fo

washed with cold

mercaptoethanol, pr

lysates were clarifie

removed and the re

for 30 min at 0°C.

Proteins were sep

phospho-Ser10 hi

blot with Ponceau

Inhibition of v

expressing eithe

cmk or fmk for

1% NP-40, 50

orthovanadate

inhibitor II cock

by Western bl

and reprobed

Morphologic

WT v-Src or

hours. Cells

PMA-stimulated histone H3 phosphorylation in nontransfected NIH-3T3 cells. Confluent NIH-3T3 cells were deprived of serum for 24 hours and then treated with fmk (10 μM) or DMSO for 90 min. Cells were stimulated with PMA (100 ng/mL) for 20 min, washed with cold PBS, and lysed in NIB containing 0.65% NP-40, 0.1% β-mercaptoethanol, protease inhibitor cocktail, and phosphatase inhibitor I/II cocktail. The lysates were clarified by centrifugation at 3,000 rpm for 5 min. The supernatant was removed and the resulting pellet was resuspended in 50 μL 0.2 N HCl. After incubation for 30 min at 0°C, lysates were clarified by centrifugation at 13,000 rpm for 10 min. Proteins were separated by 12.5% SDS-PAGE and analyzed by Western blot with phospho-Ser10 histone H3 antibodies. Total histones were visualized by staining the blot with Ponceau S.

Inhibition of v-Src: global tyrosine phosphorylation. NIH-3T3 cells stably expressing either WT or V281C v-Src were treated with the indicated concentrations of cmk or fmk for 1 hour. Cells were washed with PBS and lysed at 4°C (Src lysis buffer: 1% NP-40, 50 mM Tris [pH 7.4], 2 mM EDTA, 150 mM NaCl, 2 mM sodium orthovanadate, protease inhibitor cocktail (Roche Diagnostics), and phosphatase inhibitor II cocktail (Sigma)). Proteins were separated by 10% SDS-PAGE and analyzed by Western blot with the 4G10 monoclonal antibody (Upstate). The blot was stripped and reprobed with a monoclonal actin antibody (Sigma).

Morphological reversion of v-Src-expressing cells. NIH-3T3 cells expressing either WT v-Src or V281C v-Src were grown on coverslips and treated with cmk (1 μM) for 16 hours. Cells were fixed with 4% formaldehyde in cytoskeleton buffer with sucrose (CBS:

10 mM MES [pH 6.1

for 20 min. Cells we

TX) for 10 min, and

incubated with FITC

Cells were imaged

camera (Coolsnap

software (Universa

presence of actin s

Labeling of V281

WT v-Src were tr

were washed with

40, 50 mM Tris

protease inhibito

centrifugation at

(2 μM) was add

added for 10 m

were incubated

Institute) for 2

(Jackson) for 1

slurry (Amersh

buffer (3 x 20

Immune com

nitrocellulose

Streptavidin-

10 mM MES [pH 6.10], 138 mM KCl, 3 mM $MgCl_2$, 2 mM EGTA, and 320 mM sucrose) for 20 min. Cells were rinsed with TBS, permeabilized in TBS-0.5% Triton-X-100 (TBS-TX) for 10 min, and blocked in TBS-TX with 2% BSA for 10 min. Cells were then incubated with FITC-phalloidin (1 μg/mL) for 20 min and DAPI (5 μg/mL) for 10 min. Cells were imaged with an Olympus IX-70 fluorescence microscope and a cooled CCD camera (Coolsnap HQ Monochrome). Images were processed with Metamorph software (Universal Imaging). For each condition, 100-200 cells were scored for the presence of actin stress fibers.

Labeling of V281C v-Src by cmk-biotin. NIH-3T3 cells expressing either V281C or WT v-Src were treated with increasing concentrations of cmk at 28°C. After 2 h, cells were washed with PBS, counted to normalize, and lysed at 4°C (Src lysis buffer: 1% NP-40, 50 mM Tris pH 7.4, 2 mM EDTA, 150 mM NaCl, 2 mM sodium orthovanadate, protease inhibitor cocktail tablet (Roche Diagnostics)). The lysates were clarified by centrifugation at 13,000 rpm for 15 min (typical lysate volume was 300 μL). Cmk-biotin (2 μM) was added to the lysates for 1 h at rt. β-mercaptoethanol (BME) (10 mM) was added for 10 min to quench excess cmk-biotin, followed by SDS (0.1%). Treated lysates were incubated with 1 μg of anti-v-Src antibody (generous gift from K. Shah, Novartis Institute) for 2 h at 4°C, followed by incubation with 1 μg rabbit anti-mouse IgG antibody (Jackson) for 1 h. Lysates were then incubated with 40 μL of 50% Protein A sepharose slurry (Amersham) for 1 h at 4°C. The immune complexes were washed with Src lysis buffer (3 x 200 μL), resuspended in sample buffer (100 μL), and boiled for 5 min. Immune complexes were separated on a 10% SDS-PAGE and transferred to nitrocellulose membranes. After blocking membranes were probed with either 1:5,000 streptavidin-HRP antibody (Santa Cruz biotech.) in 10 mg/mL BSA for 1 h at rt or 1:500

anti-v-Src antibody in

used for antibody dete

Labeling of NIH-3T3

per experimental co

with cmk (3 μM) or

(1 μM) for 10 min.

Detergent lysates w

Tris [pH 7.4], 1%

cocktail, and phos

by 10% SDS-PAG

scanner. Lysates

Src antibody.

anti-v-Src antibody in AbDil for 1 h at rt. Enhanced chemiluminescence (Pierce) was used for antibody detection.

Labeling of NIH-3T3 cells with cmk-BODIPY. Confluent NIH-3T3 cells (1 x 10 cm plate per experimental condition) stably expressing either WT or V281C v-Src were treated with cmk (3 μM) or DMSO for 10 min at 37°C, followed by treatment with cmk-BODIPY (1 μM) for 10 min. Cells were washed with cold PBS and frozen in liquid nitrogen. Detergent lysates were prepared by extracting cell pellets with 1% NP-40 buffer (50 mM Tris [pH 7.4], 1% NP40, 5 mM EDTA, 150 mM NaCl, 10% glycerol, protease inhibitor cocktail, and phosphatase inhibitor I/II cocktail). Proteins (40 μg/lane) were separated by 10% SDS-PAGE, and BODIPY-labeled proteins were detected with a Typhoon gel scanner. Lysates were analyzed in parallel by Western blot with the 327 monoclonal v-Src antibody.

References

1. Manning, G
protein kinat
2. Druker, B. J
growth of B
3. Barker, A.
orally activ
targeted to
4. Liu, Y. et a
Chem Bio
5. Schindler
tyrosine k
6. Zhu, X. e
with non
7, 651-6
7. Buchdun
signal
recepto
8. Fry, D.
recepto
Sci U S
9. Hanau
featur

References

1. Manning, G., Whyte, D. B., Martinez, R., Hunter, T. & Sudarsanam, S. The protein kinase complement of the human genome. *Science* **298**, 1912-34 (2002).
2. Druker, B. J. et al. Effects of a selective inhibitor of the Abl tyrosine kinase on the growth of Bcr-Abl positive cells. *Nat Med* **2**, 561-6 (1996).
3. Barker, A. J. et al. Studies leading to the identification of ZD1839 (IRESSA): an orally active, selective epidermal growth factor receptor tyrosine kinase inhibitor targeted to the treatment of cancer. *Bioorg Med Chem Lett* **11**, 1911-4 (2001).
4. Liu, Y. et al. Structural basis for selective inhibition of Src family kinases by PP1. *Chem Biol* **6**, 671-8 (1999).
5. Schindler, T. et al. Crystal structure of Hck in complex with a Src family-selective tyrosine kinase inhibitor. *Mol Cell* **3**, 639-48 (1999).
6. Zhu, X. et al. Structural analysis of the lymphocyte-specific kinase Lck in complex with non-selective and Src family selective kinase inhibitors. *Structure Fold Des* **7**, 651-61 (1999).
7. Buchdunger, E. et al. Abl protein-tyrosine kinase inhibitor STI571 inhibits in vitro signal transduction mediated by c-kit and platelet-derived growth factor receptors. *J Pharmacol Exp Ther* **295**, 139-45 (2000).
8. Fry, D. W. et al. Specific, irreversible inactivation of the epidermal growth factor receptor and erbB2, by a new class of tyrosine kinase inhibitor. *Proc Natl Acad Sci U S A* **95**, 12022-7 (1998).
9. Hanauer, A. & Young, I. D. Coffin-Lowry syndrome: clinical and molecular features. *J Med Genet* **39**, 705-13 (2002).

10. Sturgill, T. W
kinase phos
715-8 (1988
11. Frodin, M. &
(RSK) in sig
12. Shahbazian
to control i
13. Wang, X.
S6 kinase
14. Roux, P.
phorbol
suppress
13489-94
15. Yang, X
osteobla
(2004).
16. Chen, P
domain
Proc N
17. Rivera
respon
6260-
18. Bonn
trans
(199

10. Sturgill, T. W., Ray, L. B., Erikson, E. & Maller, J. L. Insulin-stimulated MAP-2 kinase phosphorylates and activates ribosomal protein S6 kinase II. *Nature* **334**, 715-8 (1988).

11. Frodin, M. & Gammeltoft, S. Role and regulation of 90 kDa ribosomal S6 kinase (RSK) in signal transduction. *Mol Cell Endocrinol* **151**, 65-77 (1999).

12. Shahbazian, D. et al. The mTOR/PI3K and MAPK pathways converge on eIF4B to control its phosphorylation and activity. *Embo J* **25**, 2781-91 (2006).

13. Wang, X. et al. Regulation of elongation factor 2 kinase by p90(RSK1) and p70 S6 kinase. *Embo J* **20**, 4370-9 (2001).

14. Roux, P. P., Ballif, B. A., Anjum, R., Gygi, S. P. & Blenis, J. Tumor-promoting phorbol esters and activated Ras inactivate the tuberous sclerosis tumor suppressor complex via p90 ribosomal S6 kinase. *Proc Natl Acad Sci U S A* **101**, 13489-94 (2004).

15. Yang, X. et al. ATF4 is a substrate of RSK2 and an essential regulator of osteoblast biology; implication for Coffin-Lowry Syndrome. *Cell* **117**, 387-98 (2004).

16. Chen, R. H., Abate, C. & Blenis, J. Phosphorylation of the c-Fos transrepression domain by mitogen-activated protein kinase and 90-kDa ribosomal S6 kinase. *Proc Natl Acad Sci U S A* **90**, 10952-6 (1993).

17. Rivera, V. M. et al. A growth factor-induced kinase phosphorylates the serum response factor at a site that regulates its DNA-binding activity. *Mol Cell Biol* **13**, 6260-73 (1993).

18. Bonni, A. et al. Cell survival promoted by the Ras-MAPK signaling pathway by transcription-dependent and -independent mechanisms. *Science* **286**, 1358-62 (1999).

19. Lizcano, J. M
protein kinas
349, 547-57
20. Anjum, R.,
suppressor
15, 1762-7
21. Woo, M. S
kinase (R
site. *Mol C*
22. Buzko, O
and famil
23. Tsigelny
flexible
(1999).
24. Arnold,
as pote
(2000)
25. Chrest
kinase
41 (20
26. Cana
mech
(199
27. Vik,
auto
398

Lizcano, J. M., Morrice, N. & Cohen, P. Regulation of BAD by cAMP-dependent protein kinase is mediated via phosphorylation of a novel site, Ser155. *Biochem J* **349**, 547-57 (2000).

Anjum, R., Roux, P. P., Ballif, B. A., Gygi, S. P. & Blenis, J. The tumor suppressor DAP kinase is a target of RSK-mediated survival signaling. *Curr Biol* **15**, 1762-7 (2005).

Woo, M. S., Ohta, Y., Rabinovitz, I., Stossel, T. P. & Blenis, J. Ribosomal S6 kinase (RSK) regulates phosphorylation of filamin A on an important regulatory site. *Mol Cell Biol* **24**, 3025-35 (2004).

Buzko, O. & Shokat, K. M. A kinase sequence database: sequence alignments and family assignment. *Bioinformatics* **18**, 1274-5 (2002).

Tsigelny, I. et al. 600 ps molecular dynamics reveals stable substructures and flexible hinge points in cAMP dependent protein kinase. *Biopolymers* **50**, 513-24 (1999).

Arnold, L. D. et al. Pyrrolo[2,3-d]pyrimidines containing an extended 5-substituent as potent and selective inhibitors of lck I. *Bioorg Med Chem Lett* **10**, 2167-70 (2000).

Chrestensen, C. A. & Sturgill, T. W. Characterization of the p90 ribosomal S6 kinase 2 carboxyl-terminal domain as a protein kinase. *J Biol Chem* **277**, 27733-41 (2002).

Canagarajah, B. J., Khokhlatchev, A., Cobb, M. H. & Goldsmith, E. J. Activation mechanism of the MAP kinase ERK2 by dual phosphorylation. *Cell* **90**, 859-69 (1997).

Vik, T. A. & Ryder, J. W. Identification of serine 380 as the major site of autophosphorylation of Xenopus pp90rsk. *Biochem Biophys Res Commun* **235**, 398-402 (1997).

28. Dalby, K. N.
regulatory
activated p
1496-505 (
29. Frodin, M.
regulated
PDK1. *Em*
30. Soloaga,
phosphor
31. Burchat,
substitue
2171-4
32. Dinsmo
Mcloug
5,6,7,8
letters
33. Bisho
signal
34. Liu, Y
prote
35. Bish
inhib
Soc

Dalby, K. N., Morrice, N., Caudwell, F. B., Avruch, J. & Cohen, P. Identification of regulatory phosphorylation sites in mitogen-activated protein kinase (MAPK)-activated protein kinase-1a/p90rsk that are inducible by MAPK. *J Biol Chem* **273**, 1496-505 (1998).

Frodin, M., Jensen, C. J., Merienne, K. & Gammeltoft, S. A phosphoserine-regulated docking site in the protein kinase RSK2 that recruits and activates PDK1. *Embo J* **19**, 2924-34 (2000).

Soloaga, A. et al. MSK2 and MSK1 mediate the mitogen- and stress-induced phosphorylation of histone H3 and HMG-14. *Embo J* **22**, 2788-97 (2003).

Burchat, A. F. et al. Pyrrolo[2,3-d]pyrimidines containing an extended 5-substituent as potent and selective inhibitors of lck II. *Bioorg Med Chem Lett* **10**, 2171-4 (2000).

Dinsmore, C. Z., C. Blair; Baginsky, W.F.; O'neill, T.J.; Koblan, K.S.; Chen, I-Wu; Mclouglin, D.A; Olah, T.V.; Huff, J.R. Synthesis of conformationally constrained 5,6,7,8-tetrahydroimidazo[1,5-a]pyridine inhibitors of farnesyltransferase. *organic letters* **2**, 3473-2476 (2000).

Bishop, A. C. et al. Design of allele-specific inhibitors to probe protein kinase signaling. *Current Biology* **8**, 257-266 (1998).

Liu, Y., Shah, K., Yang, F., Witucki, L. & Shokat, K. M. Engineering Src family protein kinases with unnatural nucleotide specificity. *Chem Biol* **5**, 91-101 (1998).

Bishop, A. C. et al. Generation of monospecific nanomolar tyrosine kinase inhibitors via a chemical genetic approach. *Journal of the American Chemical Society* **121**, 627-631 (1999).

IRCE LIBRARY

Chapter 3

A clickable inhibitor reveals context-dependent autoactivation of p90 RSK

Abstract

p90 ribo
inputs through t
C-terminal kina
terminal kinase
recently reporte
describe a pro
"clickable" tag
mammalian ce
RSK1 and RS
(click reaction
and downstre
RSK activati
context-depe
physiological

) ribosomal protein S6 kinases (RSK) integrate and respond to signaling ugh two catalytic domains. Autophosphorylation of Ser386 by the regulatory kinase domain (CTD) is thought to be essential for activation of the N- ıase domain (NTD), which phosphorylates multiple downstream targets[1]. We ported fmk, an irreversible inhibitor of the CTD of RSK1 and RSK2[2]. Here, we propargylamine variant (fmk-pa), which has improved cellular potency and a tag for assessing the extent and selectivity of covalent RSK modification. In ı cells, fmk-pa achieved selective and saturable modification of endogenous RSK2, revealed by copper-catalyzed conjugation of an azidoalkyl reporter ion). Saturating concentrations of fmk-pa inhibited Ser386 phosphorylation tream signaling in response to phorbol ester stimulation, but had no effect on ıtion by lipopolysaccharide. RSK autoactivation by the CTD is therefore pendent, suggesting that NTD and CTD inhibitors will have distinct al effects.

Introduction

RSK are s

extracellular reg

(PDK1)[5-7]. ERK

Ser386 (RSK2 r

mechanism[8-10].

PDK1[5], which p

all known RSK

is thought to be

mutants do no

kinase-inactive

phosphorylati

phosphorylati

activation pat

Using

selective inh

the ATP-bin

CTD. A b

lysates, but

membrane

proteins. T

we sough

determine

relationsh

endogeno

Introduction

RSK are serine/threonine kinases that are activated by signaling inputs from extracellular regulated kinase[3,4] (ERK) and phosphoinositide-dependent kinase 1 (PDK1)[5-7]. ERK phosphorylates and activates the CTD, which can autophosphorylate Ser386 (RSK2 numbering) in a hydrophobic motif, most likely via an intramolecular mechanism[8-10]. The phosphorylated hydrophobic motif serves as a docking site for PDK1[5], which phosphorylates and activates the NTD, resulting in the phosphorylation of all known RSK substrates[8,9,11]. CTD-medated phosphorylation of the hydrophobic motif is thought to be essential for RSK function, as Ser386Ala (RSK2) and Ser381Ala (RSK1) mutants do not support NTD-mediated signaling[6,9]. However, overexpression of CTD kinase-inactive[12] or deletion[5] mutants of RSK2 results in constitutive Ser386 phosphorylation (albeit with reduced NTD activity), suggesting that hydrophobic motif phosphorylation can occur in the absence of the CTD. Whether a CTD-independent activation pathway exists for endogenous RSK remains unknown.

Using a structural bioinformatics approach, we recently designed fmk, the first selective inhibitor of the CTD of RSK1 and RSK2[2]. Fmk exploits two selectivity filters in the ATP-binding site: a cysteine and a threonine that together are found only in the RSK CTD. A biotinylated derivative of fmk selectively modified RSK1 and RSK2 in cell lysates, but this probe was inappropriate for targeting RSK in intact cells due to reduced membrane permeability and the presence of abundant endogenously biotinylated proteins. To extend the utility of fmk as a cellular probe of RSK CTD-mediated signaling, we sought a tagged membrane-permeable derivative. This probe would allow us to determine the selectivity of covalent modification in intact cells, as well as the relationship between CTD inactivation and hydrophobic motif phosphorylation in endogenous RSK.

Results and Di

A fluorescent d

We initi

membrane-perm

to fmk-biotin). T

the BODIPY ta

this position is p

Scheme 3-1. S
DIPEA, DMF (7

Fmk-BODIP

electrophore

fmk-BODIP

in vitro (IC_{5}

reduced po

acetate (PI

fmk-BODIP

(**Figure 3.**

cells treat

detected

(Figure 3

Results and Discussion

A fluorescent derivative of fmk is not effective in cells

We initially synthesized fmk-BODIPY, a derivative of fmk containing a membrane-permeable fluorescent tag (**Scheme 3-1**, synthesized using the same route to fmk-biotin). The primary hydroxyl group of fmk was chosen as the attachment site for the BODIPY tag since a homology model of fmk bound to the CTD of RSK2 suggested this position is partially solvent exposed.

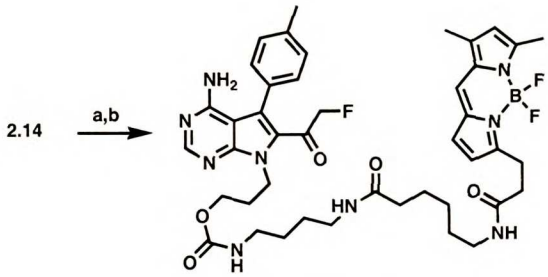

3.1 (fmk-BODIPY)

Scheme 3-1. Synthesis of fmk-BODIPY. Reagents and conditions: a. TFA, CH_2Cl_2; b. BODIPY FL-NHS, DIPEA, DMF (71% yield over 2 steps).

Fmk-BODIPY irreversibly modified RSK2 CTD, as shown by denaturing gel electrophoresis followed by in-gel fluorescence detection (**Figure 3-1a**). Unfortunately, fmk-BODIPY was ~100-fold less potent than fmk at inhibiting RSK2 CTD kinase activity *in vitro* (IC_{50} values of 1.7 μM versus 0.015 μM, respectively) and exhibited similarly reduced potency in cellular assays. Compared to fmk, which inhibited phorbol myristate acetate (PMA)-induced Ser386 phosphorylation with an EC_{50} of ~150 nM (**Figure 3-1b**), fmk-BODIPY weakly inhibited this phosphorylation event, with an EC_{50} of ~10 μM (**Figure 3-1c**). Fluorescent bands corresponding to RSK were detected in lysates from cells treated with fmk-BODIPY, but saturation of RSK was not achieved. Moreover, we detected extensive off-target modification at concentrations of fmk-BODIPY above 1 μM (**Figure 3-1d**).

Figure 3-1. Fmk
(a) Covalent la
concentrations o
resolved by 10%
with an antibody
cells were depri
stimulated with
PAGE and dete
(c) Effect of fm
of serum for 2 h
were stimulate
Proteins were
Ser386 RSK a
cell lysates fro
and Coomassie

Labeling of

with fmk-BO

potency of

We hypoth

binding bu

sought a le

reporter a

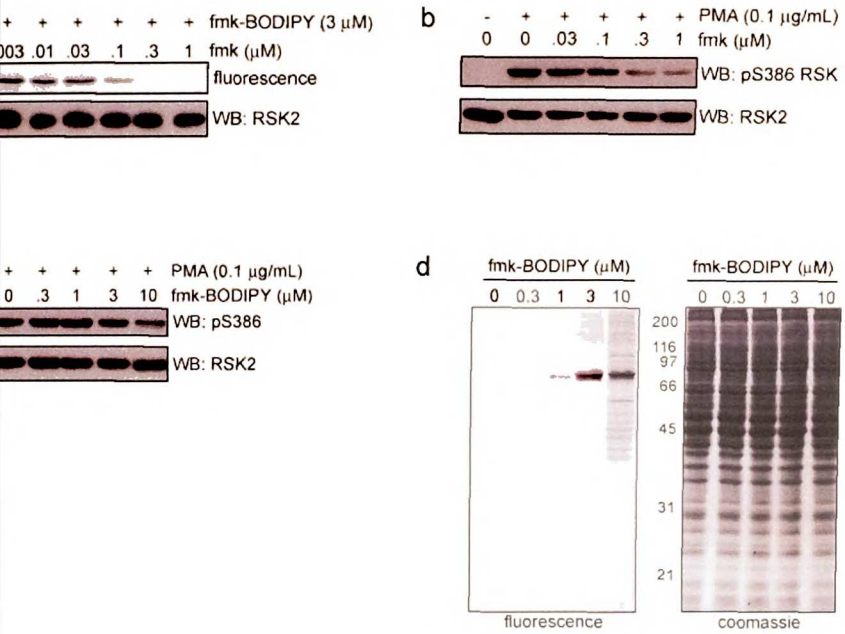

mk-BODIPY irreversibly targets RSK, but displays only modest selectivity and potency in cells. labeling of RSK2 CTD by fmk-BODIPY. RSK2 CTD was treated with the indicated s of unlabeled fmk for 1 h and subsequently with 3 μM fmk-BODIPY for 1 h. Proteins were 0% SDS-PAGE and detected by in-gel fluorescence scanning, followed by Western blotting dy to RSK2. (**b**) Inhibition of PMA-stimulated RSK Ser386 phosphorylation by fmk. HEK-293 rived of serum for 2 h and treated with the indicated concentrations of fmk for 1 h. Cells were n PMA (100 ng/mL) for 30 min and harvested in PBS. Proteins were resolved by 10% SDS- ected by Western blotting with antibodies to phospho-Ser386 RSK and total RSK2.
mk-BODIPY on PMA-stimulated RSK Ser386 phosphorylation. HEK-293 cells were deprived h and subsequently treated with the indicated concentrations of fmk-BODIPY for 1 h. Cells ed with PMA (100 ng/mL) for 30 min and harvested in phosphate buffered saline (PBS). resolved by 10% SDS-PAGE and detected by Western blotting with antibodies to phospho- and RSK2. (**d**) Selectivity of protein modification by fmk-BODIPY in intact cells. Proteins in m (**c**) were resolved by 10% SDS-PAGE and detected by in-gel fluorescence scanning (left) e blue staining (right).

RSK and off-target proteins was nearly abolished when cells were treated DIPY in media containing 10% serum (**Figure 3-2**), whereas the inhibitory mk itself was unchanged in serum-containing media (unpublished results). sized that the large, hydrophobic BODIPY tag not only interfered with RSK also promoted non-specific modification of cellular proteins. We therefore s intrusive tag that could be bioorthogonally conjugated to a fluorescent r covalent modification of RSK.

Figure 3-2. Co
whereas covale
either fmk-pa (C
for 1 h. Cells w
with TAMRA-N
scanning (left).

Click chem

Bioc

irreversible

click reacti

stable tria

inhibitor in

followed b

pa) (Sche

Schema
b. propa

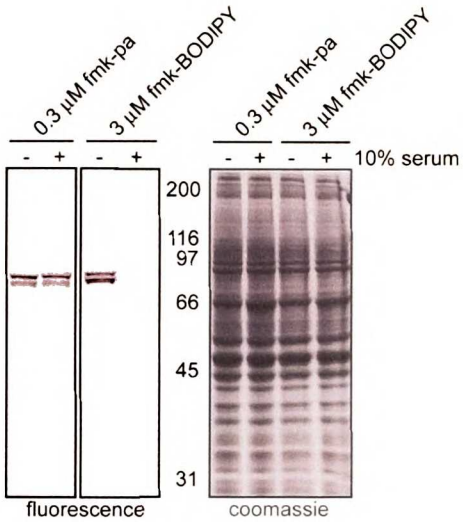

'igure 3-2. Covalent modification of RSK by fmk-pa is unaffected by serum in the incubation medium, vhereas covalent modification by fmk-BODIPY is significantly decreased. HEK-293 cells were treated with ither fmk-pa (0.3 μM) or fmk-BODIPY (3 μM) in the presence or absence of 10% fetal bovine serum (FBS) or 1 h. Cells were harvested in PBS and click reactions were performed in lysates from fmk-pa treated cells vith TAMRA-N_3 for 1 h. Proteins were resolved by 10% SDS-PAGE and detected by in-gel fluorescence canning (left). Total protein was visualized by Coomassie blue staining (right).

Click chemistry to the rescue

Bioorthogonal conjugation methods have been used to identify protein targets of rreversible inhibitors added to cell lysates[13-15], intact cells[14-18], and animals[14,15,17]. The click reaction, in which copper(I) catalyzes a [3+2] azide/alkyne cycloaddition to yield a stable triazole, is particularly effective. We therefore synthesized a clickable RSK nhibitor in a three-step sequence involving the formation of a mesylate intermediate **3.2**, ollowed by S_N2 displacement with propargylamine and *N*-boc removal to yield **3.3** (fmk-pa) (**Scheme 3-2**).

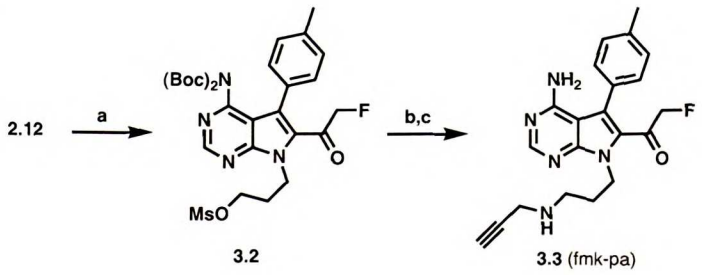

cheme 3-2. Synthesis of fmk-pa. Reagents and conditions: a. methanesulfonyl chloride, DIPEA, CH_2Cl_2; propargylamine (neat); c. TFA, CH_2Cl_2 (33% yield over 3 steps).

RSK2 CTD was treat

azide reporter (TAM

labeling of RSK2 CT

scanning (**Figure 3**

(**Figure 3-3a**) and i

values of 0.021 μM

Figure 3-3. Irreven
detection of RSK2 C
by 3 μM fmk-BODIP
by 10% SDS-PAG
TAMRA and BODIP
were deprived of se
Cells were stimulat
Selectivity of prote
conjugation with T
fluorescence scann
(c). (e) Fmk-pa co
293 cells were tre
lysates (0.7 mg to
followed by incuba
immunoprecipitate
10% SDS-PAGE
to RSK1 and RSK

2 CTD was treated with fmk-pa, followed by conjugation to a tetramethylrhodamine-

e reporter (TAMRA-N_3) using click chemistry (see **Experimental**). Saturable

ing of RSK2 CTD was achieved by fmk-pa, as determined by in-gel fluorescence

ning (**Figure 3-3a**). Fmk-pa prevented labeling of RSK2 CTD by fmk-BODIPY

ıre 3-3a) and inhibited CTD kinase activity *in vitro* with similar potency to fmk (IC_{50}

es of 0.021 μM versus 0.015 μM, respectively).

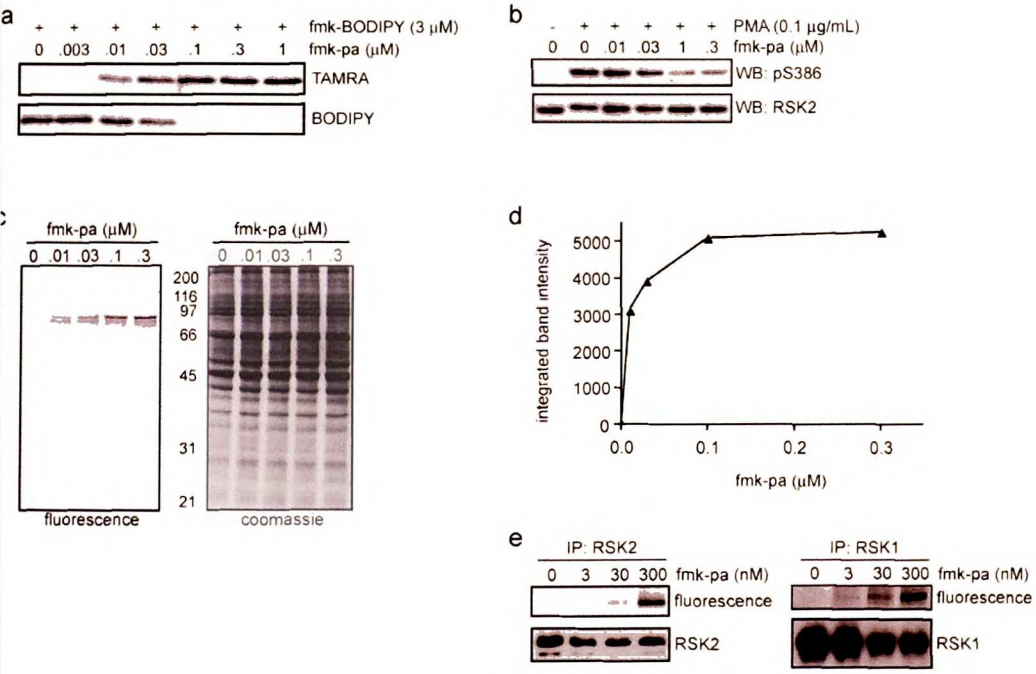

3-3. Irreversible, selective, and potent inhibition of RSK by fmk-pa. (**a**) Click chemistry-mediated on of RSK2 CTD. RSK2 CTD was treated with the indicated concentrations of fmk-pa for 1 h followed M fmk-BODIPY for 1 h. After click conjugation with TAMRA-N_3 (see Methods), proteins were resolved % SDS-PAGE and detected by sequential in-gel fluorescence scanning using filters specific for A and BODIPY. (**b**) Effect of fmk-pa on PMA-stimulated Ser386 RSK phosphorylation. HEK-293 cells eprived of serum for 2 h and subsequently treated with the indicated concentrations of fmk-pa for 1 h. vere stimulated with PMA (100 ng/mL) for 30 min and processed as described in **Figure 3-1b,c**. (**c**) vity of protein modification by fmk-pa in intact cells. Cell lysates from (**b**) were subjected to click ation with TAMRA-N_3. Proteins were resolved by 10% SDS-PAGE and detected by in-gel cence scanning (left) and Coomassie blue staining (right). (**d**) Quantification of fluorescent bands in) Fmk-pa covalently modifies RSK1 and RSK2 in intact cells as determined by click chemistry. HEK-lls were treated with the indicated concentrations of fmk-pa for 1 h and harvested in PBS. Clarified (0.7 mg total protein) were incubated with 2 μg of either RSK2 or RSK1 antibodies for 2 h at 4°C, d by incubation with 25 μL of Protein G/Sepharose (30 μL of 50% slurry in PBS) for 3 h at 4°C. The oprecipitates were subjected to the click reaction with TAMRA-N_3 for 1 h. Proteins were resolved by DS-PAGE and detected by in-gel fluorescence scanning, followed by Western blotting with antibodies 1 and RSK2.

In contrast to

RSK Ser386 phosph

fold increase in cell

1b) may be due to

length endogenous

activity *in vitro*. Th

was examined by

treated cells. La

indicated by the p

these bands were

antibodies (**Figure**

inhibition of Ser38

100 nM fmk-pa (F

block Ser386 p

modification and

serum in the inc

advantage of cli

conjugation of a

non-specific prot

Fmk-pa reveals

Having

by fmk-pa, we

ribosomal pro

involved in t

phosphorylatio

In contrast to fmk-BODIPY, fmk-pa was even more potent than fmk at inhibiting RSK Ser386 phosphorylation in HEK-293 cells (EC_{50} ~ 30 nM, **Figure 3-3b**). The five-fold increase in cellular potency of fmk-pa compared to fmk (EC_{50} ~ 150 nM, **Figure 3-1b**) may be due to increased membrane permeability or increased potency toward full-length endogenous RSK, since the two inhibitors are equipotent against RSK2 CTD activity *in vitro*. The extent and selectivity of covalent modification of RSK by fmk-pa was examined by performing the click reaction in lysates prepared from the above-treated cells. Labeling of RSK1 and RSK2 by fmk-pa was remarkably specific, as indicated by the prominent fluorescent bands at ~90 kD (**Figure 3-3c**). The identities of these bands were confirmed as RSK1 and RSK2 by immunoprecipitation with specific antibodies (**Figure 3-3e**). Importantly, the extent of covalent modification correlated with inhibition of Ser386 phosphorylation. Maximum labeling and inhibition were achieved at 100 nM fmk-pa (**Fig. 3-3b-d**), although even saturating concentrations of fmk-pa failed to block Ser386 phosphorylation completely. In contrast to fmk-BODIPY, covalent modification and inhibition of RSK in intact cells were unaffected by the presence of 10% serum in the incubation medium (**Figure 3-2**). Together, these results demonstrate the advantage of click chemistry as an alternative labeling strategy in cases where direct conjugation of a reporter tag to an irreversible inhibitor reduces potency and promotes non-specific protein modification.

Fmk-pa reveals a parallel pathway for phosphorylation of ribosomal protein s6

Having demonstrated selective and saturable modification of endogenous RSK by fmk-pa, we next tested whether RSK CTD activity is required for phosphorylation of ribosomal protein S6 (rpS6), an essential component of the 40S ribosomal subunit involved in translation initiation and regulation of cell size[19]. Until recently, phosphorylation of rpS6 at Ser235/236 was thought to be mediated exclusively by p70

S6 kinases 1 and 2

kinase, the mammal

protein complexes,

insensitive))[20]. How

phosphorylation wa

ERK[21]. These resu

of rpS6 under certa

a

. + + + +

0 0 .3 1 3 1

c . + + +

0 0 .01 1

Figure 3-4. Fmk-

rapamycin and fm

indicated concentra

for 1 h and stimula

detected by Weste

RSK2. (**b**) Dose-

(black triangles), r

determined by qu

Data represent

phosphorylation a

the indicated co

subsequently lys

with antibodies to

(**d**) Inhibition of

containing 10%

absence of fmk-

blotting with anti

To d

fmk-pa on

S6 kinases 1 and 2 (S6K1 and S6K2), the activation of which requires another protein kinase, the mammalian target of rapamycin (mTOR, which exists in cells as part of two protein complexes, mTOR/rapator (rapamycin sensitive) and mTOR/rictor (rapamycin-insensitive))[20]. However, in cells derived from S6K1/S6K2 double knockout mice, rpS6 phosphorylation was still observed and was sensitive to pharmacological inhibition of ERK[21]. These results led to the proposal that p90 RSK might promote phosphorylation of rpS6 under certain conditions[21].

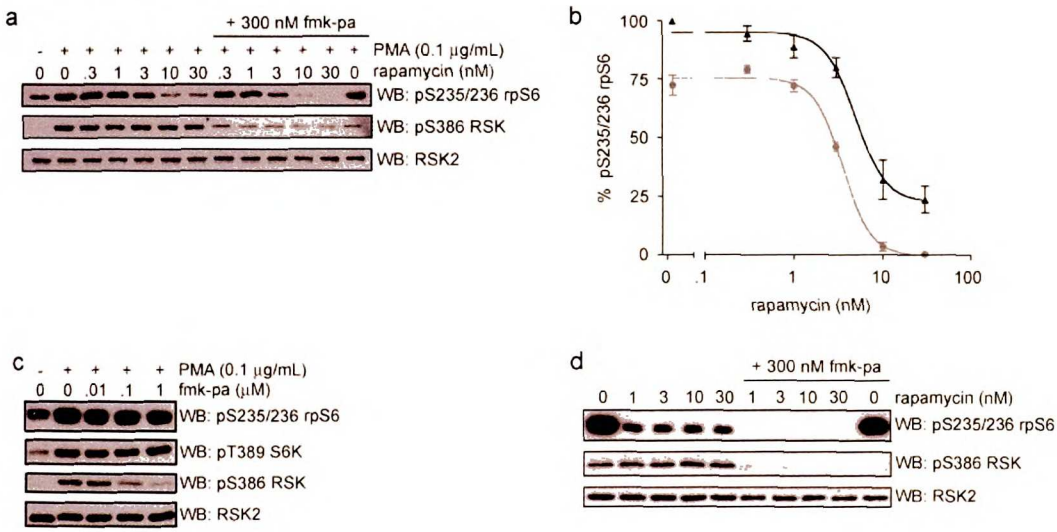

Figure 3-4. Fmk-pa reveals a RSK CTD-dependent pathway for rpS6 phosphorylation. (**a**) Effects of rapamycin and fmk-pa on rpS6 phosphorylation. Serum-starved HEK-293 cells were treated with the indicated concentrations of rapamycin in the absence (left lanes) or presence (right lanes) of 300 nM fmk-pa for 1 h and stimulated with PMA (100 ng/mL) for 30 min. Proteins were resolved by 10% SDS-PAGE and detected by Western blotting with antibodies to phospho-Ser235/236 rpS6, phospho-Ser386 RSK, and total RSK2. (**b**) Dose-response curves showing additive inhibition of rpS6 phosphorylation: rapamycin alone (black triangles), rapamycin + 300 nM fmk-pa (gray circles). Percent rpS6 Ser235/236 phosphorylation was determined by quantification of Western blots (e.g., **Figure 3-4a**) relative to DMSO controls using ImageJ. Data represent mean ± s.e.m. from 3 independent experiments. (**c**) Fmk-pa does not inhibit S6K phosphorylation at Thr389, an essential activation site[22]. Serum-starved HEK-293 cells were treated with the indicated concentrations of fmk-pa for 1 h, stimulated with PMA (100 ng/mL) for 30 min, and subsequently lysed in PBS. Proteins were resolved by 10% SDS-PAGE and detected by Western blotting with antibodies to phospho-Ser235/236 rpS6, phospho-Thr389 S6K, phospho-Ser386 RSK, and total RSK2. (**d**) Inhibition of rpS6 Ser235/236 phosphorylation by rapamycin and fmk-pa. MDA-MB-231 cells in media containing 10% FBS were treated with the indicated concentrations of rapamycin in the presence or absence of fmk-pa (300 nM) for 1 h. Proteins were resolved by 10% SDS-PAGE and detected by Western blotting with antibodies to phospho-Ser235/236 rpS6, phospho-Ser386 RSK, and total RSK2.

To directly test this hypothesis, we examined the effects of rapamycin and fmk-pa on rpS6 phosphorylation in HEK-293 cells. Increasing concentrations of

rapamycin, which p

rpS6 phosphorylatio

triangles). The max

contrast, fmk-pa alo

4a,b) without affect

produced additive e

3-4b, gray circles)

rapamycin. Simila

serum (**Figure** 3

contributes to rpS

shown to directly

RSK NTDs are hi

therefore share

shown that RSK

and eIF4B[25].

Figure 3-5. Pan

probably depend

each pathway ma

revents S6K activation by mTOR/raptor, inhibited PMA-stimulated on at Ser235/236 (**Figure 3-4a**, left lanes, and **Figure 3-4b**, black imum extent of rapamycin-mediated inhibition was only 76 ± 8%. By ne (300 nM) inhibited rpS6 phosphorylation by 28 ± 6% (**Figure 3-** ng S6K activation (**Figure 3-4c**). Combining fmk-pa and rapamycin ffects on rpS6 phosphorylation (**Figure 3-4a**, right lanes, and **Figure** which was abolished in the presence of 300 nM fmk-pa and 30 nM results were obtained in MDA-MB-231 breast cancer cells growing in **4d**). Together, these results demonstrate that the RSK CTD phosphorylation, most likely by activating the NTD, which has been osphorylate rpS6 at Ser235/236 *in vitro* (**Figure 3-5**)[8]. S6K1/2 and ly homologous, phosphorylate a similar consensus motif[23], and may ltiple substrates. Consistent with this idea, recent studies have ediates phosphorylation of two additional S6K substrates, eEF2K[24]

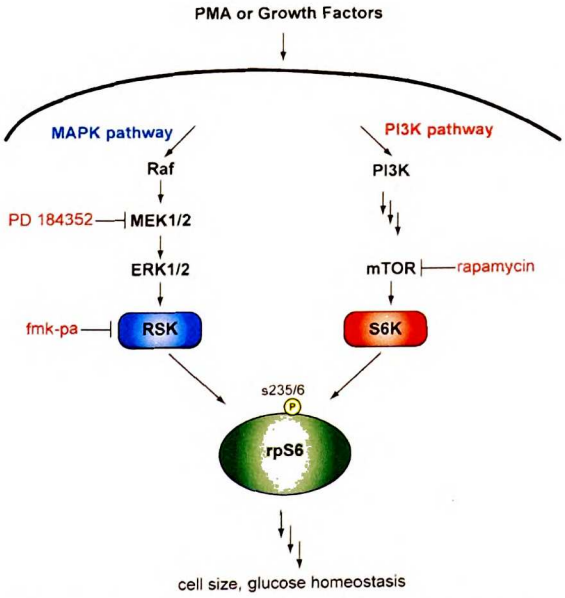

hways leading to rpS6 phosphorylation. The contribution from each pathway is ne stimulus as well as the cell type. Moreover, the signal duration propagated by erent, offering temporal control of rpS6 phosphorylation.

CTD-independent S

Saturating co

to inhibit Ser386 phe

raising the possibil

manner in certain c

Mammalian Cell lin

MDA-MB-231
COS7
HEK-293
HEK-293
COS7
HUVEC
A431
RAW 246.7
RAW 246.7

*cycling cells in DM
**cycling cells in E

Table 3-1. Variabil
phosphorylation was

To test this po

pretreatment o

type. In additi

by varying co

PMA-mediate

presence of

lipopolysacch

complete mo

a biotin-azid

enrichment

lependent Ser386 phosphorylation: Evidence for an alternative HM kinase

Saturating concentrations of fmk-pa (as revealed by click chemistry) or fmk failed t Ser386 phosphorylation completely (**Figure 3-3b**, **Figure 3-4a**, and **Table 3-1**), the possibility that Ser386 phosphorylation can occur in a CTD-independent in certain cellular contexts.

alian Cell line	Stimulus (ng/mL)	Inhibitor (μM)	Percent inhibition of Ser386 RSK phosphorylation
A-MB-231	None*	fmk-pa (0.3)	100
COS7	PMA (100)	fmk-pa (0.3)	91
IEK-293	PMA (100)	fmk (1)	80
IEK-293	PMA (100)	fmk-pa (0.3)	80
COS7	EGF (100)	fmk-pa (0.3)	78
HUVEC	None**	fmk (10)	70
A431	EGF (100)	fmk (10)	60
AW 246.7	PMA (100)	fmk-pa (1)	59
AW 246.7	LPS (1000)	fmk-pa (1)	8

cells in DMEM H12 medium containing 10% fetal bovine serum
g cells in EGM-2 (Cambrex) medium

-1. Variable inhibition of Ser386 RSK phosphorylation by fmk and fmk-pa. Percentage Ser386 rylation was determined by quantitating Western blots (ImageJ) and normalizing to DMSO controls.

t this possibility more rigorously, we compared the inhibitory effects of fmk-pa tment on Ser386 phosphorylation induced by two distinct stimuli in the same cell n addition, we used click chemistry to determine the extent of RSK modification ying concentrations of fmk-pa. In primary bone marrow-derived macrophages, nediated Ser386 phosphorylation was maximally inhibited by 67 ± 10% in the ce of 300 nM fmk-pa; by contrast, Ser386 phosphorylation induced by ysaccharide (LPS) was unaffected by up to 1 μM fmk-pa (**Figure 3-6a**), despite te modification of RSK at this concentration (**Figure 3-6c**). Click conjugation with n-azide reporter in lysates derived from LPS-stimulated cells, followed by nent of biotinylated proteins with avidin-agarose, confirmed that RSK1/RSK2 that

had been modified by

reasons that are und

reaction and trichlo

Nevertheless, our c

alternative hydropho

the RSK hydrophob

macrophages, utiliz

maximally in respon

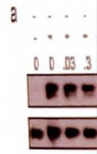

Figure 3-6. Fmk
Ser386 phosphor
macrophages sti
serum for 20 h a
stimulated with e
resolved by 10%
total RSK2. (**b**)
Figure 3-5a) rel
(**c**) Saturable R
stimulated macr
TAMRA-N_3 und
in-gel fluoresce
pa are phosph
(pretreated wit
conditions for
were resolved
RSK1, RSK2,

d been modified by fmk-pa were also phosphorylated on Ser386 (**Figure 3-6d**). For asons that are unclear, avidin affinity purification of RSK following the biotin click action and trichloroacetic acid precipitation was less efficient than expected. vertheless, our combined results provide strong evidence for the existence of an ernative hydrophobic motif (HM) kinase (or kinases) that mediates phosphorylation of e RSK hydrophobic motif (Ser386) in the absence of a functional CTD. In primary acrophages, utilization of the alternative HM kinase is context-dependent, occurring aximally in response to LPS and to a lesser extent in response to PMA (**Figure 3-7**).

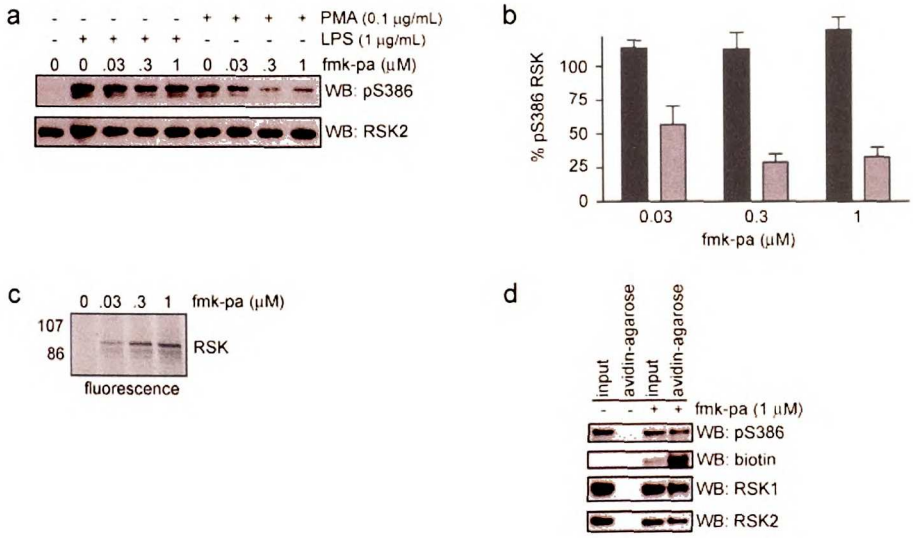

ure 3-6. Fmk-pa and click chemistry reveal the existence of a CTD-independent pathway for RSK r386 phosphorylation. (**a**) Effect of fmk-pa on Ser386 phosphorylation in primary bone marrow-derived crophages stimulated with lipopolysaccharide (LPS) and PMA. Macrophages were cultured in 0.5% um for 20 h and subsequently treated with the indicated concentrations of fmk-pa for 1 h. Cells were nulated with either PMA (100 ng/mL) or LPS (1 μg/mL) for 30 min and harvested in PBS. Proteins were olved by 10% SDS-PAGE and detected by Western blotting with antibodies to phospho-Ser386 RSK and al RSK2. (**b**) Percent Ser386 phosphorylation was determined by quantification of Western blots (e.g., **ure 3-5a**) relative to DMSO controls. Data represent mean ± s.e.m. from 3 independent experiments. Saturable RSK modification by pretreatment of intact macrophages with fmk-pa. Lysates from LPS-nulated macrophages (pretreated for 1 h with the indicated concentrations of fmk-pa) were incubated with MRA-N_3 under the click reaction conditions. Proteins were resolved by 10% SDS-PAGE and detected by gel fluorescence scanning. (**d**) Use of click chemistry to demonstrate that RSK1/RSK2 modified by fmk- are phosphorylated at Ser386 in response to LPS stimulation. Lysates from LPS-stimulated cells etreated with 1 μM fmk-pa or DMSO control) were incubated with biotin-N_3 under the click reaction nditions for 1 h. Biotinylated proteins were affinity purified with avidin-agarose beads. Eluted proteins re resolved by 10% SDS-PAGE and detected by Western blotting with streptavidin-HRP or antibodies to K1, RSK2, and phospho-Ser386 RSK.

Figure 3-7. Alternat
bypasses the CTD.

Lastly, w

pharmacological

MAPK inhibitor,

respiratory sync

cells[26]. Based

downstream of

induced RSK H

protein kinase

stimulated Se

phosphorylate

Ser386 phosp

Thus, the alter

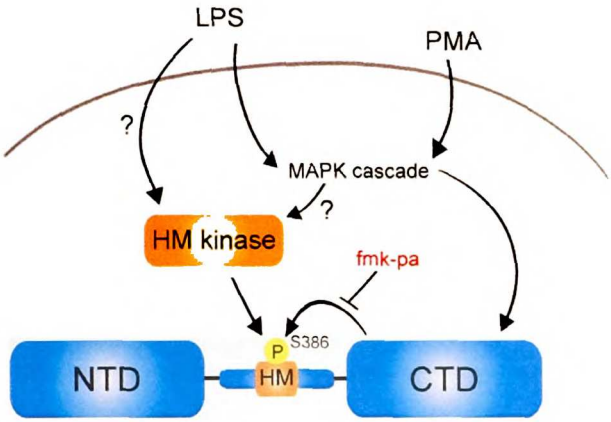

igure 3-7. Alternative RSK Ser386 phosphorylation by a putative hydrophobic motif (HM) kinase, which ypasses the CTD.

Lastly, we attempted to identify the alternative RSK HM kinase by taking a harmacological approach. Recently, it was shown that SB203580, a selective p38 IAPK inhibitor, completely abolished Ser386 phosphorylation induced by severe acute espiratory syndrome (SARS)-coronavirus (CoV) infection of monkey kidney Vero E6 ells[26]. Based on this result, we hypothesized that p38 MAPK itself, or a kinase ownstream of p38 MAPK (e.g. MAPK-activated protein kinase-2, MK-2) is the LPS iduced RSK HM kinase. Both p38 MAPK and MK-2 are candidate HM kinases for rotein kinase B[27-31]. Treatment of Bmdm with SB203580 (20 μM) did not block LPS-timulated Ser386 (**Figure 3-8a**). We then tested whether mTOR/raptor can hosphorylate Ser386, since it is the proposed S6K HM kinase[27,32]. LPS-stimulated er386 phosphorylation was unaffected by up to 100 nM rapamycin (**Figure 3-8b**). hus, the alternative RSK HM kinase remains elusive.

a

- + + +

- - - -

0 0 .03 .3

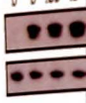

Figure 3-8. Neither
stimulated Ser386 p
inhibitors for 1 hour
proteins were resolve
RSK and RSK2.

Conclusion

Fmk-pa

mammalian cell

reaction. These

by fmk-pa, an

signaling. In

unidentified ki

previously de

targeted inhib

of RSK-media

studies with t

heart damag

fmk-pa shou

ischemia-rep

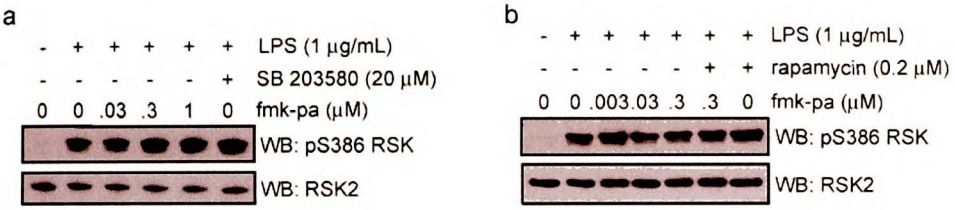

Figure 3-8. Neither rapamycin (mTOR/raptor inhibitor) nor SB 203580 (p38 MAPK inhibitor) block LPS-stimulated Ser386 phosphorylation. Primary Bmdm were treated with the indicated concentrations of inhibitors for 1 hour and then stimulated with LPS (1 μg/mL) for 30 min. Cells were lysed in PBS and proteins were resolved by SDS-PAGE and detected by Western blot with antibodies to phospho-Ser386 RSK and RSK2.

Conclusion

Fmk-pa selectively and irreversibly modifies endogenous RSK in intact mammalian cells and can be conjugated to a fluorescent or biotinylated tag via the click reaction. These properties allowed us to determine the extent of RSK CTD modification by fmk-pa, and in parallel, its effects on Ser386 phosphorylation and downstream signaling. In certain cellular contexts (e.g., LPS-stimulated macrophages), an as yet unidentified kinase bypasses the CTD requirement and phosphorylates RSK at Ser386, previously demonstrated to be essential for activation of the NTD[5,6,9]. Thus, CTD-targeted inhibitors, in contrast to NTD-targeted inhibitors, are predicted to block a subset of RSK-mediated signaling events *in vivo*, depending on the cellular context. Recent studies with transgenic mice indicate that RSK hyperactivation significantly exacerbates heart damage following ischemia-reperfusion injury[33,34]. Clickable inhibitors such as fmk-pa should facilitate determination of the specific roles played by the RSK CTD in ischemia-reperfusion injury as well as other model systems relevant to human disease.

Experimental

Chemical synthes

General. ^{1}H and ^{1}

and 100 MHz, res

downfield from a

solvent reference

recorded on a V

performed on a V

210 nm and 260

impact mass sp

Yuequan Sun

Spectrometry C

flame-dried pric

dimethylforman

using the solv

Beach, CA). A

further purifica

were used wit

indacene-3-p

purchased fro

dipyrimidine c

solvent often

were perform

was conduc

liquid chrom

ıtal

ynthesis

and ^{13}C NMR spectra were recorded on a Varian 400 spectrometer at 400 Hz, respectively. Chemical shifts were reported as parts per million (ppm) om an internal tetramethylsilane standard (δ = 0.0 for ^{1}H NMR) or from rences. Low-resolution electrospray ionization mass spectra (EI^{+}-MS) were ı a Waters Micromass ZQ 4000 spectrometer. LC/MS (MS: EI^{+}) was n a Waters AllianceHT LC/MS with a flow rate of 0.2 mL/min (monitored at 260 nm) using an Xterra MS C18 column (Waters). High-resolution electron s spectra (HRMS) were recorded on a Micromass VG70E spectrometer by Sun at the University of California-San Francisco Biomedical Mass y Center. For air- and water-sensitive reactions, glassware was oven- or prior to use and reactions were performed under argon. Dichloromethane, amide, methanol, tetrahydrofuran, toluene, and diisopropylamine were dried olvent purification system manufactured by Glass Contour, Inc. (Laguna All other solvents were of ACS chemical grade (Fisher) and used without cation unless otherwise indicated. Commercially available starting reagents vithout further purification. 6-((4,4-difluoro-5,7-dimethyl-4-bora-3a,4a-diaza-*s*-propionyl)amino)hexanoic acid, succinimidyl ester (BODIPY FL-NHS) was om Invitrogen and used without further purification. Many of the pyrrolo[2,3- compounds were sparingly soluble in acetonitrile and concentration from this yielded a nice solid. Analytical and preparative thin layer chromatography ned with silica gel 60 F_{254} glass plates (EM Science). Flash chromatography ted with 230-400 mesh silica gel (Selecto Scientific). High performance atography (HPLC) was performed on a Prostar 210 (Varian) with a flow rate

of 10 mL/min (mo

column (Peeke Sci

Fmk-BODIPY **3.1**

(0.3 mL) was add

RT over a period

deprotected prod

FL-NHS (5 mg,

stirring for 12 h

Purification by p

desired **3.1** (fm

(400 MHz, CDC

1H), 6.89 (d, 1

4.75 (t, J = 6.8

7.2 Hz, 2H), 2

LC/MS (LC: g

MS: EI$^+$): rete

Mesylate **3.2**

DIPEA (0.05

mL, 0.17 m

the reaction

mL) followe

concentrat

in the nex

MHz, CDC

2H), 4.31

of 10 mL/min (monitored at 210 nm and 260 nm) using a COMBI-A C18 preparatory column (Peeke Scientific).

Fmk-BODIPY **3.1** (fmk-BODIPY). To a solution of **2.14** (20 mg, 0.026 mmol) in CH_2Cl_2 (0.3 mL) was added TFA (0.3 mL) at 0˚C. After slowly warming the reaction mixture to RT over a period of 2 h, solvent was removed *in vacuo*. A portion of the crude boc-deprotected product (5.6 mg, 0.0084 mmol) was dissolved in DMF (0.1 mL). BODIPY FL-NHS (5 mg, 0.01 mmol) was added followed by DIPEA (3.9 mg, 0.03 mmol). After stirring for 12 h at room temperature, the reaction mixture was concentrated *in vacuo*. Purification by preparative thin layer chromatography (10:1 CH_2Cl_2/MeOH) afforded the desired **3.1** (fmk-BODIPY) (5 mg, 71% yield over 2 steps) as an off-white solid: ^{1}H NMR (400 MHz, $CDCl_3$) δ 8.35 (s, 1H), 7.37 (d, J = 8 Hz, 2H), 7.31 (d, J = 8 Hz, 2H), 7.10 (s, 1H), 6.89 (d, 1H), 6.29 (d, 1H), 6.12 (s, 1H), 5.86 (m, 1H), 5.78 (m, 1H), 4.94 (m, 2H), 4.75 (t, J = 6.8 Hz, 2H), 4.62 (d, J_{HF} = 47 Hz, 2H), 4.08 (m, 2H), 3.20 (m, 6H), 2.62 (t, J = 7.2 Hz, 2H), 2.55 (s, 2H), 2.48 (s, 3H), 2.26 (s, 3H), 2.13 (m, 4H), 1.59-1.24 (m, 12H); LC/MS (LC: gradient 0-100% MeCN [0.1% HCO_2H] over 30 min, 0.2 mL/min flow rate, MS: EI$^+$): retention time, 12.42 min; purity, >95%; 844.3 $[M+H]^+$.

Mesylate **3.2**. To a solution of **2.12** (75 mg, 0.14 mmol) in CH_2Cl_2 (3 mL) was added DIPEA (0.057 mL, 0.317 mmol) at 0˚C. Methanesulfonyl chloride (1 M in CH_2Cl_2, 0.17 mL, 0.17 mmol) was added and the reaction mixture was stirred at 0˚C. After 30 min, the reaction mixture was diluted with ethyl acetate and washed with saturated NH_4Cl (10 mL) followed by brine (10 mL). The organic fraction was dried over Na_2SO_4, filtered, and concentrated *in vacuo* to give 82 mg (96% yield) of crude mesylate **3.2**, which was used in the next reaction without purification (>95% pure based on ^{1}H NMR): ^{1}H NMR (400 MHz, $CDCl_3$) δ 8.92 (s, 1H), 7.22 (m, 4H), 4.81 (t, J = 6.8 Hz, 2H), 4.62 (d, J_{HF} = 47 Hz, 2H), 4.31 (t, J = 6.8 Hz, 2H), 2.96 (s, 3H), 2.43 (s, 3H), 2.33 (m, 2H), 1.29 (s, 18H).

Fmk-propargylam

added propargyl

The solvent was

mL) and TFA (

removed *in vacu*

TFA, over 23 m

yield): ^{1}H NMR

7.31 (d, J = 8 H

2H), 3.24 (m, 2

MeCN [0.1% H

min; purity, >95

Proteins, re

expressed in

previously de

(benzyltriazol

described[15,27

Biotechnolog

and phosph

Streptavidin-

anti-rabbit H

Cell Cultur

Eagle's me

murine bon

-propargylamine **3.3** (fmk-pa). To the crude mesylate **3.2** (57 mg, 0.092 mmol) was d propargylamine (0.5 mL) and the reaction mixture was stirred for 30 h at 40°C. solvent was removed *in vacuo* and the crude product was dissolved in CH_2Cl_2 (1 and TFA (1 mL). After stirring for 2 h at room temperature, the solvent was ved *in vacuo*. Purification by preparative HPLC (gradient 0-65% acetonitrile, 0.1 % over 23 min, 10 mL/min flow rate) afforded the desired **3.3** (fmk-pa) (4.4 mg, 35% : ^{1}H NMR (400 MHz, $CDCl_3$) δ 11.1 (br s, 1H), 8.31 (s, 1H), 7.44 (d, J = 8 Hz, 2H), (d, J = 8 Hz, 2H), 5.42 (br s, 2H), 4.76 (t, 2H), 4.67 (d, J_{HF} = 47 Hz, 2H), 3.92 (s, 3.24 (m, 2H), 2.58 (s, 1H), 2.50 (s, 3H), 2.41 (m, 2H); LC/MS (LC: gradient 0-100% N [0.1% HCO_2H] over 30 min, 0.2 mL/min flow rate, MS: EI^+): retention time, 9.28 urity, >95%; 380.0 $[M+H]^+$.

eins, reagents and antibodies. RSK2 CTD with a hexahistidine tag was ssed in *E. coli* and purified by immobilized nickel affinity chromatography as usly described[2]. PMA and LPS were purchased from Sigma. TBTA [tris- yltriazolylmethyl)amine], TAMRA-N_3 and biotin-N_3 were synthesized as previously bed[15,27]. Antibodies against RSK1 and RSK2 were purchased from Santa Cruz chnology. Antibodies against phospho-Ser386 RSK, phospho-Ser235/236 rpS6, phospho-Thr389 S6K were purchased from Cell Signaling Technology. avidin-HRP was purchased from Jackson ImunnoResearch. Anti-mouse HRP and bbit HRP secondary antibodies were purchased from Pierce.

Culture. HEK-293 and MDA-MB-231 cells were cultured in Dulbecco's modified s medium (DMEM) supplemented with 10% fetal bovine serum (FBS). Primary e bone marrow-derived macrophages were kindly provided by Melissa Pak and

Eric Brown (UCS

[pH 7.4], 10% FE

stimulating facto

Western Blottin

in either PBS ly

mM KCl, 0.5 m

inhibitor cockta

NaCl, 25% gly

phosphatase

Bradford assa

were resolve

transferred to

primary and

(ECL).

Labeling of

treated with

(3 μM) for 1

buffer. Pro

scanning wi

Click Che

RSK2 CTD

from fmk-p

Eric Brown (UCSF) and were maintained in DMEM supplemented with 20 mM Hepes [pH 7.4], 10% FBS, and 10% CMG14-12 cell supernatant (source of macrophage-colony stimulating factor)[28].

Western Blotting. Cells were washed with cold PBS and lysed by freezing and thawing in either PBS lysis buffer (1.5 mM KH_2PO_4, 8 mM Na_2HPO_4 [pH 7.4], 137 mM NaCl, 2.7 mM KCl, 0.5 mM $MgCl_2$, 0.9 mM $CaCl_2$, protease inhibitor cocktail [Roche], phosphatase inhibitor cocktail [Sigma]) or hypertonic lysis buffer (20 mM Hepes [pH 7.9], 450 mM NaCl, 25% glycerol, 3 mM $MgCl_2$, 0.5 mM EDTA, protease inhibitor cocktail [Roche], phosphatase inhibitor cocktail [Sigma]). Clarified lysates were normalized using the Bradford assay (BioRad). Laemmli sample buffer was added to samples and proteins were resolved by 10% SDS-polyacrylamide gel electrophoresis (SDS-PAGE), transferred to a nitrocellulose membrane, blocked with 5% (w/v) nonfat milk, probed with primary and secondary antibodies, and detected by enhanced chemiluminescence (ECL).

Labeling of RSK2 CTD with fmk-BODIPY. RSK2 CTD (30 nM) in PBS [pH 7.4] was treated with increasing concentrations of fmk or fmk-pa for 1 h, then with fmk-BODIPY (3 μM) for 1 h. The labeling reaction was terminated by the addition of Laemmli sample buffer. Proteins were resolved by 10% SDS-PAGE and detected by in-gel fluorescence scanning with a Typhoon 9400 flatbed laser-induced scanner (Amersham Biosciences).

Click Chemistry. Click reactions were performed as previously described[15]. Briefly, RSK2 CTD (30 nM) pretreated with the indicated concentrations of fmk-pa, or lysates from fmk-pa-pretreated cells were incubated with TAMRA-N_3 or biotin-N_3 (50 μM), TCEP

(1 mM), $CuSO_4$ (

at room temperat

fluorescence sc

detected by Wes

PMA-stimulate

cells. Conflue

subsequently tr

stimulation wit

harvested in e

Click chemistr

Proteins were

LPS and PM

in 12-well pl

and 0.5% FB

1 h at 37°C.

cells were w

performed

fluorescenc

Avidin pu

macrophag

Hepes [pH

pa for 1 h

(1 mM), $CuSO_4$ (1 mM), and TBTA (100 μM) in PBS [pH 7.4] containing 1% SDS for 1 h at room temperature. Proteins were resolved by 10% SDS-PAGE and detected by in-gel fluorescence scanning (TAMRA-N_3) or were affinity purified with avidin-agarose and detected by Western blotting (biotin-N_3).

PMA-stimulated RSK Ser386 and rpS6 Ser235/236 phosphorylation in HEK-293 cells. Confluent HEK-293 cells in 12-well plates were deprived of serum for 2 h and subsequently treated with the indicated concentrations of inhibitors for 1 h at 37°C. After stimulation with PMA (0.1 μg/mL) for 30 min, cells were washed with cold PBS and harvested in either PBS lysis buffer (**Fig. 1c** and **2c**) or hypertonic lysis buffer (**Fig. 3**). Click chemistry was performed with TAMRA-N_3 in lysates from cells treated with fmk-pa. Proteins were analyzed by in-gel fluorescence scanning or Western blotting.

LPS and PMA stimulation of primary mouse macrophages. Confluent macrophages in 12-well plates were incubated in DMEM supplemented with 20 mM Hepes [pH 7.4] and 0.5% FBS for 12 h prior to treatment with the indicated concentrations of fmk-pa for 1 h at 37°C. After stimulation with either PMA (0.1 μg/mL) or LPS (1 μg/mL) for 30 min, cells were washed with cold PBS and harvested in PBS lysis buffer. Click chemistry was performed with TAMRA-N_3 and proteins were subsequently analyzed by in-gel fluorescence scanning or Western blotting.

Avidin pulldown from LPS-stimulated primary macrophages. Confluent primary macrophages in 15 cm plates were incubated in DMEM supplemented with 20 mM Hepes [pH 7.4] and 0.5% FBS for 12 h prior to treatment with either DMSO or 1 μM fmk-pa for 1 h at 37 ^{0}C. Lysates (200 μL, 5 mg/mL) prepared in PBS were subjected to click

chemistry to con

proteins were p

centrifugation (1

pellet was washe

was solubilized

Samples were c

Avidin-agarose

overnight at 4

washed with P

proteins were

biotin (100 μL

mistry to conjugate biotin-N_3 to fmk-pa-modified RSK. After the click reaction, eins were precipitated using 15% (v/v) tricloroacetic acid (TCA) and pelleted by trifugation (13,000 rpm, 5 min, 4°C). The supernatant was removed and the protein et was washed twice with ice-cold acetone (2 x 200 μL). The resulting acetone pellet solubilized in PBS (40 μL) containing 2% (w/v) SDS by heating and sonication. nples were diluted 10-fold in PBS containing 0.5 % (v/v) NP40 (400 μL, 0.9 mg/mL). lin-agarose (30 μL of 50% slurry in PBS) was added and samples were rotated rnight at 4°C. The post-avidin supernatant was removed and the beads were hed with PBS containing 0.5% NP40 and 0.1% SDS (2 x 1 mL). Affinity purified eins were eluted from the beads with 2X Laemmli sample buffer containing 1 mM n (100 μL), resolved by 10% SDS-PAGE, and detected by Western blotting.

References

1. Frodin, M.
(RSK) in si
2. Cohen, M
based de
(2005).
3. Smith, J.
extracell
sequenc
4. Gavin,
phosph
(1999).
5. Frodin
regula
PDK1
6. Jense
by 3-
(199
7. Rich
kina
MA
8. Fis
pp
9. De
re

ences

Frodin, M. & Gammeltoft, S. Role and regulation of 90 kDa ribosomal S6 kinase (RSK) in signal transduction. *Mol Cell Endocrinol* **151**, 65-77 (1999).

Cohen, M. S., Zhang, C., Shokat, K. M. & Taunton, J. Structural bioinformatics-based design of selective, irreversible kinase inhibitors. *Science* **308**, 1318-21 (2005).

Smith, J. A., Poteet-Smith, C. E., Malarkey, K. & Sturgill, T. W. Identification of an extracellular signal-regulated kinase (ERK) docking site in ribosomal S6 kinase, a sequence critical for activation by ERK in vivo. *J Biol Chem* **274**, 2893-8 (1999).

Gavin, A. C. & Nebreda, A. R. A MAP kinase docking site is required for phosphorylation and activation of p90(rsk)/MAPKAP kinase-1. *Curr Biol* **9**, 281-4 (1999).

Frodin, M., Jensen, C. J., Merienne, K. & Gammeltoft, S. A phosphoserine-regulated docking site in the protein kinase RSK2 that recruits and activates PDK1. *Embo J* **19**, 2924-34 (2000).

Jensen, C. J. et al. 90-kDa ribosomal S6 kinase is phosphorylated and activated by 3-phosphoinositide-dependent protein kinase-1. *J Biol Chem* **274**, 27168-76 (1999).

Richards, S. A., Fu, J., Romanelli, A., Shimamura, A. & Blenis, J. Ribosomal S6 kinase 1 (RSK1) activation requires signals dependent on and independent of the MAP kinase ERK. *Curr Biol* **9**, 810-20 (1999).

Fisher, T. L. & Blenis, J. Evidence for two catalytically active kinase domains in pp90rsk. *Mol Cell Biol* **16**, 1212-9 (1996).

Dalby, K. N., Morrice, N., Caudwell, F. B., Avruch, J. & Cohen, P. Identification of regulatory phosphorylation sites in mitogen-activated protein kinase (MAPK)-

activated
1496-50
10. Vik, T.
autopho
398-40
11. Bjorbac
kinase
12. Chrest
kinase
41 (20
13. Vocad
glyco
(2004
14. Spee
using
125,
15. Spe
che
16. Ova
two
17. Ale
im
en
18. Ev
in
B

vated protein kinase-1a/p90rsk that are inducible by MAPK. *J Biol Chem* **273**,)6-505 (1998).

, T. A. & Ryder, J. W. Identification of serine 380 as the major site of ophosphorylation of Xenopus pp90rsk. *Biochem Biophys Res Commun* **235**, -402 (1997).

rbaek, C., Zhao, Y. & Moller, D. E. Divergent functional roles for p90rsk ase domains. *J Biol Chem* **270**, 18848-52 (1995).

estensen, C. A. & Sturgill, T. W. Characterization of the p90 ribosomal S6 ase 2 carboxyl-terminal domain as a protein kinase. *J Biol Chem* **277**, 27733- (2002).

adlo, D. J. & Bertozzi, C. R. A strategy for functional proteomic analysis of cosidase activity from cell lysates. *Angew Chem Int Ed Engl* **43**, 5338-42 04).

ers, A. E., Adam, G. C. & Cravatt, B. F. Activity-based protein profiling in vivo ng a copper(i)-catalyzed azide-alkyne [3 + 2] cycloaddition. *J Am Chem Soc* , 4686-7 (2003).

ers, A. E. & Cravatt, B. F. Profiling enzyme activities in vivo using click mistry methods. *Chem Biol* **11**, 535-46 (2004).

a, H. et al. Chemistry in living cells: detection of active proteasomes by a -step labeling strategy. *Angew Chem Int Ed Engl* **42**, 3626-9 (2003).

ander, J. P. & Cravatt, B. F. Mechanism of carbamate inactivation of FAAH: ications for the design of covalent inhibitors and in vivo functional probes for ymes. *Chem Biol* **12**, 1179-87 (2005).

ns, M. J., Saghatelian, A., Sorensen, E. J. & Cravatt, B. F. Target discovery nall-molecule cell-based screens by in situ proteome reactivity profiling. *Nat echnol* **23**, 1303-7 (2005).

19. Ruvinsk
size an
20. Hay, N
1926-4
21. Pende
rapam
mitoge
3112-
22. Weng
Analy
1662
23. Leigh
Com
a rel
MAF
93 (
24. Wa
S6
25. Sha
He
MA
En
26. Mi
p
5

Ruvinsky, I. et al. Ribosomal protein S6 phosphorylation is a determinant of cell size and glucose homeostasis. *Genes Dev* **19**, 2199-211 (2005).

Hay, N. & Sonenberg, N. Upstream and downstream of mTOR. *Genes Dev* **18**, 1926-45 (2004).

Pende, M. et al. S6K1(-/-)/S6K2(-/-) mice exhibit perinatal lethality and rapamycin-sensitive 5'-terminal oligopyrimidine mRNA translation and reveal a mitogen-activated protein kinase-dependent S6 kinase pathway. *Mol Cell Biol* **24**, 3112-24 (2004).

Weng, Q. P. et al. Regulation of the p70 S6 kinase by phosphorylation in vivo. Analysis using site-specific anti-phosphopeptide antibodies. *J Biol Chem* **273**, 16621-9 (1998).

Leighton, I. A., Dalby, K. N., Caudwell, F. B., Cohen, P. T. & Cohen, P. Comparison of the specificities of p70 S6 kinase and MAPKAP kinase-1 identifies a relatively specific substrate for p70 S6 kinase: the N-terminal kinase domain of MAPKAP kinase-1 is essential for peptide phosphorylation. *FEBS Lett* **375**, 289-93 (1995).

Wang, X. et al. Regulation of elongation factor 2 kinase by p90(RSK1) and p70 S6 kinase. *Embo J* **20**, 4370-9 (2001).

Shahbazian, D. R., P.P.; Mieulet, V.; Cohen, M.S.; Raught, B.; Taunton, J.; Hershey J.W.B.; Blenis, J.; Pende, M.; Sonenberg, N. The mTOR/PI3K and MAPK pathways converge on eIF4B to control its phosphorylation and activity. *Embo J*, In Press (2006).

Mizutani, T., Fukushi, S., Saijo, M., Kurane, I. & Morikawa, S. Regulation of p90RSK phosphorylation by SARS-CoV infection in Vero E6 cells. *FEBS Lett* **580**, 1417-24 (2006).

Dong, L. Q. & Liu, F. PDK2: the missing piece in the receptor tyrosine kinase signaling pathway puzzle. *Am J Physiol Endocrinol Metab* **289**, E187-96 (2005).

Alessi, D. R. et al. Mechanism of activation of protein kinase B by insulin and IGF-1. *Embo J* **15**, 6541-51 (1996).

Baudhuin, L. M., Cristina, K. L., Lu, J. & Xu, Y. Akt activation induced by lysophosphatidic acid and sphingosine-1-phosphate requires both mitogen-activated protein kinase kinase and p38 mitogen-activated protein kinase and is cell-line specific. *Mol Pharmacol* **62**, 660-71 (2002).

Gonzalez, I. et al. Akt2, a novel functional link between p38 mitogen-activated protein kinase and phosphatidylinositol 3-kinase pathways in myogenesis. *Mol Cell Biol* **24**, 3607-22 (2004).

Rane, M. J. et al. p38 Kinase-dependent MAPKAPK-2 activation functions as 3-phosphoinositide-dependent kinase-2 for Akt in human neutrophils. *J Biol Chem* **276**, 3517-23 (2001).

Isotani, S. et al. Immunopurified mammalian target of rapamycin phosphorylates and activates p70 S6 kinase alpha in vitro. *J Biol Chem* **274**, 34493-8 (1999).

Itoh, S. et al. Role of p90 ribosomal S6 kinase-mediated prorenin-converting enzyme in ischemic and diabetic myocardium. *Circulation* **113**, 1787-98 (2006).

Maekawa, N. et al. Inhibiting p90 ribosomal S6 kinase prevents (Na+)-H+ exchanger-mediated cardiac ischemia-reperfusion injury. *Circulation* **113**, 2516-23 (2006).

Feldman, A. K., Colasson, B. & Fokin, V. V. One-pot synthesis of 1,4-disubstituted 1,2,3-triazoles from in situ generated azides. *Org Lett* **6**, 3897-9 (2004).

Stamm, L. M. et al. Mycobacterium marinum escapes from phagosomes and is propelled by actin-based motility. *J Exp Med* **198**, 1361-8 (2003).

Chapter 4

Isoform-selective p90 RSK inhibitors identified by a two-step competition labeling approach

Abstract

A sr
acceptors d
the C-termin
and isoform
labeling in
that can b
extent of c
bearing a
more RS
electroph
slightly m
isoform s
the cyste
react m
revealed
demons
rate of

Abstract

A small series of electrophilic pyrrolo[2,3-*d*]pyrimidines containing Michael acceptors designed to react with a nonconserved cysteine in the ATP binding pocket of the C-terminal kinase domain (CTD) of RSK1 and RSK2 were synthesized. The potency and isoform selectivity of these compounds were rapidly evaluated by competition labeling in living cells with fmk-pa, an alkyne-containing, irreversible RSK CTD inhibitor that can be conjugated to an azidoalkyl reporter via the click reaction to assess the extent of covalent RSK CTD modification. Using this strategy, we found that compounds bearing an electrophile at the C-6 position of the pyrrolo[2,3-*d*]pyrimidine scaffold were more RSK1 selective; however, the degree of selectivity varied greatly among the electrophilic inhibitors. By contrast, the parent scaffold, a reversible inhibitor, was slightly more selective for RSK2. Together, these results support the hypothesis that isoform selectivity is achieved by a mechanism involving covalent bond formation with the cysteine in the CTD. Consistent with this idea, electrophilic pyrrolo[2,3-*d*]pyrimidines react much more rapidly with recombinant RSK1 CTD than RSK2 CTD *in vitro* as revealed by electrospray mass spectrometry. To our knowledge, this is the first example demonstrating that isoform selectivity can be achieved by exploiting differences in the rate of covalent bond formation.

Introduction

Many

overlapping p

in which man

physiological

poorly under

distinguish

hindered, in

several kina

commonly

time consu

Herein, we

in living c

(RSK), RS

inhibitors

Co

of a give

reversible

active s

fluoroph

bioortho

referred

covalen

and se

RSK2

inhibit

man enzymes are expressed as isoforms that often have distinct, non-siological roles. This is especially pertinent to the protein kinase family, of its members consist of a subfamily of closely related isoforms[1]. The les of individual kinase isoforms within a closely related family are often od due to the lack of cell-permeable, small molecule inhibitors that can ween them[2]. The discovery of isoform selective kinase inhibitors is rt, by the lack of methods to rapidly screen potential inhibitors against isoforms simultaneously in a cellular context. Isoform selectivity is most essed *in vitro* using kinase activity assays, which can be laborious and g, requiring the expression and purification of individual isoforms[3,4]. ort a two-step competition labeling approach to rapidly profile compounds against two closely related isoforms of the p90 ribosomal S6 kinases nd RSK2. This strategy led to the identification of several RSK1-selective chieve isoform selectivity through covalent bond formation.

tion assays exploiting activity based probes that target several members yme family have been used to quickly screen irreversible[5-7] as well as nibitors in cell lysates. These activity based probes are composed of cted, electrophilic inhibitors and a reporter tag, such as biotin or a s reporter tags are often quite large and interfere with probe binding, ethods, such as the [3+2] azide/alkyne cycloaddition reaction (commonly e click reaction), have been developed to conjugate the reporter tag after ation of the protein target[11,12]. We recently described fmk-pa, a potent ickable inhibitor of the C-terminal kinase domains (CTD) of RSK1 and **4-1**). Fmk-pa is a structurally related variant of fmk, an irreversible cts specifically with a nonconserved cysteine (Cys436, human RSK2

numbering) fo

(HEK-293) co

be conjugate

reaction in ce

Figure 4-1.
position. Fr
methylketone
derivative of
modification

The mole

distinct b

scanning

RSK2 as

4-2). C

vitro, w

library o

Figure
fmk-pa
were i
detecti

umbering) found in the ATP-binding site of the RSK CTD[13]. In human epithelial kidney HEK-293) cells, fmk-pa irreversibly modified endogenous RSK1 and RSK2 and could e conjugated to a tetramethylrhodamine-azide reporter (TAMRA-N_3) via the click eaction in cell lysates.

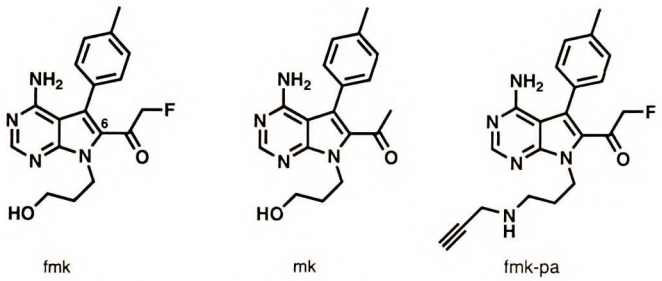

gure 4-1. Chemical structures of pyrrolo[2,3-*d*]pyrimidines substituted with an electrophile at the C-6 osition. Fmk is a potent and selective irreversible inhibitor of the CTD of RSK1 and RSK2. The ethylketone (mk) analog of fmk was designed as a reversible covalent RSK CTD inhibitor. Fmk-pa is a rivative of fmk that can be conjugated to an azidoalkyl reporter via the click reaction to assess covalent odification of RSK CTD in cells.

ne molecular weight of RSK1 and RSK2 differ enough to enable detection of two stinct bands by denaturing gel electrophoresis followed by in-gel fluorescence anning. We demonstrate here that the lower band is RSK1 whereas the upper band is SK2 as determined by quantitative immunodepletion using specific antibodies (**Figure 2**). Consequently, using a cellular competition assay followed by click chemistry *in tro*, we could determine, in parallel, the potency and isoform selectivity of a small rary of electrophilic compounds against endogenous RSK1 and RSK2.

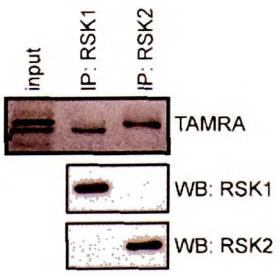

ure 4-2. Two distinct RSK bands are targeted by fmk-pa in intact cells. HEK-293 cells were treated with k-pa (0.3 μM). Cells were harvested and click reactions were performed with TAMRA-N_3. Cell lysates re incubated with either RSK1 or RSK2 antibodies. Proteins were resolved by 10% SDS-PAGE and ected by in-gel fluorescence scanning, followed by Western blotting.

Results an

Design and

We c

on a pyrro

electrophile

Scheme
condition
Et_3N, DM
1-(3-dime
THF (21

Briefly

bromo

acrylat

Acrylat

remo

benz

sults and Discussion

sign and synthesis of electrophilic RSK CTD inhibitors

We designed and synthesized a small set of potential RSK CTD inhibitors based a pyrrolo[2,3-*d*]pyrimdine chemotype that contain various Michael acceptor ctrophiles at the C-6 position according to **Schemes 4-1** and **4-2**.

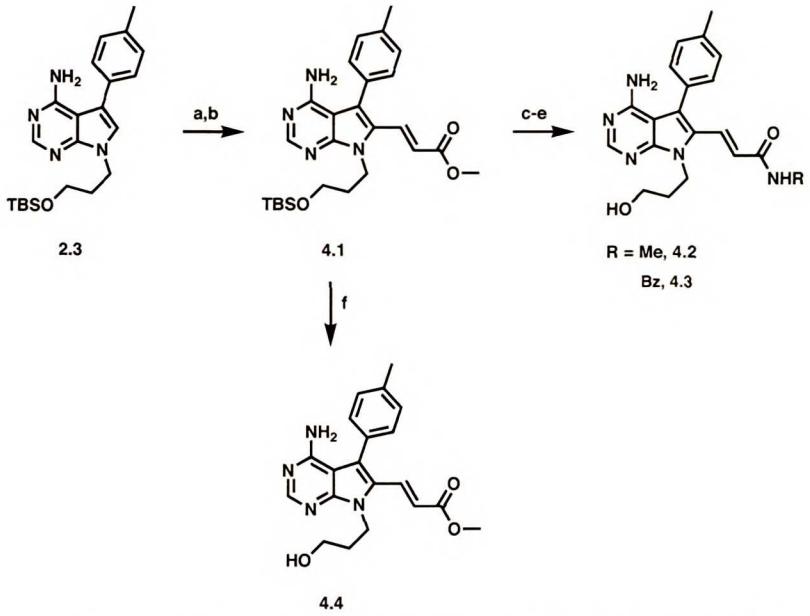

eme 4-1. Synthesis of Michael acceptor-substituted pyrrolo[2,3-*d*]pyrimidines I. Reagents and itions: a. *N*-bromosuccinimide, DMF (99% yield); b. Methyl acrylate, $Pd(OAc)_2$, tri(ortho-tolyl)phosphine, , DMF (76% yield); c. LiOH, THF, MeOH, H_2O (60% yield); d. methylamine (**4.2**) or benzylamine (**4.3**), dimethylaminopropyl)-3-ethylcarbodiimide hydrochloride (EDCI-HCl), DIPEA, DMF, CH_2Cl_2; e. 1 N HCl, (21% yield over two steps); f. 1 N HCl, THF (46% yield).

efly, enoate **4.1** was obtained via bromination of scaffold **2.3** with *N*-mosuccinimide, followed by a palladium-catalyzed Heck coupling with methyl late. Facile removal of the silyl protecting group with 1 N HCl afforded enoate **4.4**. lamides **4.2** and **4.3** were conveniently prepared from **4.1** in three steps involving oval of the methyl ester, coupling of the free acid with either methylamine or zylamine using the standard amino acid coupling reagent, 1-(3-

dimethylamin

silyl protectin

2,3 $\xrightarrow{a,b}$ N

TBS

Scheme 4
conditions:
OsO_4, NaI
2-propano
cyanoacet
(89% yie
CH_2Cl_2; m

The oth

from th

Lemieu

Wittig

and O

Knoev

and C

dimethylaminopropyl)-3-ethylcarbodiimide hydrochloride (EDCI-HCl), and removal of the silyl protecting group.

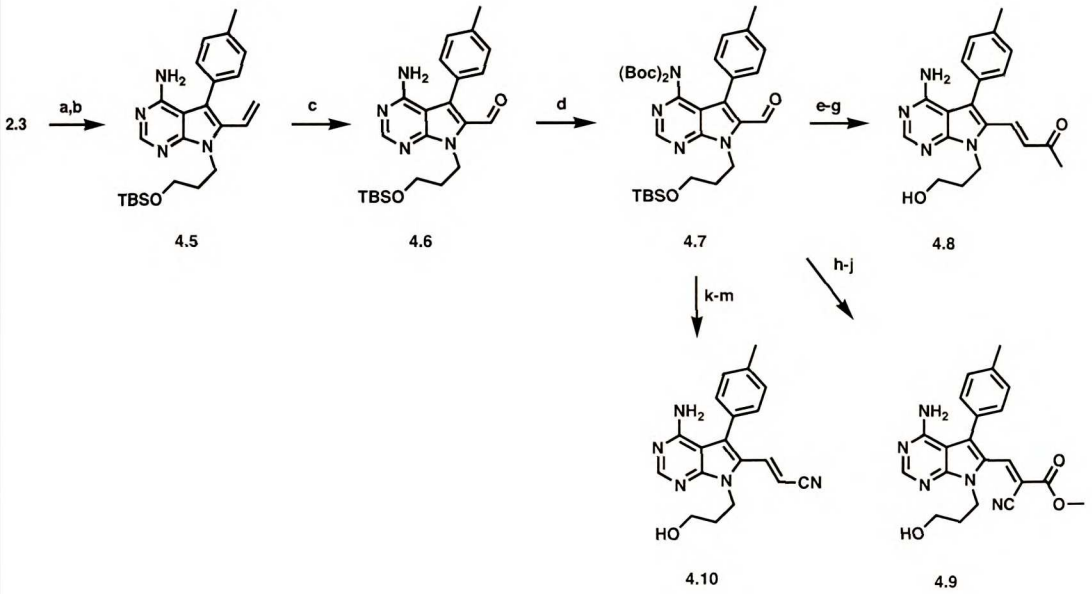

Scheme 4-2. Synthesis of Michael acceptor-substituted pyrrolo[2,3-*d*]pyrimidines II. Reagents and conditions: a. *N*-bromosuccinimide, DMF (99% yield); b. tributylvinyltin, $Pd[P(Ph)_3]_4$, toluene (88% yield); c. OsO_4, $NaIO_4$, THF, H_2O (86% yield); d. $(Boc)_2O$, DMAP, THF (70% yield); e. 1-triphenyl-phosphoranylidene-2-propanone, CH_2Cl_2 (95% yield); f. TFA, CH_2Cl_2; g. 1 N HCl, THF (89% yield over 2 steps); h. methyl cyanoacetate, 1,8-diazabicyclo(5.4.0)undec-7-ene (DBU), THF (78% yield); i. TFA, CH_2Cl_2; j. 1 N HCl, THF (89% yield over 2 steps); k. 1-triphenyl-phosphoranylidene-2-acetonitrile, CH_2Cl_2 (80% yield); l. TFA, CH_2Cl_2; m. 1 N HCl, THF (80% yield over 2 steps)

The other Michael acceptor derivatives used in this study could readily be synthesized from the aldehyde intermediate **4.7**, which was prepared from vinyl **4.5** according to the Lemieux oxidation protocol. Enone **4.8** and acrylonitrile **4.10** were prepared by the Wittig reaction with the appropriate phosphoranylidene, followed by removal of the *N*-boc and *O*-silyl protecting groups. Finally, acrylonitrile-enoate **4.9** was synthesized via the Knoevenagel condensation with methyl cyanoacetate, followed by removal of the *N*-boc and *O*-silyl protecting groups.

Competitio

To d

substituted

clickable R

competition

scaffold (a

treated wi

saturating

TAMRA-N

electrophi

was quan

Table 4-1

a

Figure
(a) C
RSK2
0.3 μ
TAMR
scann
black
4.9: b

petition profiling reveals isoform selectivity of RSK CTD inhibitors

To determine the cellular potency and isoform selectivity of the Michael acceptor-tuted compounds, we used a two-step competition labeling approach exploiting our ble RSK CTD inhibitor, fmk-pa. We also included three other compounds in this etition analysis: fmk, mk (**Figure 4-1**), and the parent pyrrolo[2,3-*d*]pyrimidine old (absent the electrophile at the C-6 position). Human HEK-293 cells were ed with increasing concentrations of the electrophilic compounds followed by ating fmk-pa (0.3 μM). Cell lysates were subjected to click conjugation with RA-N_3, and labeled RSK1 and RSK2 were separated by denaturing gel ophoresis and detected by in-gel fluorescence scanning (**Figure 4-3**). Competition quantified by determining the IC_{50} values against RSK1 and RSK2 (**Figure 4-3b** and **4-1**).

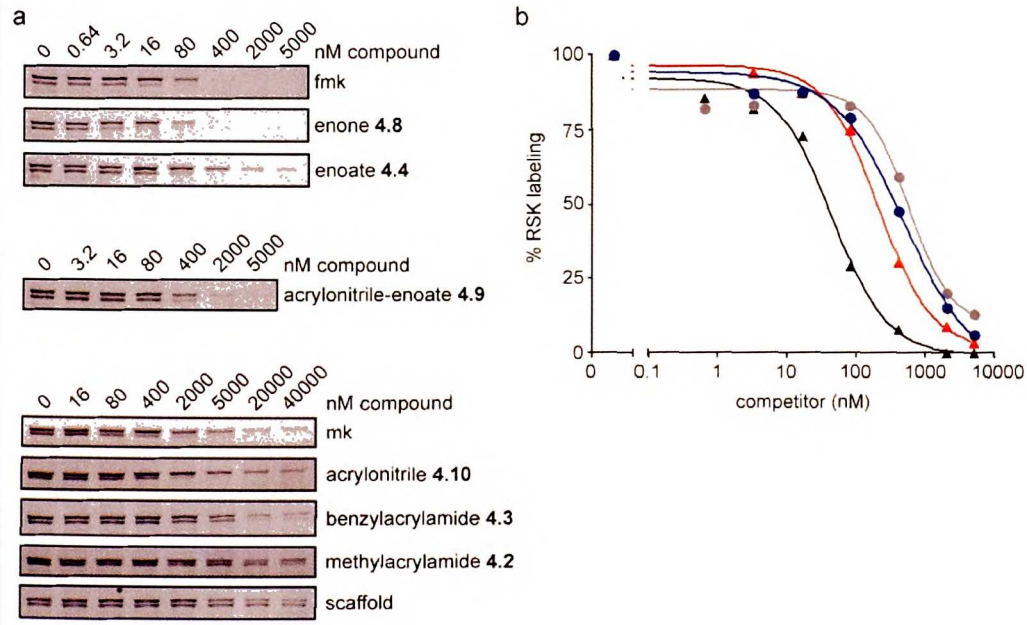

4-3. Two-step competition labeling as a method to screen RSK1 and RSK2 CTD inhibitors in cells. mpetition labeling profiles of pyrrolo[2,3-*d*]pyrimidines derivatives (competitor) against RSK1 and HEK-293 cells were treated with the indicated concentrations of the competitor for 1 h followed by fmk-pa for 1 h. Cells were harvested in PBS and click reactions were performed in lysates with -N_3 for 1h. Proteins were resolved by 10% SDS-PAGE and detected by in-gel fluorescence g. (**b**) Representative dose-response curves obtained by quantification of fluorescent bands in (**a**); iangles, RSK1/enoate **4.4**; gray circles, RSK2/enoate **4.4**; red triangles, RSK1/acrylonitrile-enoate e circles, RSK2/acrylonitrile-enoate.

Table 4-1.
from quanti
last column
isoform sel

T

selectivi

pyrrolo[

tested,

potent

fmk a

relativ

cystei

corre

reac

acc

acr

be

compound	IC_{50} (nM) RSK1	RSK2	RSK2/RSK1
fmk	5	97	19
enone **4.8**	4	57	14
enoate **4.4**	45	577	13
mk	200	1600	8
acrylonitrile **4.10**	1000	6000	6
acrylonitrile-enoate **4.9**	212	484	2
methylacrylamide **4.2**	~10000	~10000	~1
benzylacrylamide **4.3**	~10000	~10000	~1
scaffold	~40000	~20000	~0.5

Table 4-1. IC_{50} values of pyrrolo[2,3-*d*]pyrimidines derivatives against RSK1 and RSK2 in cells (obtained from quantitative analysis of the two-step competition labeling experiments described in **Figure 4-3**). The last column shows the IC_{50} values against RSK2 divided by the IC_{50} values against RSK1, which gives the isoform selectivity for each compound.

The IC_{50} values shown in **Table 4-1** demonstrate that the potency and isoform selectivity can vary significantly as a function of the electrophile at the C-6 position of the pyrrolo[2,3-*d*]pyrimidine scaffold. Fmk was the most RSK1-selective of the compounds tested, exhibiting a 19-fold greater potency over RSK2. The fluoride atom is required for potent inhibition, as the ketone isosteric variant, mk, was 40- and 16-fold weaker than fmk against RSK1 and RSK2, respectively. Despite the decreased potency of mk relative to fmk, its greater chemical stability toward proteinogenic nucleophiles, such as cysteine, may give it more therapeutic value.

Within the Michael acceptor series, potency and RSK1 selectivity generally correlated with the intrinsic reactivity of the electrophile. The predicted order of reactivity, based on kinetic analysis of the Michael acceptor fragment, for the Michael acceptor pyrrolo[2,3-*d*]pyrimidine derivatives toward thiolates[14] is as follows: enone **4.8** > acrylonitrile-enoate **4.9** > enoate **4.4** > acrylonitrile **4.10** > methylacrylamide **4.2** ≅ benzylacrylamide **4.3**. Indeed enone **4.8** exhibited the greatest potency against RSK1

(IC_{50} = 4 n

and **4.3** w

RSK1 and

RSK1 and

enoate **4.**

potent ag

selective

in the lo

parent s

RSK2),

electrop

exploite

Isofor

88% i

formin

carrie

RSK

RSK

mod

mod

sec

wer

= 4 nM) and RSK2 (IC_{50} = 57 nM) and RSK1 selectivity whereas acrylamides **4.2** **.3** weakly inhibited both RSK1 and RSK2 (IC_{50} values of ~10 μM against both and RSK2). Enoate **4.4** was ~10-fold less potent than enone **4.8** against both and RSK2. On the basis of Michael acceptor reactivity, we expected acrylonitrile- e **4.9** to be more potent than enoate **4.4**; however, this compound was ~5-fold less against RSK1 and equipotent against RSK2, and, moreover, was only 2-fold more ive for RSK1. The less reactive compound, acrylonitrile **4.10**, exhibited IC_{50} values low-micromolar range and was 6-fold more selective for RSK1. Intriguingly, the scaffold, although a weak cellular inhibitor (IC_{50} > 10 μM for both RSK1 and), was slightly more selective for RSK2. Together, these results demonstrate that ophiles at the C-6 position of the pyrrolo[2,3-*d*]pyrimidine chemotype can be ed to achieve isoform selectivity.

rm selectivity is likely governed by covalent chemistry

We hypothesize that subtle differences in the CTD of RSK1 and RSK2, which are dentical, can influence the rate of covalent bond formation with Cys436, thus g the basis for isoform-selective inhibition. To test this notion experimentally, we out kinetic analyses *in vitro* of the reaction of fmk with the CTD of RSK1 and in the presence of 2 mM ATP (physiologically relevant concentration). Irreversible TD modification was analyzed by mass spectrometry. Remarkably, complete ation of RSK1 CTD by fmk occurred in less than 10 min; by contrast, complete ation of RSK2 CTD required greater than 35 min (**Figure 4-4**). The apparent -order rate constants for fmk against RSK1 CTD and RSK2 CTD modification 2 X 10^5 $M^{-1}min^{-1}$ and ~2 X 10^4 $M^{-1}min^{-1}$ ($k_{obs}/[I]$), respectively. The ~10-fold higher

ation of RSK1 CTD relative to RSK2 CTD is consistent with the idea that
vity is governed by covalent bond formation with Cys436.

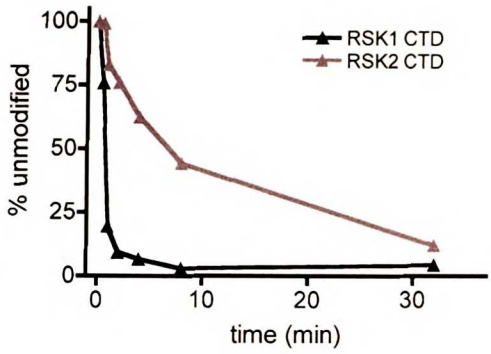

dependent, covalent modification of the CTD of RSK1 and RSK2. human RSK1 CTD (1
SK2 CTD (1 μM) (the CTD of mouse and human RSK2 are 100% identical) were treated
the presence of 2 mM ATP at 0^0C for various times. Reactions were quenched by the
acid (0.4% v/v) and analyzed by liquid chromatography/mass spectrometry (LC/MS).
btained by H. Hadjivassiliou in the Taunton laboratory.

mary factors that can influence the rate of covalent bond formation of
cted, electrophilic inhibitors are the position and reactivity of the targeted
These factors are intimately connected to the local environment that
he nucleophilic residue. In RSK1 and RSK2, Cys436, targeted by fmk[13]
electrophilic inhibitors described in this study, is located at the C-terminal
ible glycine-rich loop (Gly-rich loop), which contains a highly conserved
(G-X-G-X-Y/F-G/S)[15]. This loop is situated at the roof of the active site
ributes to ATP as well as inhibitor binding. Interestingly, sequence
e CTD Gly-rich loop of RSK1 and RSK2 revealed three non-homologous
ferences (**Figure 4-5**). We speculate that isoform selectivity emanates
erences in the Gly-rich loop. Although the residues in this loop do not
t the active site (based on the analysis of multiple kinase crystals
ey could influence the position (proximity to electrophile) and/or
pKa) of Cys436.

Figure 4-
RSK2. Cy
glycines a

Conclu

screen

RSK1

electro

Micha

were

the el

differ

the C

dete

Gly-rich loop

```
RSK1    YVVKETIGVGSYSEC
RSK2    YEVKEDIGVGSYSVC
```

4-5. Sequence alignment of the Gly-rich loop located in the CTD active site of human RSK1 and Cys436 (colored red) is the nucleophile that reacts with the electrophilic inhibitors. The conserved are highlighted in yellow.

lusion

In this study, we have developed a two-step competition labeling strategy to irreversible as well as reversible inhibitors in intact cells against endogenous and RSK2. Using this approach, we profiled the potency and isoform selectivity of philic pyrrolo[2,3-*d*]pyrimidine derivatives, including several newly described l acceptor-substituted compounds. Intriguingly, we found that these compounds SK1-selective, and that this selectivity was dependent on the intrinsic reactivity of ctrophiles. We provide evidence that isoform selectivity is achieved by exploiting nces in the rate of covalent bond formation with Cys436 at the C-terminal end of -rich loop in the CTD of RSK1 and RSK2. Future studies will be directed toward ining the origin of this rate difference.

Experim

Chemica

General.

and 100

downfiel

solvent

recorde

perform

210 nm

impact

Yueqi

Spect

flame

dimet

using

Beac

furth

wer

wer

nic

sili

23

(H

(n

S

ıl

thesis

nd ^{13}C NMR spectra were recorded on a Varian 400 spectrometer at 400 respectively. Chemical shifts were reported as parts per million (ppm) n an internal tetramethylsilane standard (δ = 0.0 for ^{1}H NMR) or from ıces. Low-resolution electrospray ionization mass spectra (EI^{+}-MS) were a Waters Micromass ZQ 4000 spectrometer. LC/MS (MS: EI^{+}) was a Waters AllianceHT LC/MS with a flow rate of 0.2 mL/min (monitored at 50 nm) using an Xterra MS C18 column (Waters). High-resolution electron spectra (HRMS) were recorded on a Micromass VG70E spectrometer by ı at the University of California-San Francisco Biomedical Mass Center. For air- and water-sensitive reactions, glassware was oven- or or to use and reactions were performed under argon. Dichloromethane, nide, methanol, tetrahydrofuran, toluene, and diisopropylamine were dried ent purification system manufactured by Glass Contour, Inc. (Laguna All other solvents were of ACS chemical grade (Fisher) and used without ion unless otherwise indicated. Commercially available starting reagents hout further purification. Many of the pyrrolo[2,3-*d*]pyimidine compounds soluble in acetonitrile and concentration from this solvent often yielded a alytical and preparative thin layer chromatography were performed with 254 glass plates (EM Science). Flash chromatography was conducted with silica gel (Selecto Scientific). High performance liquid chromatography performed on a Prostar 210 (Varian) with a flow rate of 10 mL/min 210 nm and 260 nm) using a COMBI-A C18 preparatory column (Peeke

Enoate-O

(0.26 mL

was deg

0.38 mm

was hea

concen

chroma

yellow

1H), 7.

4.45 (t

0.88 (

138.3

25.9,

Meth

THF

H_2O

mix

The

vac

ga

so

wi

us

D

Enoate-OTBS **4.1**. To bromide-OTBS **2.4** (300 mg, 0.63 mmol) in DMF (2 mL) and Et_3N (0.26 mL, 1.90 mmol) was added palladium acetate (42.4 mg, 0.19 mmol). The mixture was degassed by two cycles of freeze-pump-thaw and tri-*o*-tolylphosphine (115.4 mg, 0.38 mmol) was added, followed by methyl acrylate (0.206 mL, 2.90 mmol). The mixture was heated to 100 ^{0}C in a sealed-tube reaction vessel. After 4 h, the mixture was concentrated *in vacuo* and the crude product was rapidly purified by flash chromatography (1:1 hexanes/ethyl acetate) to give 231 mg (76% yield) of **4.1** a pale-yellow solid: R_f 0.40 (1:1 hexanes/ethyl acetate); ^{1}H NMR (400 MHz, $CDCl_3$) δ 8.27 (s, 1H), 7.59 (d, J = 16.4 Hz, 2H), 7.26 (s, 4H), 6.14 (d, J = 16.4 Hz, 2H), 5.10 (br s, 2H), 4.45 (t, J = 5.6 Hz, 2H), 3.72 (t, J = 5.6 Hz, 2H), 3.69 (s, 3H), 2.40 (s, 3H), 2.10 (m, 2H), 0.88 (s, 9H), 0.05 (s, 6H); ^{13}C NMR (100 MHz, $CDCl_3$) δ 167.5, 157.4, 153.5, 152.0, 138.3, 131.8, 130.6, 130.0, 129.9, 127.9, 120.9, 117.7, 102.0, 60.5, 51.5, 40.2, 33.1, 25.9, 21.3, 18.3.

Methylacrylamide **4.2**. Saponification of **4.1**: To a solution of **4.1** (78 mg, 0.16 mmol) in THF (2 mL) was added MeOH (1 mL) and H_2O (1 mL). LiOH (0.8 mL of 1 M solution in H_2O) was added and reaction mixture was stirred at room temperature. After 20 h, the mixture was partitioned between 50 % (v/v) aq. acetic acid (10 mL) and CH_2Cl_2 (10 mL). The organic fraction was dried over anhydrous Na_2SO_4, filtered, and concentrated *in vacuo*. Rapid purification by flash column chromatography (1:1 hexanes/ethyl acetate) gave 52 mg (60% yield) of the acid derivative of **4.1** (acrylic acid-OTBS) as a yellow solid: EI$^+$-MS 467 $[M+H]^+$. This compound exhibited poor solubility in many solvents, which made purification by flash chromatography problematic. The crude acid could be used in the next reaction without column purification.

To a heterogeneous suspension of the acrylic acid-OTBS (16 mg, 0.034 mmol) in DMF (0.5 mL) and CH_2Cl_2 (0.5 mL) was added diisopropylethylamine (DIPEA) (0.008

5 mmol), followed by 1-(3-dimethylaminopropyl)-3-ethylcarbodiimide
de (EDCI-HCl) (8.6 mg, 0.045 mmol). Methylamine (0.026 mL of 2 M in THF)
and reaction mixture was stirred in a sealed-tube reaction vessel at room
e. After 18 h, the mixture was diluted with ethyl acetate (10 mL) and washed
w/v) aq. Citrate buffer [pH = 4.0] (10 mL), saturated $NaHCO_3$, and brine
he organic fraction was dried over anhydrous Na_2SO_4, filtered, and
d *in vacuo*. The crude product was dissolved in THF (2 mL) and stirred at
HCl (0.2 mL) was added and reaction mixture was slowly warmed to room
e over a period of two hours. Mixture was partitioned between CH_2Cl_2 (5 mL)
ed $NaHCO_3$ (5 mL). The collected organic fraction was washed with brine (5
over anhydrous Na_2SO_4, filtered, and concentrated *in vacuo*. Purification by
HPLC (30-100% MeOH gradient over 15 min; 10 mL/min; retention time, 7.3
ed the desired methylacrylamide **4.2** (pp-ma) (2.6 mg, 21% yield) as a white
MR (400 MHz, $CDCl_3$) δ 8.30 (s, 1H), 7.60 (d, J = 16.8 Hz, 2H), 7.31 (s, 4H),
15.6 Hz, 2H), 5.3 (br s, 1 H), 5.0 (br s, 2H), 4.50 (m, 2H), 3.45 (m, 2H), 2.86
Hz, 2H), 2.44 (s, 3H), 2.0 (m, 2H); LC/MS (LC: gradient 5-100% MeCN [0.1%
er 35 min, 0.2 mL/min flow rate, MS: EI^+): retention time, 9.84 min; purity,
1 $[M+H]^+$.

amide **4.3**. To a suspension of the acrylic acid-OTBS (9 mg, 0.019 mmol) in
mL) was added DIPEA (0.005 mL), followed by EDC (4.8 mg, 0.025 mmol).
ion of EDCI-HCl, reaction mixture became homogeneous. Benzylamine
0.025 mmol) was added and reaction mixture was stirred at room
. . After 18 h, the mixture was diluted with ethyl acetate (10 mL) and
10% (w/v) aq. Citrate buffer [pH = 4.0] (10 mL), saturated $NaHCO_3$, and
). The organic fraction was dried over anhydrous Na_2SO_4, filtered, and

ntrated *in vacuo*. The crude product was dissolved in THF (2 mL) and stirred at 1 N HCl (0.2 mL) was added and reaction mixture was slowly warmed to room erature over a period of two hours. Mixture was partitioned between CH_2Cl_2 (5 mL) aturated $NaHCO_3$ (5 mL). The collected organic fraction was washed with brine (5 dried over anhydrous Na_2SO_4, filtered, and concentrated *in vacuo*. Purification by arative HPLC (30-100% MeOH gradient over 15 min; 10 mL/min; retention time, min) afforded the desired benzylacrylamide **4.3** (1.7 mg, 20% yield) as a white ^{1}H NMR (400 MHz, $CDCl_3$) δ 8.30 (s, 1H), 7.70 (d, *J* = 16.8 Hz, 2H), 7.31 (m, 4H), d, *J* = 15.6 Hz, 2H), 5.6 (br t, 1 H), 5.0 (br s, 2H), 4.50 (m, 4H), 3.45 (m, 2H), 2.43 H), 2.0 (m, 2H); LC/MS (LC: gradient 5-100% MeCN [0.1% HCO_2H] over 35 min, 0.2 in flow rate, MS: EI^+): retention time, 13.59 min; purity, ~95%; 442.0 $[M+H]^+$.

te **4.4**. To a solution of **4.1** (22 mg, 0.046 mmol) in THF (2 mL) at 0 ^{0}C was added 1 Cl (0.3 mL). After stirring for 1 h 30 min at 0 ^{0}C and 1 h at room temperature, the ion was diluted with ethyl acetate (5 mL) and washed with saturated $NaHCO_3$ (5 and brine (5 mL). The organic fraction was dried over anhydrous Na_2SO_4, filtered, concentrated *in vacuo*. Purification by preparative TLC (10% $MeOH/CH_2Cl_2$) ded 7.3 mg (46% yield) of enoate **4.4** as a pale-yellow solid; ^{1}H NMR (400 MHz, $_3$) δ 8.29 (s, 1H), 7.61 (d, *J* = 16.4 Hz, 1H), 7.31 (d, *J* = 8.0 Hz, 2H), 7.30 (d, *J* = lz, 2H), 6.05 (d, *J* = 16.4 Hz, 1H), 5.2 (br s, 2H), 4.53 (t, *J* = 5.6 Hz, 2H), 3.73 (s, 3.46 (m, 2H), 2.45 (s, 3H), 2.01 (m, 2H); LC/MS (LC: gradient 5-100% MeCN [0.1% $_2$H] over 35 min, 0.2 mL/min flow rate, MS: EI^+): retention time, 12.7 min; purity, ; 367.1 $[M+H]^+$.

OTBS **4.5**. To a solution of bromide-OTBS **2.4** (350 mg, 0.74 mmol) in toluene (16 vas added tributyl(vinyl)tin (0.260 mL, 0.89 mmol). Argon gas was bubbled through

the solutio

quickly ad

and the c

to give v

MHz, CD

18 Hz, 1

4.89 (br

2H), 0.8

130.9,

MS 42

Aldeh

THF/

mixtu

turne

over

prec

and

filte

ac

^{1}H

=

2

1

the solution for 5 min. Tetrakis(triphenylphosphine)palladium (60 mg, 0.052 mmol) was quickly added and the mixture was refluxed for 10 h. The solvent was removed *in vacuo* and the crude product was purified by flash chromatography (2:1 ethyl acetate/hexanes) to give vinyl-OTBS **4.5** (271 mg, 88% yield): R_f 0.45 (100% ethyl acetate); ^{1}H NMR (400 MHz, $CDCl_3$) δ 8.28 (s, 1H), 7.31 (d, *J* = 8.0 Hz, 2H), 7.26 (d, *J* = 8.0 Hz, 2H), 6.65 (dd, 18 Hz, 12 Hz, 1H), 5.44 (dd, *J* = 18 Hz, 1.2 Hz, 1H), 5.24 (dd, *J* = 12 Hz, 1.2 Hz, 1H), 4.89 (br s, 2H), 4.43 (t, *J* = 7.6 Hz, 2H), 3.72 (t, *J* = 6.0 Hz, 2H), 2.42 (s, 3H), 2.05 (m, 2H), 0.89 (s, 9H), 0.05 (s, 6H); ^{13}C NMR (100 MHz, $CDCl_3$) δ 156.7, 152.0, 137.4, 131.8, 130.9, 130.4, 129.6, 124.9, 118.1, 114.4, 102.3, 60.3, 39.8, 33.2, 25.9, 21.2, 18.2; EI$^+$-MS 423.1 $[M+H]^+$.

Aldehyde-OTBS **4.6.** To a solution of vinyl-OTBS **4.5** (50 mg, 0.12 mmol) in 3:1 THF/H_2O (1 mL) was added OsO_4 (2.5 wt. % in *t*-butanol, 0.030 mL, 0.0024 mmol). The mixture was stirred for 10 min at room temperature, during which time the solution turned dark brown. $NaIO_4$ (45 mg, 0.21 mmol) in H_2O (0.20 mL) was added dropwise over a period of 10 min, during which time the solution turned yellow and a white precipitate formed. After 1 h, the reaction mixture was diluted with ethyl acetate (10 mL) and washed with sat. Na_2SO_3 (10 mL). The organic fraction was dried over Na_2SO_4, filtered, and concentrated *in vacuo*. Purification by flash chromatography (2:1 ethyl acetate/hexanes) gave 43 mg (86% yield) of aldehyde **4.6**: R_f 0.51 (100% ethyl acetate); ^{1}H NMR (400 MHz, $CDCl_3$) δ 9.62 (s, 1H), 8.39 (s, 1H), 7.38 (d, *J* = 8 Hz, 2H), 7.33 (d, *J* = 8 Hz, 2H), 5.1 (br s, 2H), 4.72 (t, *J* = 7.6 Hz, 2H), 3.73 (t, *J* = 6.0 Hz, 2H), 2.45 (s, 3H), 2.04 (m, 2H), 0.89 (s, 9H), 0.05 (s, 6H); ^{13}C NMR (100 MHz, $CDCl_3$) δ 182.0, 159.1, 155.8, 151.0, 138.9, 130.6, 130.3, 129.8, 129.7, 128.8, 128.3, 101.7, 60.9, 41.0, 33.6,

25.8, 21

mL/min t

N-diboc

in THF

was qu

reactio

mL) fo

conce

afford

aceta

Hz. 2

3H),

δ 184

33.8

HCO

>95

En

(2

the

5

by

O

C

4

, 21.2, 18.2; LC/MS (LC: gradient 5-100% MeCN [0.1% HCO_2H] over 35 min, 0.2 min flow rate, MS: EI^+): retention time, 23.4 min; purity, >95%; 425.1 $[M+H]^+$.

boc aldehyde-OTBS **4.7**. To a solution of aldehyde-OTBS **4.6** (135 mg, 0.32 mmol) HF (3 mL) was added $(Boc)_2O$ (207 mg, 0.95 mmol). DMAP (8 mg, 0.064 mmol) quickly added and the mixture was stirred for 2 h at room temperature. The tion mixture was diluted with ethyl acetate (10 mL) and washed with 0.5 N HCl (10 follwed by brine (10 mL). The organic fraction was dried over Na_2SO_4, filtered, and entrated *in vacuo*. Purification by flash chromatography (1:6 ethyl acetate/hexanes) ded the desired *N*-diboc aldehyde-OTBS **4.7** (140 mg, 70% yield): R_f 0.75 (1:1 ethyl ate/hexanes); ^1H NMR (400 MHz, $CDCl_3$) δ 9.84 (s, 1H), 8.96 (s, 1H), 7.34 (d, J = 8 2H), 7.26 (d, J = 8 Hz, 2H), 4.82 (t, J = 7.6 Hz, 2H), 3.74 (t, J = 6.0 Hz, 2H), 2.44 (s, 2.05 (m, 2H), 1.31 (s, 18H), 0.92 (s, 9H), 0.06 (s, 6H); ^{13}C NMR (100 MHz, $CDCl_3$) , 156.2, 155.4, 155.1, 150.3, 131.7, 130.3, 128.7, 113.3, 94.6, 83.6, 60.9, 41.8, 28.8, 28.2, 28.1, 27.9, 27.2, 26.3, 25.9; LC/MS (LC: gradient 5-100% MeCN [0.1% $_2H$] over 35 min, 0.2 mL/min flow rate, MS: EI^+): retention time, 34 min; purity, ; 625.1 $[M+H]^+$.

e **4.8**. To a solution of *N*-diboc-aldehyde-OTBS **4.7** (75 mg, 0.12 mmol) in CH_2Cl_2) was added 1-triphenyl-phosphoranylidene-2-propanone (153 mg, 0.48 mmol) and ixture was stirred at room temperature. Reaction mixture turned bright yellow after . After 12 h, the solvent was removed *in vacuo* and the crude product was purified sh chromatography (1:5 ethyl acetate/hexanes) to give the desired *N*-diboc enone- S (76 mg, 95% yield): R_f 0.40 (1:4 ethyl acetate/hexanes); ^1H NMR (400 MHz,) δ 8.84 (s, 1H), 7.53 (d, J = 16.4 Hz, 1H), 7.23 (m, 4H), 6.51 (d, J = 16.4 Hz, 1H), (t, J = 7.6 Hz, 2H), 3.77 (t, J = 6.0 Hz, 2H), 2.42 (s, 3H), 2.23 (s, 3H), 2.0 (m, 2H),

1.3 (s, 1

152.5, 1

60.4, 40

was ad

remove

mL).

satura

Na_2SO

MeOH

MeOH

(d, J

J = 6

(LC

rete

Ac

mm

fol

m

fla

m

, 0.93 (s, 9H), 0.05 (s, 6H); ^{13}C NMR (100 MHz, $CDCl_3$) δ 197.2, 154.2, , 150.3, 137.6, 132.3, 130.2, 129.9, 129.8, 129.3, 129.2, 119.8, 114.4, 83.1, 3.0, 28.1, 27.8, 25.9, 21.3, 18.4.

solution of the diboc enone-OTBS (21 mg, 0.03 mmol) in CH_2Cl_2 (0.25 mL) TFA (0.25 mL). After stirring for 2 h at room temperature, the solvent was *vacuo* and the crude product was dissolved in THF (1 mL) and 1 N HCl (0.3 3 h, the reaction mixture was diluted with CH_2Cl_2 (5 mL) and washed with $aHCO_3$ (5 mL) followed by brine (5 mL). The organic fraction was dried over ered, and concentrated *in vacuo*. Purification by flash chromatography (1:20 Cl_2) gave enone **4.8** (9.6 mg, 89% yield) as a yellow solid: R_f 0.20 (1:20 Cl_2); ^1H NMR (400 MHz, $CDCl_3$) δ 8.29 (s, 1H), 7.41 (d, J = 16 Hz, 1H), 7.33 , 2H), 7.29 (d, J = 8 Hz, 2H), 6.38 (d, J = 16 Hz, 1H), 5.20 (br s, 2H), 4.53 (t, 2H), 3.48 (t, J = 5.6 Hz, 2H), 2.45 (s, 3H), 2.20 (s, 3H), 2.01 (m, 2H); LC/MS nt 5-100% MeCN [0.1% HCO_2H] over 35 min, 0.2 mL/min flow rate, MS: EI^+): e, 11.4 min; purity, >95%; 351.1 $[M+H]^+$.

-enoate **4.9**. To a solution of *N*-diboc-aldehyde-OTBS **4.7** (23 mg, 0.037 HF (0.5 mL) was added methyl cyanoacetate (0.037 mL of 1 M in THF), DBU (0.04 mL of 1 M in THF). Reaction mixture turned bright yellow after 5 h, the solvent was removed *in vacuo* and the crude product was purified by atography (1:3 ethyl acetate/hexanes) to give the desired *N*-diboc vinylnitrile- e-OTBS (20.3 mg, 78% yield): R_f 0.50 (2:3 ethyl acetate/hexanes); ^1H NMR DCl_3) δ 8.86 (s, 1H), 8.27 (s, 1H), 7.18 (s, 4H), 4.55 (t, J = 7.6 Hz, 2H), 3.85 (t, J = 6.0 Hz, 2H), 2.37 (s, 3H), 1.27 (s, 18H), 0.89 (s, 9H), 0.05 (s, 6H).

solution of the *N*-diboc acrylonitrile-enoate-OTBS (20 mg, 0.028 mmol) in mL) was added TFA (0.25 mL). After stirring for 2 h at room temperature,

the solvent was

and 1 N HCl (0.

washed with sa

was dried ove

chromatograph

as a yellow so

1H), 8.30 (s, 1

2H), 3.87 (s, 3

MeCN [0.1% I

min; purity, >9

acrylonitrile **4**

CH_2Cl_2 0.5 m

mmol). After

by flash chr

(*E*-isomer, 8

δ 8.86 (s, 1H

J = 7.6 Hz,

9H), 0.05 (s

To a

was added

removed in

mL). After

saturated N

Na_2SO_4, fi

MeOH/CH

e solvent was removed *in vacuo* and the crude product was dissolved in THF (1 mL) d 1 N HCl (0.3 mL). After 3 h, the reaction mixture was diluted with CH_2Cl_2 (5 mL) and ashed with saturated $NaHCO_3$ (5 mL) followed by brine (5 mL). The organic fraction as dried over Na_2SO_4, filtered, and concentrated *in vacuo*. Purification by flash romatography (1:20 MeOH/CH_2Cl_2) gave acrylonitrile-enoate **4.9** (9.6 mg, 89% yield) a yellow solid: R_f 0.20 (1:20 MeOH/CH_2Cl_2); ^{1}H NMR (400 MHz, $CDCl_3$) δ 8.36 (s, l), 8.30 (s, 1H), 7.24 (d, J = 8.0 Hz, 2H), 7.27 (d, J = 8.0 Hz, 2H), 4.5 (t, J = 6.0 Hz,), 3.87 (s, 3H), 3.4 (m, 2H), 2.43 (s, 3H), 1.95 (m, 2H); LC/MS (LC: gradient 5-100% eCN [0.1% HCO_2H] over 35 min, 0.2 mL/min flow rate, MS: EI^+): retention time, 11.8 n; purity, >95%; 392.0 $[M+H]^+$.

ylonitrile **4.10**. To a solution of *N*-diboc-aldehyde-OTBS **4.7** (10 mg, 0.016 mmol) in $_2Cl_2$ 0.5 mL) was added 1-triphenyl-phosphoranylidene-2-acetonitrile (19 mg, 0.064 nol). After 12 h, the solvent was removed *in vacuo* and the crude product was purified flash chromatography (1:5 ethyl acetate/hexanes) to give *N*-diboc vinylnitrile-OTBS isomer, 8 mg, 80%): R_f 0.50 (1:4 ethyl acetate/hexanes); ^{1}H NMR (400 MHz, $CDCl_3$) 86 (s, 1H), 7.39 (d, J = 17.2 Hz, 1H), 7.23 (m, 4H), 5.79 (d, J = 17.2 Hz, 1H), 4.56 (t, 7.6 Hz, 2H), 3.75 (t, J = 6.0 Hz, 2H), 2.44 (s, 3H), 2.0 (m, 2H), 1.3 (s, 18H), 0.93 (s, , 0.05 (s, 6H).

To a solution of the acrylonitrile-OTBS (8 mg, 0.012 mmol) in CH_2Cl_2 (0.25 mL) added TFA (0.25 mL). After stirring for 2 h at room temperature, the solvent was oved *in vacuo* and the crude product was dissolved in THF (1 mL) and 1 N HCl (0.3 . After 3 h, the reaction mixture was diluted with CH_2Cl_2 (5 mL) and washed with rated $NaHCO_3$ (5 mL) followed by brine (5 mL). The organic fraction was dried over SO_4, filtered, and concentrated *in vacuo*. Purification by flash chromatography (1:20 OH/CH_2Cl_2) gave acrylonitrile **4.10** (3.2 mg, 80% yield) as a white solid: R_f 0.20 (1:20

MeOH/CH_2Cl_2);

(d, J = 7.6 Hz,

4.47 (t, J = 6.0

100% MeCN [(

11.9 min; purity

Proteins, reag

RSK2 (aa414

purified by im

and LPS we

TAMRA-N_3 w

RSK2 were p

HRP seconda

Cell culture

(DMEM) sup

Lysate prep

by freezing

7.4], 137 m

cocktail [Ro

Laemmli sa

polyacrylam

membrane

antibodies

H_2Cl_2); ^{1}H NMR (400 MHz, $CDCl_3$) δ 8.31 (s, 1H), 7.35 (d, *J* = 7.6 Hz, 2H), 7.28 .6 Hz, 2H), 7.25 (d, *J* = 17.2 Hz, 1H), 5.42 (d, *J* = 17.2 Hz, 1H), 5.0 (br s, 2H), = 6.0 Hz, 2H), 3.49 (m, 2H), 2.46 (s, 3H), 1.97 (m, 2H); LC/MS (LC: gradient 5- eCN [0.1% HCO_2H] over 35 min, 0.2 mL/min flow rate, MS: EI^+): retention time, ; purity, >95%; 334.1 $[M+H]^+$.

, reagents and antibodies. The CTD of human RSK1 (aa419-744) and mouse a414-740) with a C-terminal hexahistidine tag was expressed in *E. coli* and y immobilized nickel affinity chromatography as previously described[13]. PMA S were purchased from Sigma. TBTA [tris-(benzyltriazolylmethyl)amine], N_3 were synthesized as previously described[12,16]. Antibodies against RSK1 and re purchased from Santa Cruz Biotechnology. Anti-mouse HRP and anti-rabbit ondary antibodies were purchased from Pierce.

ure. HEK-293 cells were cultured in Dulbecco's modified Eagle's medium supplemented with 10% fetal bovine serum (FBS).

eparation and western blotting. Cells were washed with cold PBS and lysed g and thawing in either PBS lysis buffer (1.5 mM KH_2PO_4, 8 mM Na_2HPO_4 [pH mM NaCl, 2.7 mM KCl, 0.5 mM $MgCl_2$, 0.9 mM $CaCl_2$, protease inhibitor Roche]). Clarified lysates were normalized using the Bradford assay (BioRad). sample buffer was added to samples and proteins were resolved by 7.5% SDS- amide gel electrophoresis (SDS-PAGE), transferred to a nitrocellulose e, blocked with 5% (w/v) nonfat milk, probed with primary and secondary , and detected by enhanced chemiluminescence (ECL).

Two-step competition labeling assay. Confluent HEK-293 cells in 12-well plates were treated with the indicated concentrations of the electrophilic pyrrolo[2,3-*d*]pyrimidines (competitors) for 1 h at 37°C, followed by fmk-pa (0.3 μM) for 1 h at 37°C. Cells were washed with cold PBS and harvested in PBS lysis buffer as described above. Click reactions were performed as previously described. Briefly, HEK-293 cell lysates (~1 mg/mL) from competitor and fmk-pa-pretreated cells (0.3 μM) were incubated with TAMRA-N_3 (50 μM), TCEP [tris(carboxyethyl)phosphine] (1 mM), $CuSO_4$ (1 mM), and TBTA (100 μM) in PBS [pH 7.4] containing 1% SDS for 1 h at room temperature. Laemmli sample buffer was added and proteins were resolved by 7.5% SDS-PAGE and detected by in-gel fluorescence scanning with a Typhoon 9400 flatbed laser-induced scanner (Amersham Biosciences). TAMRA-labeled RSK1 and RSK2 bands were quantified (ImageJ). Data were fit using Prism 4.0 to obtain IC_{50} values.

Immunodepletion of TAMRA-labeled proteins with monospecific antibodies against RSK1 and RSK2. A HEK-293 cell lysate (5 mg/mL, 400 μL) from fmk-pa treated cells was incubated with TAMRA-N_3 under the click reaction conditions for 1 h. 10 μL was removed for the input lane and diluted with 40 μL PBS lysis buffer (containing 1% NP-40 and 0.1% SDS) and 50 μL 2X Laemmli sample buffer. The remaining lysate was diluted with 4 mL PBS containing 1% NP-40. The diluted lysate (1.5 mL each) was incubated with 4 μg (20 μL) of either a RSK2 monoclonal antibody or affinity purified RSK1 polyclonal antibodies for 2 hours at 4°C, followed by incubation with 50 μL Protein G/Sepharose (Amersham) overnight at 4°C. The immune complexes were washed three times with PBS lysis buffer (containing 0.1 %SDS and 1% NP-40), resuspended in 50 μL of PBS lysis buffer (containing 0.1 % SDS and 1% NP-40) and 100 μL 2X Laemmli sample buffer, and boiled for 10 min. To 50 μL of the supernatants from each condition

was added 50 μL of Laemmli sample buffer. Proteins were subsequently analyzed by in-gel fluorescence scanning or Western blotting.

Determination of the rate of reaction of fmk with RSK1 CTD and RSK2 CTD using mass spectrometry. Human RSK1 CTD (1 μM) or mouse RSK2 CTD (1 μM) in 12.5 mM Tris [pH 8], 100 mM NaCl, and 1 mM DTT was incubated with 2 mM ATP at room temperature for 10 min. Proteins were then transferred to a 96-well plate on ice and incubated with fmk (3 μM) for various times and the reaction was quenched by the addition of ice cold aqueous formic acid (0.4% v/v). The reactions were diluted 1:10 in aqueous formic acid and analyzed by mass spectrometry using a CIT Analytics Autosampler and a QStar Electrospray mass spectrometer (Applied Biosystems). Percent modification was quantified by dividing the intensity of the fmk-modified peak by the unmodified peak. Determination of the apparent second-order rate constants (k_{obs}/[I]): k_{obs} was determined by plotting $\ln(E_o/E)$ vs. preincubation time (where E_o = % fmk-modification at time 0 and E = % fmk-modification at time *t*).

ces

anning, G., Whyte, D. B., Martinez, R., Hunter, T. & Sudarsanam, S. The rotein kinase complement of the human genome. *Science* **298**, 1912-34 (2002).

night, Z. A. & Shokat, K. M. Features of selective kinase inhibitors. *Chem Biol* 2, 621-37 (2005).

avies, S. P., Reddy, H., Caivano, M. & Cohen, P. Specificity and mechanism of tion of some commonly used protein kinase inhibitors. *Biochem J* **351**, 95-105 000).

ain, J., McLauchlan, H., Elliott, M. & Cohen, P. The specificities of protein nase inhibitors: an update. *Biochem J* **371**, 199-204 (2003).

ito, D. et al. Activity-based probes that target diverse cysteine protease milies. *Nat Chem Biol* **1**, 33-8 (2005).

eenbaum, D., Medzihradszky, K. F., Burlingame, A. & Bogyo, M. Epoxide ectrophiles as activity-dependent cysteine protease profiling and discovery ols. *Chem Biol* **7**, 569-81 (2000).

eenbaum, D. C. et al. Small molecule affinity fingerprinting. A tool for enzyme mily subclassification, target identification, and inhibitor design. *Chem Biol* **9**, 85-94 (2002).

ung, D., Hardouin, C., Boger, D. L. & Cravatt, B. F. Discovering potent and ective reversible inhibitors of enzymes in complex proteomes. *Nature otechnology* **21**, 687-691 (2003).

ger, D. L. et al. Discovery of a potent, selective, and efficacious class of ersible alpha-ketoheterocycle inhibitors of fatty acid amide hydrolase effective analgesics. *J Med Chem* **48**, 1849-56 (2005).

ung, D. et al. Discovery of an exceptionally potent and selective class of fatty d amide hydrolase inhibitors enlisting proteome-wide selectivity screening:

t optimization of enzyme inhibitor potency and selectivity. *Bioorg Med t* **15**, 1423-8 (2005).

. E., Adam, G. C. & Cravatt, B. F. Activity-based protein profiling in vivo opper(i)-catalyzed azide-alkyne [3 + 2] cycloaddition. *J Am Chem Soc* -7 (2003).

. E. & Cravatt, B. F. Profiling enzyme activities in vivo using click methods. *Chem Biol* **11**, 535-46 (2004).

. S., Zhang, C., Shokat, K. M. & Taunton, J. Structural bioinformatics-sign of selective, irreversible kinase inhibitors. *Science* **308**, 1318-21

M., Cavins, J.F., Wall, J.S. Relative Nucleophilic Reactivities of Amino and Mercaptide Ions in Addition Reactions with α,β-Unsaturated ds. *J Am Chem Soc* **87**, 3672-2682 (1965).

T., Hemmer, W. & Taylor, S. S. Serine-53 at the tip of the glycine-rich MP-dependent protein kinase: role in catalysis, P-site specificity, and with inhibitors. *Biochemistry* **39**, 8325-32 (2000).

A. K., Colasson, B. & Fokin, V. V. One-pot synthesis of 1,4-ed 1,2,3-triazoles from in situ generated azides. *Org Lett* **6**, 3897-9

Chapter 5

Third-generation p90 RSK inhibitors

:hapter describes efforts to identify more potent inhibitors of the CTD of SK2. We synthesized variants of our previously described inhibitor, fmk, diverse substituents at the N-7 position of the pyrrolo[2,3-*d*]pyrimidine placement of hydroxyl group emanating from the substituent at the N-7 nk with secondary amines led to improved cellular potency. By contrast, r piperidinyl N-7 derivatives exhibited reduced potency. We also explored e hydrophobic pocket occupied by the C-5 *p*-tolyl group of fmk. A small cturally related, reversible pyrazolo[3,4-*d*]pyrimidines with diverse aromatic at a position analogous to the C-5 position of fmk were screened against sing a competition labeling assay *in vitro*. The results of this experiment aromatic substituents at the C-5 position larger than the tolyl group will sed affinity relative to fmk.

UCSF LIBRARY

ntroduction

p90 ribosomal protein S6 kinases (RSK) are serine/threonine kinases that are ctivated by signaling inputs from extracellular regulated kinase (ERK)[1,2] and hosphoinositide-dependent kinase 1 (PDK1)[3-5]. In humans there are four RSK isoforms RSK1-4) and they all contain two, non-identical kinase domains: a regulatory C-erminal kinase domain (CTD) and an N-terminal kinase domain (NTD), which hosphorylates all downstream RSK targets[6,7]. The CTD is thought to be essential for ctivation of the N-terminal kinase domain (NTD) by autophosphorylation of Ser386 numan RSK2 numbering). Previous work in our laboratory led to the rational design of mk (**Figure 4-1**), an irreversible inhibitor of the CTD of RSK1 and RSK2 that exploits wo selectivity filters in the ATP-binding site of the RSK CTD: a non-conserved cysteine Cys436, human RSK2 numbering), which is covalently modified by the electrophile of mk, and a semi-conserved threonine (Thr493, known at the gatekeeper residue) in the TP binding site[8]. We recently designed a second-generation RSK CTD inhibitor, amed fmk-pa (**Figure 4-1**), a propargylamine variant that not only can be conjugated to n azidoalkyl reporter via click chemistry to monitor covalent CTD modification in cells, ut also has a 5-fold greater cellular potency than fmk against the CTD of RSK2. Both hibitors have been integral for probing the requirement of the CTD for endogenous SK signaling and identifying new, physiologically relevant RSK substrates.

In an effort to identify alternative electrophilic inhibitors with improved potency, e recently synthesized a series of Michael acceptor-substituted pyrrolo[2,3-pyrimidines. From this set, we identified enone **4.8** (refer to **Scheme 4-2**), which was ore potent than fmk against RSK2 in cells; however, because of the intrinsically greater emical reactivity of the enone electrophile relative to the fluoromethylketone of fmk, we ere concerned that enone **4.8** would exhibit less proteome-wide, kinetic selectivity. deed, in HEK-293 cells, a fluorophore-conjugated derivative of enone **4.8**, enone-

DIPY (**Scheme 5-1**, synthesized using a similar route to fmk-BODIPY), demonstrated re extensive off-target modification compared to fmk-BODIPY at the same centrations (**Figure 5-1**).

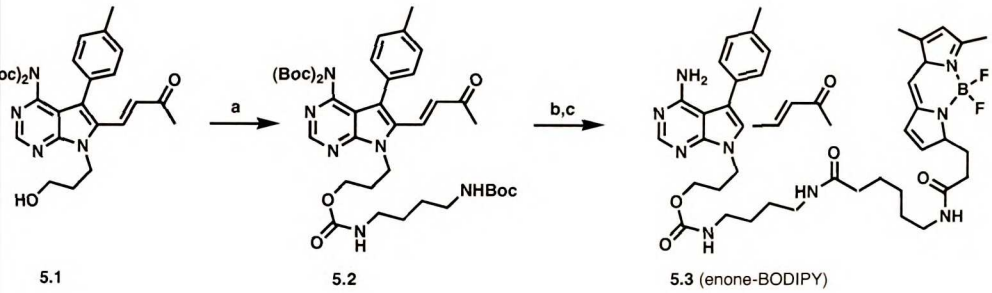

eme 5-1. Synthesis of enone-BODIPY. Reagents and conditions: a. carbonyldiimidazole, DIPEA, Cl_2, then *N*-Boc-1,4-diaminobutane; b. TFA, CH_2Cl_2; c. BODIPY FL-NHS, DIPEA, DMF.

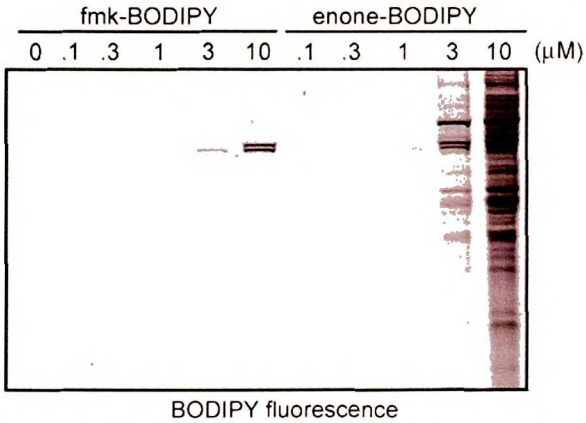

ure 5-1. Fmk-BODIPY is more kinetically selectivity than enone-BODIPY in intact cells. HEK-293 cells e treated with the indicated concentrations of fmk-BODIPY or enone-BODIPY for 1 h. Cells were vested in PBS and proteins were resolved by 7.5% SDS-PAGE and detected by in-gel fluorescence nning.

reover, enone **4.8** was 6-fold more potent than fmk against the Thr-gatekeeper ase, Src (IC_{50} of 0.2 μM and 1.2 μM, respectively), which is a potential reversible off- et of our designed electrophilic compounds since it is potently inhibited by related olo[2,3-*d*]pyridines. We therefore chose not to pursue the synthesis of electrophilic olo[2,3-*d*]pyrimidines that incorporated the enone electrophile. Instead, we turned efforts toward the synthesis of fmk variants with improved cellular potency. We

in particular, on preparing third-generation fmk analogs with variations at the N-

n.

s and Discussion

is and evaluation of fmk variants with various N-7 substituents

Based on the unanticipated result that fmk-pa is more potent than fmk in cells, ared a small set of fmk analogs that contain secondary or tertiary amines in the hydroxyl group at the N-7 substituent (**Scheme 5-2**). Our strategy rapidly ed the amine derivatives from the common mesylate intermediate **3.2** via a wo-step sequence involving S_N2 displacement with primary or secondary amines, by removal of the Boc protecting group.

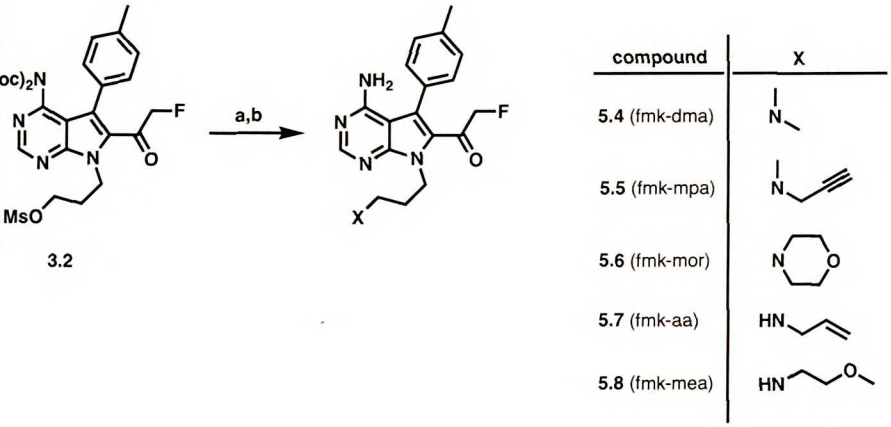

-2. Synthesis of secondary amine derivatives of fmk. Reagents and conditions: a. amine (neat or); b. TFA, CH_2Cl_2 (30-100% yield over 2 steps).

synthesized two other fmk analogs that contained cyclopentyl or piperidinyl t the N-7 position (**Schemes 5-2** and **5-3**, similar to route used to prepare fmk). inspired by studies from Abbott that showed that 7-cycloalkyl substituents on yrrolo[2,3-*d*]pyrimidine inhibitors of the Src family tyrosine kinase, Lck,

improved their potency relative to their lead compound that contained a *t*-

at the N-7 position[9].

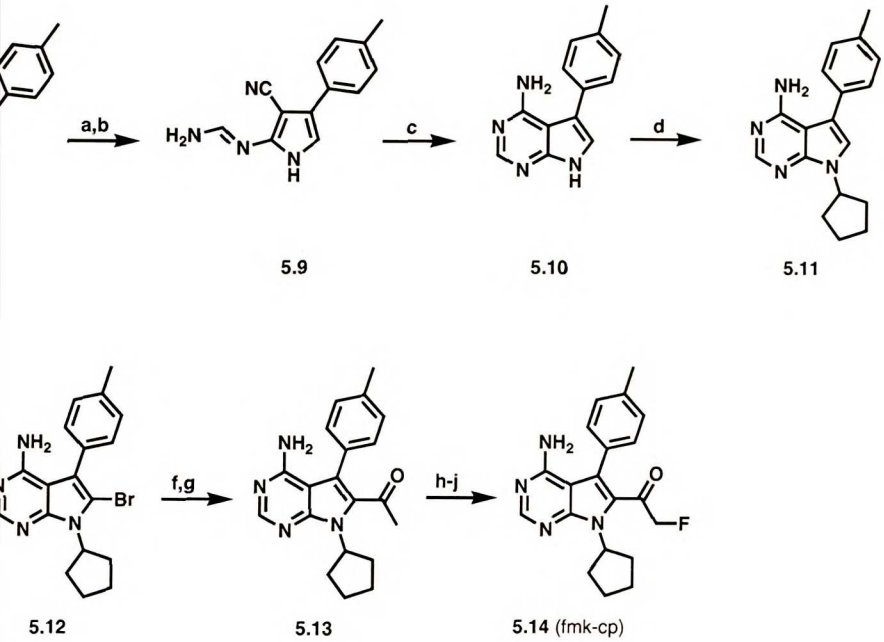

ynthesis of fmk-cp. Reagents and conditions: a. triethylorthoformate; b. 7 N NH_3, MeOH; c. H (60% yield over 2 steps); d. NaH, cyclopentyl bromide, DMF (61 % yield); e. *N*-ide, DMF (60% yield); f. α-(ethoxyvinyl)tributyl tin, $Pd[P(Ph)_3]_4$, toluene; g. 1 N HCl, THF over 2 steps); h. $(Boc)_2O$, DMAP, THF (80% yield); i. LDA, THF, then N-ulfonimide; j. TFA, CH_2Cl_2.

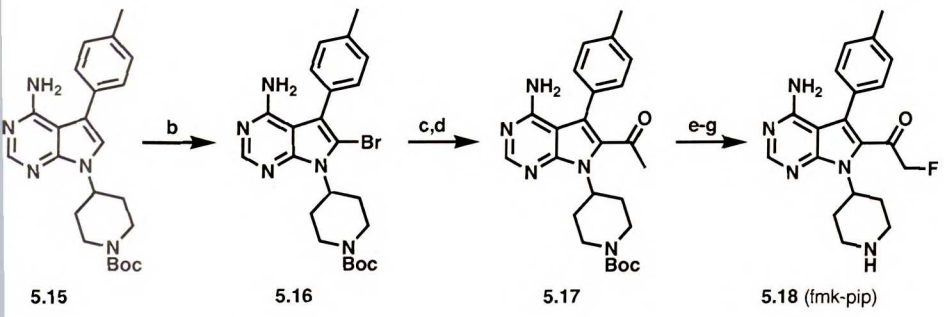

ynthesis of fmk-pip. Reagents and conditions: a. K_2CO_3, 18 crown-6-ether, *N*-boc 4-tosylate-F (38% yield); b. *N*-bromosuccinimide, DMF (50% yield); c. α-(ethoxyvinyl)tributyl tin, uene (72% yield); d. 1 N HCl, THF (86% yield); e. $(Boc)_2O$, DMAP, THF (79% yield); f. LDA, robenzenesulfonimide; g. TFA, CH_2Cl_2.

ested some of the N-7 fmk derivatives, at a concentration of 1 μM, for CTD cellular activity by monitoring PMA-induced autophosphorylation of in HEK-293 cells (**Figure 5-2**). The dimethyl amine derivative, fmk-dma, more potent than fmk in this experiment; however, a more careful dose alysis demonstrated that they are equipotent. Interestingly, the morpholino nk-mor, was significantly less active than fmk-dma, demonstrating that only roups attached to the amine are tolerated. Fmk-pip weakly inhibited Ser386 tion, whereas fmk-cp had no effect. This dramatically reduced potency nk could be the result of an altered conformation of the electrophile, making ptible to nucleophilic attack by Cys436. Indeed, molecular modeling studies the conformation of the electrophile is different in fmk-cp and fmk-pip than not shown).

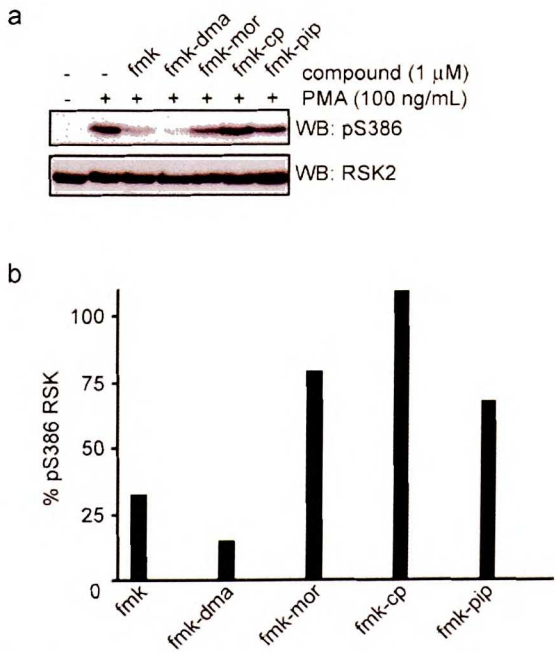

cts of N-7 fmk derivatives on PMA-stimulated RSK Ser386 phosphorylation. (**a**) HEK-293 ved of serum for 2 h and subsequently treated with 1 μM compound for 90 min. Cells were PMA (100 ng/mL) for 30 min and harvested in RSK lysis buffer. Proteins were resolved by and detected by Western blotting with antibodies to phospho-Ser386 RSK and RSK2. (**b**) Western blot data in (**a**).

The cellular activities of the secondary amine derivatives, fmk-aa and fmk-mea, were directly compared to fmk-pa. Both fmk-aa and fmk-mea potently inhibited PMA-stimulated RSK Ser386 phosphorylation, achieving complete inactivation at a concentration of 100 nM (**Figure 5-3**). These compounds are our most potent RSK CTD inhibitors to date. Future studies will involve the synthesis of a library of secondary amine variants to develop the structure activity relationship (SAR) of this region of fmk.

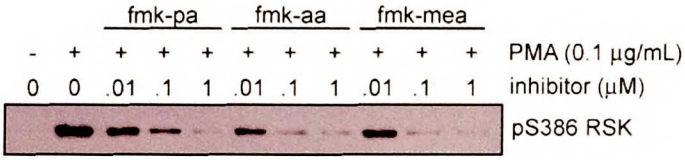

Figure 5-3. Secondary amine fmk variants exhibit remarkable cellular potency. HEK-293 cells were deprived of serum for 2 h and subsequently treated with the indicated concentrations of the compounds for 90 min. Cells were stimulated with PMA (100 ng/mL) for 30 min and harvested in RSK lysis buffer. Proteins were resolved by 10% SDS-PAGE and detected by Western blotting with antibodies to phospho-Ser386 RSK.

The *N*-methyl propargylamine derivative, fmk-mpa, was originally synthesized as a potential clickable probe of the RSK CTD. The extent and selectivity of covalent RSK CTD modification by fmk-mpa was compared to fmk-pa. In contrast to fmk-pa (3 μM), modification of endogenous RSK1 and RSK2 by fmk-mpa (3 μM) was undetectable following click chemistry (**Figure 5-4**). Future experiments are required to understand why this compound did not work as a clickable probe. In particular, its effects on PMA-stimulated Ser386 phosphorylation need to be evaluated. If fmk-mpa exhibits similar potency to fmk-pa, then it is possible that the *N*-methyl group adversely affects the click reaction.

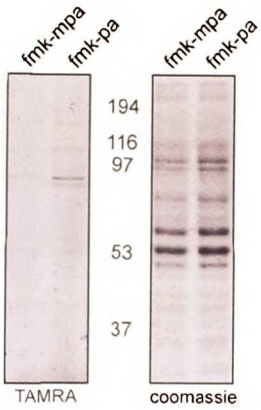

-mpa is not an effective clickable probe of the CTD of RSK1 and RSK2. HEK-293 cells were M of either fmk-mpa or fmk-pa for 1h. Cells were harvested in PBS and lysates were k conjugation with TAMRA-N_3. Proteins were resolved by 10% SDS-PAGE and detected by ce scanning (left) and Coomassie blue staining (right).

size of the gatekeeper pocket with a small library of reversible -d]pyrimidines

olyl substituent at the C-5 position of fmk is hypothesized to occupy a pocket that is defined by Thr493, which is referred to as the gatekeeper e Chapter 1). Among the Thr gatekeeper kinases (~25% of the human ne), there are considerable differences in the size and character of this ially in the autoinhibited states[11]. In fact, various inhibitors have been exploit these differences to achieve remarkable selectivity, even among d kinases. Since no crystal structures of the CTD of RSK are available, the acter of this pocket are unknown. Therefore, we screened a small panel of ble (from the Shokat laboratory at UCSF) pyrazolo[3,4-*d*]pyrimidines with atic substituents at the C-5 position to map the Thr gatekeeper pocket in **igure 5-5a**). The pyrazolo[3,4-*d*]pyrimidine scaffold is essentially identical o[2,3-*d*]pyrimidine scaffold of fmk, the only differences being the f the substituted-carbon at C-2 with a nitrogen and the hydroxypropyl at N- l group. To facilitate the rapid analysis of the pyrazolo[3,4-*d*]pyrimidine C-

c variants against RSK2 CTD, we used a competition labeling assay with fmk-
Competition labeling assays have been used to screen irreversible[12-14] as well
ble[15] covalent inhibitors, but to our knowledge have not been used to screen
rsible inhibitors. Nevertheless, we reasoned that under conditions of
e modification of RSK2 CTD by fmk-BODIPY, reversible inhibitors, similar to
covalent inhibitors but perhaps to a lesser extent, should effectively compete
g.

e therefore performed a time course of RSK2 CTD (50 nM) labeling by 1 μM
PY (**Figure 5-5b**). Based on this experiment, we decided that 30 min would
ptimal time for the competition labeling reaction. To determine if these
could be used to effectively measure the affinity of a reversible inhibitor, we
SK2 CTD with increasing concentrations of PP1, a pyrazolo[3,4-*d*]pyrimidine
yl group at C-5. A dose dependent decrease in RSK2 CTD labeling was
upon PP1 pretreatment (**Figure 5-5c**). Quantification of the labeled bands
n IC_{50} of ~3 μM for PP1. Next, we screened 10 other pyrazolo[3,4-
nes with various aromatic groups at the C-5 position at a concentration of 3
ppointingly, none of the tested compounds were more potent than PP1. Only
pund, c284, was equipotent to PP1. This compound contains a *m*-hydroxyl
stituted phenyl ring at C-5, which has previously been suggested to form a
pond to the threonine gatekeeper side chain in the Src-family kinases. The *m*-
ative (c302) and the acetal-protected catechol derivative (c215) blocked
~50%. The benzyl derivative (c299) was less potent than PP1, blocking
~30%. Replacement of the *p*- *or m*-methyl group of the tolyl substituent with
nitro, *t*-butyl, or phenylether, led to a substantial loss in activity (< 25% block
). Together our results demonstrate that the Thr gatekeeper pocket in the

CTD of RSK2 cannot accommodate aromatic groups much larger than the original tolyl group, although more inhibitors need to be tested and IC_{50} values determined.

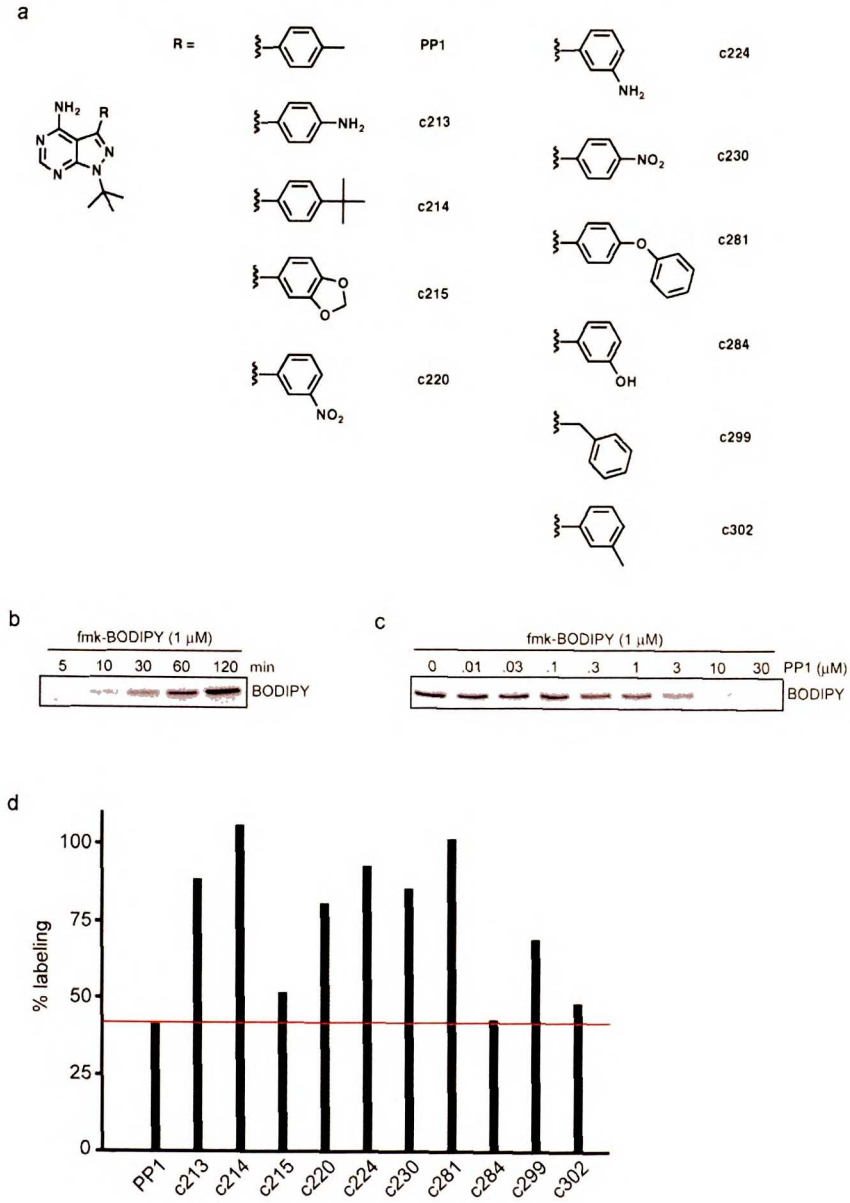

Figure 5-5. Exploring the size threonine gatekeeper pocket of RSK2 CTD using a competition labeling assay. (**a**) Panel of pyrazolo[3,4-*d*]pyrimidines with various aromatic groups at the C-5 position. (**b**) Time-course of RSK2 CTD labeling by fmk-BODIPY. RSK2 CTD (50 nM) was treated with 1 μM fmk-BODIPY for the indicated times and reaction was quenched by the addition of Laemmli sample buffer. Proteins were resolved by 10% SDS-PAGE and detected by in-gel fluorescence scanning. (**c**) PP1 inhibits the labeling of RSK2 CTD in a concentration-dependent manner. RSK2 CTD (50 nM) was treated with increasing concentrations of PP1 followed by 1 μM fmk-BODIPY for 30 min. Analyzed as described in (**b**). (**d**) Screening of compounds shown in (**a**). RSK2 CTD (50 nM) was treated with 3 μM of the indicated inhibitors, followed by 1 μM fmk-BODIPY for 30 min. Analyzed as described in (**b**).

imental

cal synthesis

al. ^{1}H and ^{13}C NMR spectra were recorded on a Varian 400 spectrometer at 400)0 MHz, respectively. Chemical shifts were reported as parts per million (ppm) eld from an internal tetramethylsilane standard (δ = 0.0 for ^{1}H NMR) or from t references. Low-resolution electrospray ionization mass spectra (EI^{+}-MS) were ed on a Waters Micromass ZQ 4000 spectrometer. LC/MS (MS: EI^{+}) was ned on a Waters AllianceHT LC/MS with a flow rate of 0.2 mL/min (monitored at ı and 260 nm) using an Xterra MS C18 column (Waters). High-resolution electron mass spectra (HRMS) were recorded on a Micromass VG70E spectrometer by an Sun at the University of California-San Francisco Biomedical Mass ɔmetry Center. For air- and water-sensitive reactions, glassware was oven- or dried prior to use and reactions were performed under argon. Dichloromethane, ylformamide, methanol, tetrahydrofuran, toluene, and diisopropylamine were dried the solvent purification system manufactured by Glass Contour, Inc. (Laguna CA). All other solvents were of ACS chemical grade (Fisher) and used without purification unless otherwise indicated. Commercially available starting reagents sed without further purification. Many of the pyrrolo[2,3-*d*]pyimidine compounds ɔaringly soluble in acetonitrile and concentration from this solvent often yielded a lid. Analytical and preparative thin layer chromatography were performed with el 60 F_{254} glass plates (EM Science). Flash chromatography was conducted with 0 mesh silica gel (Selecto Scientific). High performance liquid chromatography was performed on a Prostar 210 (Varian) with a flow rate of 10 mL/min red at 210 nm and 260 nm) using a COMBI-A C18 preparatory column (Peeke ic).

Diboc enone **5.1**. Diboc enone-OTBS (76 mg, 0.11 mmol) was dissolved in THF (3 mL) and stirred at 0°C. 1 N HCl (1 mL) was added and reaction mixture was slowly warmed to room temperature over a period of two hours. Mixture was partitioned between CH_2Cl_2 (10 mL) and saturated $NaHCO_3$ (10 mL). The collected organic fraction was washed with brine (10 mL), dried over anhydrous Na_2SO_4, filtered, and concentrated *in vacuo*. Purification by flash chromatography (100% ethyl acetate) gave diboc enone **5.1** (55 mg, 92% yield) as a yellow film; ^{1}H NMR (400 MHz, $CDCl_3$) δ 8.85 (s, 1H), 7.53 (d, *J* = 16.8 Hz, 1H), 7.24 (m, 4H), 6.49 (d, *J* = 16.4 Hz, 1H), 4.62 (t, *J* = 6.0 Hz, 2H), 4.02 (t, 2H), 3.54 (m, 2H), 2.43 (s, 3H), 2.23 (s, 3H), 2.01 (m, 2H); ^{13}C NMR (100 MHz, $CDCl_3$) δ 198.0, 152.5, 150.2, 137.9, 132.6, 130.1, 129.9, 129.5, 129.4, 83.3, 57.7, 39.2, 32.7, 28.2, 27.8, 21.3.

Enone carbamate **5.2**. To a solution of **5.1** (15 mg, 0.027 mmol) in CH_2Cl_2 (0.25 mL) was added DIPEA (0.045 mL of 1 M in CH_2Cl_2), followed by carbonyldiimidazole (5.3 mg, 0.033 mmol). After stirring for 2 h at room temperature, *N*-Boc-1,4-diaminobutane (26 mg, 0.14 mmol) was added. After 3 h, additional *N*-Boc-1,4-diaminobutane (12 mg, 0.065 mmol) was added and the reaction was stirred for 2 h at room temperature. The reaction mixture was diluted with ethyl acetate (10 mL) and washed with 0.5 N HCl (10 mL) followed by brine (10 mL). The organic fraction was dried over Na_2SO_4, filtered, and concentrated *in vacuo*. Purification by flash chromatography (3:2 ethyl acetate/hexanes) gave 13.1 mg (65% yield) of enone carbamate **5.2**; ^{1}H NMR (400 MHz, $CDCl_3$) δ 8.86 (s, 1H), 7.56 (d, *J* = 16.8 Hz, 1H), 7.26 (m, 4H), 6.74 (d, *J* = 16.8 Hz, 1H), 4.62 (t, *J* = 7.6 Hz, 2H), 4.18 (t, *J* = 5.2 Hz, 2H), 3.16 (m, 4H), 2.45 (s, 3H), 2.0 (s, 3H), 2.0 (m, 2H), 1.42 (s, 9H), 1.30 (s, 18H), 1.28 (m, 4H).

Enone-BODIPY **5.3**. To a solution of **5.2** (13 mg, 0.017 mmol) in CH_2Cl_2 (0.8 mL) at 0°C was added TFA (0.7 mL). After warming to room temperature and stirring for 3 h, solvents were removed *in vacuo* to yield the boc deprotected product, which was used in the next reaction without further purification.

To a solution of the crude enone amine in DMF (0.1 mL) at room temperature was added BODIPY FL-NHS (5 mg, 0.009 mmol), followed by DIPEA (0.003 mL, 0.016 mmol). After 24 h in the dark, the solvents were removed *in vacuo* and the mixture was purified by flash chromatography (10:1 CH_2Cl_2/MeOH) to give **5.3** (enone-BODIPY) as a red solid in quantitative yield: ^{1}H NMR (400 MHz, $CDCl_3$) δ 8.22 (s, 1H), 8.00 (s, 1H), 7.50 (d, J = 16.8 Hz, 2H), 7.35 (d, J = 8 Hz, 2H), 7.30 (d, J = 8.4 Hz, 2H), 7.1 (s, 1H), 6.86 (d, J = 3.6 Hz, 1H), 6.65 (d, J = 16.8 Hz, 2H), 6.21 (d, J = 3.6 Hz, 1H), 6.0 (s, 1H), 5.80 (m, 2H), 4.45 (t, 2H), 4.04 (m, 2H), 3.25-3.06 (m, 6H), 2.60 (t, 2H), 2.48 (s, 3H), 2.39 (s, 3H), 2.18 (s, 3H), 2.11 (s, 3H), 2.0 (t, 2H), 1.46-1.37 (m, 10H).

Fmk-dimethylamine **5.4** (fmk-dma). To a solution of mesylate **3.2** (7.5 mg, 0.012 mmol) in THF (0.1 mL) was added dimethylamine (0.5 mL of 2 M in THF) and the reaction was stirred for 50 h at room temperature. The reaction mixture was diluted with ethyl acetate (10 mL) and washed with H_2O (10 mL). The organic fraction was dried over Na_2SO_4, filtered, and concentrated *in vacuo*. The crude amine was dissolved in CH_2Cl_2 (1 mL) and cooled to 0°C. After 5 min, TFA (1 mL) was then added and reaction mixture was slowly warmed to room temperature. After 3 h, solvents were removed *in vacuo* and the mixture was purified by preparative layer chromatography (5% MeOH, 1% TEA in CH_2Cl_2) to give 4.3 mg (100% yield) of **5.4** (fmk-dma): R_f 0.3 (5% MeOH, 1% TEA in CH_2Cl_2); ^{1}H NMR (400 MHz, $CDCl_3$) δ 8.34 (s, 1H), 7.39 (d, J = 8 Hz, 2H), 7.36 (d, J = 8.4 Hz, 2H), 4.71 (t, J = 8 Hz, 2H), 4.65 (d, J_{HF} = 47 Hz, 2H), 3.1 (m, 2H), 2.80 (s, 6H), 2.49 (s, 3H), 2.35 (m, 2H).

Fmk-*N*-methylpropargylamine **5.5** (fmk-mpa). To a solution of mesylate **3.2** (20 mg, 0.032 mmol) in THF (0.5 mL) was added *N*-methylpropargylamine (0.5 mL of 4 M in THF) and the reaction was stirred for 50 h at room temperature, and 9 h at 45°C. The reaction mixture was diluted with ethyl acetate (10 mL) and washed with H_2O (10 mL), followed by brine (10 mL). The organic fraction was dried over Na_2SO_4, filtered, and concentrated *in vacuo*. Purification by preparative layer chromatography (2:1 ethyl acetate/hexanes) afforded the desired diboc fmk-*N*-methylpropargylamine (fmk-mpa) (5 mg, 30% yield): R_f 0.5 (100% ethyl acetate); ^{1}H NMR (400 MHz, $CDCl_3$) δ 8.96 (s, 1H), 7.25 (m, 4H), 4.72 (t, J = 8 Hz, 2H), 4.65 (d, J_{HF} = 47 Hz, 2H), 3.37 (s, 2H), 2.52 (t, J = 8 Hz, 2H), 2.45 (s, 3H), 2.3 (s, 3H), 2.02 (m, 2H), 1.3 (s, 18H).

To a solution of *N*-diboc fmk-mpa (5 mg, 0.084 mmol) in CH_2Cl_2 (1 mL) was added TFA (1 mL) and reaction was stirred at room temperature. After 2.5 h, the solvents were removed *in vacuo* to give 4.3 mg (82% yield) of **5.5** (fmk-mor); ^{1}H NMR (400 MHz, $CDCl_3$) δ 8.26 (s, 1H), 7.43 (d, J = 8 Hz, 2H), 7.35 (d, J = 8 Hz, 2H), 5.38 (br s, 2H), 4.76 (m, 2H), 4.69 (d, J_{HF} = 46 Hz, 2H), 3.99 (br s, 2H), 3.26 (m, 2H), 2.89 (s, 3H), 2.69 (s, 1H), 2.51 (s, 3H), 2.35 (m, 2H); desired compound was found to be > 99% pure by analytical HPLC (0-100% MeCN gradient [0.1% TFA] over 15 min; 1 mL/min flow rate; retention time for **5.5** was 7.17 min).

Fmk-morpholine **5.6** (fmk-mor). To a solution of mesylate **3.2** (7.5 mg, 0.012 mmol) in THF (0.1 mL) was added morpholine (0.5 mL of 2 M in THF) and the reaction was stirred for 50 h at room temperature. The reaction mixture was diluted with ethyl acetate (10 mL) and washed with H_2O (10 mL). The organic fraction was dried over Na_2SO_4, filtered, and concentrated *in vacuo*. The crude amine was dissolved in CH_2Cl_2 (1 mL) and cooled to 0°C. After 5 min, TFA (1 mL) was then added and reaction mixture was slowly

oom temperature. After 3 h, solvents were removed *in vacuo* and the purified by preparative layer chromatography (5% MeOH, 1% TEA in ve 4.6 mg (94% yield) of **5.6** (fmk-mor): R_f 0.2 (5% MeOH, 1% TEA in MR (400 MHz, $CDCl_3$) δ 8.34 (s, 1H), 7.39 (d, J = 8 Hz, 2H), 7.34 (d, J = 8 (t, J = 8 Hz, 2H), 4.65 (d, J_{HF} = 47 Hz, 2H), 3.81 (m, 2H), 2.71 (m, 4H), 2.17 (m, 2H).

cedure for the synthesis of fmk-allylamine **5.7** (fmk-aa) and fmk-amine **5.8** (fmk-mea): To mesylate **3.2** (30 mg, 0.048 mmol) was added allylamine or methoxyethylamine) and the reaction was stirred at 40°C. e solvent was removed *in vacuo.* ^{1}H NMR analysis indicated that both *N*-vere removed under these reaction conditions. Purification by preparative ent 10-65% acetonitrile [0.1 % TFA] over 23 min, 5 mL/min flow rate) desired amine derivatives. Preparation of the HCl salt and removal of ophilic plasticizers: the purified product was dissolved in 0.01 M HCl (10 acted against ether (2 x 10 mL). The aqueous layer was concentrated *in* ed vigorously under high vacuum.

e **5.7** (fmk-aa). ^{1}H NMR (400 MHz, ~3:1 $CDCl_3$/MeOD) [TFA salt] δ 8.34 (s, J = 8 Hz, 2H), 7.37 (d, J = 8 Hz, 2H), 5.9 (m, 1H), 5.52 (m, 2H), 4.72 (m, J_{HF} = 47 Hz, 2H), 3.62 (d, J = 7 Hz, 2H), 3.36 (m, 2H), 3.05 (t, J = 8 Hz, 3H), 2.32 (M, 2H). LC/MS (LC: gradient 0-100% MeCN [0.1% HCO_2H] over nL/min flow rate, MS: EI^+): retention time, 9.44 min; purity, >95%; 382.1

Fmk-methyoxyethylamine **5.8** (fmk-mea). ^{1}H NMR (400 MHz, ~3:1 $CDCl_3$/MeOD) [TFA salt] δ 8.34 (s, 1H), 7.46 (d, *J* = 8 Hz, 2H), 7.37 (d, *J* = 8 Hz, 2H), 4.71 (t, *J* = 8 Hz, 2H), 4.66 (d, J_{HF} = 47 Hz, 2H), 3.68 (t, *J* = 4 Hz, 2H), 3.44 (s, 3H), 3.36 (m, 2H), 3.18 (t, *J* = 8 Hz, 2H), 3.06 (t, *J* = 8 Hz, 2H), 2.52 (s, 3H), 2.36 (m, 2H). LC/MS (LC: gradient 0-100% MeCN [0.1% HCO_2H] over 30 min, 0.2 mL/min flow rate, MS: EI^+): retention time, 9.22 min; purity, >95%; 400.1 $[M+H]^+$.

Formamidine **5.9**. A solution of pyrrole **2.1** (61 g, 0.31 mol) in triethyl orthoformate (300 mL) was refluxed for 1 h. After cooling to room temperature, the solvent was removed *in vacuo*. The crude pyrrole iminoether, which was pure by ^{1}H NMR, was azeotropically dried with toluene (2 x 10 mL) and carried on directly to the next step; ^{1}H NMR (400 MHz, $CDCl_3$) δ 8.38 (s, 1H), 7.49 (d, *J* = 8 Hz, 2H), 7.18 (d, *J* = 8 Hz, 2H), 5.1 (s, 1H), 4.28 (q, *J* = 7 Hz, 2H), 2.29 (s, 3H), 1.32 (t, *J* = 7 Hz, 3H).

The crude pyrrole iminoether was dissolved in 7 N NH_3 in MeOH (1000 mL) and the reaction was stirred at room temperature for 4 h. The solvent was removed *in vacuo* and the desired formamidine **5.9**, which was pure by ^{1}H NMR, was carried on directly to the next step; ^{1}H NMR (400 MHz, $CDCl_3$) δ 8.0 (t, *J* = 9 Hz, 1H), 7.47 (d, *J* = 8 Hz, 2H), 7.15 (d, *J* = 8 Hz, 2H), 6.76 (s, 1H), 2.28 (s, 3H).

Pyrrolo[2,3-*d*]pyrimidine-7-H **5.10**. To a suspension of **5.9** (78 g, 0.35 mol) in MeOH (1000 mL) was added sodium methoxide (40 mL, 25 wt. % in MeOH). Reaction mixture was brought to reflux, upon which the reaction became homogenous. After stirring at reflux for 30 min, a brown solid precipitated. The reaction was cooled to room temperature and the solid was collected by filtration and vigorously dried under vacuum over P_2O_5 to yield 39.2 g (57% yield) of **5.10** as a tan solid; ^{1}H NMR (400 MHz, $CDCl_3$) δ

8.09 (s, 1H), 7.35 (d, J = 8 Hz, 2H), 7.26 (d, J = 8 Hz, 2H), 7.17 (s, 1H), .34 (s, 3H).

yrimidine-7-cyclopentyl **5.11**. To a suspension of **5.10** (695 mg, 3.10 (20 mL) at 0°C was added NaH (103 mg, 4.3 mmol, 95 wt. % as an oil After stirring for 2 min, H_2 gas evolved and the reaction became The reaction mixture was stirred at 0°C for an additional 30 min, and then ure for 5 min. Cyclopentyl bromide (693 mg, 4.65 mmol) was added and tirred at room temperature. After 23 h, the reaction mixture was diluted 00 mL) and washed with H_2O (200 mL). The aqueous layer was back- austively, with ethyl acetate. The combined organic layers were dried iltered, and concentrated *in vacuo*. Purification by flash chromatography CH_2Cl_2) afforded 550 mg (61% yield) of **5.11**: R_f 0.8 (10% MeOH in MR (400 MHz, $CDCl_3$) δ 8.29 (s, 1H), 7.36 (d, J = 8 Hz, 2H), 7.24 (d, J = 8 s, 1H), 5.41 (br s, 2H), 5.10 (m, 1H), 2.39 (s, 3H), 2.25 (m, 2H), 1.87 (m, 2H); ^{13}C NMR (100 MHz, $CDCl_3$) δ 157.4, 151.9, 137, 132.3, 129.9, 128.9, 5.1, 33.1, 24.3, 21.3.

opentyl **5.12**. To a solution of **5.10** (376 mg, 1.28 mmol) in DMF (10 mL) bromosuccinimide (250 mg, 1.4 mmol) and the mixture stirred for 15 h light. The reaction was diluted with ethyl acetate (100 mL) and washed Na_2SO_3 (200 mL) followed by brine (200 mL). The organic layer was dried s Na_2SO_4, filtered, and concentrated *in vacuo*. Purification by flash y (2:1 hexanes/ethyl acetate) afforded 282 mg (60% yield) of **5.12**: R_f es/ethyl acetate); ^1H NMR (400 MHz, $CDCl_3$) δ 8.25 (s, 1H), 7.36 (d, J = 8 d, J = 8 Hz, 2H), 5.27 (br s, 2H), 5.24 (m, 1H), 2.51 (m, 2H), 2.43 (s, 3H),

2.09 (m, 4H), 1.73 (m, 2H); ^{13}C NMR (100 MHz, $CDCl_3$) δ 155.9, 151.4, 150.2, 137.6, 130.5, 130.1, 129.4, 115.2, 109.4, 102.5, 57.4, 30.4, 24.8, 21.2, 14.1.

Methylketone-7-cyclopentyl **5.13**. To a solution of **5.12** (141 mg, 0.38 mmol) in toluene (5 mL) was added α-(ethoxyvinyl)tin (0.167 mL, 0.49 mmol). Argon gas was bubbled through the solution for 10 min. Tetrakis(triphenylphosphine)palladium (44 mg, 0.038 mmol) was quickly added and mixture was refluxed for 4 h. The solvent was removed *in vacuo* and the crude product was dissolved in THF (10 mL) and 1N HCl (3 mL). After stirring for 12 h at room temperature, the reaction mixture was diluted with ethyl acetate (50 mL) and washed with saturated $NaHCO_3$ (200 mL). The organic layer was dried over Na_2SO_4, filtered, and concentrated *in vacuo*. Purification by flash chromatography (1:1 hexanes/ethyl acetate) afforded 57 mg (45% yield) of **5.13**; ^1H NMR (400 MHz, $CDCl_3$) δ 8.31 (s, 1H), 7.31 (m, 4H), 5.45 (m, 1H), 5.0 (br s, 2H), 2.44 (s, 3H), 2.44 (m, 2H), 2.07 (m, 4H), 2.0 (s, 3H), 1.68 (m, 2H).

Fluoromethylketone-7-cyclopentyl **5.14** (fmk-cp). To a solution of **5.13** (57 mg, 0.17 mmol) in THF (2 mL) was added $(Boc)_2O$ (111 mg, 0.51 mmol). DMAP (4.15 mg, 0.34 mmol) was quickly added and the mixture was stirred for 12 h at room temperature. The reaction mixture was diluted with ethyl acetate (50 mL) and washed with 0.5 N HCl (50 mL) followed by brine (50 mL). The organic fraction was dried over Na_2SO_4, filtered, and concentrated *in vacuo*. Purification by flash chromatography (1:7 ethyl acetate/hexanes) gave 71 mg (79% yield) of *N*-diboc methylketone: R_f 0.60 (1:1 hexanes/ethyl acetate); ^1H NMR (400 MHz, $CDCl_3$) δ 8.91 (s, 1H), 7.24 (d, J = 8 Hz, 2H), 7.20 (d, J = 8 Hz, 2H), 5.25 (m, 1H), 2.48 (m, 2H), 2.42 (s, 3H), 2.06 (m, 4H), 2.06 (s, 3H), 1.70 (m, 2H), 1.3 (s, 18H).

To a solution of *N*-diboc methylketone (71 mg, 0.13 mmol) in THF at 0°C was added LDA (0.095 mL, 2 M in THF). After 30 min, the reaction mixture was cooled to –78°C. *N*-fluorobenzenesulfonimide (0.127 mL, 1.67 M in THF) was added dropwise and the reaction mixture was warmed to room temperature. After 25 min, saturated NH_4Cl (1 mL) was added and the reaction mixture was poured into saturated NH_4Cl (50 mL) and extracted with ethyl acetate (50 mL). The organic fraction was dried over Na_2SO_4, filtered, and concentrated *in vacuo*. The crude product was dissolved in CH_2Cl_2 (1 mL) and cooled to 0°C. After 5 min, TFA (1 mL) was then added and reaction mixture was slowly warmed to room temperature. After 3 h, solvents were removed *in vacuo*. Purification by preparative HPLC (gradient 50-100% methanol over 15 min, 10 mL/min flow rate) gave **5.14** (fmk-cp) as a white solid; ^{1}H NMR (400 MHz, $CDCl_3$) δ 8.34 (s, 1H), 7.35 (d, J = 8 Hz, 2H), 7.32 (d, J = 8 Hz, 2H), 5.53 (m, 1H), 4.92 (br s, 2H), 4.6 (d, J_{HF} = 47 Hz, 2H), 2.47 (s, 3H), 2.45 (m, 2H), 2.09 (m, 4H), 1.70 (m, 2H).

Pyrrolo[2,3-*d*]pyrimidine-7-*N*-boc-piperdine **5.15**. To a solution of **5.10** (750 mg, 3.35 mmol) in DMF (7 mL) was added 18 crown-6-ether (885 mg, 3.35 mmol) and K_2CO_3 (926 mg, 6.7 mmol). The heterogenous mixture was heated to 70°C, upon which the reaction became homogenous. After 30 min, *N*-boc-4-tosylate-piperidine (1.31 g, 3.68 mmol) was added and reaction was stirred for 36 h. The reaction was diluted with ethyl acetate (100 mL) and washed with H_2O (300 mL), followed by brine (300 mL). The organic layer was dried over Na_2SO_4 and concentrated *in vacuo*. Purification by flash chromatography (2% MeOH in CH_2Cl_2) afforded 489 mg (36% yield) of **5.15**; ^{1}H NMR (400 MHz, $CDCl_3$) δ 8.28 (s, 1H), 7.36 (d, J = 8 Hz, 2H), 7.25 (d, J = 8 Hz, 2H), 5.8 (br s, 2H), 4.9 (m, 2H), 4.4 (br s, 2H), 3.0 (m, 2H), 2.4 (s, 3H), 2.05 (m, 2H), 1.9 (m, 2H), 1.4 (s, 9H); ^{13}C NMR (100 MHz, $CDCl_3$) δ 157.2, 154.4, 151.5, 149.9, 136.7, 131.6, 129.7, 129.5, 128.5, 118.9, 116.5, 101, 79.7, 67.1, 51.2, 34.1, 32.2, 28.2, 20.9.

Bromide-7-*N*-boc-piperdine **5.16**. To a solution of **5.15** (45 mg, 0.11 mmol) in DMF (2 mL) was added *N*-bromosuccinimide (21 mg, 0.12 mmol) and $NaHCO_3$ (14 mg, 0.165 mmol), and the mixture stirred for 15 h protected from light. The reaction was diluted with ethyl acetate (50 mL) and washed with saturated Na_2SO_3 (100 mL) followed by brine (200 mL). The organic layer was dried over anhydrous Na_2SO_4, filtered, and concentrated *in vacuo.* Purification by flash chromatography (1:1 hexanes/ethyl acetate) afforded 26.3 mg (50% yield) of **5.16** (also contained some amount of *N*-boc-4-hydroxy-piperidine so yield may not be accurate: R_f 0.4 (1:2 hexanes/ethyl acetate); ^{1}H NMR (400 MHz, $CDCl_3$) δ 8.24 (s, 1H), 7.34 (d, J = 8 Hz, 2H), 7.27 (d, J = 8 Hz, 2H), 5.24 (br s, 1H), 4.33 (br s, 2H), 3.85 (m, 2H), 2.87 (m, 2H), 2.42 (s, 3H), 1.83 (br s, 2H), 1.51 (s, 9H).

Methylketone-7-*N*-boc-piperdine **5.17**. To a solution of **5.16** (60 mg, 0.12 mmol) in toluene (3 mL) was added α-(ethoxyvinyl)tin (0.054 mL, 0.49 mmol). Argon gas was bubbled through the solution for 10 min. Tetrakis(triphenylphosphine)palladium (14 mg, 0.012 mmol) was quickly added and mixture was refluxed for 4 h. The reaction mixture was diluted with ethyl acetate (50 mL) and washed with saturated $NaHCO_3$ (50 mL), followed by brine (50 mL). The organic layer was dried over Na_2SO_4, filtered, and concentrated *in vacuo.* Purification by flash chromatography (2:3 hexanes/ethyl acetate) afforded 42 mg (72% yield) of the enol ether derivative, which was carried on directly to the next step.

The enol ether derivative was dissolved in THF (2 mL) and 1 N HCl (1 mL). After stirring at room temperature for 3 h, the reaction was portioned between ethyl acetate (50 mL) and saturated $NaHCO_3$ (50 mL). The organic layer was collected and dried over Na_2SO_4, filtered, and concentrated *in vacuo* to give 34 mg (86% yield) of **5.17**; ^{1}H NMR

(400 MHz, $CDCl_3$) δ 8.29 (s, 1H), 7.31 (s, 4H), 5.1 (m, 1H), 4.9 (br s, 2H), 4.3 (m, 2H), 2.9 (m, 2H), 2.45 (s, 3H), 2.0 (s, 3H), 1.9 (d, 2H), 1.51 (s, 9H).

Flouromethylketone-7-*N*-boc-piperdine **5.18** (fmk-pip). To a solution of **5.17** (34 mg, 0.08 mmol) in THF (1 mL) was added $(Boc)_2O$ (0.2 mL, 1.14 M in THF). DMAP (0.064 mL, 0.23 M in THF) was quickly added and the mixture was stirred for 12 h at room temperature. The reaction mixture was diluted with ethyl acetate (50 mL) and washed with 0.5 N HCl (50 mL) followed by brine (50 mL). The organic fraction was dried over Na_2SO_4, filtered, and concentrated *in vacuo*. Purification by flash chromatography (1:7 ethyl acetate/hexanes) gave 31 mg (63% yield) of *N*-diboc methylketone: R_f 0.40 (1:1 hexanes/ethyl acetate); ^{1}H NMR (400 MHz, $CDCl_3$) δ 8.87 (s, 3H), 7.22 (m, 4H), 4.9 (m, 1H), 4.3 (br s, 2H), 2.9 (m, 4H), 2.43 (s, 3H), 2.0 (s, 3H), 1.9 (d, 2H), 1.52 (s, 9H), 1.34 (s, 18H), 1.26 (m, 2H).

To a solution of *N*-diboc methylketone (31 mg, 0.08 mmol) in THF at 0°C was added LDA (0.035 mL, 2 M in THF). After 30 min, the reaction mixture was cooled to –78°C. *N*-fluorobenzenesulfonimide (0.050 mL, 1.67 M in THF) was added dropwise and the reaction mixture was warmed to room temperature. After 25 min, saturated NH_4Cl (1 mL) was added and the reaction mixture was poured into saturated NH_4Cl (50 mL) and extracted with ethyl acetate (50 mL). The organic fraction was dried over Na_2SO_4, filtered, and concentrated *in vacuo*. The crude product was dissolved in CH_2Cl_2 (1 mL) and cooled to 0°C. After 5 min, TFA (1 mL) was then added and reaction mixture was slowly warmed to room temperature. After 3 h, solvents were removed *in vacuo*. Purification by preparative HPLC (gradient 28-35% methanol [0.1% TFA] over 15 min, 10 mL/min flow rate) gave **5.18** (fmk-pip) as a clear film; ^{1}H NMR (400 MHz, $CDCl_3$) δ 9.9 (br s, 1H), 9.0 (br s, 1H), 8.2 (br s, 1H), 7.42 (d, J = 8 Hz, 2H), 7.31 (d, J = 8 Hz, 2H),

, 2H), 4.66 (d, J_{HF} = 46 Hz, 2H), 3.7 (br s, 2H), 3.4-3.0 (m, 4H), 2.50 (s, 3H), 2.1).

ns, reagents and antibodies. Refer to Chapters 2-4.

ences

Gavin, A. C. & Nebreda, A. R. A MAP kinase docking site is required for phosphorylation and activation of p90(rsk)/MAPKAP kinase-1. *Curr Biol* **9**, 281-4 (1999).

Smith, J. A., Poteet-Smith, C. E., Malarkey, K. & Sturgill, T. W. Identification of an extracellular signal-regulated kinase (ERK) docking site in ribosomal S6 kinase, a sequence critical for activation by ERK in vivo. *J Biol Chem* **274**, 2893-8 (1999).

Frodin, M., Jensen, C. J., Merienne, K. & Gammeltoft, S. A phosphoserine-regulated docking site in the protein kinase RSK2 that recruits and activates PDK1. *Embo J* **19**, 2924-34 (2000).

Jensen, C. J. et al. 90-kDa ribosomal S6 kinase is phosphorylated and activated by 3-phosphoinositide-dependent protein kinase-1. *J Biol Chem* **274**, 27168-76 (1999).

Richards, S. A., Fu, J., Romanelli, A., Shimamura, A. & Blenis, J. Ribosomal S6 kinase 1 (RSK1) activation requires signals dependent on and independent of the MAP kinase ERK. *Curr Biol* **9**, 810-20 (1999).

6. Frodin, M. & Gammeltoft, S. Role and regulation of 90 kDa ribosomal S6 kinase (RSK) in signal transduction. *Mol Cell Endocrinol* **151**, 65-77 (1999).

7. Hauge, C. & Frodin, M. RSK and MSK in MAP kinase signalling. *J Cell Sci* **119**, 3021-3 (2006).

8. Cohen, M. S., Zhang, C., Shokat, K. M. & Taunton, J. Structural bioinformatics-based design of selective, irreversible kinase inhibitors. *Science* **308**, 1318-21 (2005).

9. Calderwood, D. J., Johnston, D. N., Munschauer, R. & Rafferty, P. Pyrrolo[2,3-d]pyrimidines containing diverse N-7 substituents as potent inhibitors of Lck. *Bioorg Med Chem Lett* **12**, 1683-6 (2002).

10. Liu, Y. et al. Structural basis for selective inhibition of Src family kinases by PP1. *Chem Biol* **6**, 671-8 (1999).

11. Huse, M. & Kuriyan, J. The conformational plasticity of protein kinases. *Cell* **109**, 275-82 (2002).

12. Greenbaum, D., Medzihradszky, K. F., Burlingame, A. & Bogyo, M. Epoxide electrophiles as activity-dependent cysteine protease profiling and discovery tools. *Chem Biol* **7**, 569-81 (2000).

13. Greenbaum, D. C. et al. Small molecule affinity fingerprinting. A tool for enzyme family subclassification, target identification, and inhibitor design. *Chem Biol* **9**, 1085-94 (2002).

14. Kato, D. et al. Activity-based probes that target diverse cysteine protease families. *Nat Chem Biol* **1**, 33-8 (2005).

15. Leung, D., Hardouin, C., Boger, D. L. & Cravatt, B. F. Discovering potent and selective reversible inhibitors of enzymes in complex proteomes. *Nature Biotechnology* **21**, 687-691 (2003).

UCSF LIBRARY

Chapter 6

Conclusions and future directions

UCSF LIBRARY

Protein kinases are essential enzymes involved in nearly all aspects of cell biology. In humans there are ~500 kinases and the development of selective inhibitors for every member promises to contribute greatly to our understanding of their roles in myriad cellular processes[1]. As most kinase inhibitors target the highly similar ATP binding site, they are often nonselective, incapable of distinguishing between family members. The identification of selective, ATP competitive inhibitors has predominately relied on intense medicinal chemistry and high-throughput screening by the pharmaceutical industry. While these efforts have generated a few incredibly potent and selective inhibitors (e.g. quinazoline-based EGFR inhibitors by Parke-Davis[2]), we sought a more rational approach that would combine structural and mutagenesis studies defining the pharmacophore of several inhibitors with structure-based sequence alignments. Toward this aim, we developed a structural bioinformatics approach to guide the rational design of selective, irreversible kinase inhibitors[3]. We were particularly interested in identifying nonconserved cysteine residues that could be exploited by electrophilic inhibitors as means to not only achieve potency, but also selectivity. This strategy led to the development of fmk, the first inhibitor of the CTD of RSK1 and RSK2. Fmk exploit two selectivity filters, a nucleophilic cysteine (found in 11 kinases) at the C-terminal end of the Gly-rich loop and a threonine gatekeeper (found in ~20% of kinases), which together are found only in the CTD of RSK1, RSK2, and RSK4. This work is a significant advance to the field of chemistry and chemical biology because it provides a potentially general strategy for the rational design of selective kinase inhibitors, traditionally a daunting challenge.

Fmk has allowed us to directly probe the role of the CTD in endogenous RSK signaling in ways not possible with NTD inhibitors and genetic techniques such as RNA interference. To extend the utility of fmk as a cellular probe of RSK CTD-dependent signaling, we developed fmk-pa, a propargylamine analog that not only exhibits

increased cellular potency, but can also be coupled to a reporter tag via the click reaction to assess covalent CTD modification in cells. These improved properties of fmk-pa were exploited to demonstrate that RSK CTD is required for S6K-independent rpS6 phosphorylation. We also used fmk-pa to show that Ser386 in the hydrophobic motif (HM) of endogenous RSK1 and RSK2 could be phosphorylated by a CTD-independent mechanism. This result led us to propose that another kinase could bypass the CTD under certain conditions, although thus far we have not able to identify this alternative RSK HM kinase. Pharmacological studies ruled out p38 MAPK (inhibited by SB203580), MK-2 (inhibited by SB203580, and mTOR/rapator (inhibited by rapamycin) as LPS-stimulated RSK HM kinases. Recent work from the Sabatini laboratory demonstrated that phosphorylation of Ser473 in the HM of protein kinase B is mediated by mTOR/rictor (insensitive to inhibition by rapamycin)[4]. Based on this result, it is possible that mTOR/rictor is the relevant, LPS-stimulated RSK HM kinase. This hypothesis could be tested by inhibition of mTOR/rictor using either RNA interference[4] or a small molecule inhibitor of mTOR kinase activity, which has recently been reported[5].

In a subsequent study, we exploited the ability of fmk-pa to report the modification of RSK1 and RSK2 simultaneously in cells to rapidly screen a small set of pyrrolo[2,3-*d*]pyrimidine-based inhibitors using two-step competition labeling assays. Intriguingly, we found that compounds bearing an electrophile at the C-6 position of the pyrrolo[2,3-*d*]pyrimidine scaffold were more selective for RSK1, although to varying degrees. By contrast, the parent scaffold, a reversible inhibitor, was slightly more selective for RSK2. Together, these results support the hypothesis that isoform selectivity is achieved by a mechanism involving covalent bond formation with the cysteine in the CTD. Consistent with this idea, fmk reacted much more rapidly with recombinant RSK1 CTD than RSK2 CTD *in vitro* as revealed by electrospray mass spectrometry. To our knowledge, this is the first demonstration that isoform selectivity

can be achieved by exploiting differences in the rate of covalent bond formation. The development of irreversible inhibitors that exhibit even greater RSK1-selectivity than fmk is worth pursuing since these compounds can be used to evaluate the specific cellular functions of RSK1.

Lastly, we pursued the identification of third-generation RSK CTD inhibitors with improved potency. Although only a limited set of compounds was synthesized, we were able to identify secondary amine derivatives of fmk (including fmk-pa) that exhibit remarkable cellular potency. One of these inhibitors, fmk-mea, ranks among the most potent and selective kinase inhibitors reported to date. Future studies will involve using this compound to explore the consequences of RSK CTD inhibition in cell-based and mouse models.

Developing electrophilic inhibitors for other cysteine containing kinases

How do we design inhibitors against the other 8 other kinases (**Figure 2-2**) that contain a cysteine corresponding to the cysteine in RSK1, RSK2, and RSK4? The latter three are the only kinases with a threonine selectivity filter in the gatekeeper position, which allows access to the hydrophobic pocket by the C-5 tolyl substituent of fmk. The other kinases have larger gatekeepers (methionine, leucine, and isoleucine) that obstruct access to this lipophilic cavity. We therefore searched for kinase inhibitors that do not extend into the gatekeeper pocket and could be easily appended with electrophiles. A class of inhibitors that meets these criteria is the oxindoles, for which there are numerous examples that target serine/threonine and tyrosine kinases that have large side chains at the gatekeeper position. Analysis of crystal structures of oxindole-based inhibitors bound to their kinase target suggested that electrophiles emanating from C-5 would be near the target cysteines. Dr. Sehat Nauli, a previous

scholar in our laboratory, synthesized a small set of electrophilic oxindoles . One of these inhibitors, B93, which contains a chloromethylketone at the of the oxindole scaffold, potently inhibited the se activities of NEK2 and MEKK1 (IC_{50} value n presence of 50 μM ATP). However, a y labeled derivative of B93, synthesized by se in our laboratory, was not selective in the

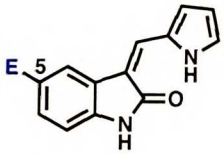

Electrophilic oxindole

Figure 6-1. Designed oxindole-based electrophilic inhibitor

mode (i.e. covalently modified many off-target proteins in cell lysates). replace the chloromethylketone with the inherently less-reactive reactive lketone resulted in a substantial loss in activity. This is likely because of the sible affinity of the oxindole scaffold for NEK2 and MEKK1 (an oxindole- itor with an ethyl group in place of the chloromethylketone exhibits an IC_{50} 5 μM). Attempts to increase the potency of B93 by replacing the pyrrole with various heterocyles have led to inhibitors with slightly increased potency K2 (Jeffrey Henise, unpublished results); however, these compounds still chloromethylketone to attain nanomolar inhibition.

do we achieve potent, irreversible inhibition exploiting weak electrophiles? to begin with an inhibitor scaffold that binds with higher affinity than the If we consider fmk as the paradigm of our rational design strategy, then an 1 μM for the starting scaffold is required. Therefore I propose that a panel kinase inhibitors be screened against the remaining 8 cysteine kinases) to identify scaffolds that adhere to this criterion. Ideally, the binding mode ied inhibitors will be known to guide attachment of the electrophiles.

UCSF LIBRARY

s

ning, G., Whyte, D. B., Martinez, R., Hunter, T. & Sudarsanam, S. The ein kinase complement of the human genome. *Science* **298**, 1912-34 (2002).

D. W. et al. A specific inhibitor of the epidermal growth factor receptor sine kinase. *Science* **265**, 1093-5 (1994).

en, M. S., Zhang, C., Shokat, K. M. & Taunton, J. Structural bioinformatics-ed design of selective, irreversible kinase inhibitors. *Science* **308**, 1318-21 05).

passov, D. D., Guertin, D. A., Ali, S. M. & Sabatini, D. M. Phosphorylation and ulation of Akt/PKB by the rictor-mTOR complex. *Science* **307**, 1098-101 05).

, Q. W. et al. A dual PI3 kinase/mTOR inhibitor reveals emergent efficacy in ma. *Cancer Cell* **9**, 341-9 (2006).

UCSF LIBRARY

Appendix A

^{1}H and ^{13}C NMR spectra

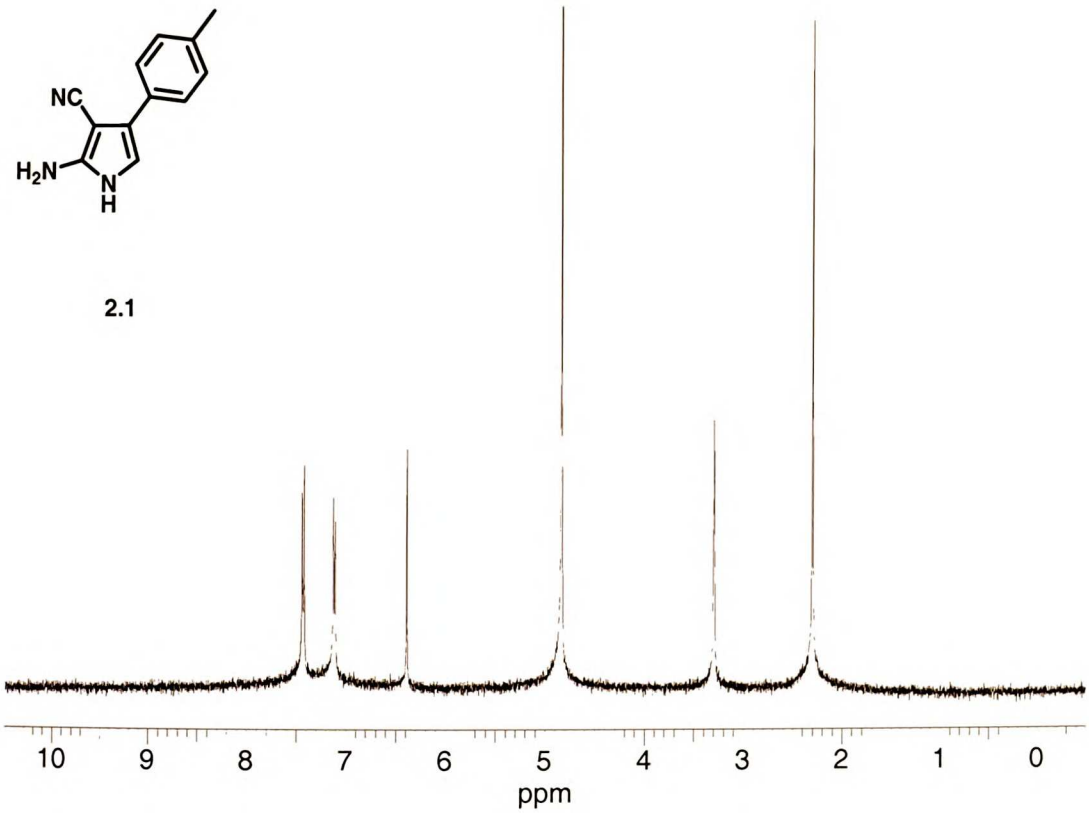
NC
H2N
N
H
2.1
10
9
8
7
6
5
4
3
2
1
0
ppm

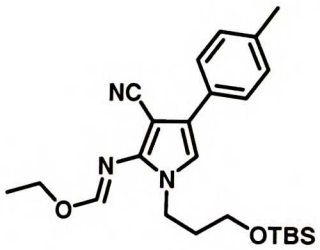

2.2

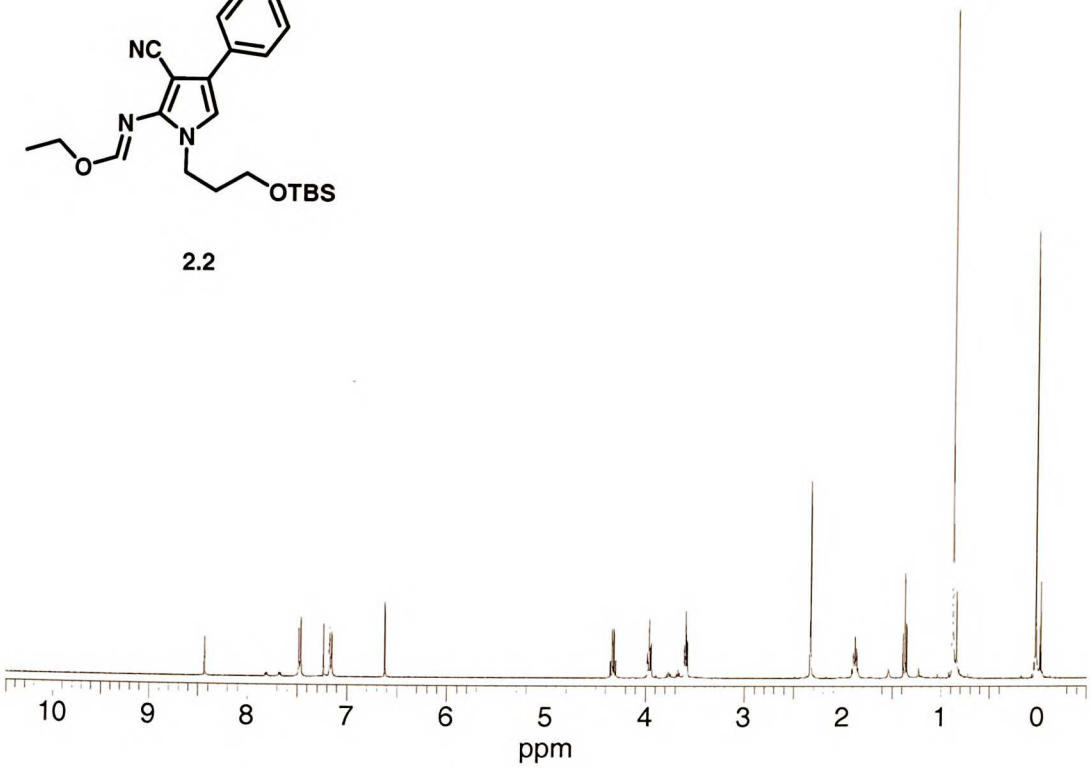

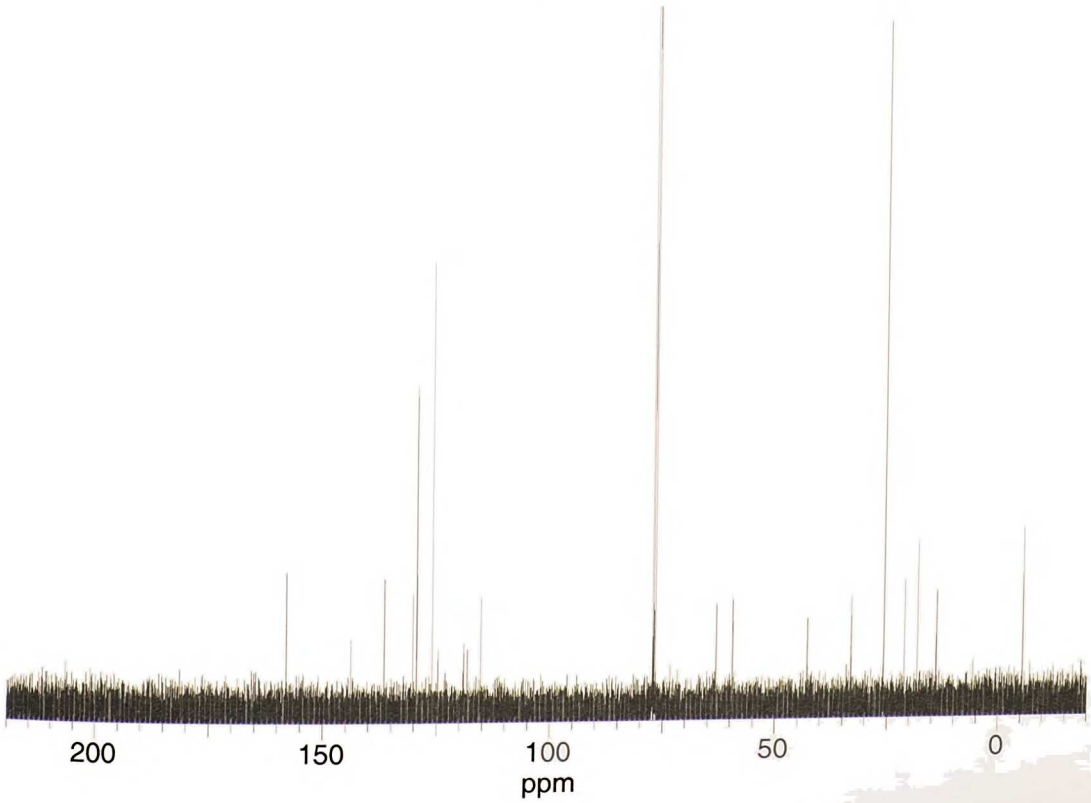

2.3

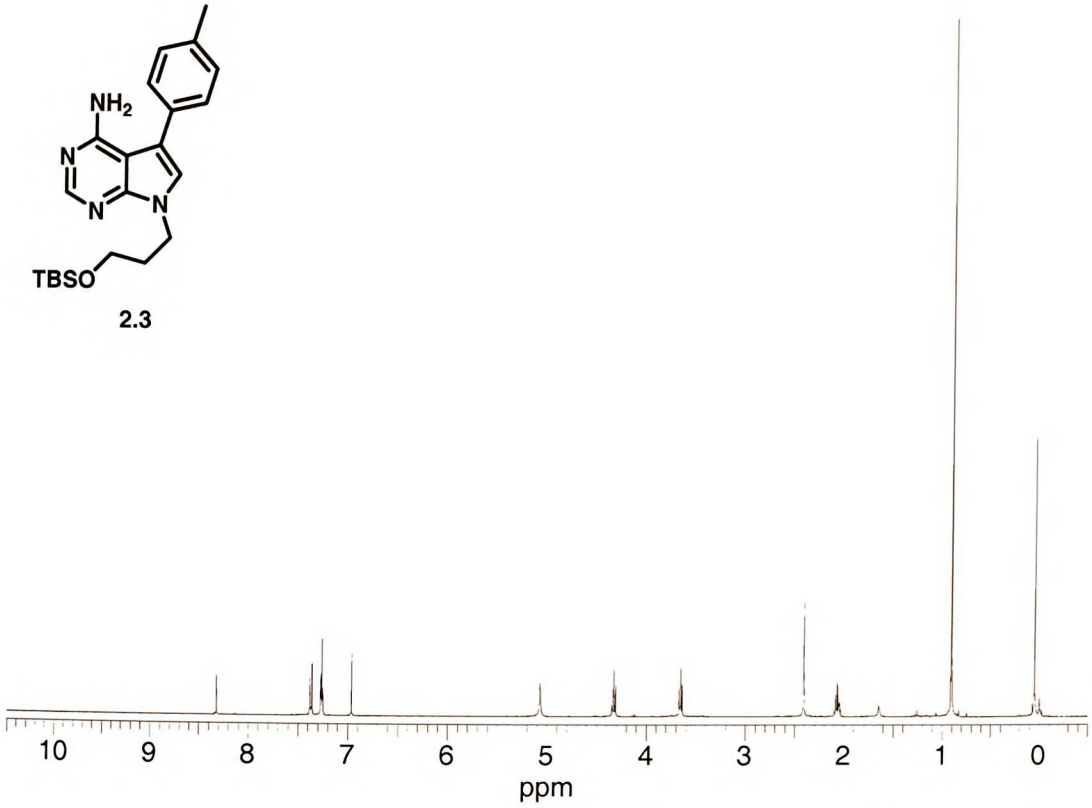

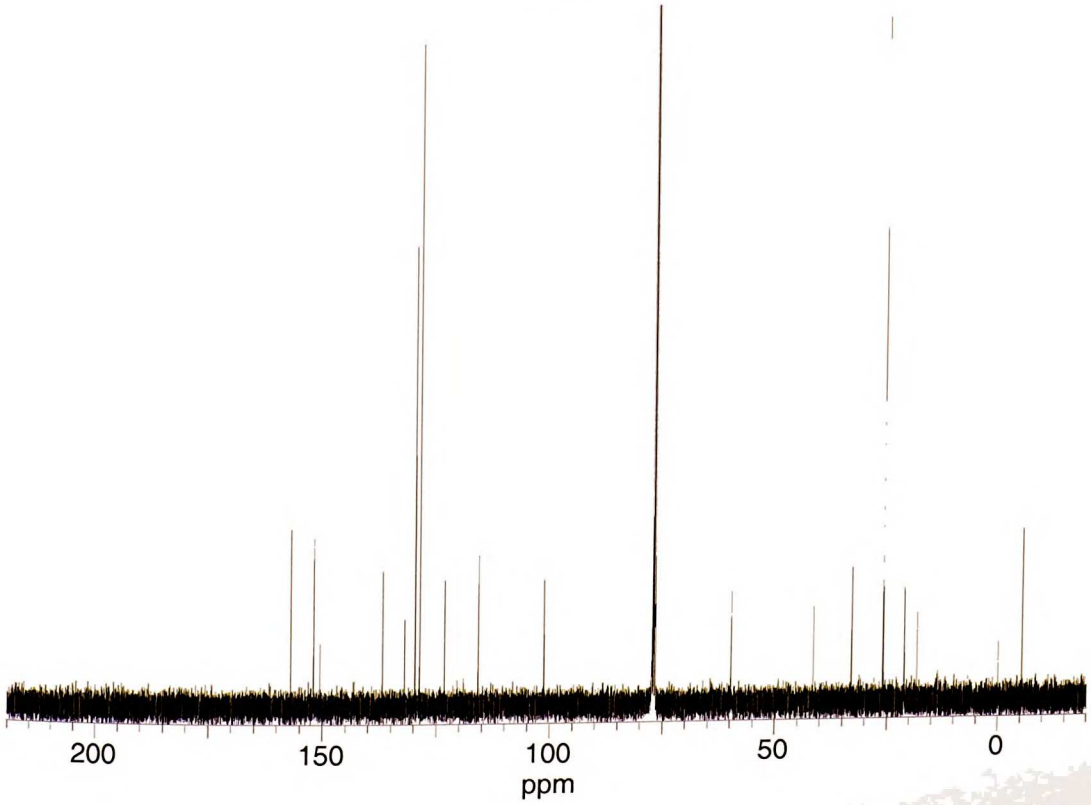

2.4

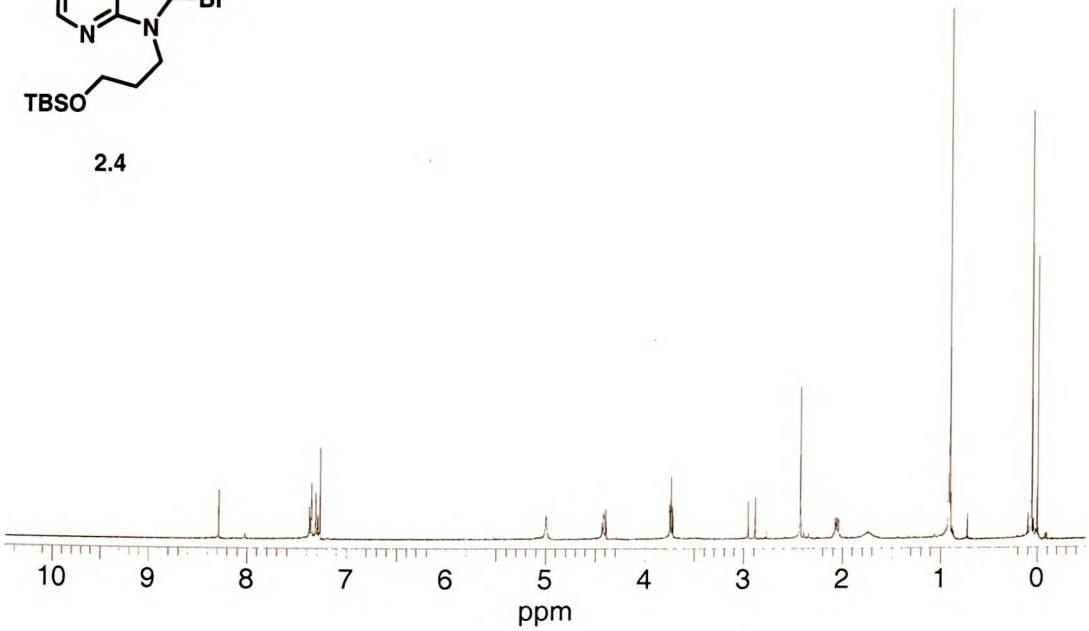

UCSF LIBRARY

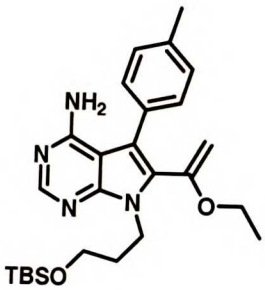

2.5

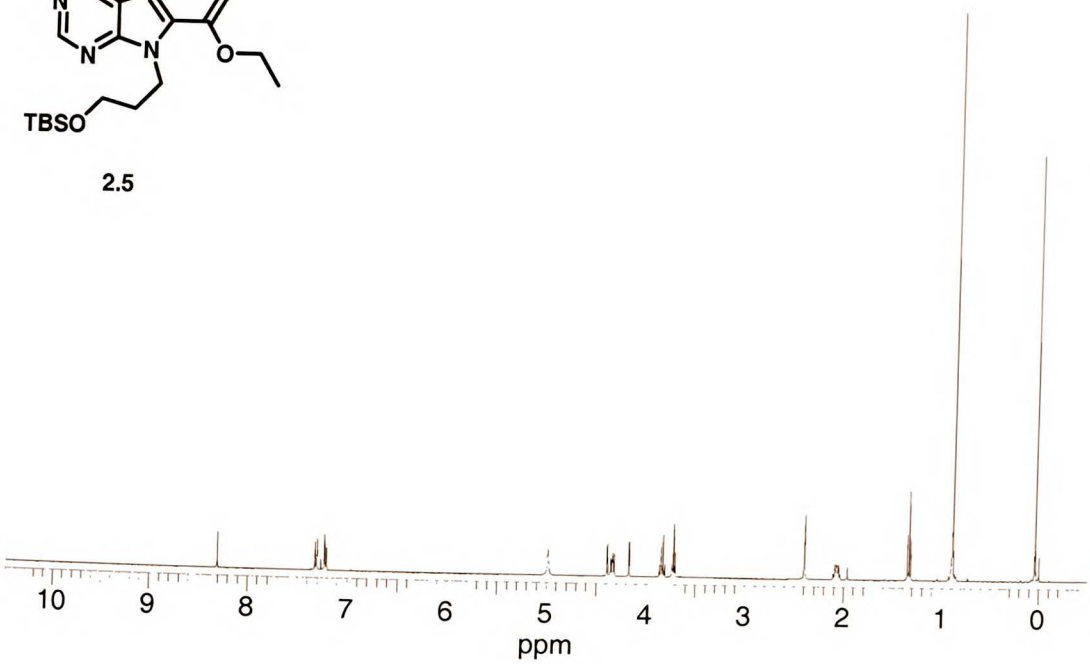

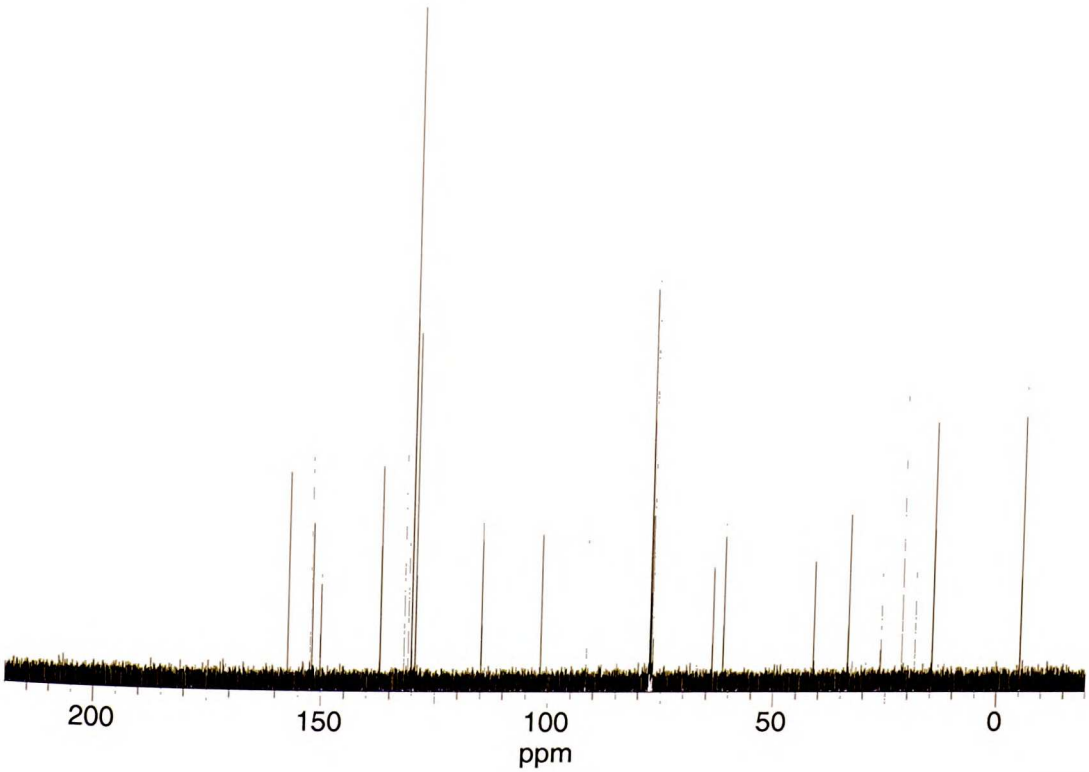

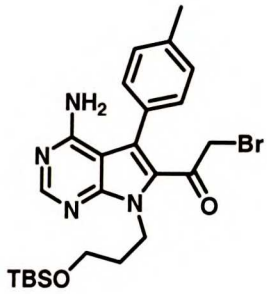

2.6

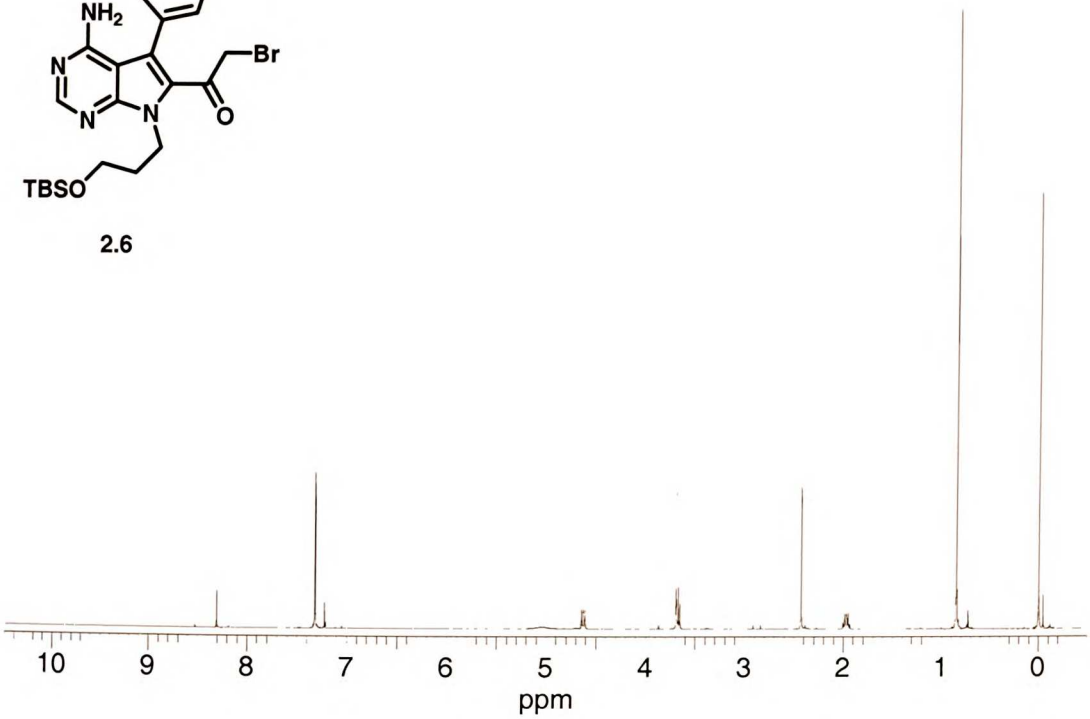

2.7

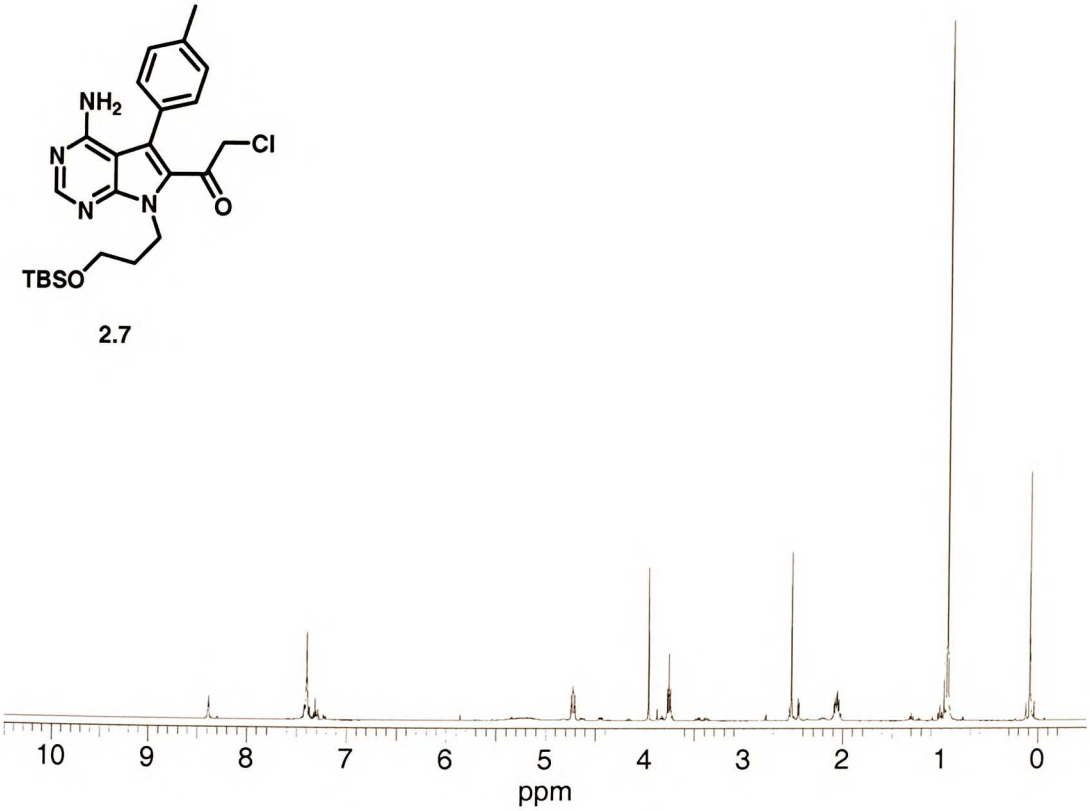

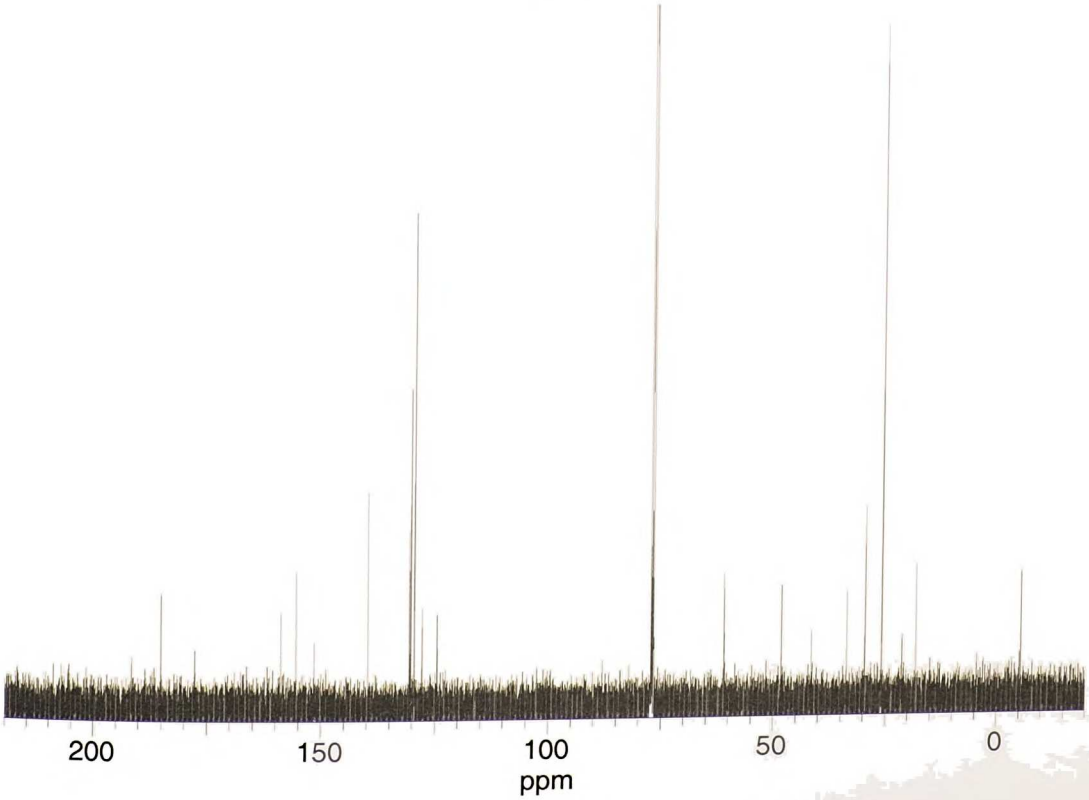

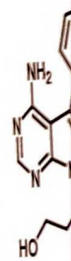

2.8

10

2.8 (bmk)

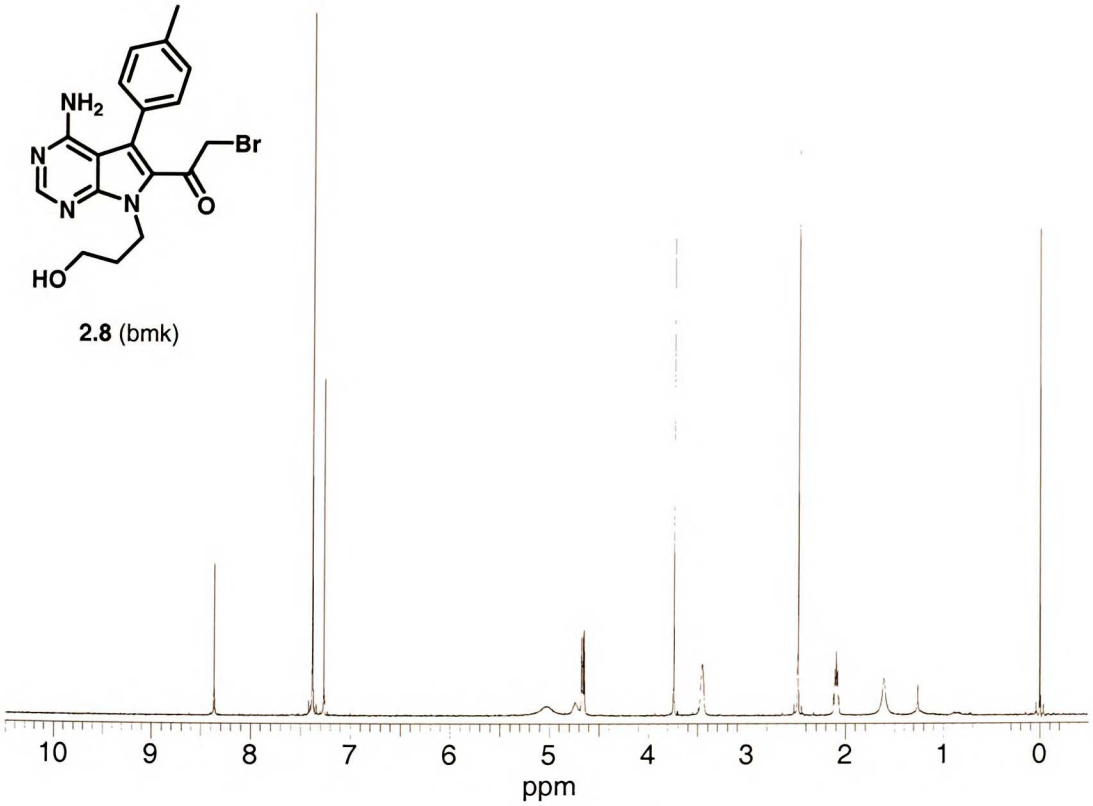

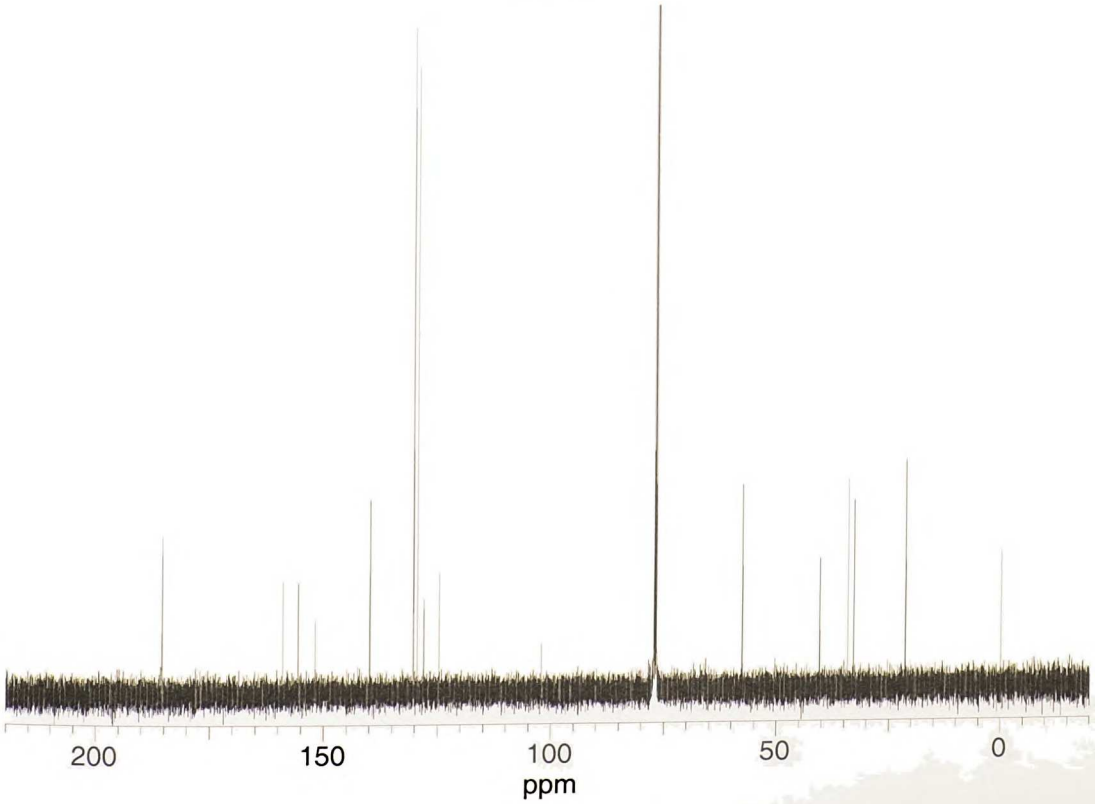

2.9 (cmk)

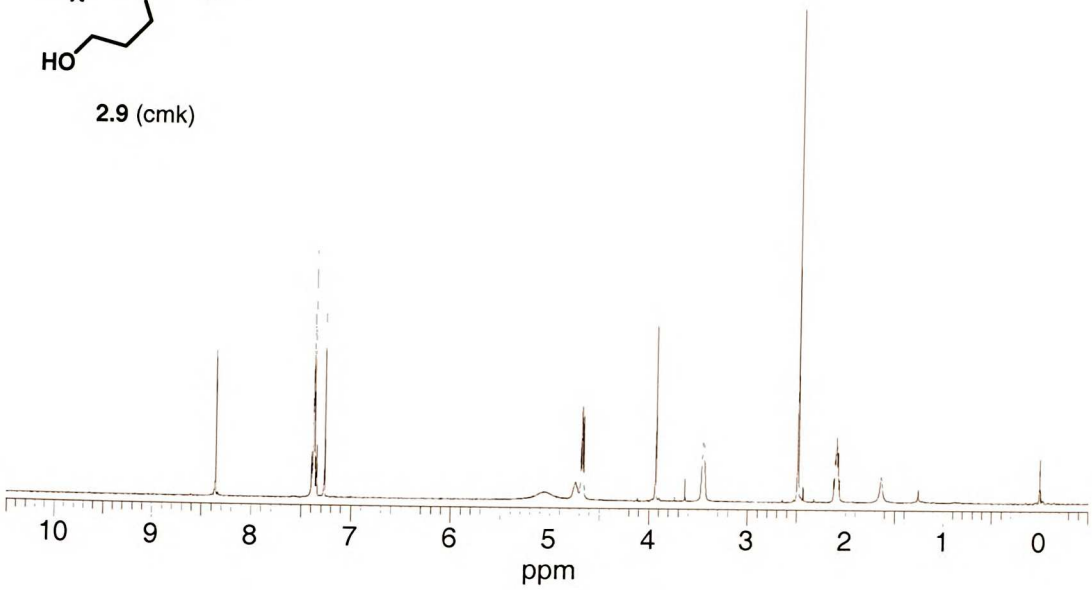

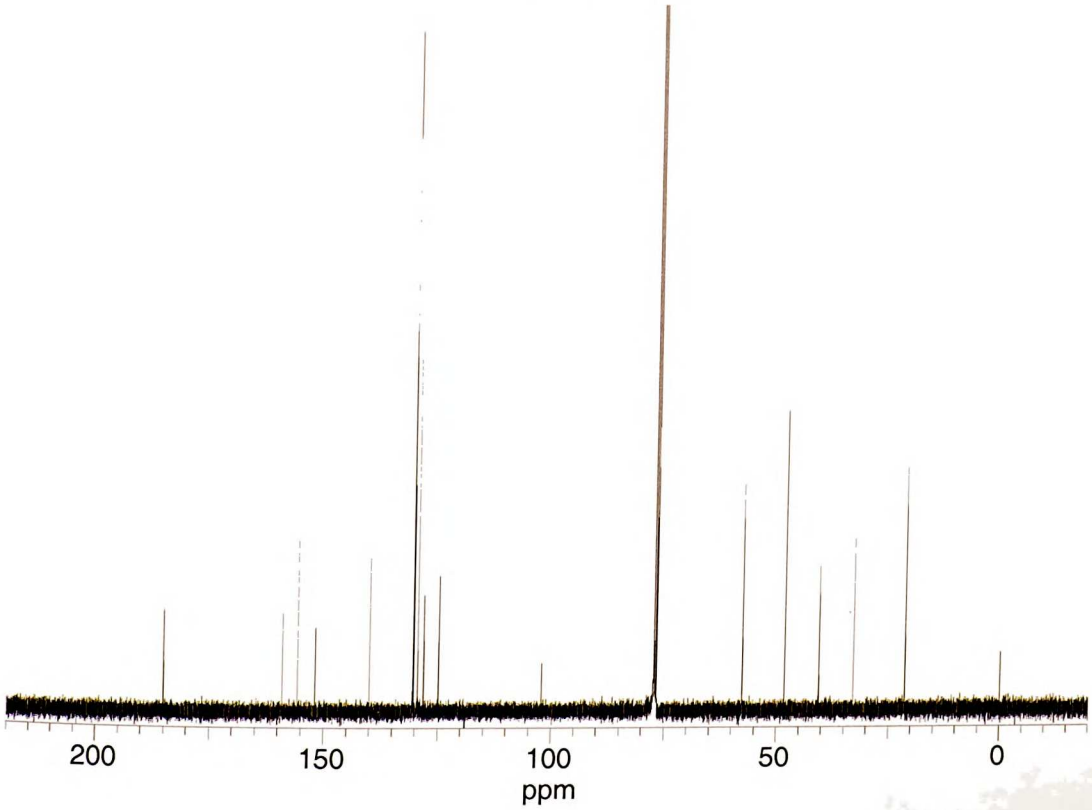

UCSD LIBRARY

2.10

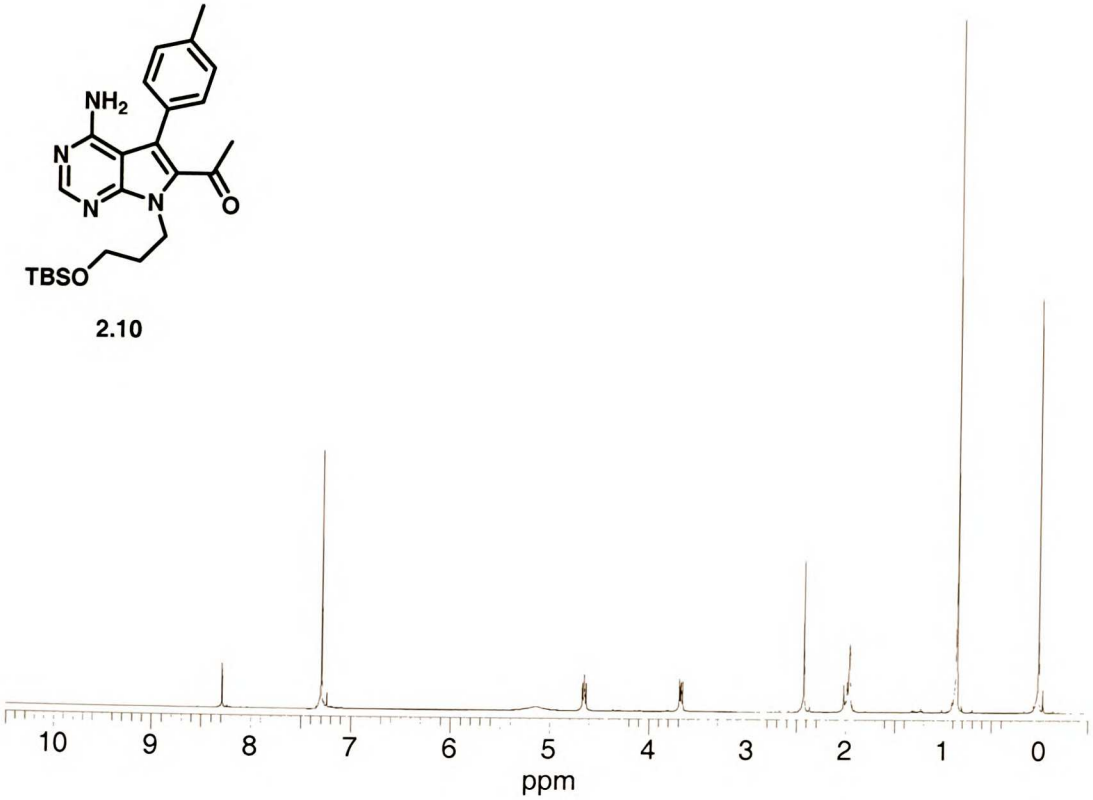

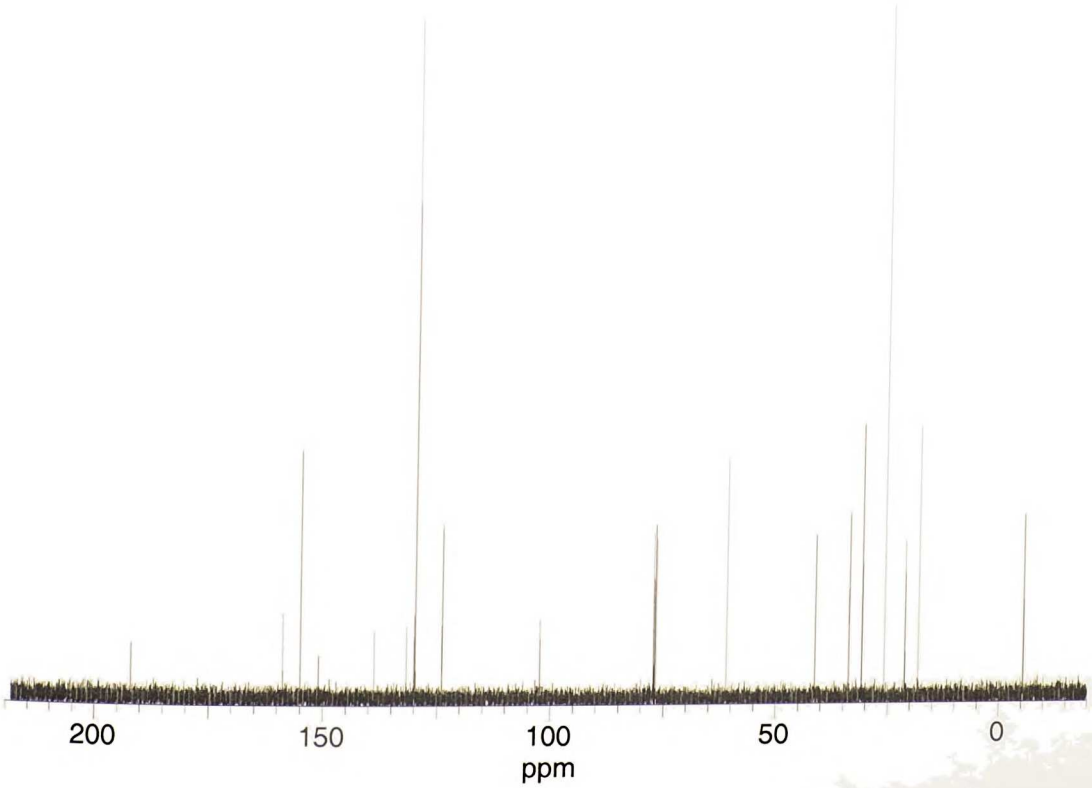

UCSF LIBRARY

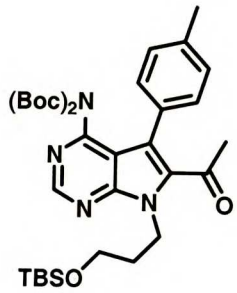

2.11

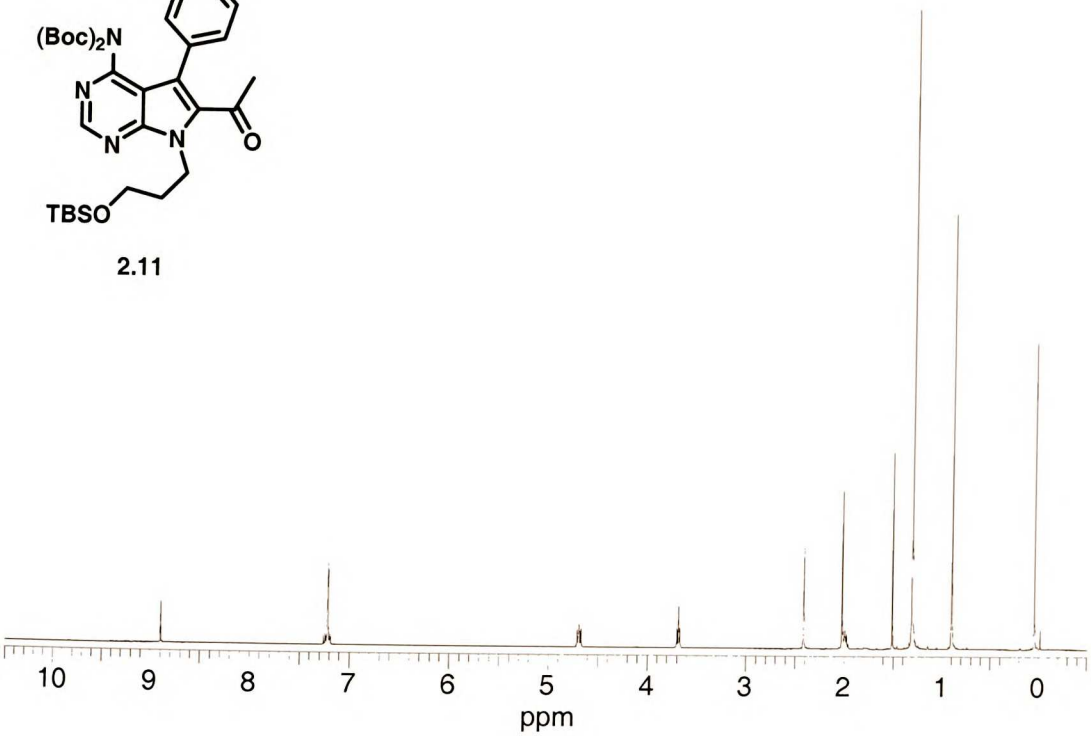

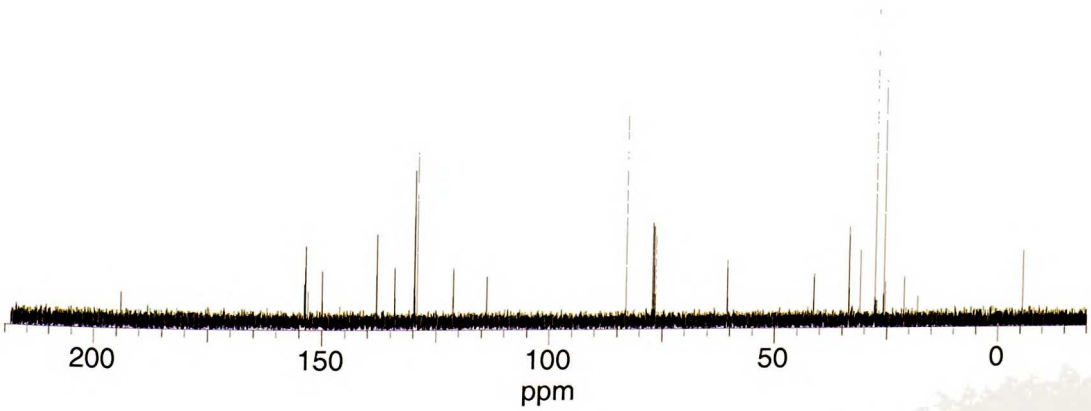

UCSF LIBRARY

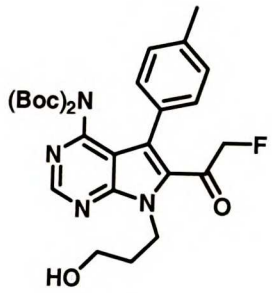

2.12

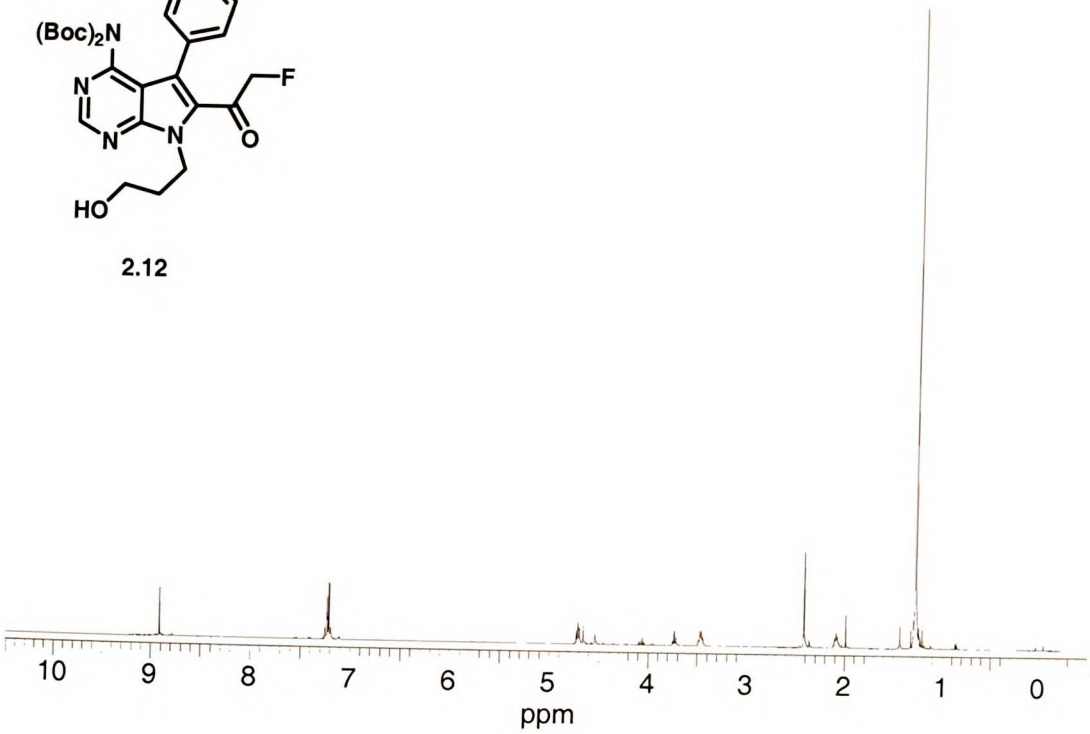

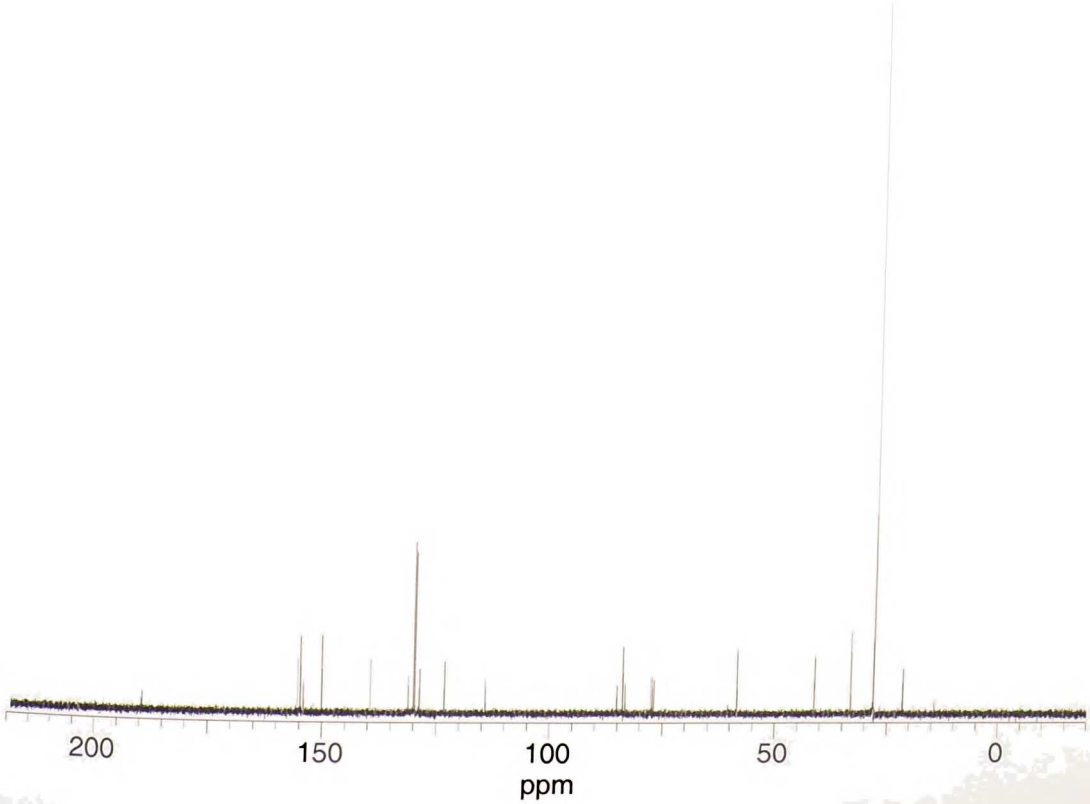

UCSF LIBRARY

2.13 (fmk)

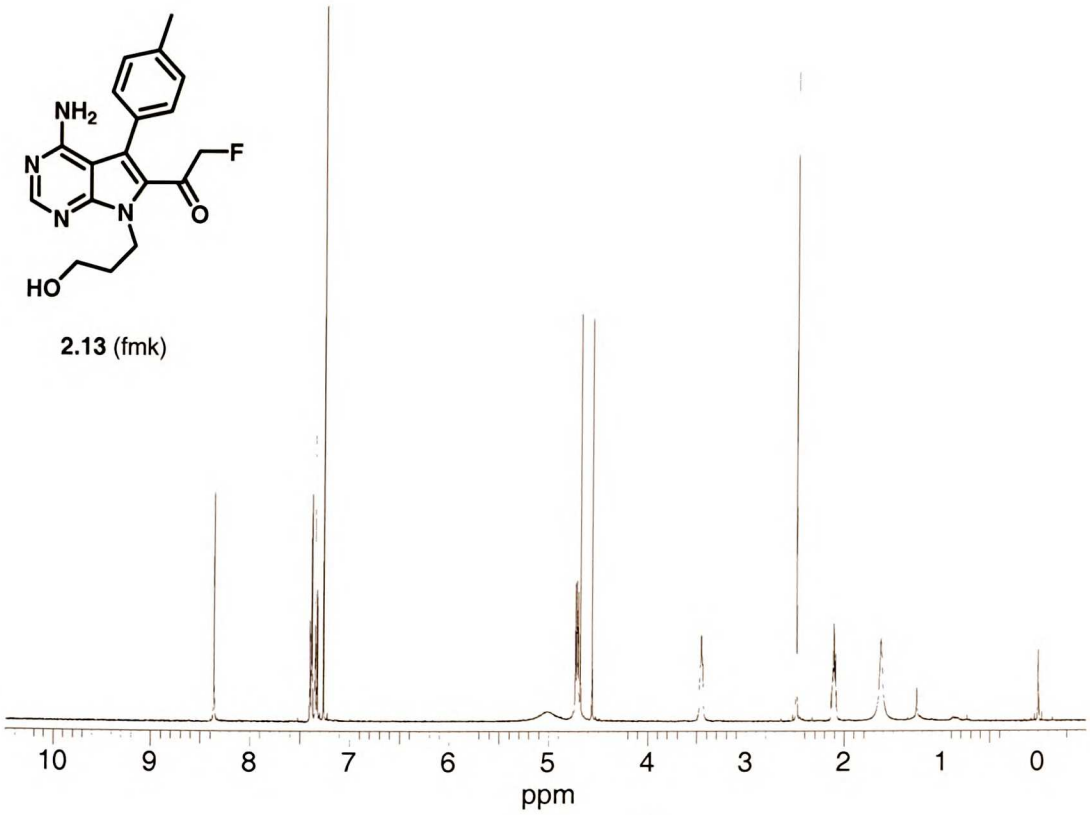

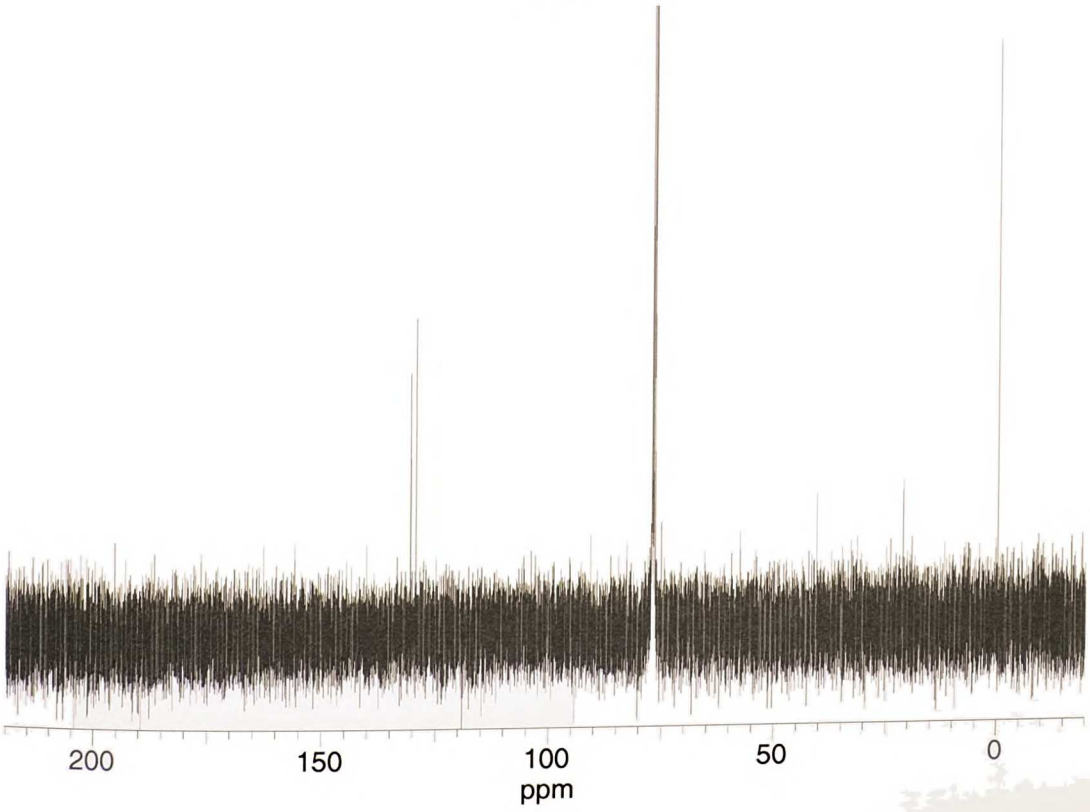

2.14 (scaffold)

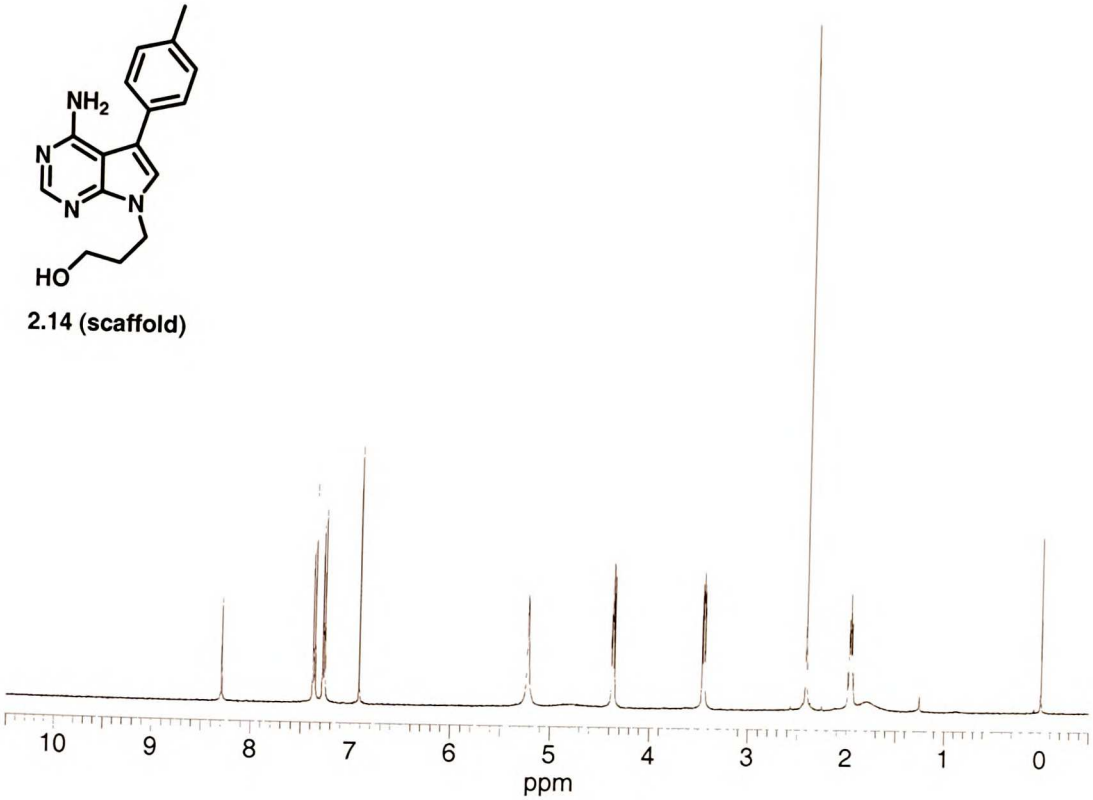

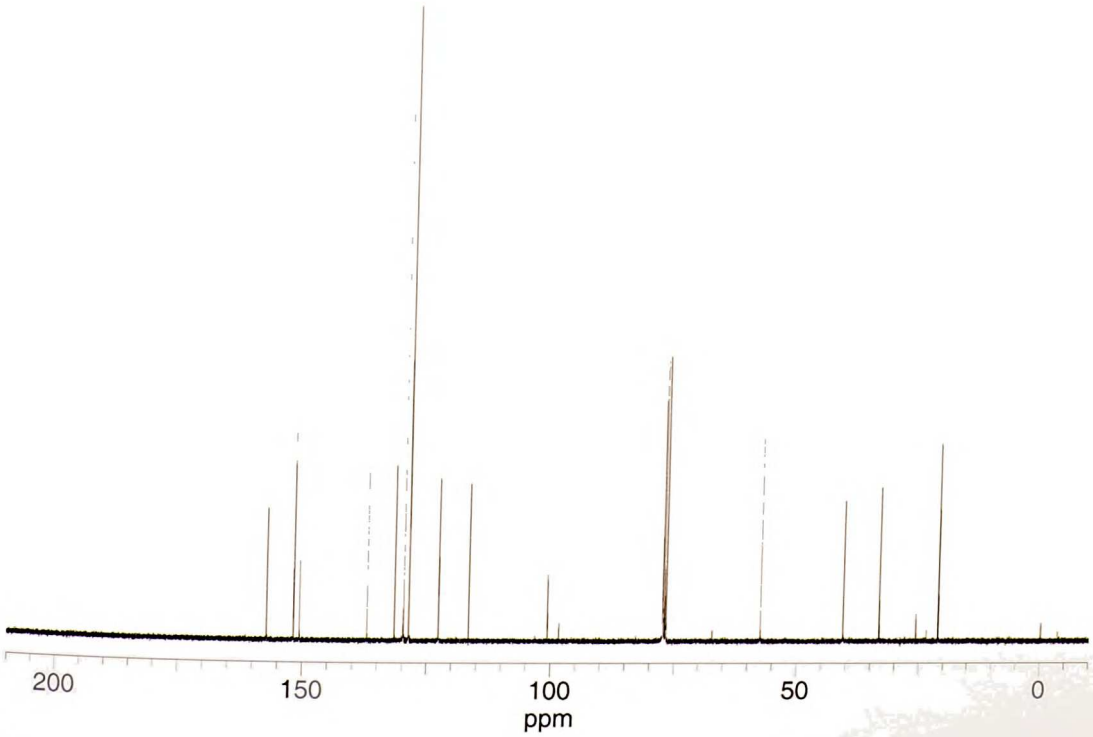

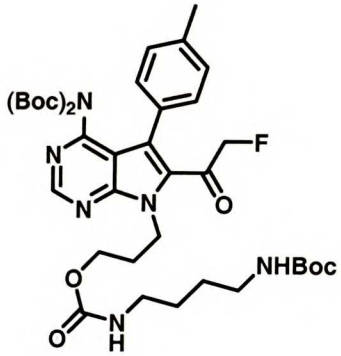

2.15

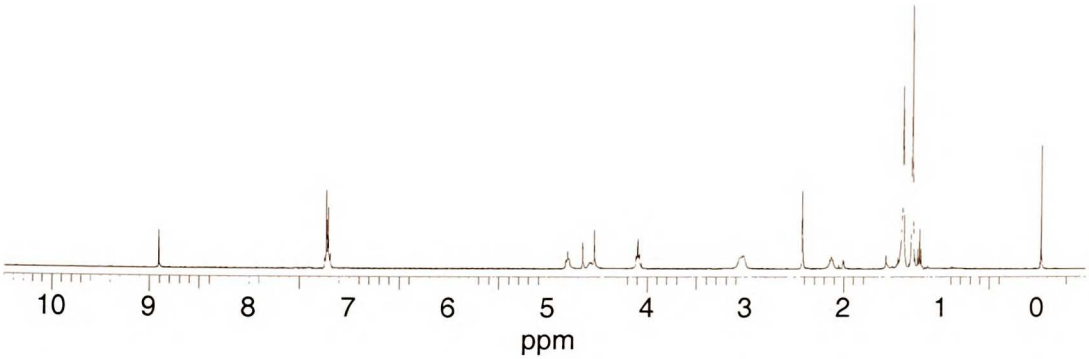

UCSF LIBRARY

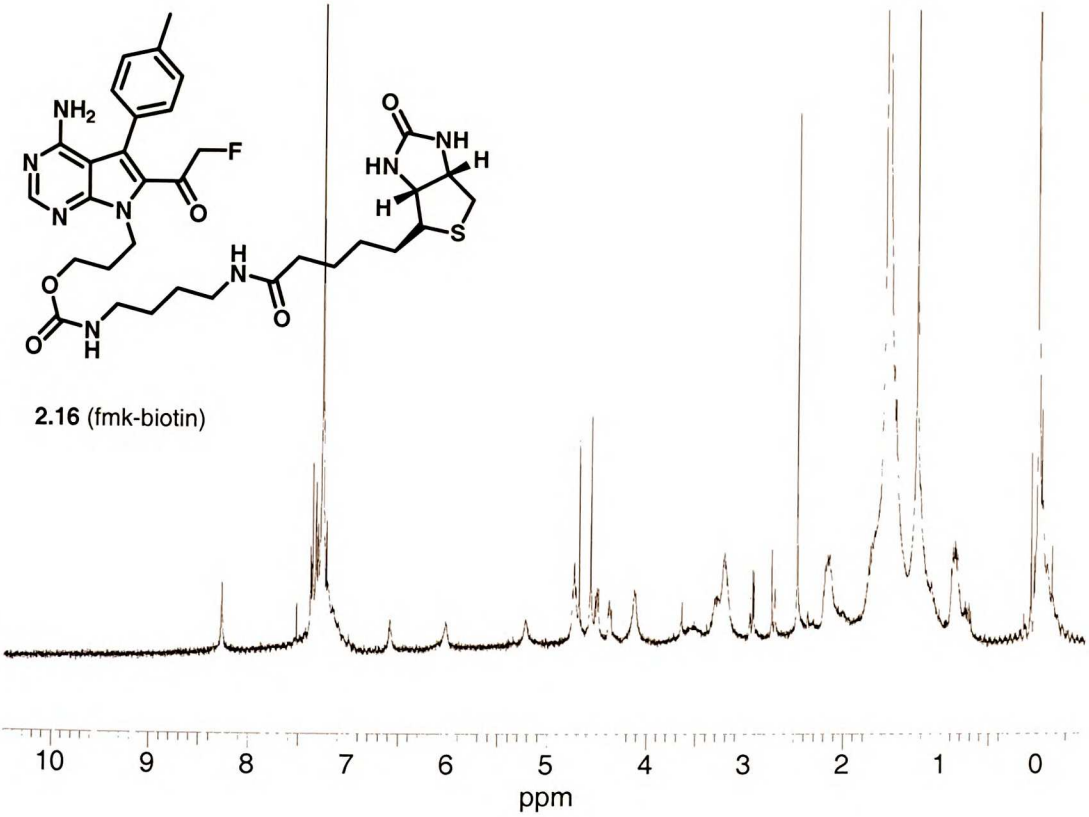

2.16 (fmk-biotin)

UCSF LIBRARY

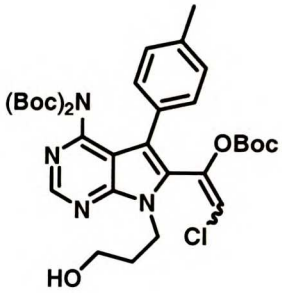

2.17

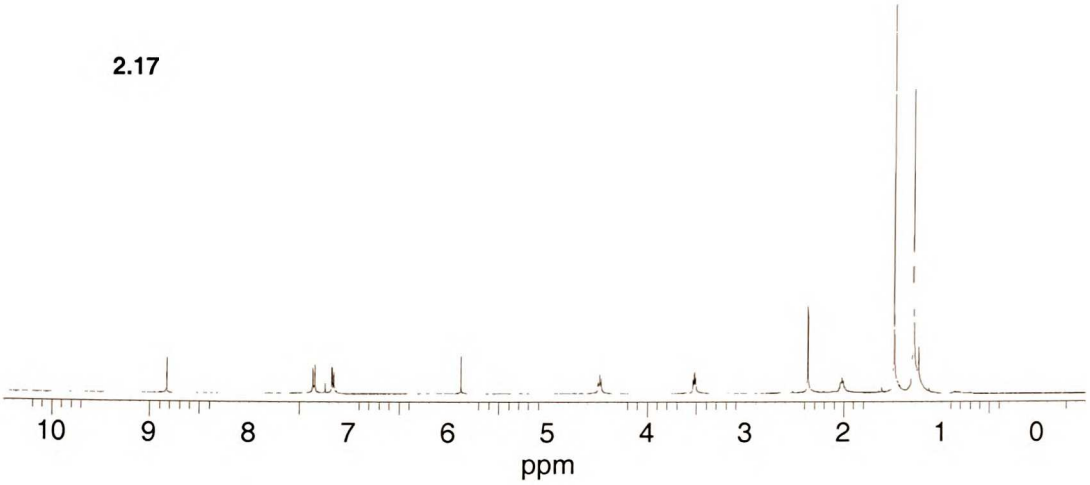

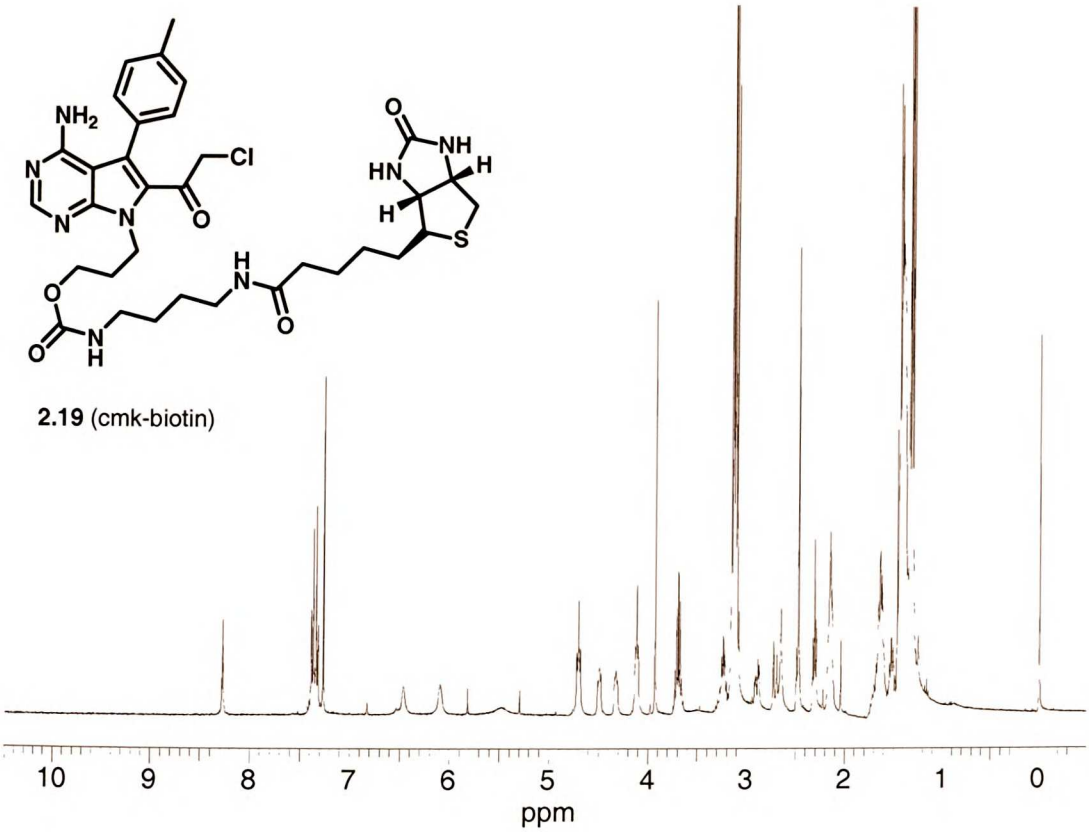

2.19 (cmk-biotin)

2.20

10

2.20 (cmk-BODIPY)

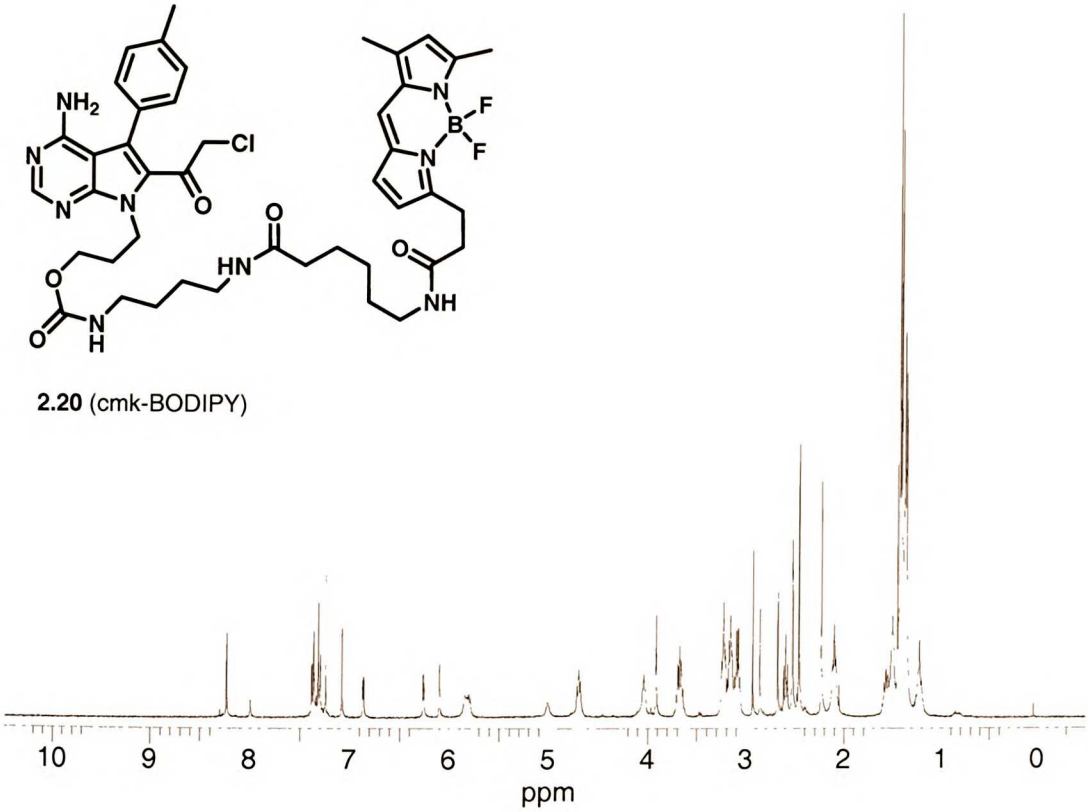

3.

10

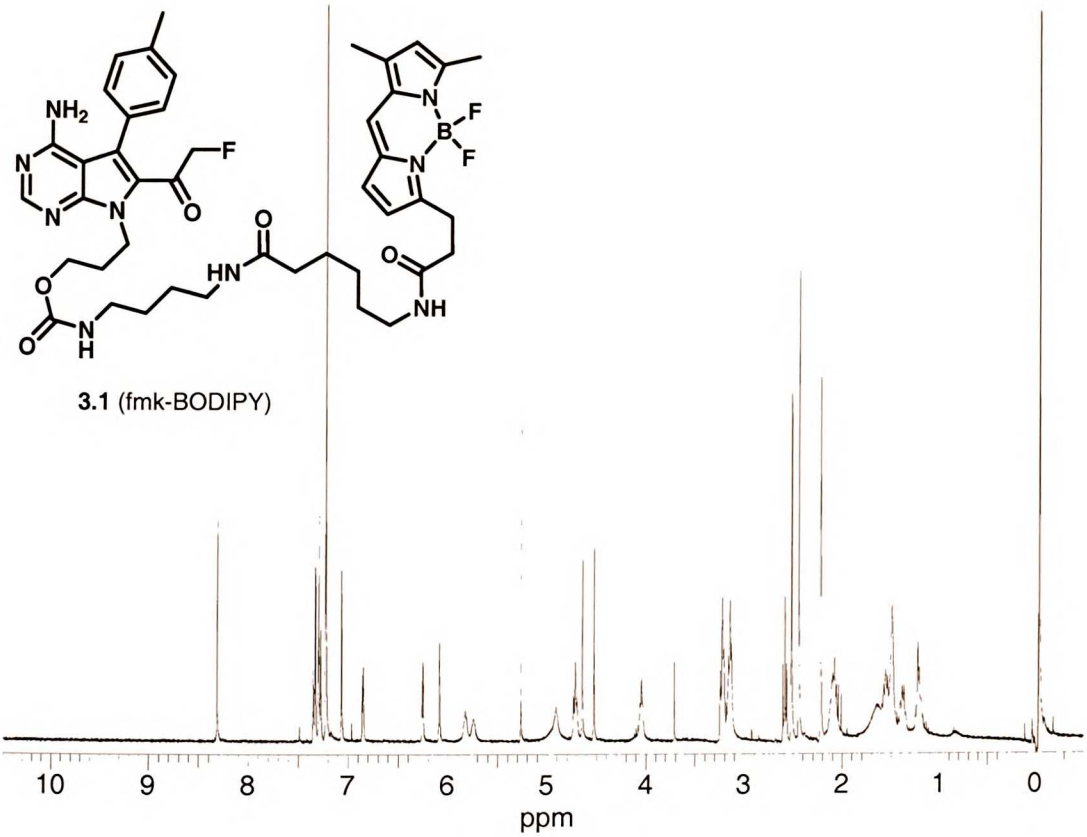

3.1 (fmk-BODIPY)

10

3.2

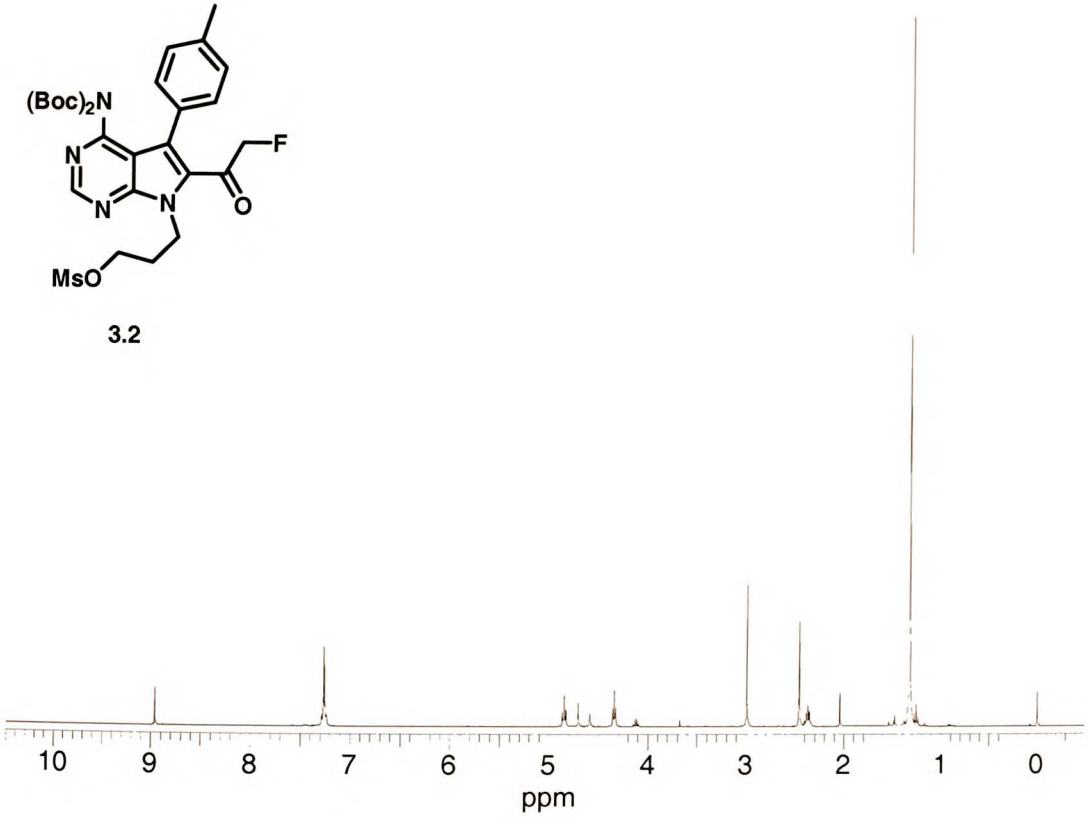

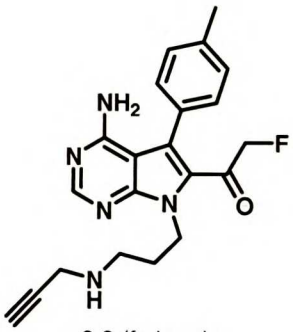

3.3 (fmk-pa)

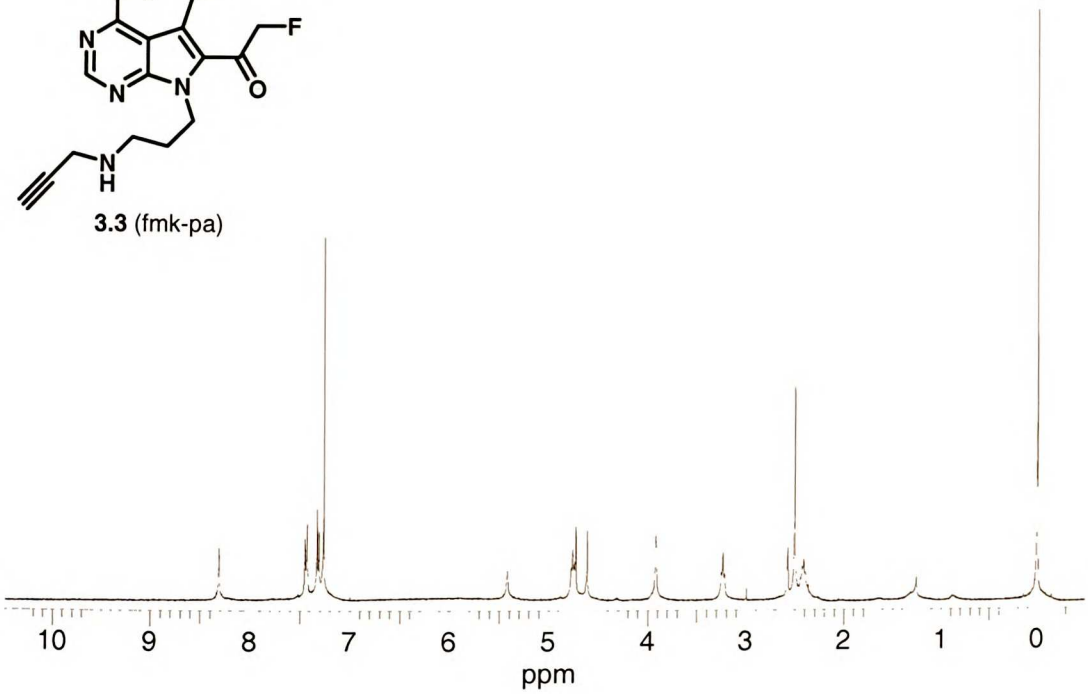

10

UNSF LIBRARY

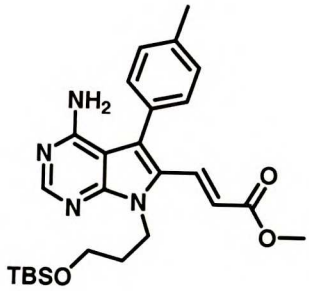

4.1

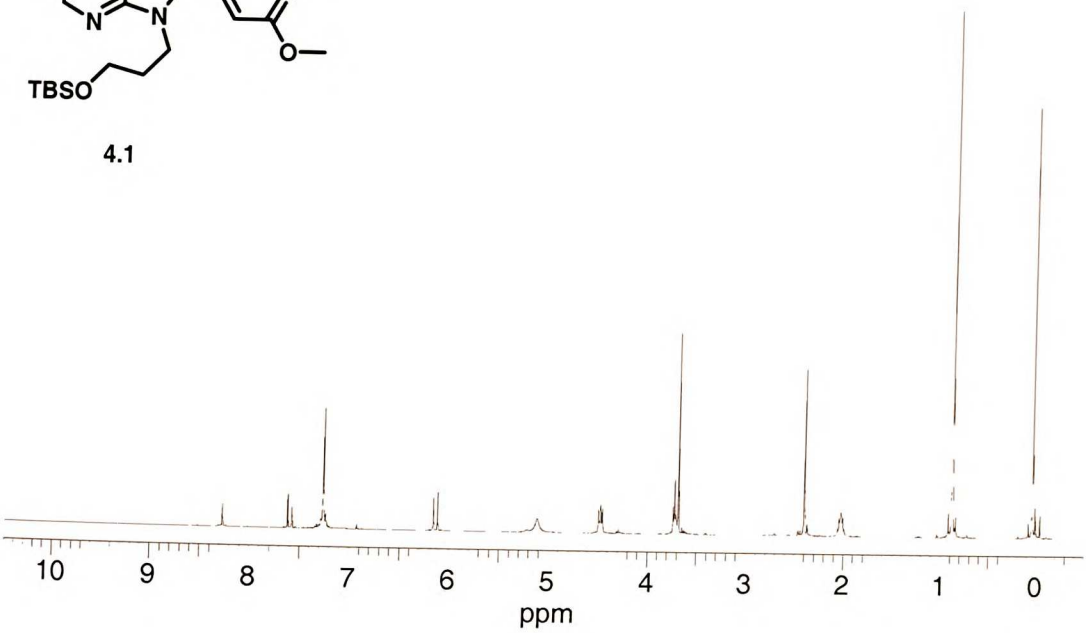

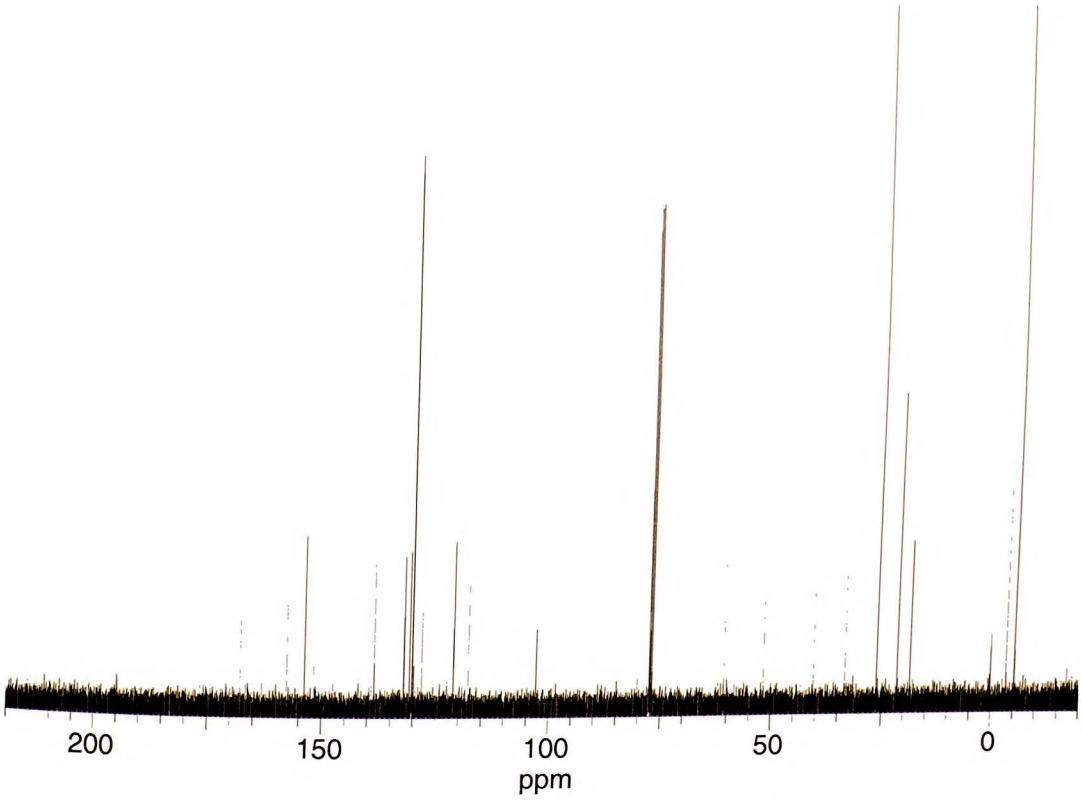

4.

10

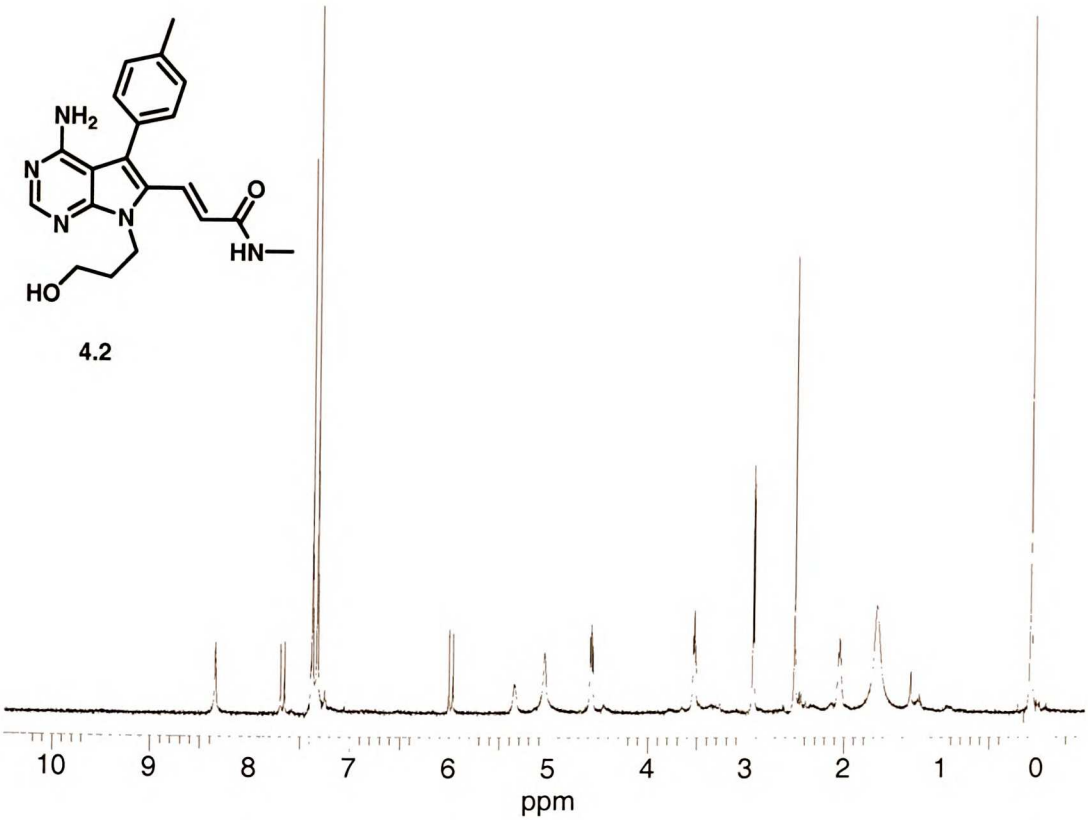
NH2
N
N
N
O
HN—
HO
4.2
10
9
8
7
6
5
4
3
2
1
0
ppm

NH2
N
N
HO

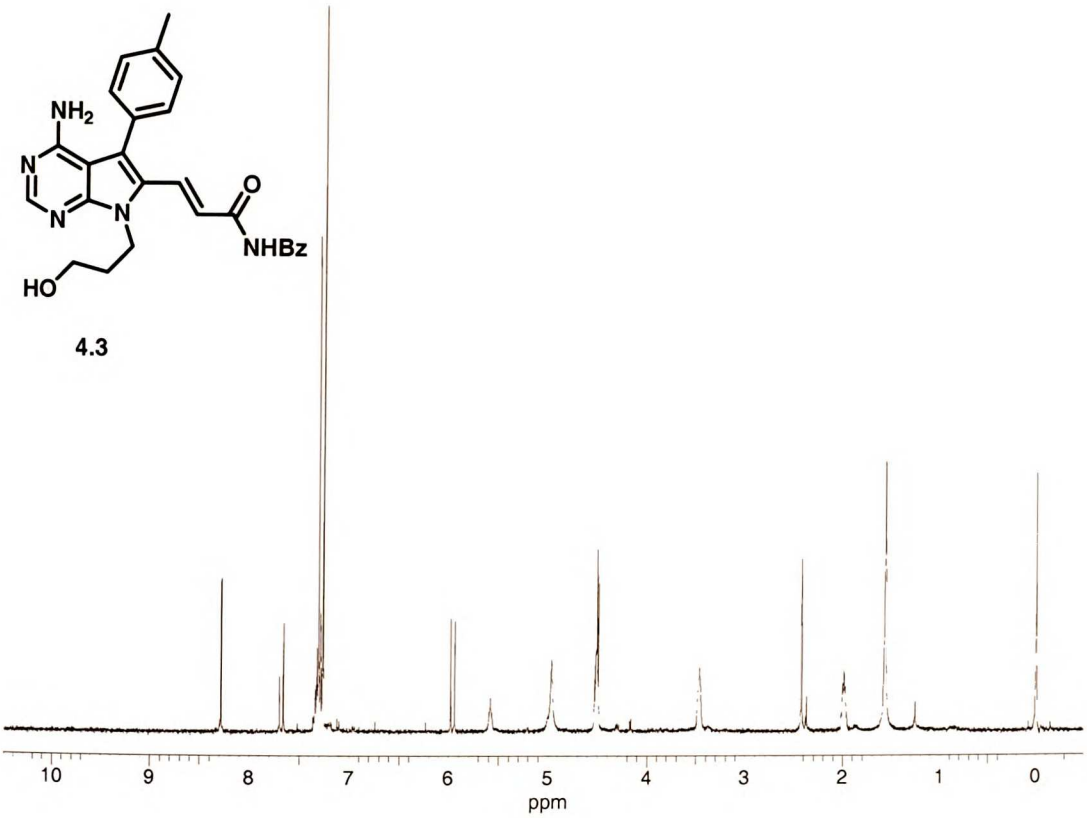
NH2
N
N
N
O
NHBz
HO
4.3
10
9
8
7
6
5
4
3
2
1
0
ppm

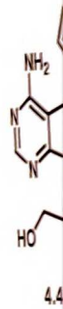

4.4

10

4.4

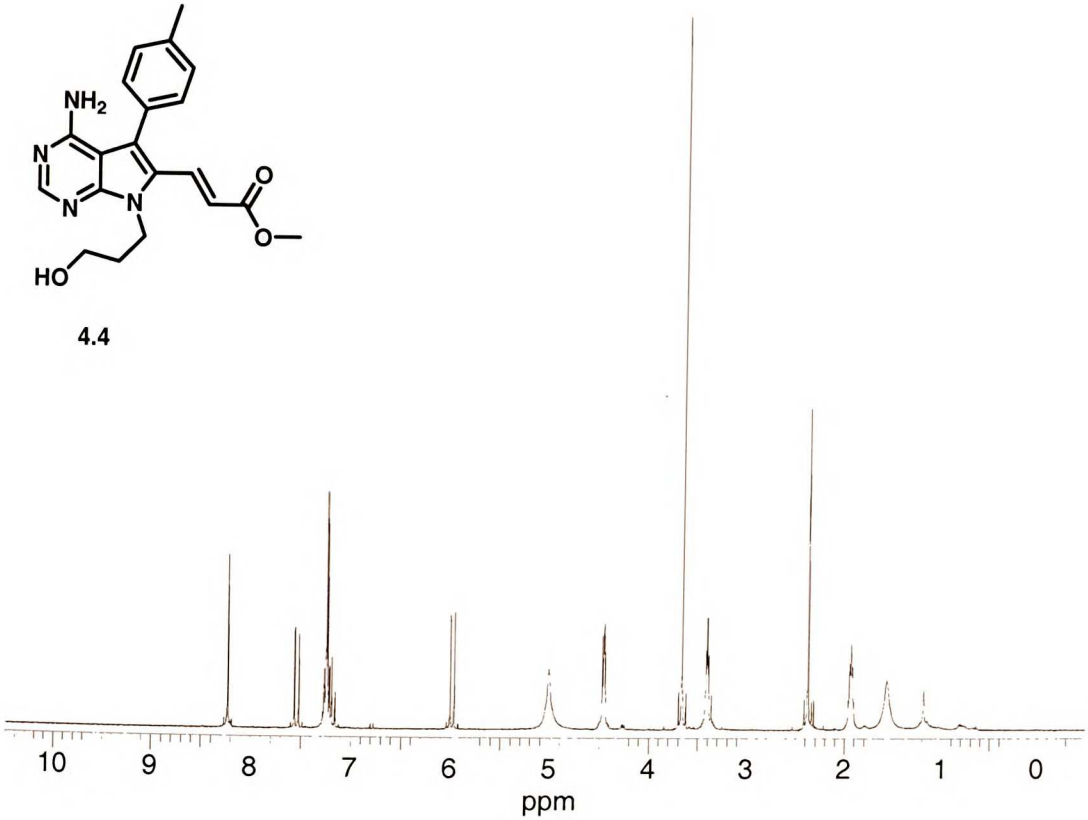

NH
N
N
TBSO

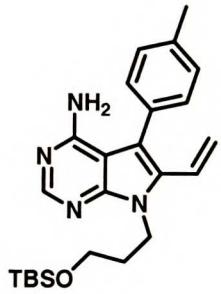

4.5

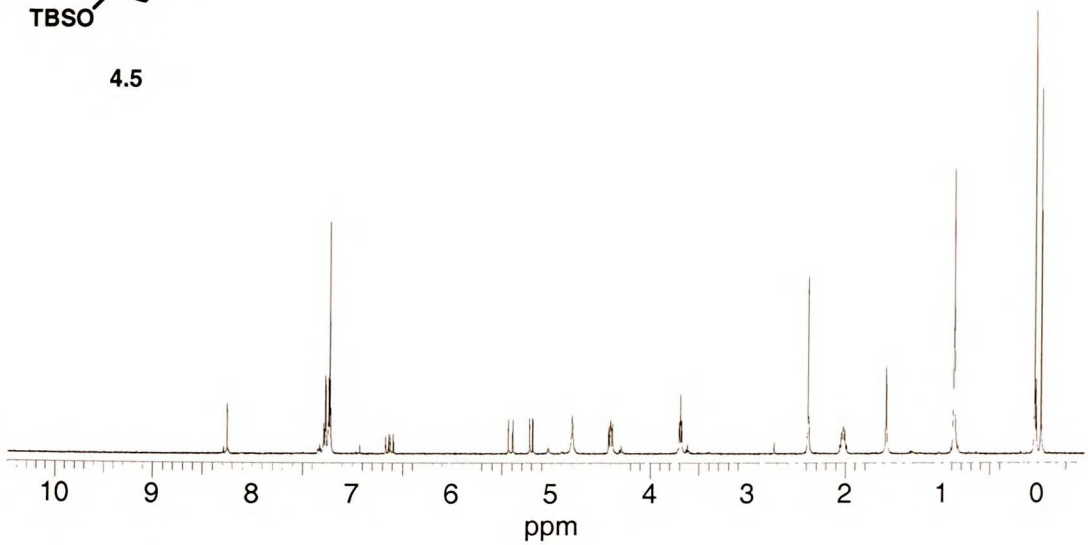

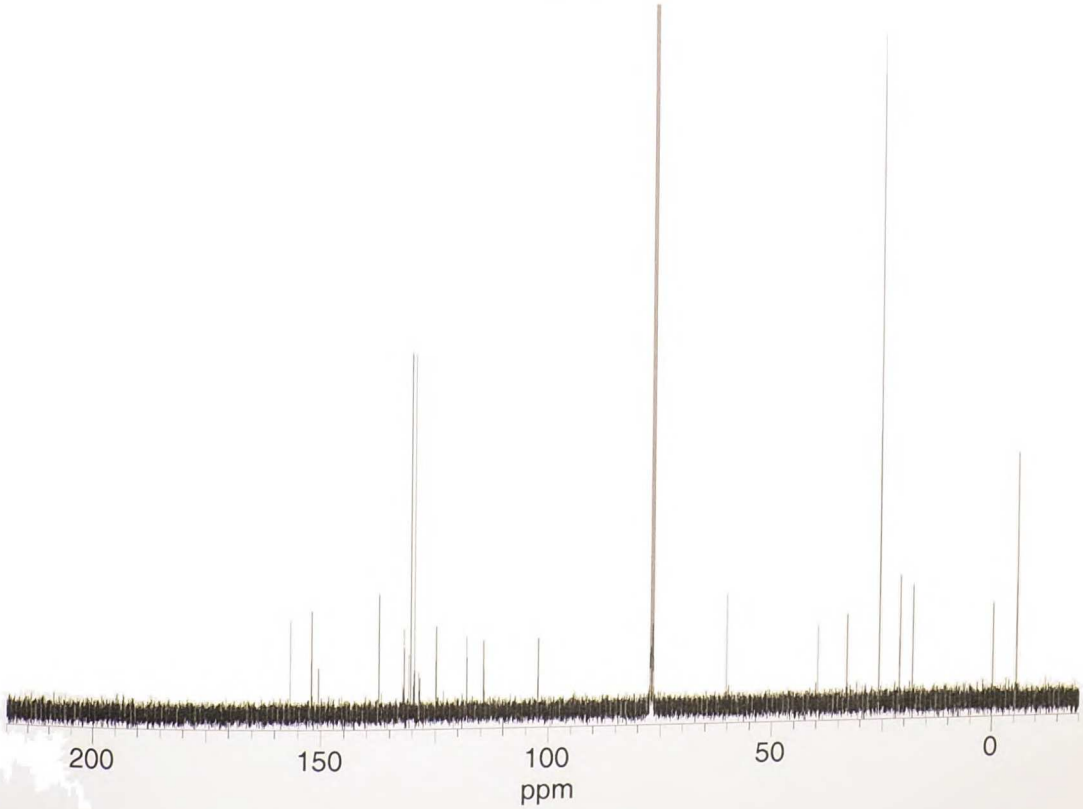

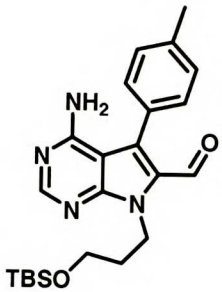

4.6

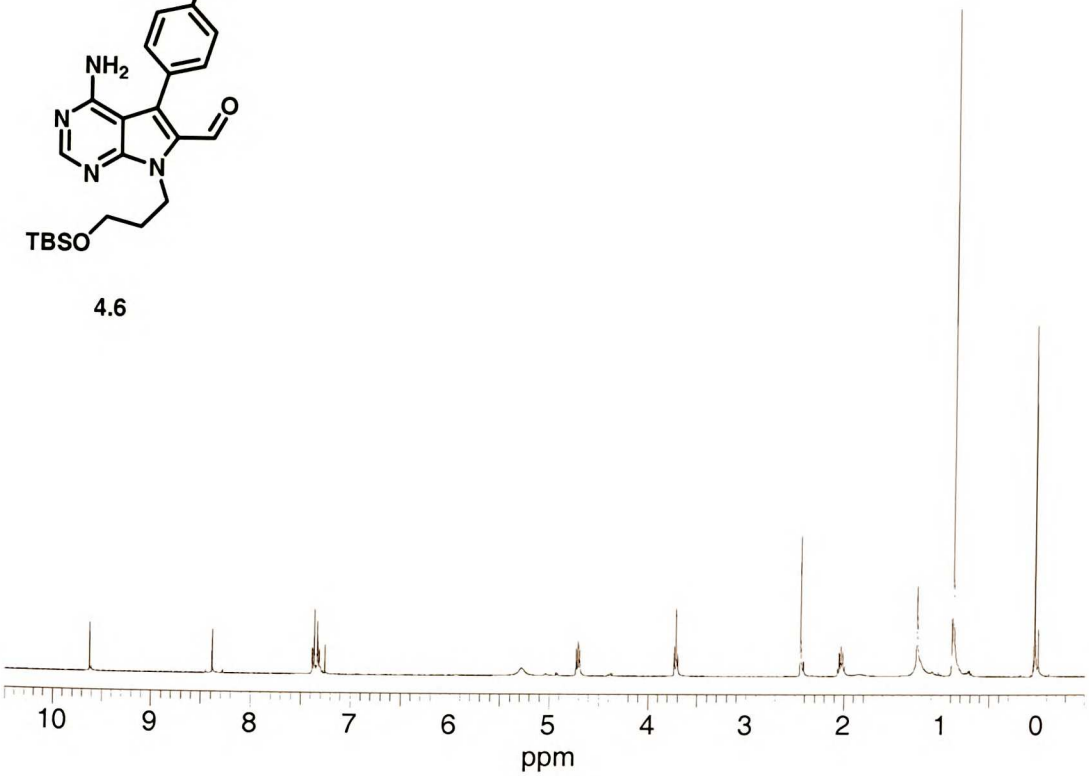

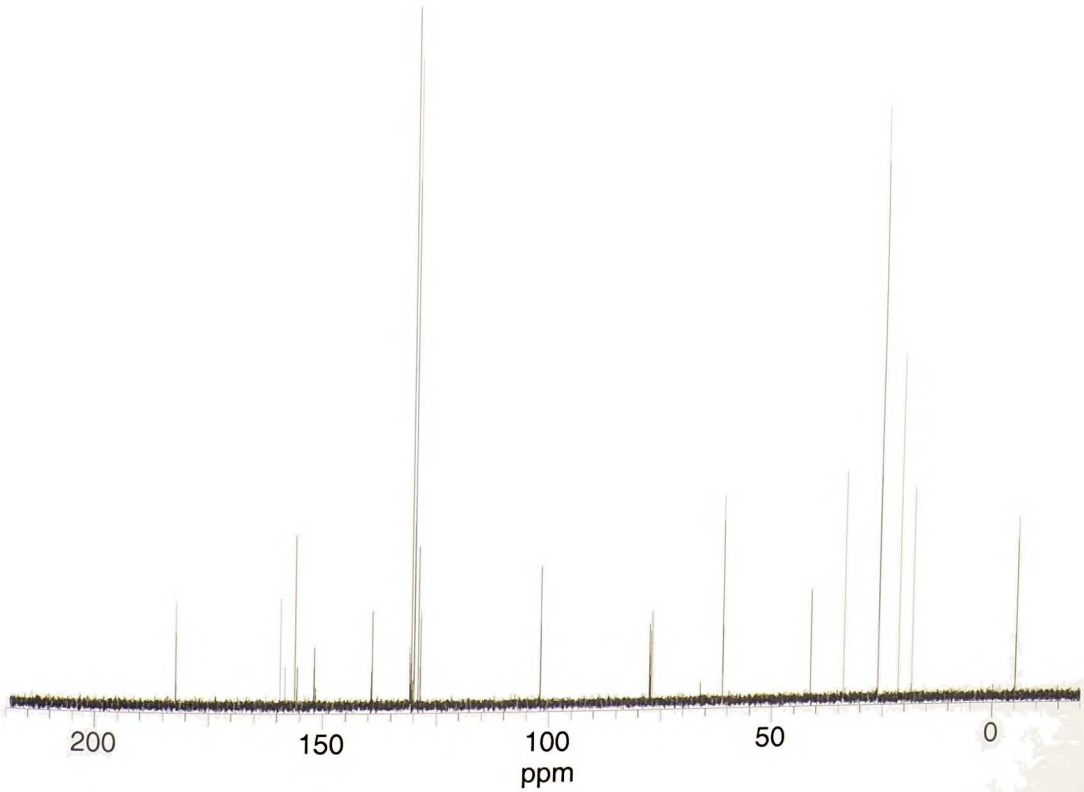

(Boc)2N
N
N
TBSO
10

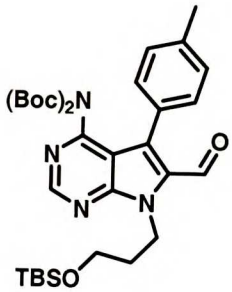

4.7

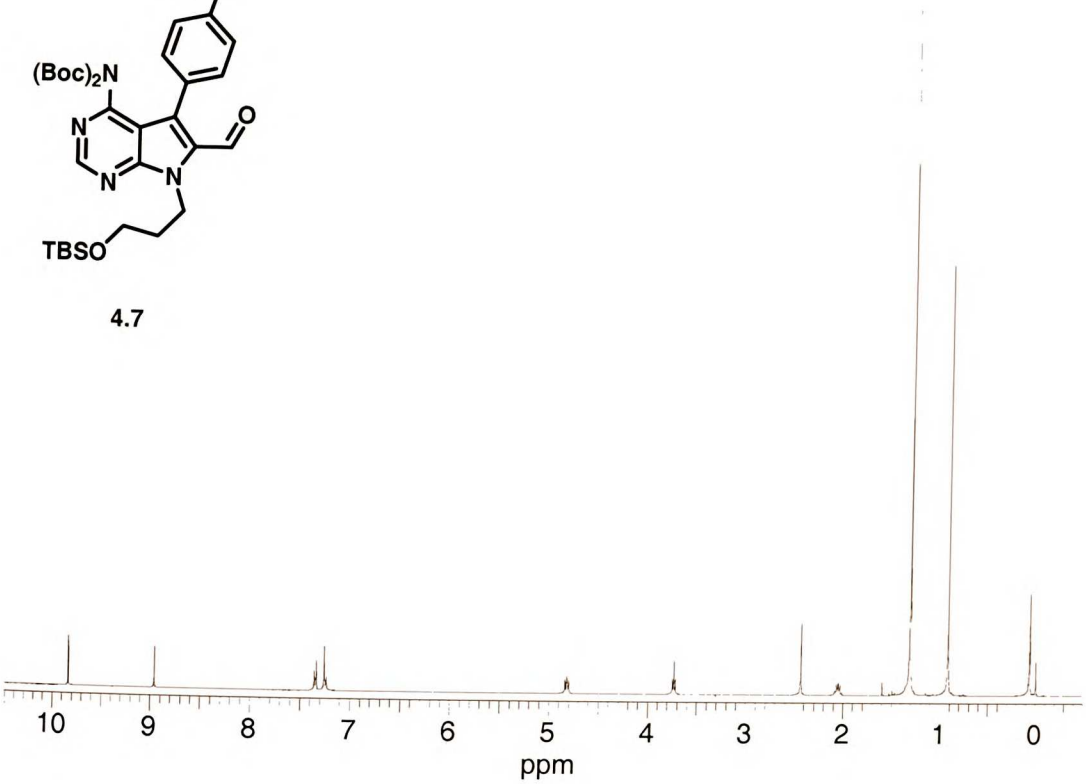

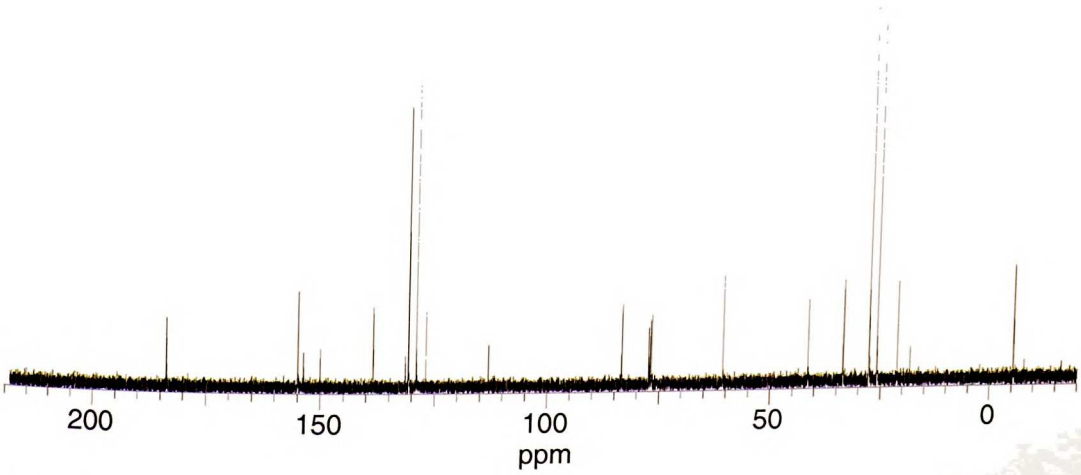

10

(Boc)2N
N
N
N
O
HO

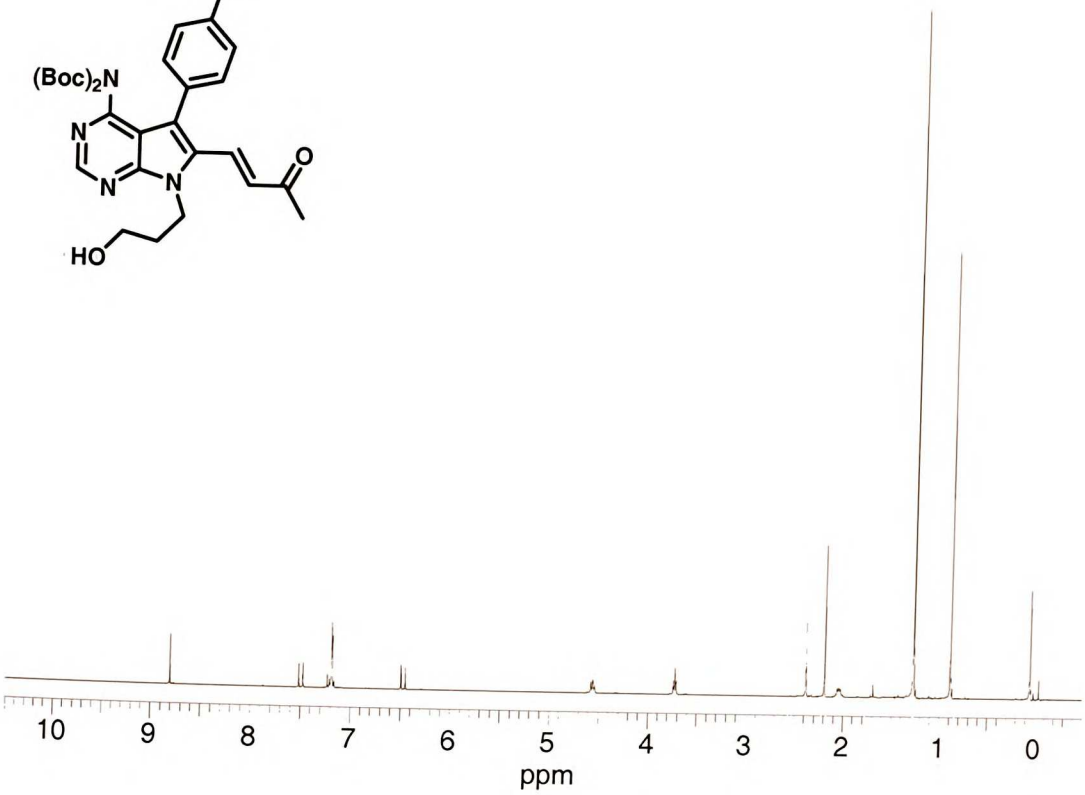
10
9
8
7
6
5
4
3
2
1
0
ppm

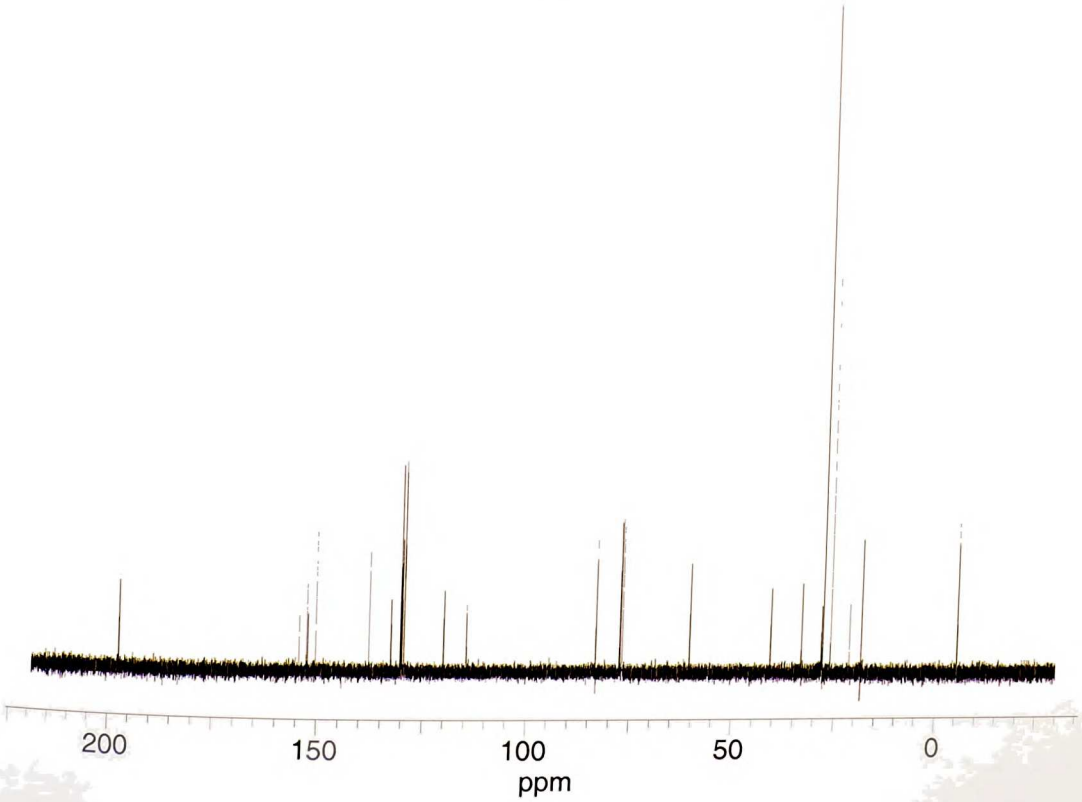
200
150
100
50
0
ppm

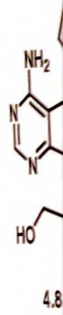

4.8

10

4.8

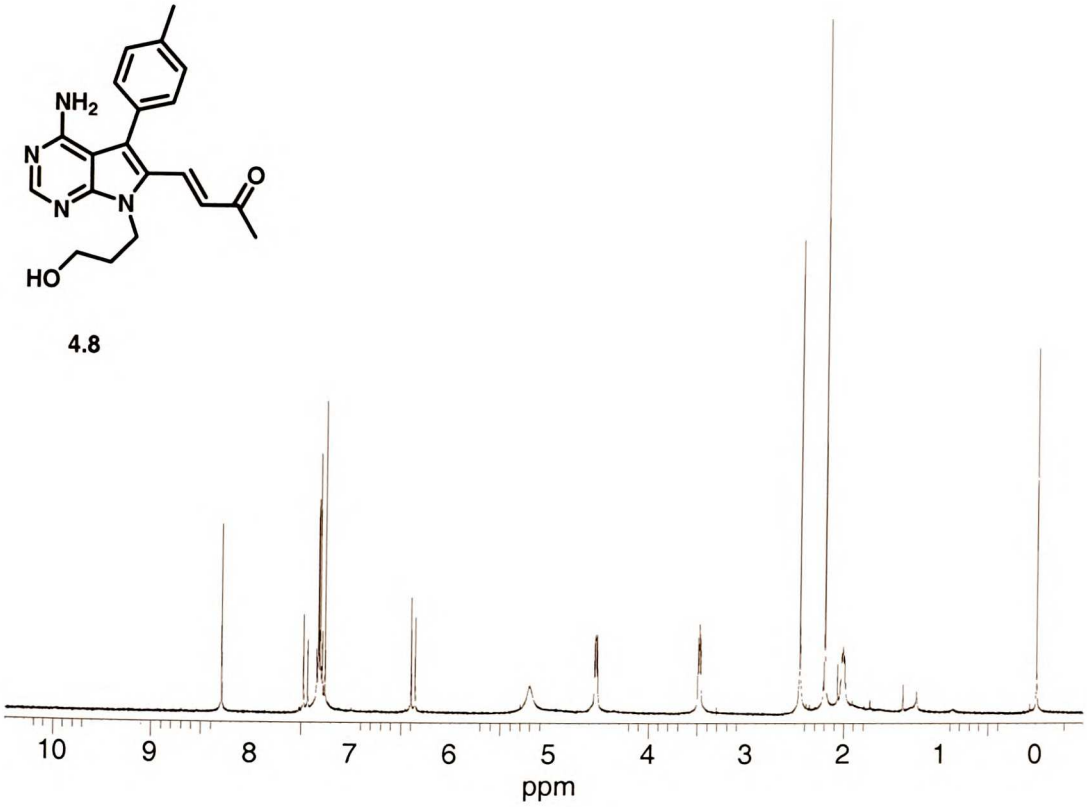

10

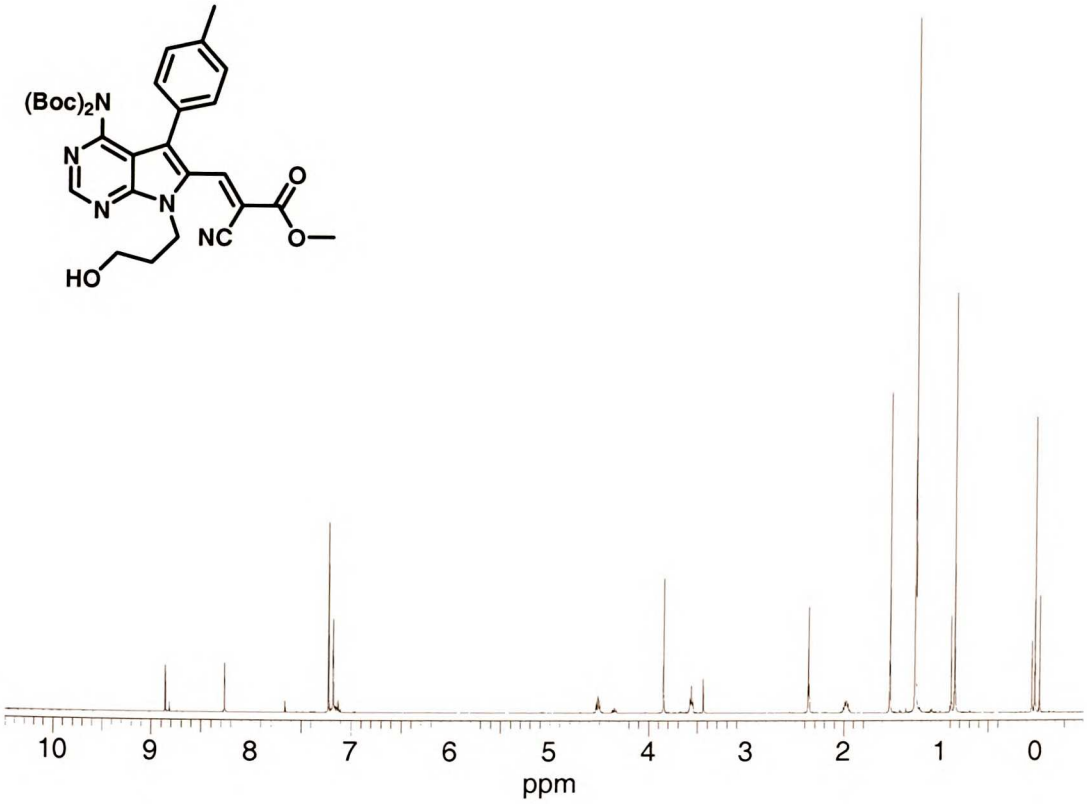
(Boc)2N
N
N
N
HO
NC
O
O—
10
9
8
7
6
5
4
3
2
1
0
ppm

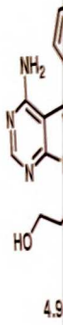

4.9

10

UCSF LIBRARY

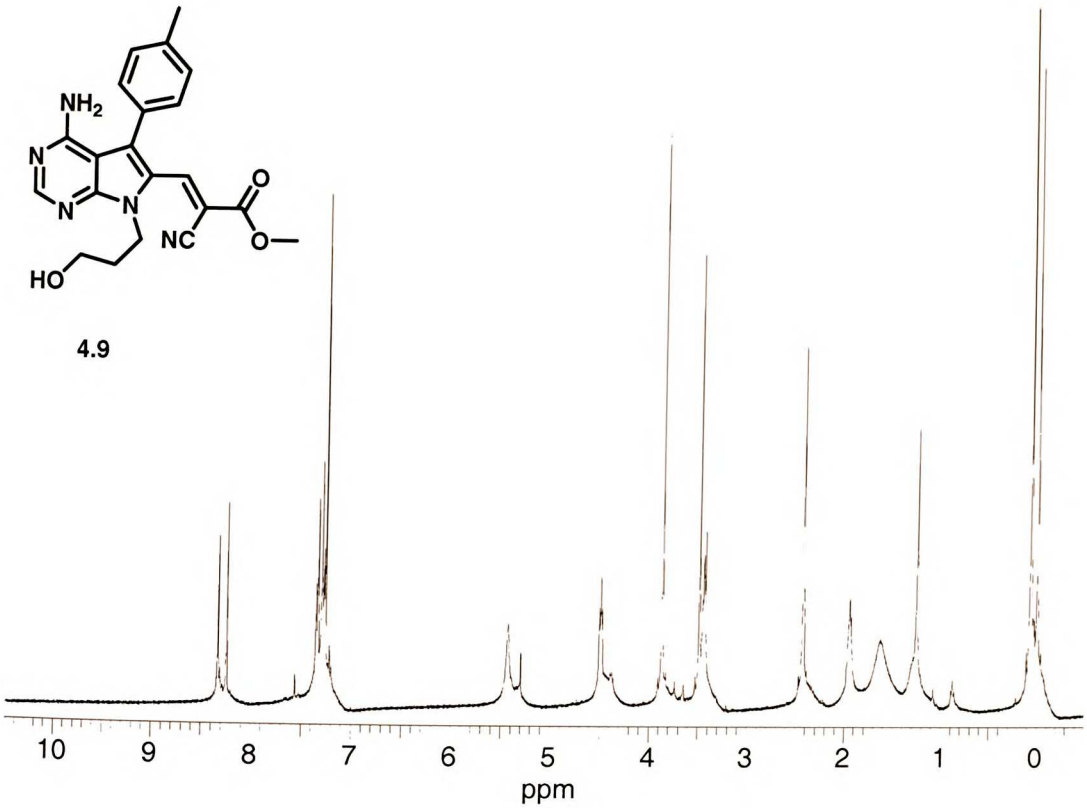
NH2
N
N
N
O
NC
O—
HO
4.9
10
9
8
7
6
5
4
3
2
1
0
ppm

USSF LIBRARY

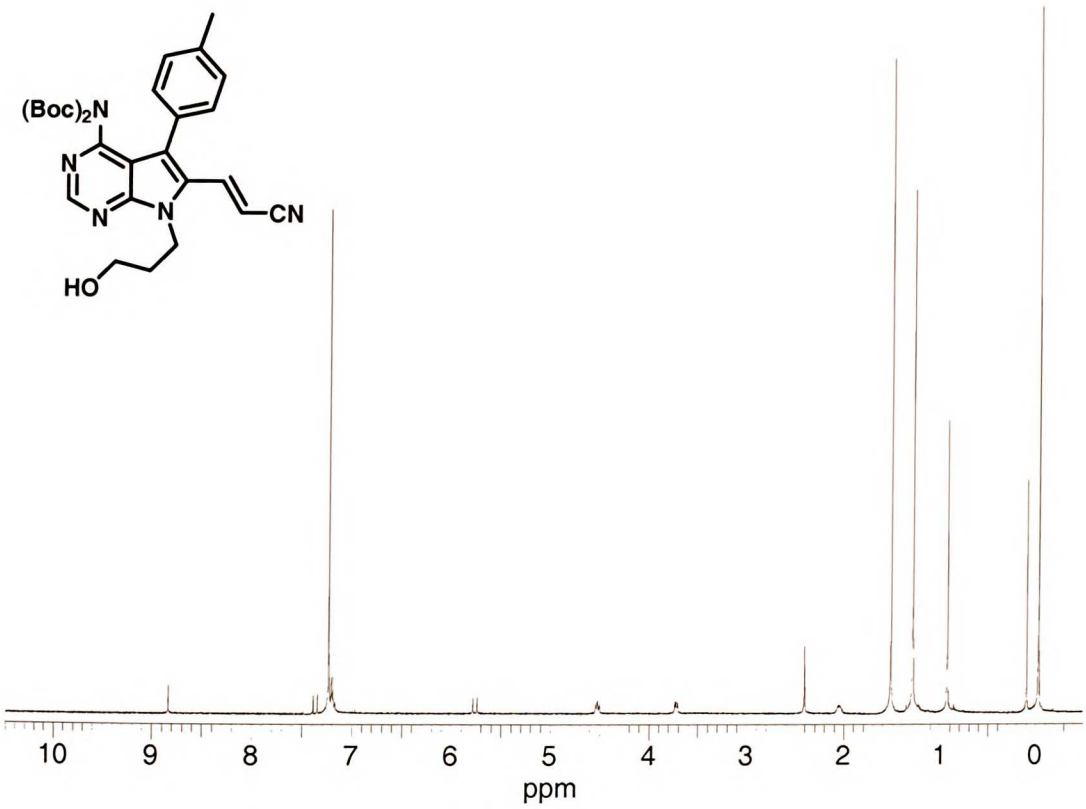
(Boc)2N
N
N
N
CN
HO
10
9
8
7
6
5
4
3
2
1
0
ppm

USF LIBRARY

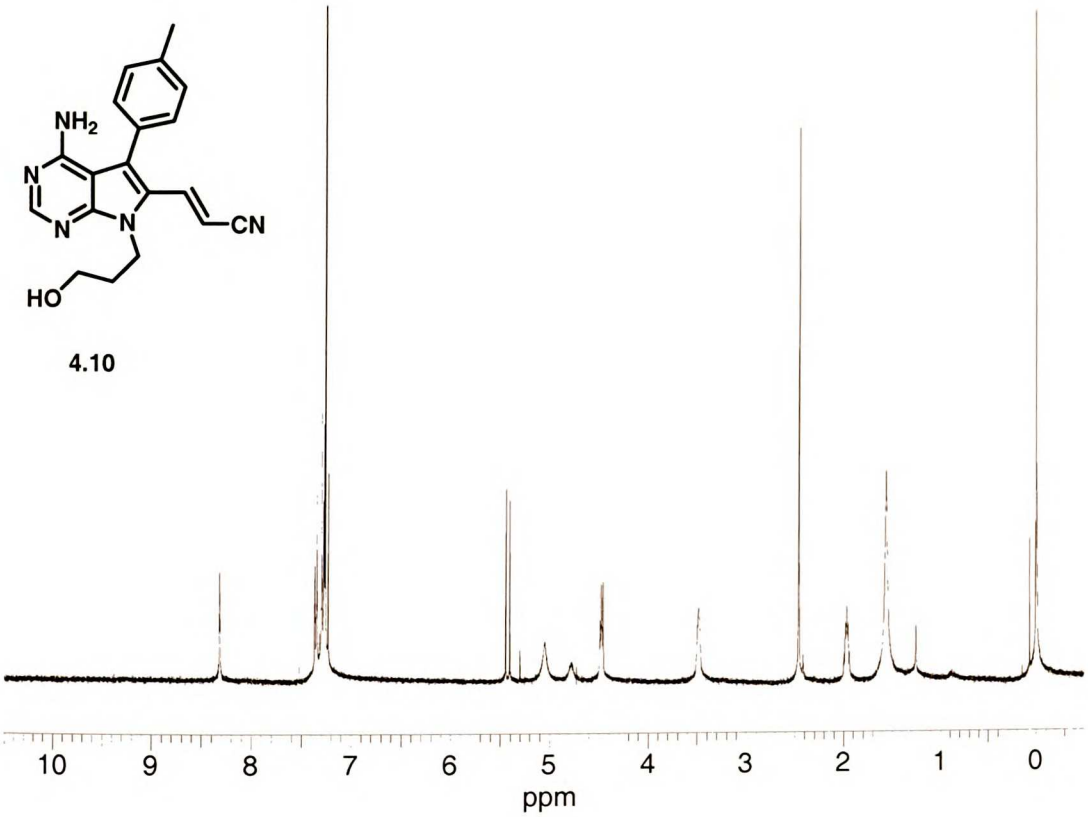
NH2
N
N
N
CN
HO
4.10
10
9
8
7
6
5
4
3
2
1
0
ppm

UCSF LIBRARY

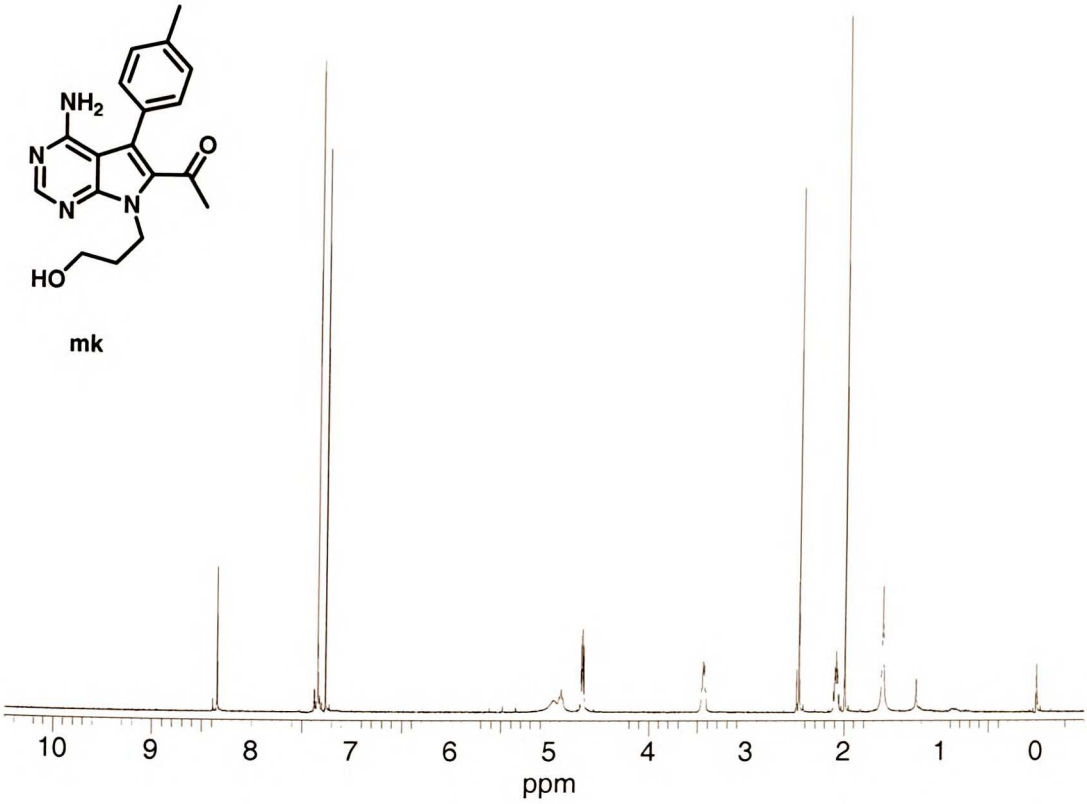
NH2
N
N
N
O
HO
mk
10
9
8
7
6
5
4
3
2
1
0
ppm

UNSE LIBRARY

5.1

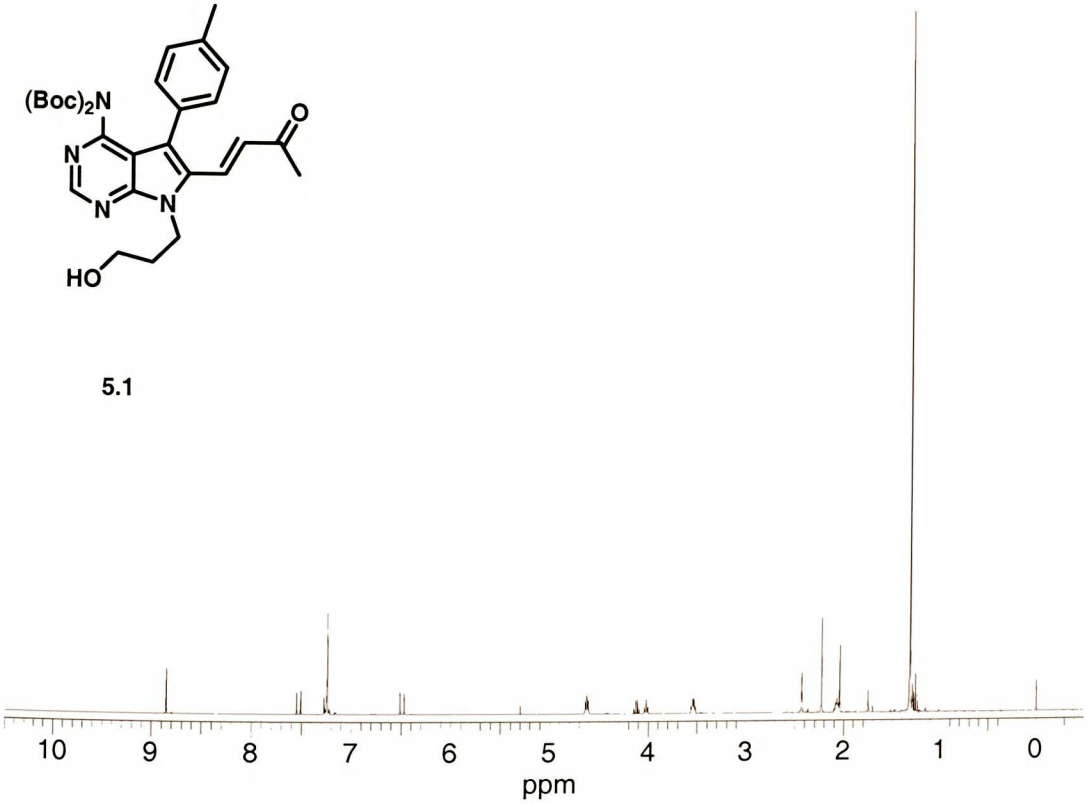

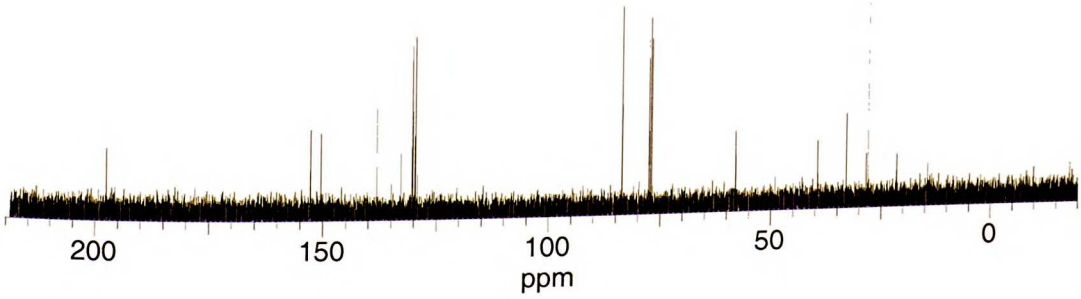

UCSF LIBRARY

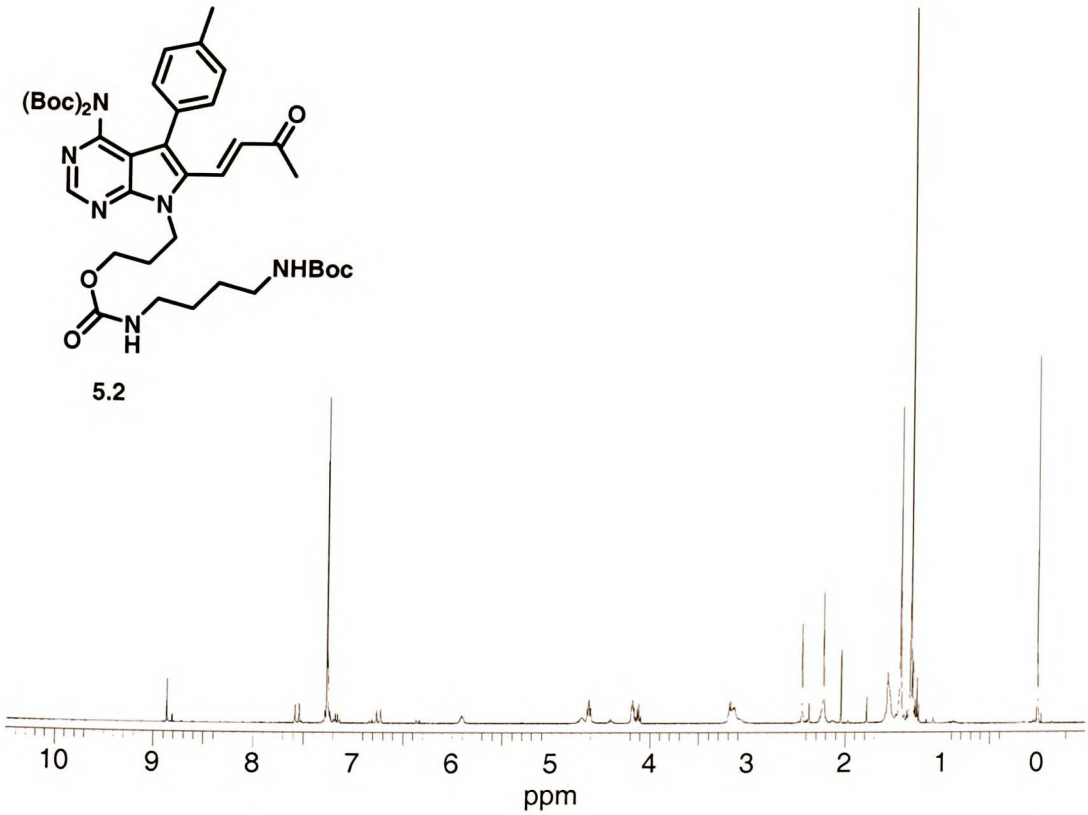
(Boc)2N
N
N
N
O
O
NHBoc
O
O
N
H
5.2
10
9
8
7
6
5
4
3
2
1
0
ppm

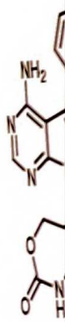

5.3 (e

1

UCSF LIBRARY

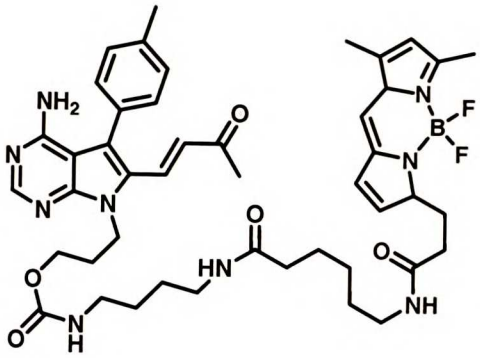

5.3 (enone-BODIPY)

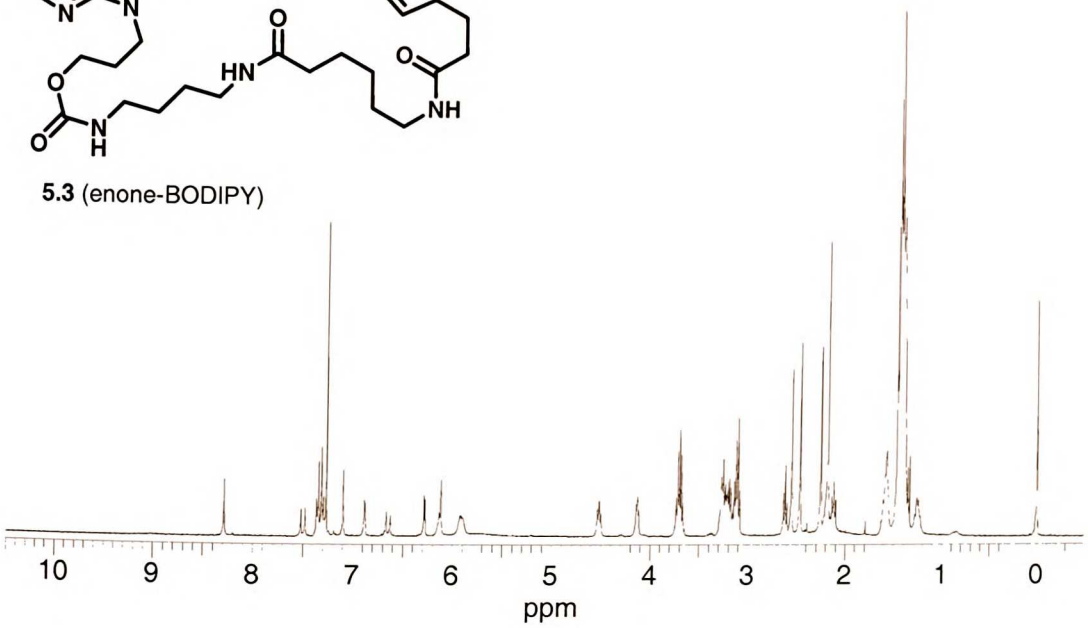

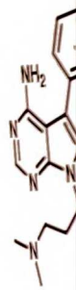

5.4

10

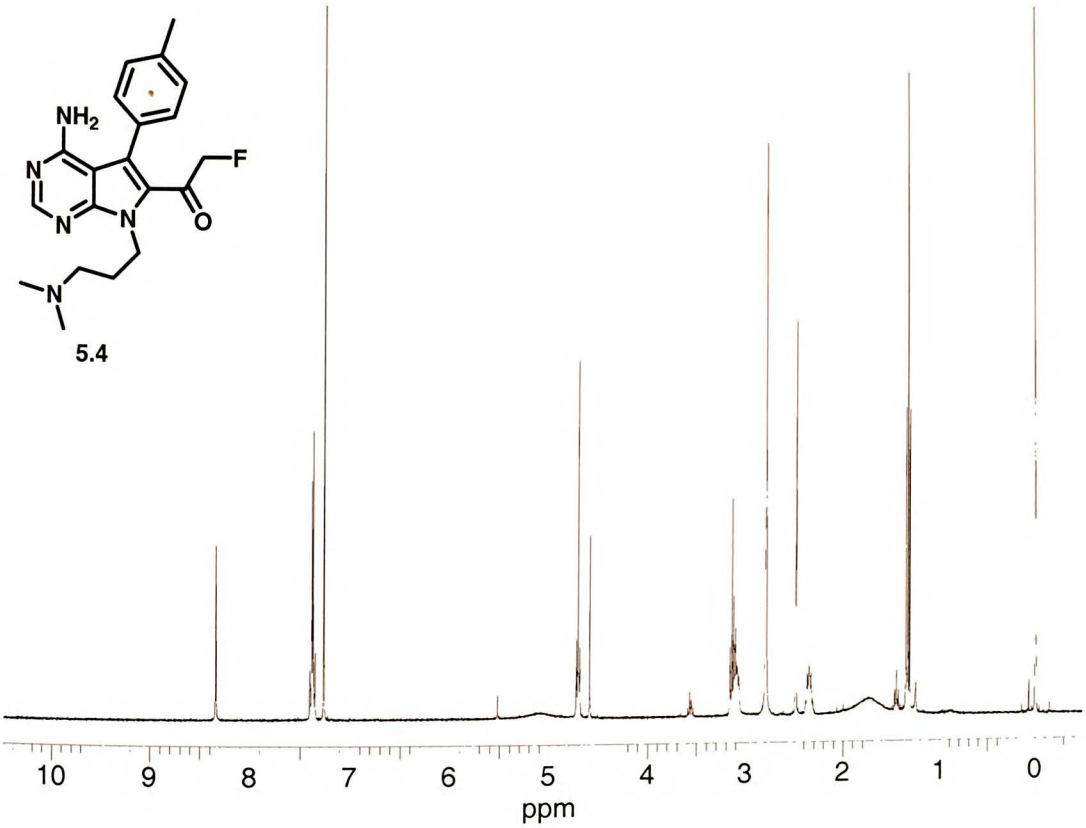
NH2
N
N
N
F
O
N
5.4
10
9
8
7
6
5
4
3
2
1
0
ppm

(Boc)2N
N
N
N

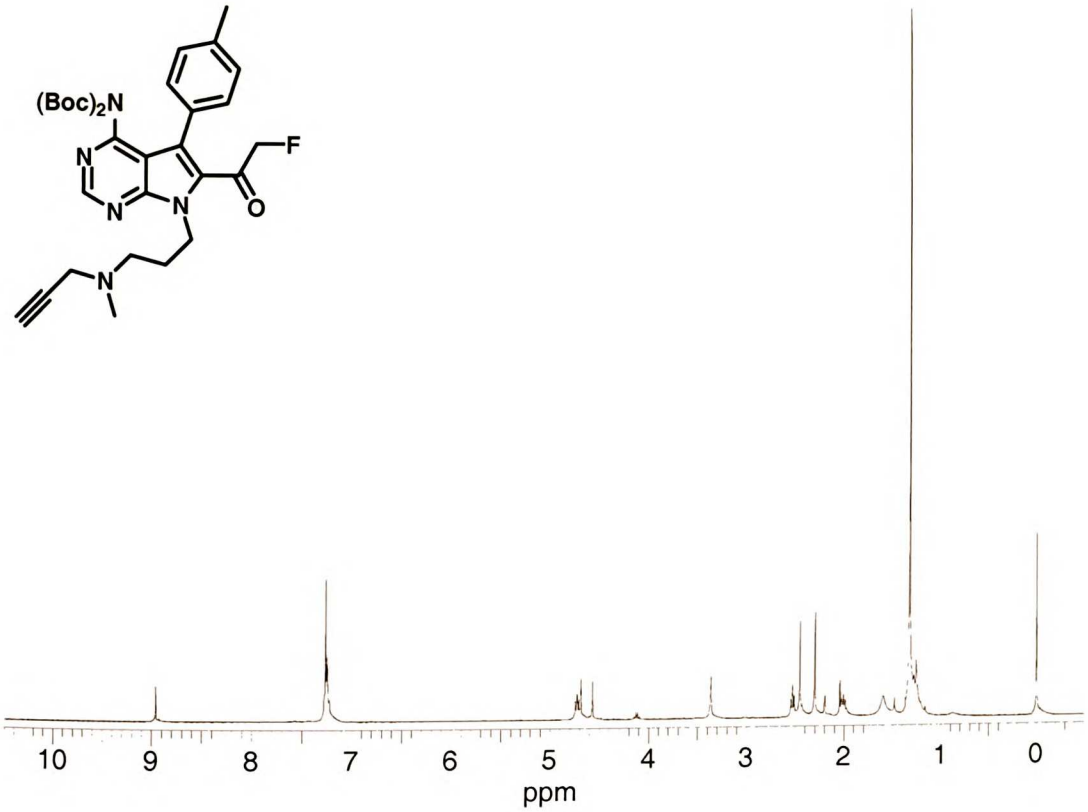
(Boc)2N
N
N
N
F
O
N
10
9
8
7
6
5
4
3
2
1
0
ppm

UCSF LIBRARY

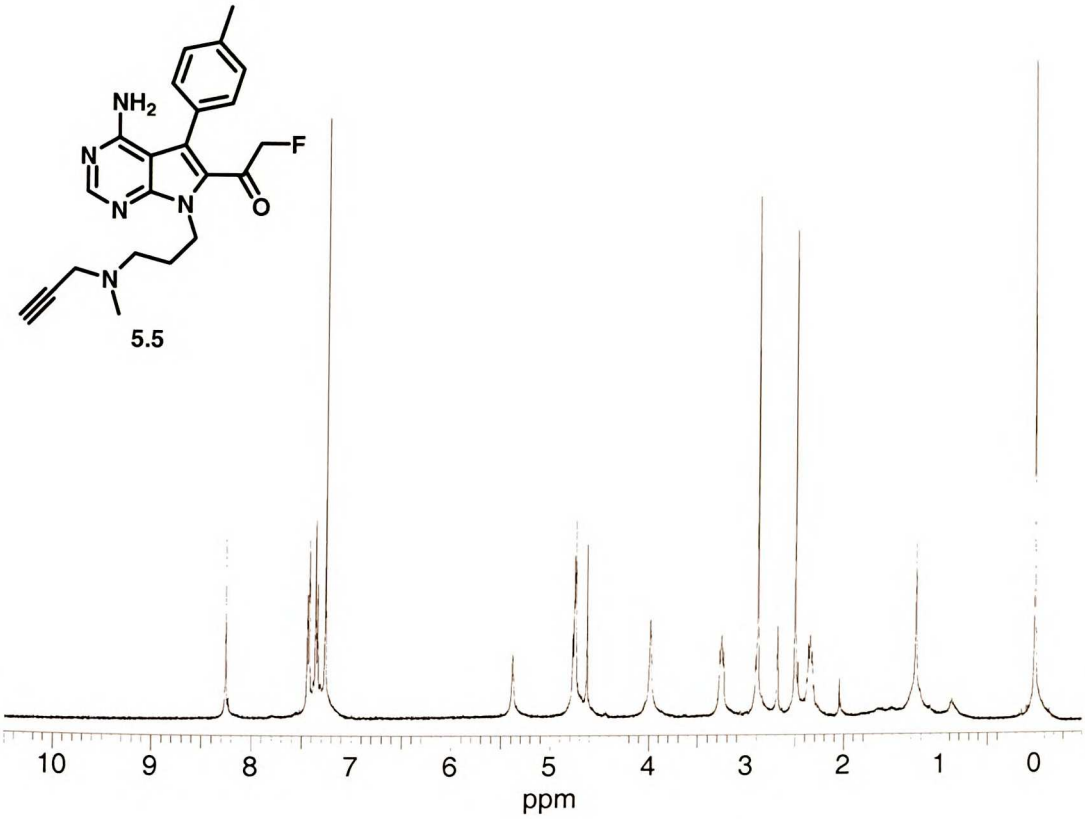
NH2
N
N
N
F
O
N
5.5
10
9
8
7
6
5
4
3
2
1
0
ppm

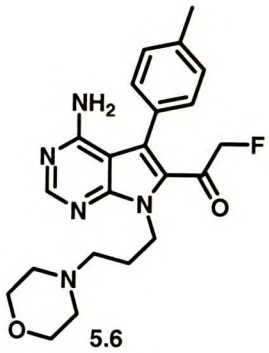

5.6

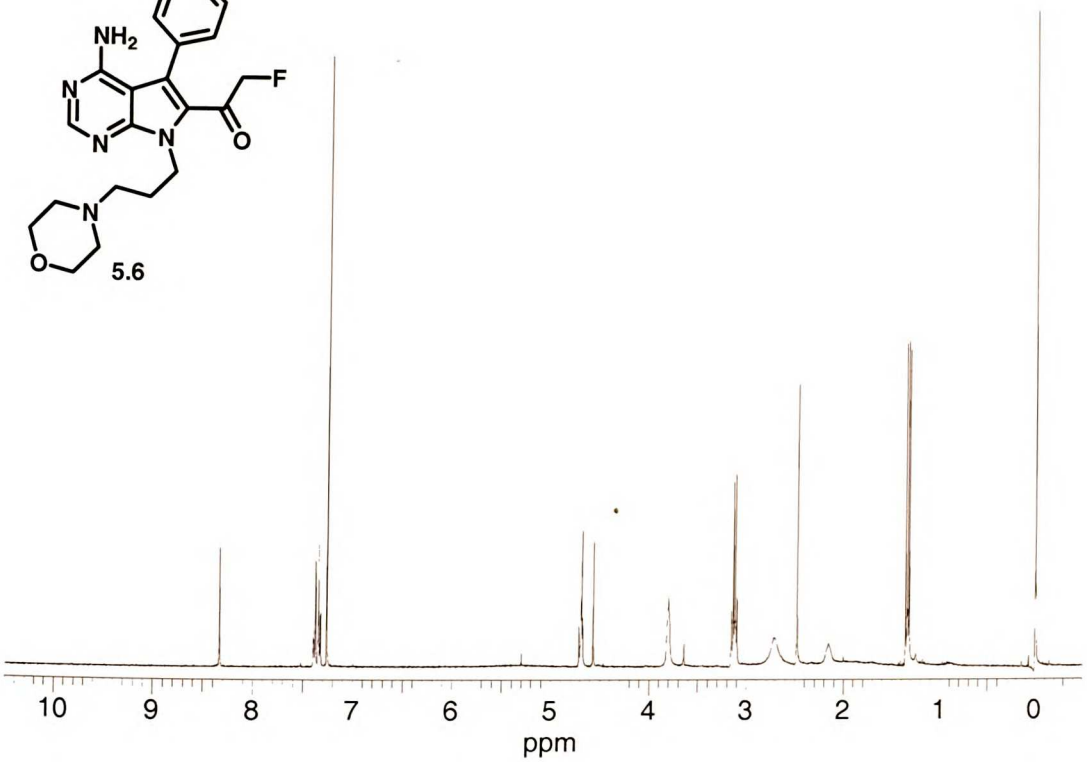

UNSF LIBRARY

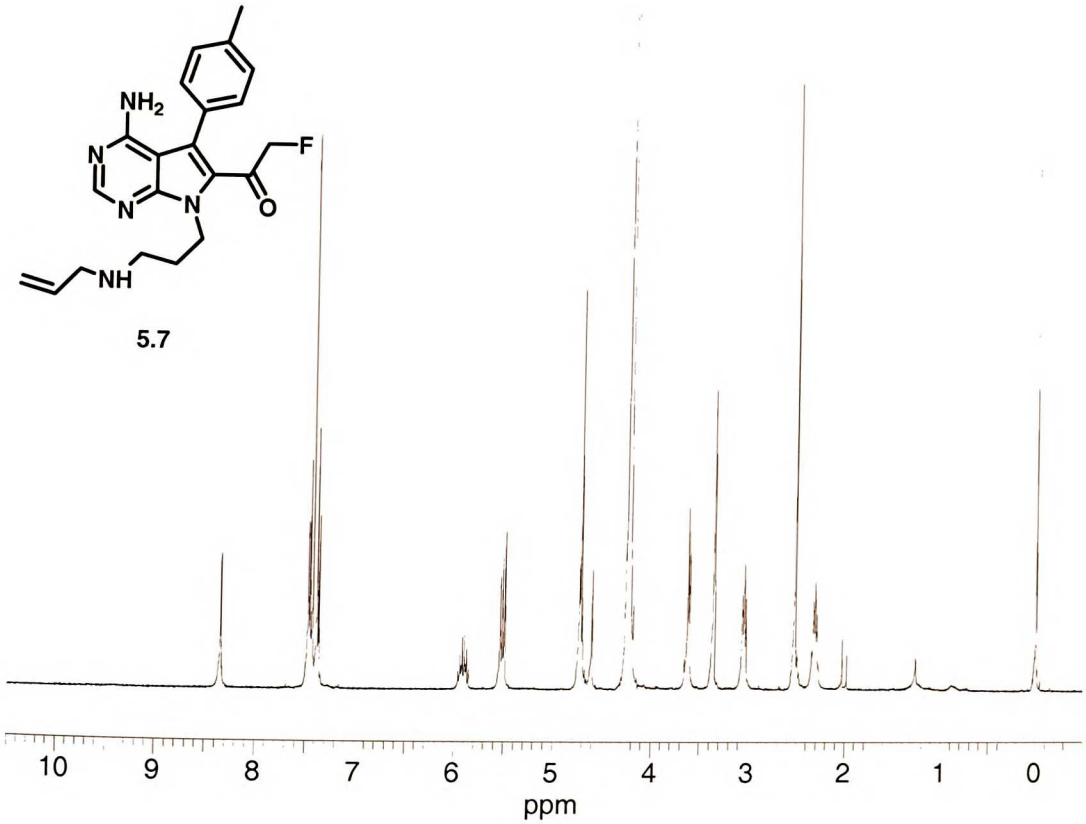
NH2
N
N
N
F
O
NH
5.7
10
9
8
7
6
5
4
3
2
1
0
ppm

UCSF LIBRARY

5.8

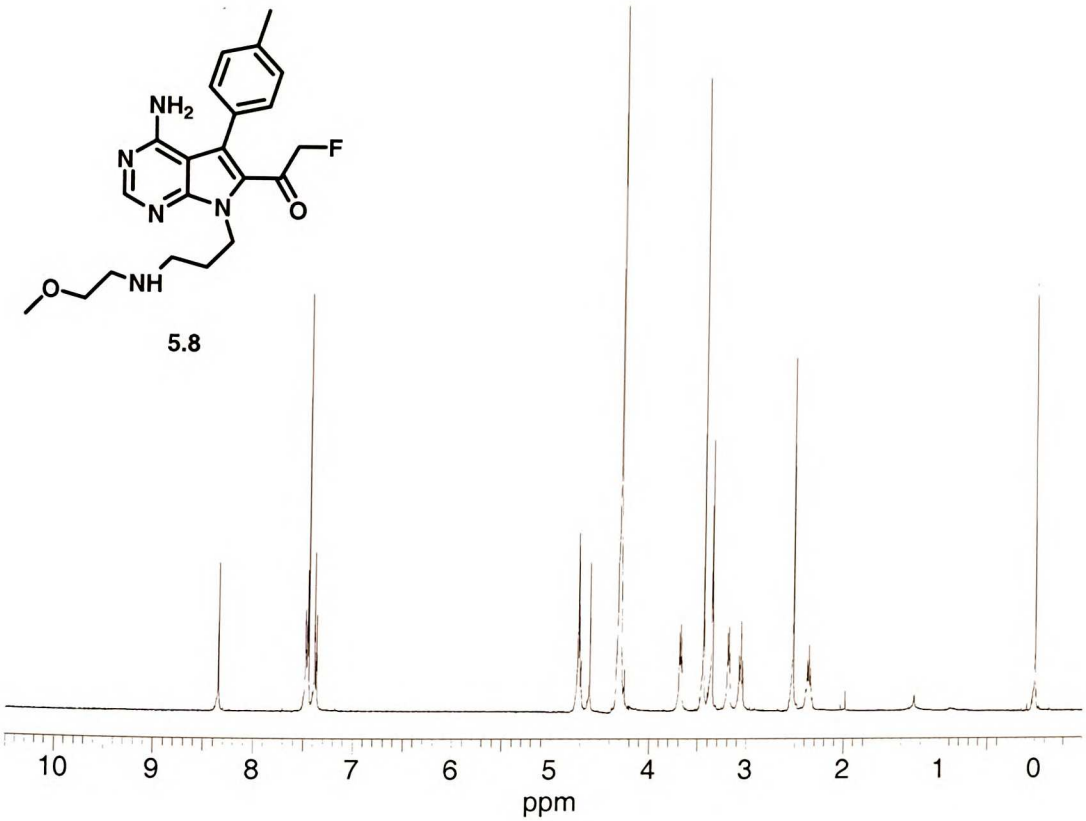

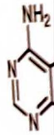

5

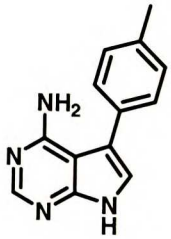

5.10

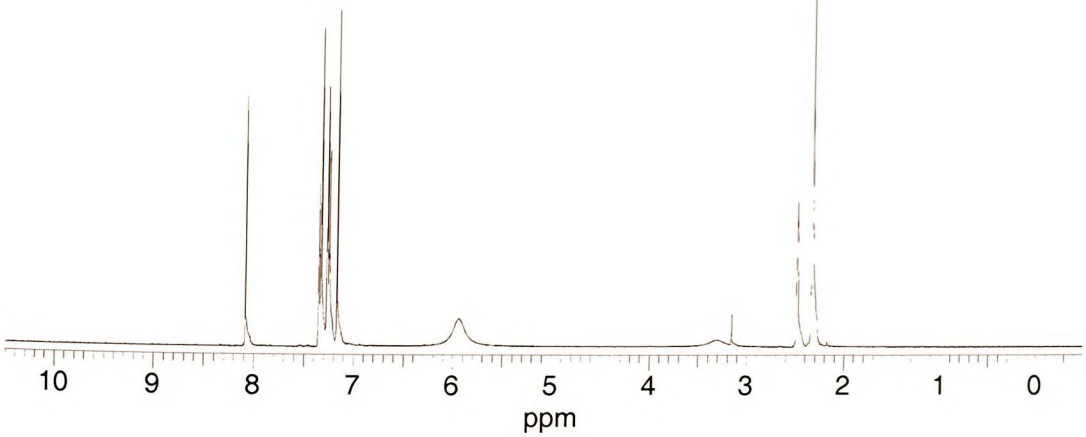

UCSF LIBRARY

5.11

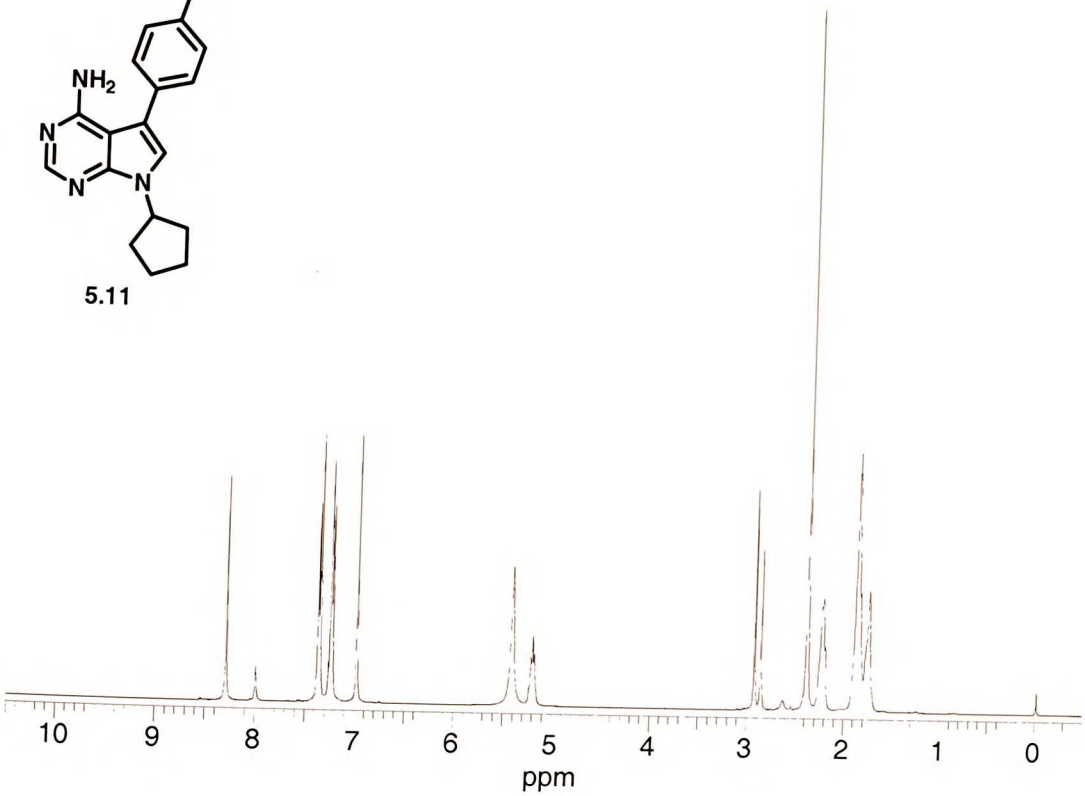

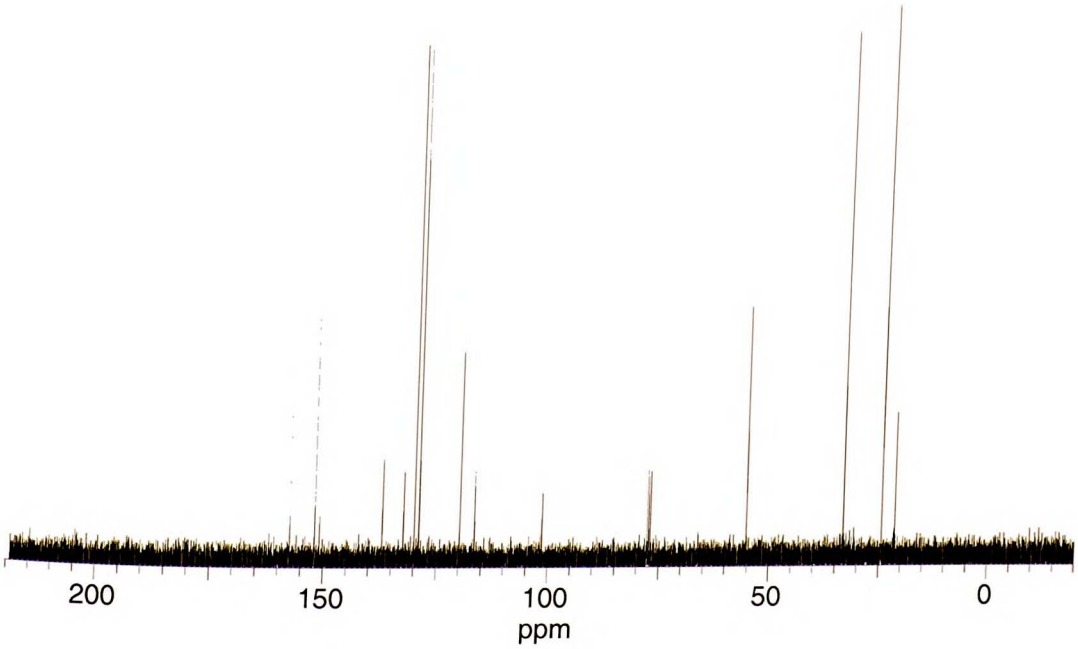

UCSF Library

5.11

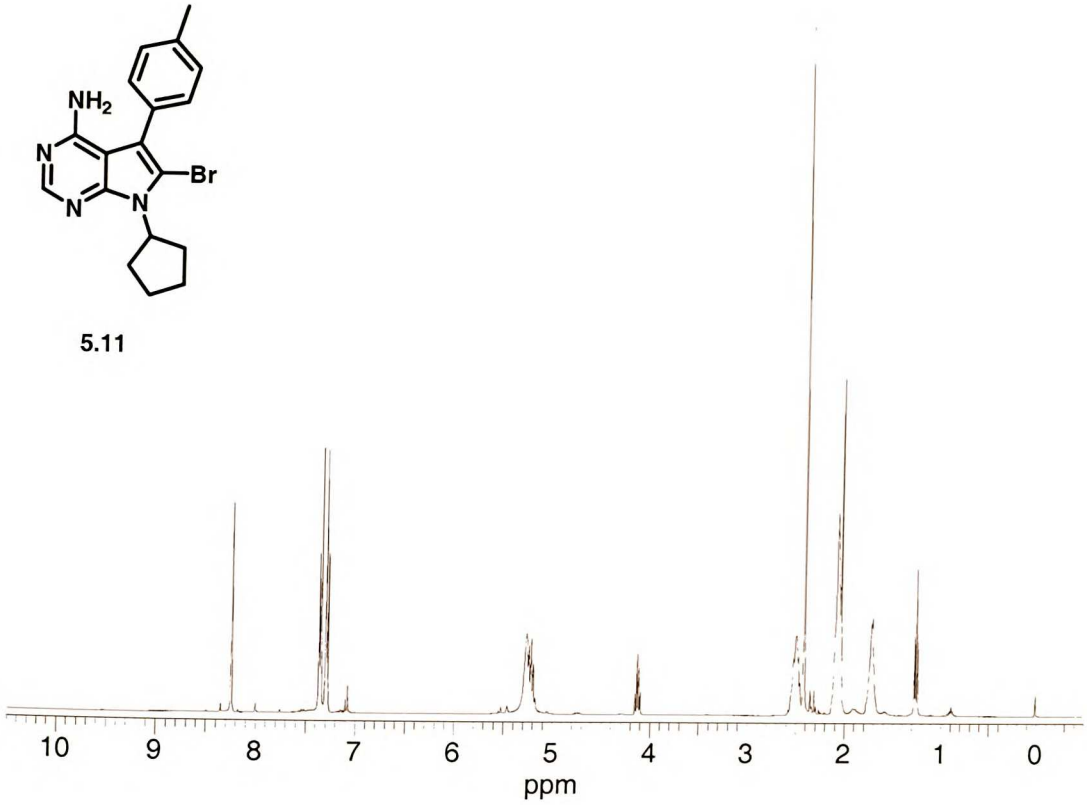

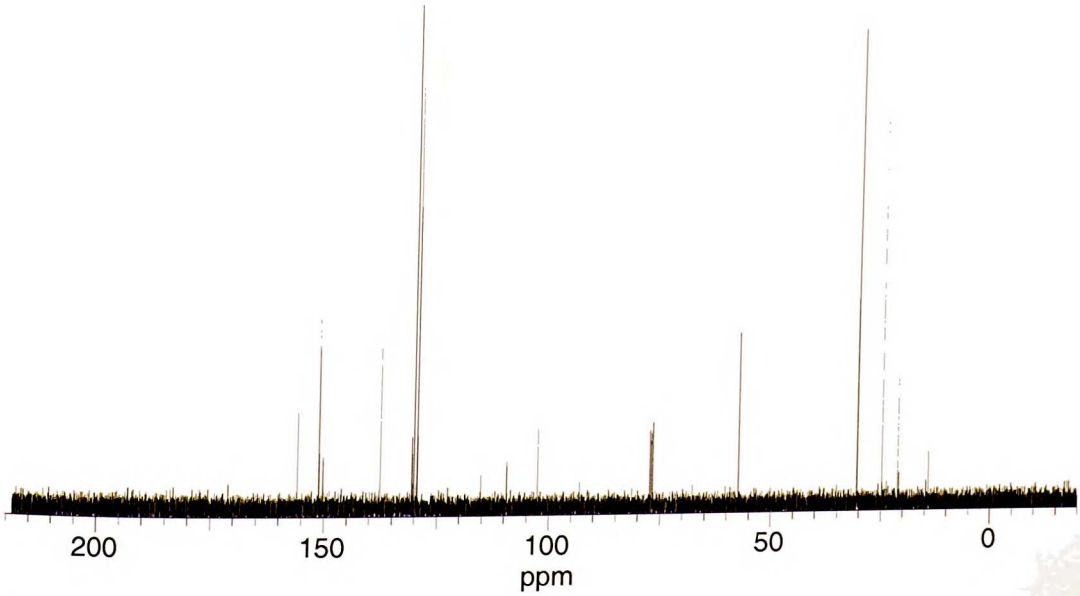

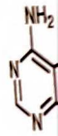

UCSF LIBRARY

5.12

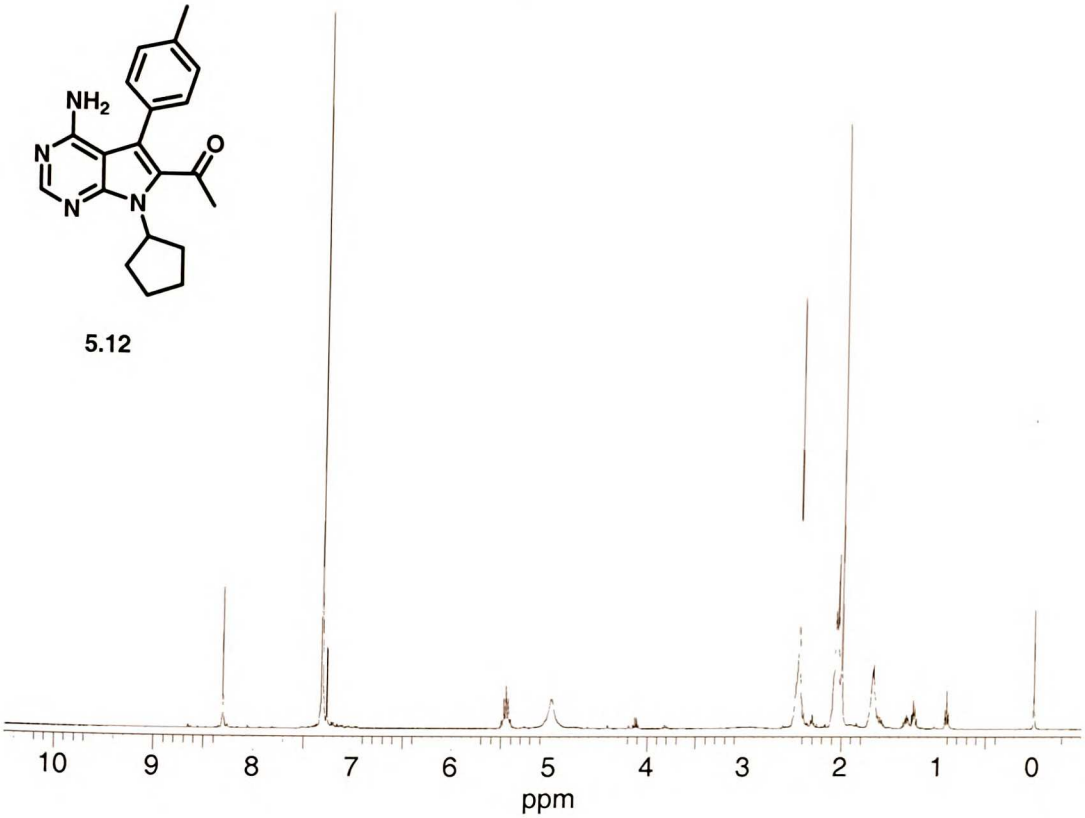

UCSF LIBRARY

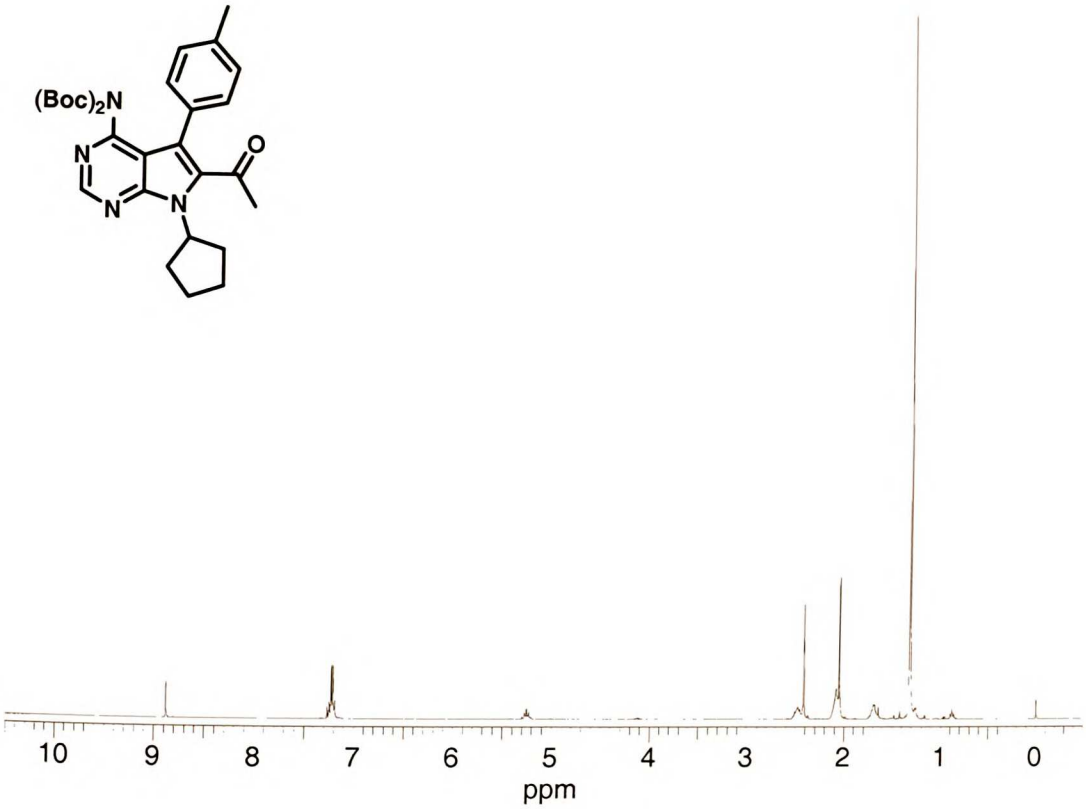
(Boc)2N
N
N
N
O
10
9
8
7
6
5
4
3
2
1
0
ppm

5.14

UCSF LIBRARY

5.14 (fmk-cp)

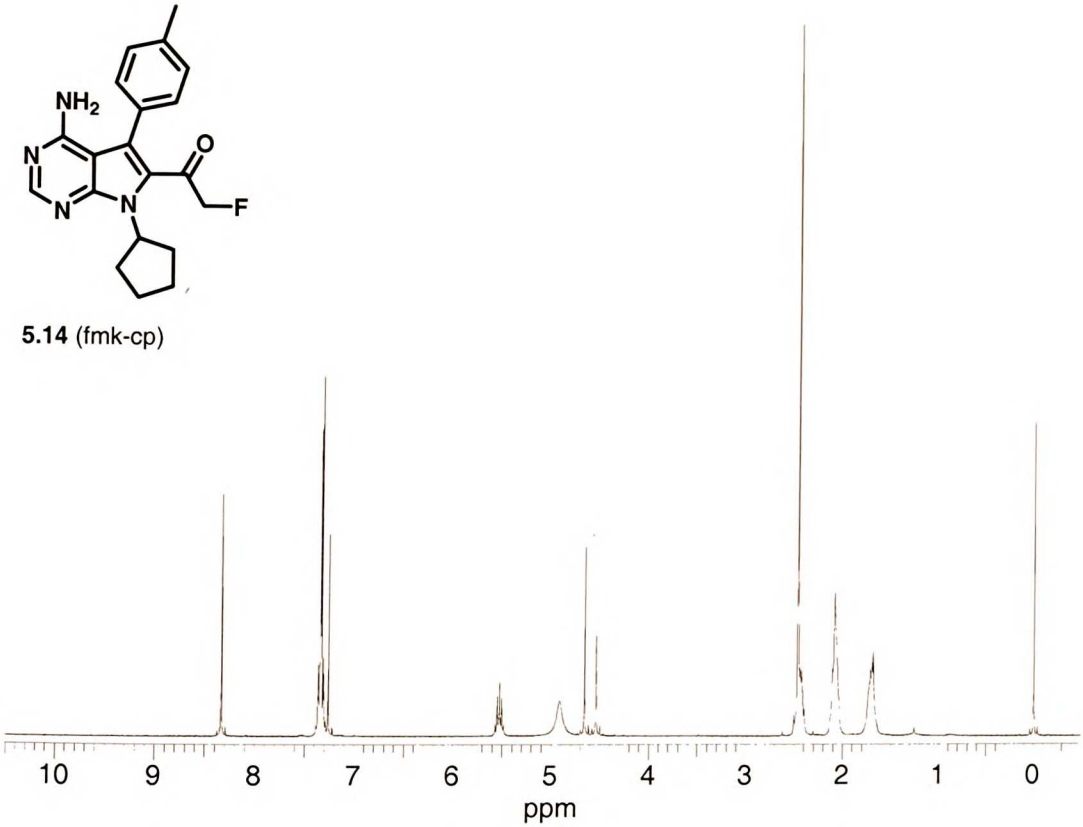

UCSF LIBRARY

5.15

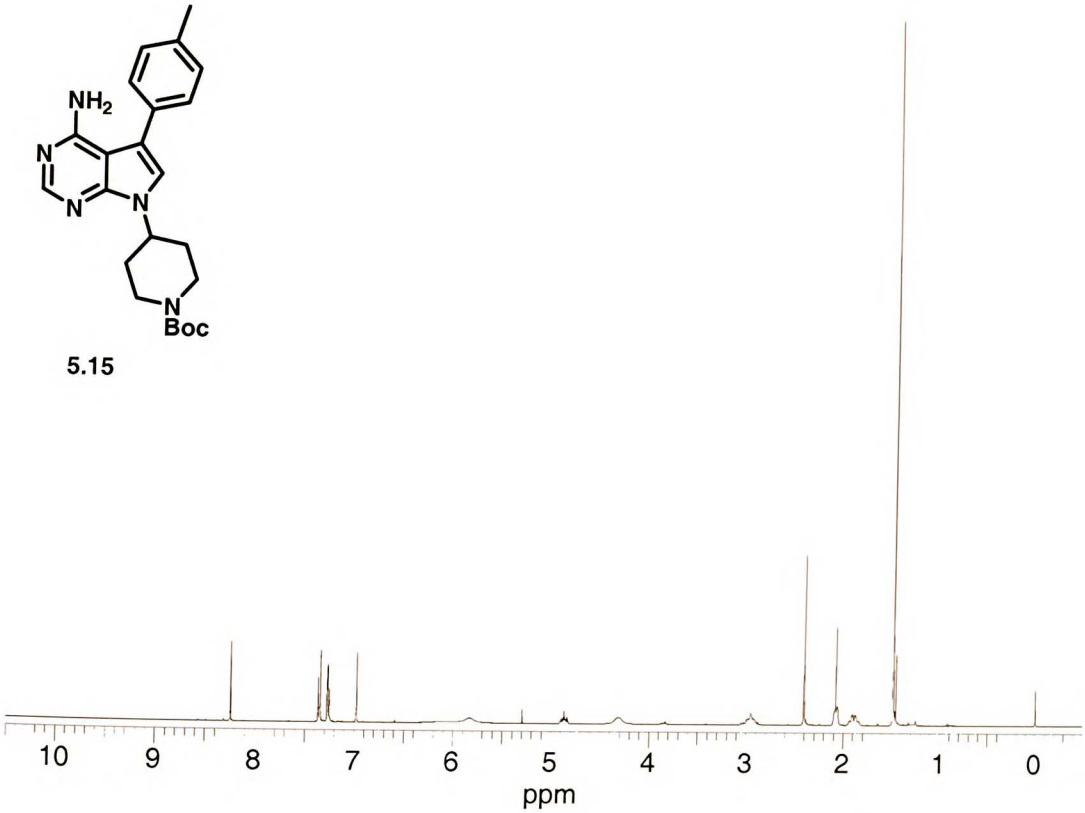

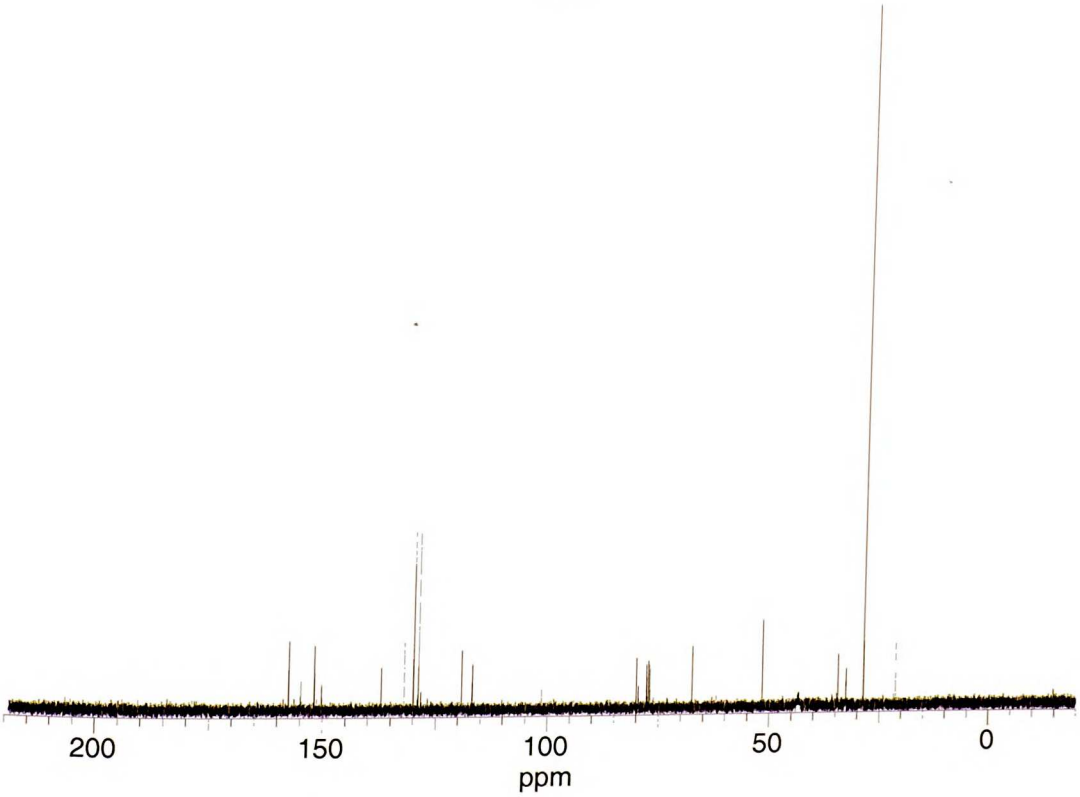

UCSF LIBRARY

5.16

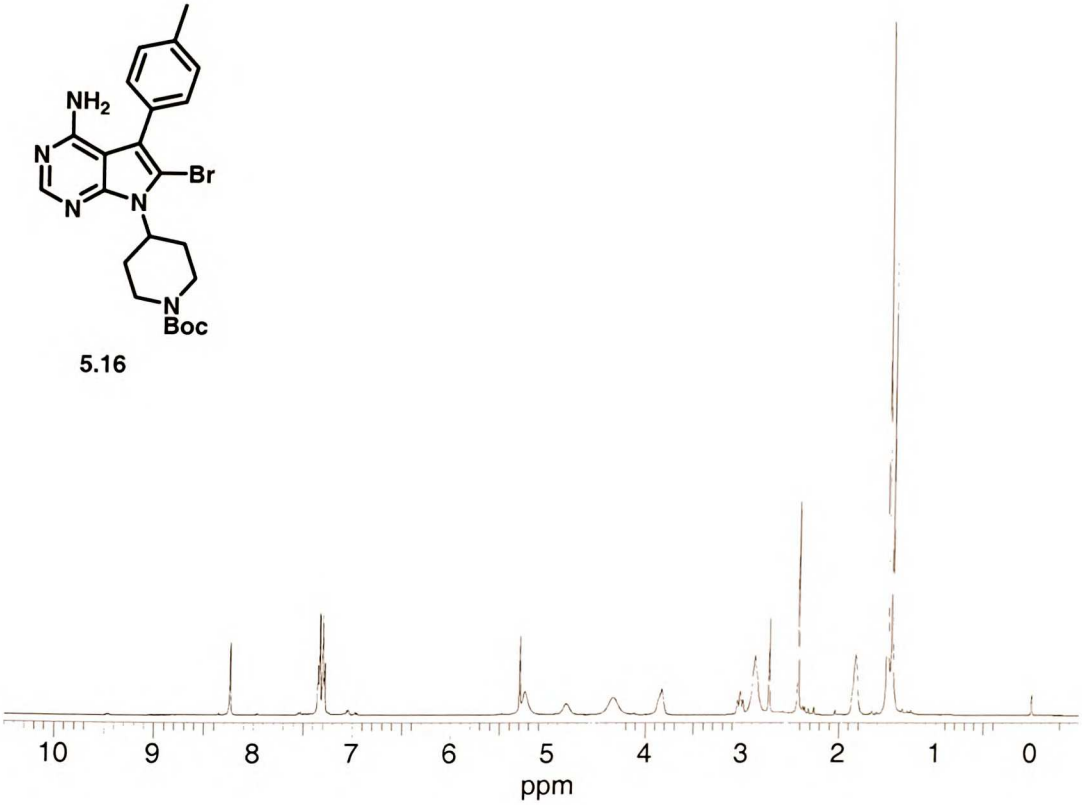

UCSF LIBRARY

5.17

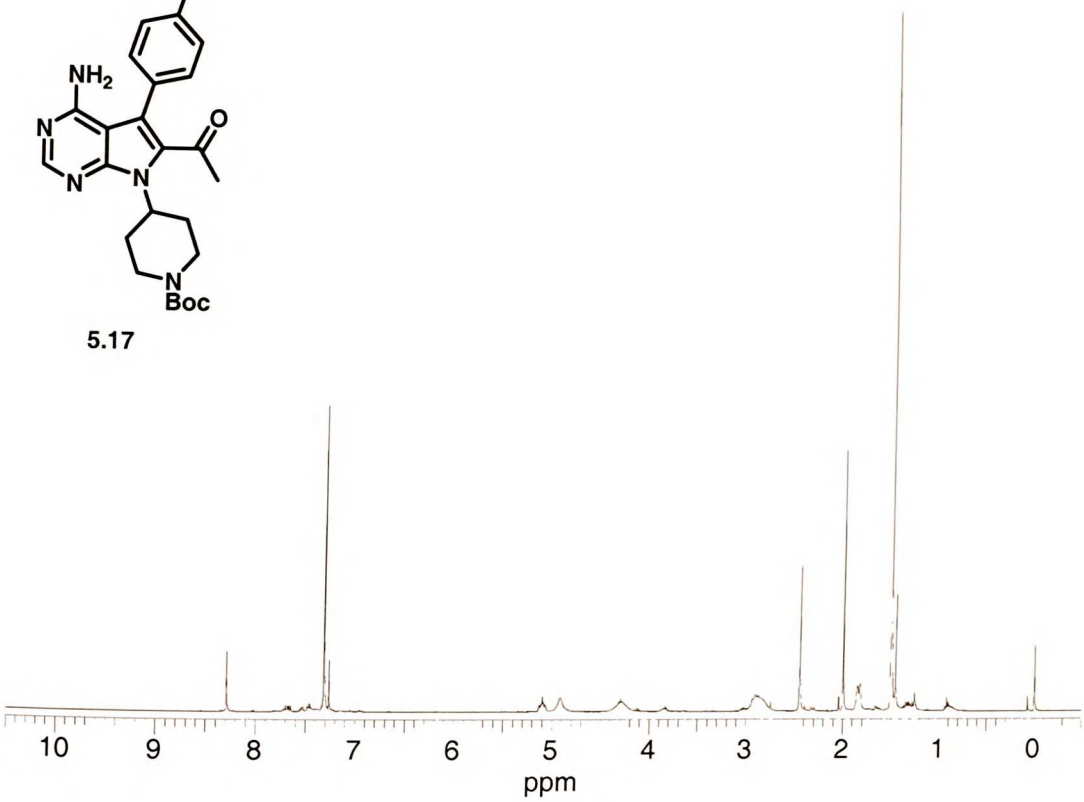

UCSF LIBRARY

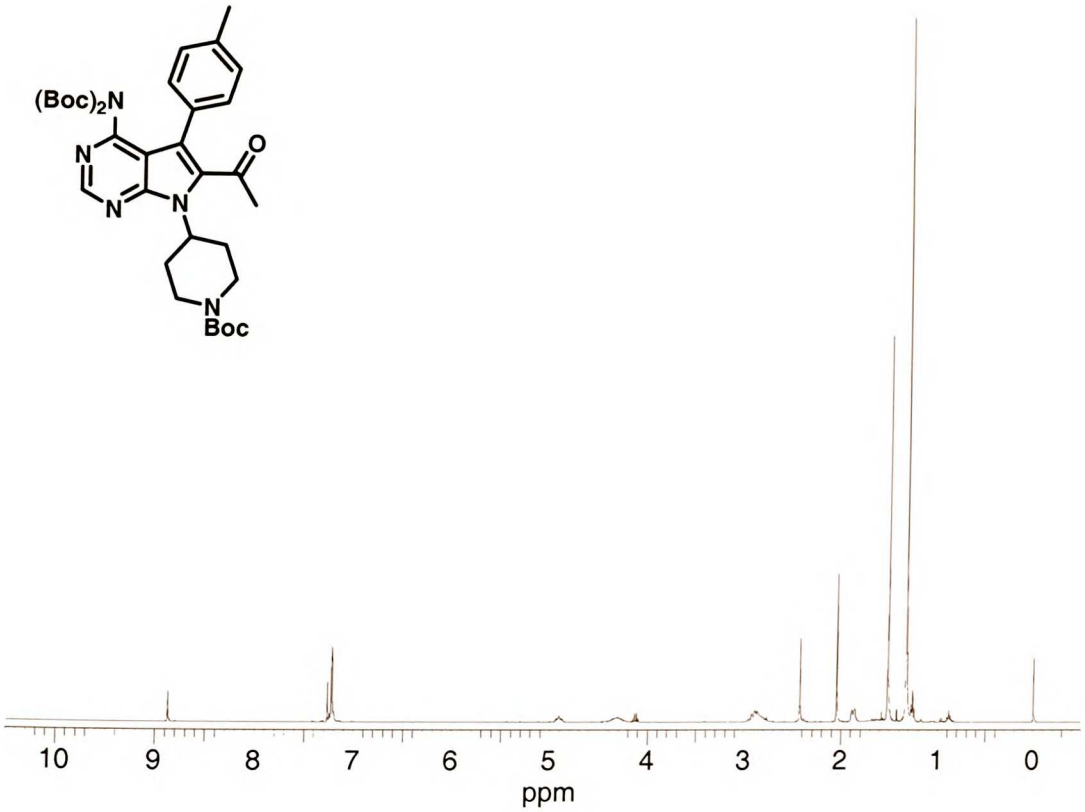
(Boc)2N
N
N
N
O
N
Boc
10
9
8
7
6
5
4
3
2
1
0
ppm

UCSF LIBRARY

5.18 (fmk-pip)

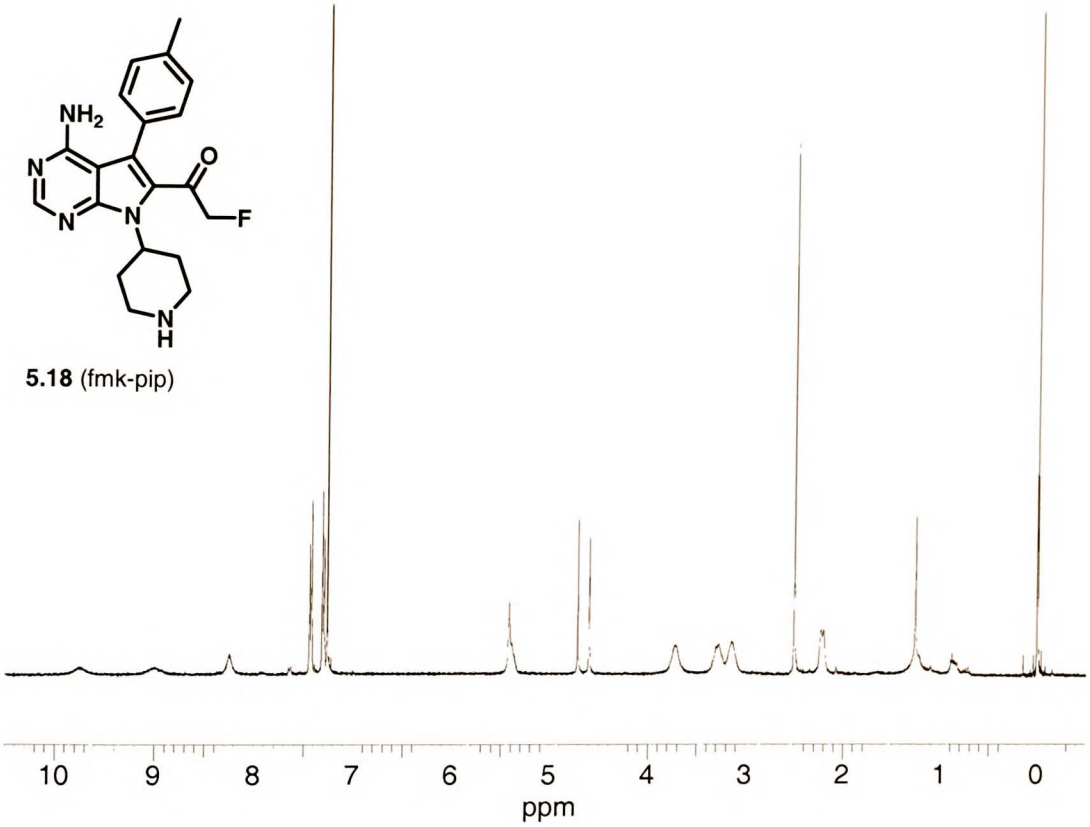

UCSF LIBRARY

6942 R

UCSF LIBRARY

UC San Francisco LIBRARY
UNIVERSITY OF CALIFORNIA

UCSF LIBRARY